DIANE SEWARD

SOME ASPECTS OF SEDIMENTOLOGY OF THE WANGANUI
BASIN, NORTH ISLAND, NEW ZEALAND

Thesis submitted for the degree of
Doctor of Philosophy
in Geology
Victoria University of Wellington
January 1974

i.

TABLE OF CONTENTS

LIST OF FIGURES

LIST OF TABLES

ABSTRACT

The thesis comprises studies of the marine Pleistocene sediments
of the Wanganui Basin, North Island, New Zealand.

Part I deals with the chronology of the sediments and correlation
of horizons within and outside the basin, by dating glass shards from
tephra horizons using the fission-track method. Correlation to similar
tephras from Hawke's Bay, to deep-sea cores taken 1000 km east of New Zealand
and to the central North Island volcanic district is attempted. These
fission-track ages fill a dating gap that previously existed in the New
Zealand marine Quaternary sequence.

Thirteen tephras were examined in the Wanganui Basin and were found to
range in age from 1.50 ± 0.21m.y.B.P. (Ohingaiti Ash) to 0.28 ± 0.05m.y.B.P.
(uppermost Finnis Road Ash). These tephras record major rhyolitic eruptive
phases in the central volcanic region. The most significant eruptive phase
began 1.06 ± 0.16m.y.B.P. with the deposition of the Makirikiri Tuff sediments,
continued to 0.88 ± 0.13m.y.B.P. and is tentatively associated with the older
ignimbrites of the King Country, west of Lake Taupo. A volcanically quiet
period followed when no volcanic glass was deposited in the sediments, until
0.74 ± 0.09m.y.B.P. Several large eruptions then occurred between 0.74 and
0.28m.y.B.P.

The age of the Plio-Pleistocene boundary, at the base of the Hautawan
Stage in the Wanganui Basin is 1.87m.y.B.P. The age of the base of the
Nukumaruan is 1.55m.y.B.P., the Okehuan, 1.06m.y.B.P., the Castlecliffian
0.45m.y.B.P., and the Hawera Series is less than 0.38m.y.B.P.

Palaeomagnetic stratigraphy was determined for the upper Nukumaruan
and lower Okehuan sequence in the Rangitikei River. Viscous components of
magnetism were removed from the samples by thermal demagnetising, extreme

care being needed to obtain consistent results. Independent dates from the palaeomagnetic stratigraphy substantially confirm the fission-track dates. The Bruhnes-Matuyama boundary is clearly defined between the Rewa and Potaka Pumice Members (aged 0.74 and 0.61m.y.B.P. respectively) of the Kaimatira Pumice Sand Formation. The Jaramillo event was not recognised and is probably represented in part of the sequence where sediments are too coarse and friable to yield palaeomagnetic cores.

Part II deals with the detailed sedimentology of the lower Okehuan Stage sequence which is composed of two volcaniclastic formations, the Makirikiri Tuff and Kaimatira Pumice Sand, separated by a non-volcaniclastic siltstone formation, the Okehu Siltstone.

Interpretations of the sedimentary structures in the Makirikiri Tuff and the Kaimatira Pumice Sand Formation confirm previous conclusions of shallow water deposition based on palaeontological evidence. Some structures also indicate the high rate of sediment accumulation during deposition of the volcanic sediments.

Size analysis statistics show influence of source material and processes acting on the sediment during transport and deposition. Rapid sediment accumulation is emphasised by poor sorting, and processes inferred from the sedimentary structures are confirmed by the grain size analyses of the same structures.

Analysis of the attitude of large and small scale cross-stratification reveals a complex polymodal palaeocurrent pattern, as might be expected of shallow water to intertidal sequences. Although often bipolar-bimodal, the dominant sediment transport appears to have been from west to east, similar to the direction of current movement along the Wanganui coast today.

Size and petrography of clasts from the conglomeratic horizons indicate sediment sources both from the central volcanic region of North Island and from the Mesozoic "greywackes" of the axial mountain ranges

which were emergent and probably significantly elevated at the time when the sediments were accumulating. No volcanic debris was deposited with the Okehu Siltstone.

The mineralogy of the sands points to the same sediment sources but also indicates that some metamorphic material was being introduced most likely from South Island.

Part III of the thesis represents a pilot study undertaken to determine whether isotopic differences in fossil shell composition could be used to distinguish shells that grew in fully marine water from those that grew in less saline conditions. Carbon and oxygen isotope ratios were determined on shells from three formations whose environments had been adequately studied by paleontologists. The horizons chosen were the Waipuru Shellbed, the Tewkesbury Formation and the Tainui Shellbed. Agreement with the palaeontological evidence and thus distinction between the fully marine and the fresh water contaminated marine environments was possible with the technique.

ACKNOWLEDGEMENTS

PART I

GEOCHRONOLOGY OF THE PLEISTOCENE SEDIMENTS OF THE WANGANUI
BASIN

CHAPTER 1

GENERAL INTRODUCTION

Location and geological setting

The area of study is on the west side of southern North Island, New Zealand, (Fig. 1), and lies within the Wanganui Basin, (Fleming, 1953) or the South Wanganui Basin, (Cope and Reed, 1967). Its western boundary is in the vicinity of the township of Patea; to the east it is bounded by the North Island axial mountain ranges, and to the north by the central volcanic region of New Zealand. The basin contains sediments ranging in age from early Pliocene in the north to Holocene in the south with a basement of Mesozoic "greywacke" like that of the central axial ranges. The Pliocene-early Pleistocene strata dip towards the centre of the basin generally at angles of less than 7°. They are composed of marine mudstones, sandstones, shellbeds and conglomerates. The latter are infrequent in the lower part of the sequence but become more widespread and increasingly dominant in the upper part.

The basin is crossed by faults trending northeast southwest, the most important of which are the Nukumaru Fault Zone, Upukongara Fault, Turakina Fault, and Pohangina Fault. A system of smaller faults has an east west strike.

Several anticlines, thought to be active (Te Punga, 1957) emphasise the northeast southwest trend and drilling has shown that the cores of some of these folds are basement ridges, with sediments thinning over the crests, (Superior, 1943).

Stratigraphic nomenclature of the Pleistocene Sequence

Fleming (1953) reviewed the early work in the Wanganui Subdivision. Crawford (1869) was the first to recognise "the great Tertiary basin". He, (1870), classified the rocks as Tertiary, Recent and Volcanic. Park (1905 and 1910) set the basis for later classifications by subdividing the sediments of the Wanganui System into Older and Newer Pliocene, with the
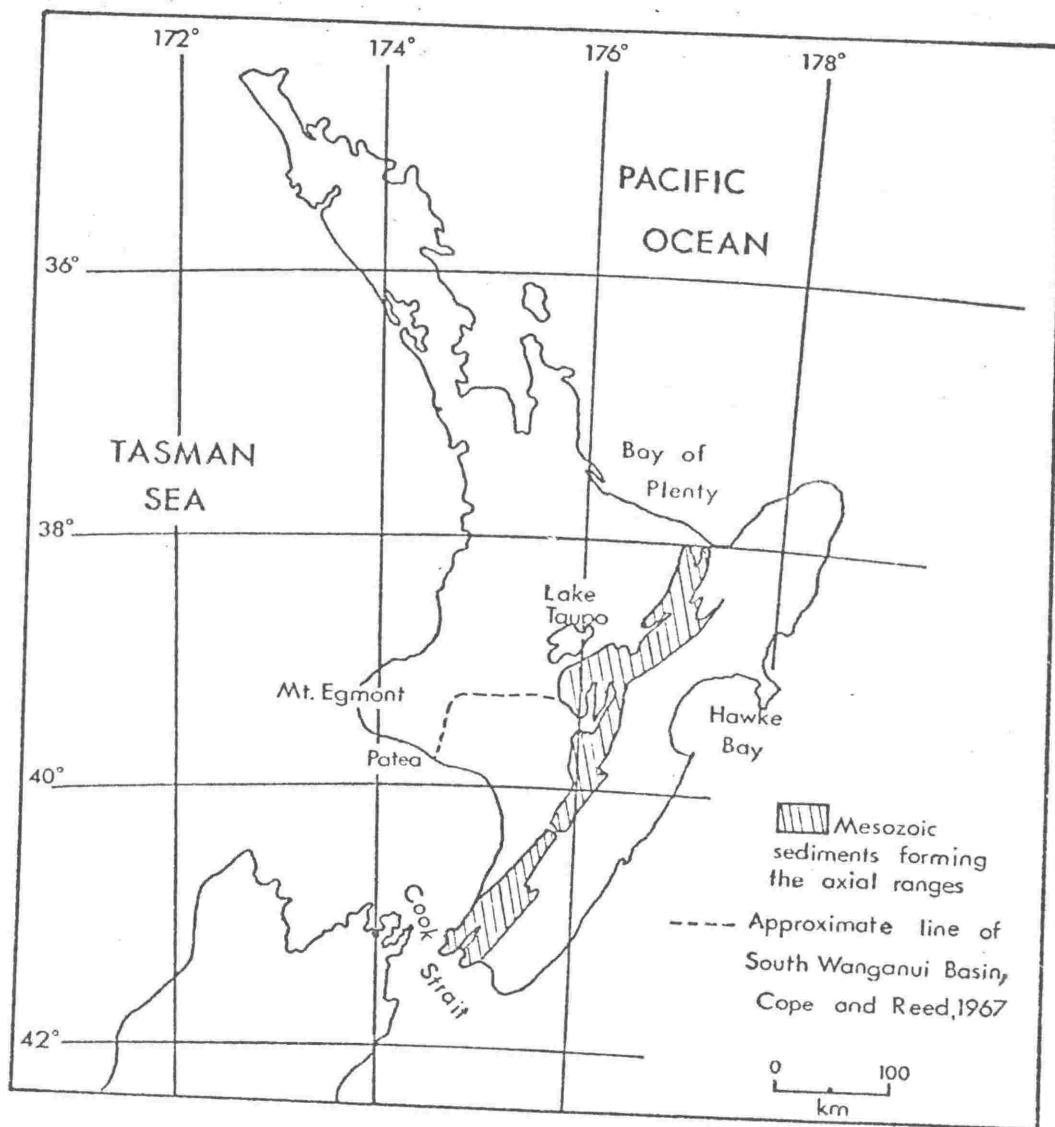
Fig. 1: Location of study area.
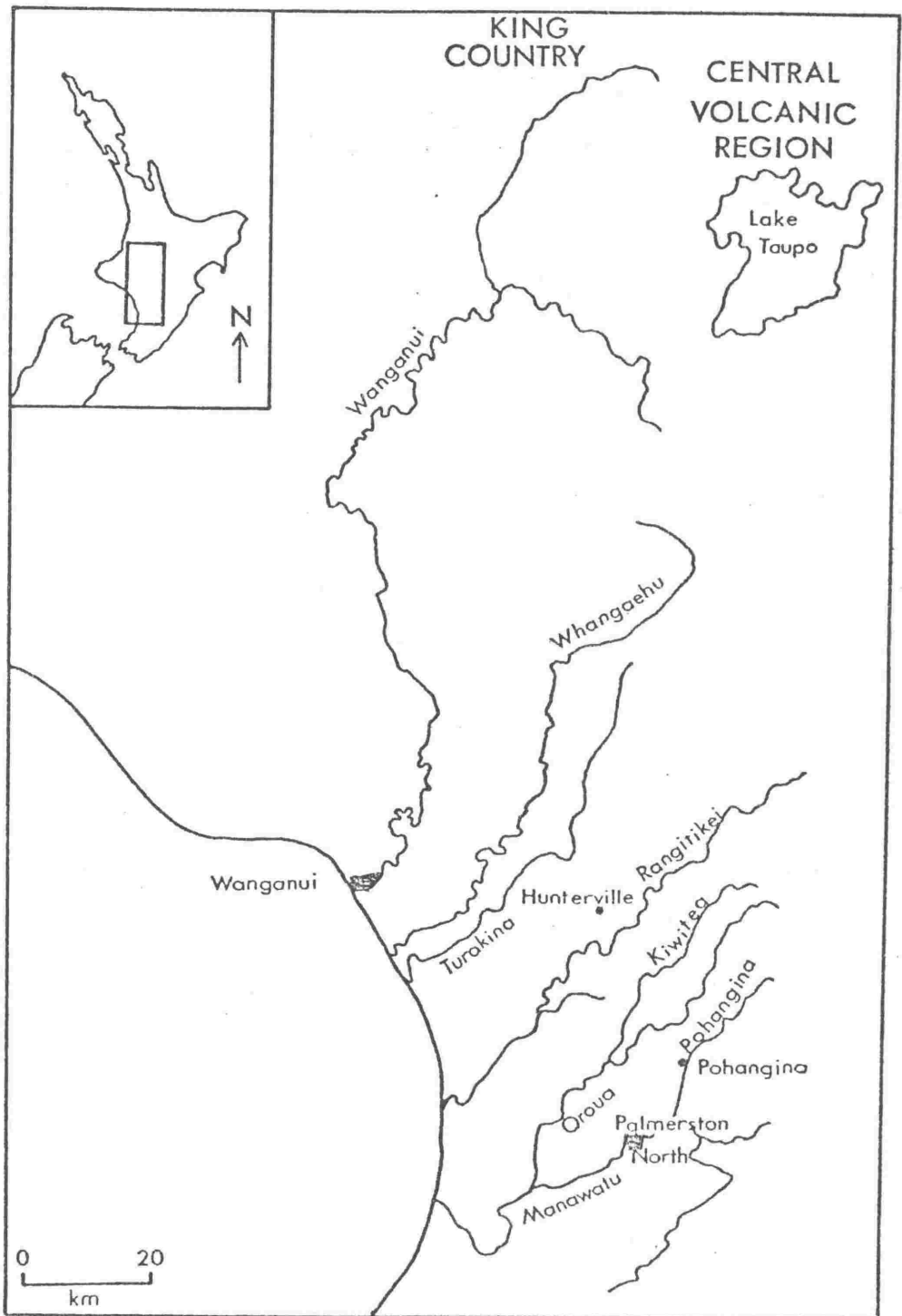
Fig. 2: Map showing geographical locations mentioned in the text.

Nukumaru Limestone at the base of the latter. Thompson (1916) renamed Park's divisions as the two stages – Castlecliffian and Waitotaran. Later workers added the Nukumaruan (Morgan, 1924) and the Opoitian (Finlay, 1939).

Geologists of the Superior Oil Company (1943) – (later cited in the text as "Superior, 1943"), grouped the Pliocene rocks into three stages, Waitotaran, Nukumaruan and Castlecliffian. On the basis of the sequence in the Rangitikei River (Fig. 2), they recognised four formations in the Waitotaran, two in the Nukumaruan and one in the Castlecliffian, (Table 1).

Te Punga (1953) recognised the same stages as Superior but defined three formations that were the direct equivalent of the stages, (Table 1).

Fleming (1953) proposed a nomenclature that followed international usage. He accepted the division of the sediments in the Wanganui Subdivision into three Series: Wanganui, Hawera (Finlay and Marwick, 1947) and Recent. In the Wanganui Series he recognised the Waitotaran, Nukumaruan and Castlecliffian Stages, and in the Hawera Series he named the interglacial Terangian and Oturian Stages. He subdivided the Waitotaran, Nukumaruan and Castlecliffian Stages into substages which were later elevated to stage rank (Fleming, 1962; Vella, 1963). Table 2 shows the time stratigraphic terminology adopted. In this account the supression of the Hautawan Stage by Beu (1969) is not followed.

Lithological terminology

Throughout the thesis two lithological terms have been used which are here qualified.

1) Tephra

The term tephra was qualified by Cole and Kohn (1972) as a general descriptive term for unconsolidated pyroclastic deposits. Although at least some of the beds of volcanic detritus in the Wanganui Basin are most probably by definition epiclastic, a term is needed to differentiate beds

SUPERIOR OIL CO. (1943)		TE PUNGA (1953)	
STAGE	FORMATION	STAGE	FORMATION
Castlecliffian	Castlecliff	Castlecliffian	Upper Rangitikei
Nukumaruan	Petane	Nukumaruan	Middle Rangitikei
	Lower Nukumaruan		
Waitotaran	Mangaweka Mudstone	Waitotaran	Lower Rangitikei
	Utiku Sand		
	Taihape Mudstone		
	Reef bearing Sands		

Pliocene

Table 1: Stratigraphic nomenclature of Superior (1943) and Te Punga (1953)
in the Wanganui Basin.

SERIES	STAGE
Hawera	
Wanganui (upper part)	Castlecliffian
	Okehuan
	Nukumaruan
	Hautawan

Table 2: Time stratigraphic divisions of the
Pleistocene sediments in the Wanganui
Basin, after Fleming (1962) and Vella
(1963).

with one hundred percent volcanic detritus from other volcaniclastic
sediment that is mixed with non-volcanic detritus. The term tephra is
therefore used for beds that are composed entirely of volcanic detritus,
even though part or all of the volcanic detritus may be epiclastic.

2) Greywacke

The term "greywacke" is commonly used in a loose sense in New Zealand
to refer to the Mesozoic sediments of the central axial ranges. It is used
in this thesis where it refers to poorly sorted sedimentary rocks of
litharenite to feldsarenite composition (Folk et al. 1970), that form
clasts in the Pleistocene sediments and are presumed to have been derived
from the central axial ranges.

Sample numbers

The sample numbers quoted in the thesis are the writer's field
numbers. All samples are listed with geographical locality in Appendix 3.
Those used for chemical analyses and fission-track dating are lodged in
the Victoria University collection, and are given Victoria University
numbers in Appendix 3.

CHAPTER 2

PALAEOMAGNETIC STRATIGRAPHY

11.

Introduction

During the past decade palaeomagnetic stratigraphy has become an increasingly important tool in the study of Quaternary and Tertiary chronologies. Most work has been carried out on deep-sea sediment cores; the advantage of studies on deep-sea sediments compared with shallow water marine or continental sediments is that at least some time planes can usually be determined independently and breaks in sedimentation tend to be fewer, more widespread if present and more easily detected.

The section studied here is the Upper Nukumaruan to Middle Okehuan, shallow water, sedimentary sequence of the Rangitikei River Valley (Fig. 2) in the Wanganui Basin. The section has relatively good exposure, no evidence of major unconformities, and a high rate of sediment accumulation. The major disadvantages of the sequence are that the magnetic intensities are generally low, and that much of the sediment is of sand size detritus which is too poorly consolidated to hold together as cores.

Field Techniques

Samples were cored at each site using a portable motorised corer: in no case were within-site cores more than 100mm stratigraphically above or below each other, which, on the basis of fission-track dates, (Chapter 3) represents a time gap of no more than 100 years. At each site at least three cores were taken and every effort was made to obtain cores from the same sedimentation units.

As sand sized material was generally too unconsolidated, sites were restricted to silts and silty fine sands.

Cores were orientated in the field prior to removal from the outcrop and were marked in the manner of figure 3. Two readings were taken on each core, declination and inclination. (By convention inclination was regarded
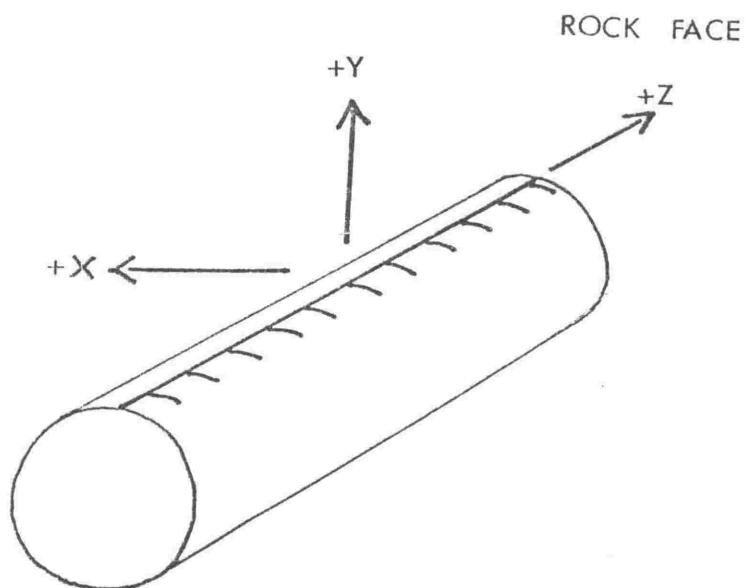
Fig. 3: Axes of orientation of palaeomagnetic cores.

negative if up, positive if down.) The +Z axis is that into the outcrop face, i.e. along the core; +Y was the vertical axis of the core in the upward direction and +X was at 90° to the left of +Z and +Y (while in the outcrop). The -X side of the Z axis was marked with hachures such that there was no possibility of reversal of the core after removal from the outcrop face. (This is not the same convention for axis nomenclature as that of Doell and Cox, 1965).

Dip and strike of bedding plane were also recorded at each locality.

Laboratory Measurements

The direction and intensity of natural remanent magnetism were measured with a 5 CPS spinner magnetometer slightly modified after the design of Foster (1966) and incorporating two fluxgate detectors. All results are tabulated in Appendix 1.

Thermal demagnetising runs

Four cores from site 83, three from site 73 and several single cores from other sites were thermally demagnetised in steps mostly at 50°C intervals.

Relative intensity was plotted against temperature. In most cases there was an increase in intensity immediately prior to samples changing direction from normal to reversed. The three cores from site 83 (Fig. 4) showed no consistent cleaning pattern but all were reversed after treatment at 250°C. Declination and inclination for the samples at each temperature plotted on a stereonet all fall closest together at 350°C (Fig. 5), with a cone of confidence of 25° (Appendix 1). Site 73 (Fig. 6) shows more consistent cleaning patterns between cores with an initial increase in relative intensity then decreasing up to about 250°C where the intensity levelled off. Of the two cores taken to 350°C one became reversed with a
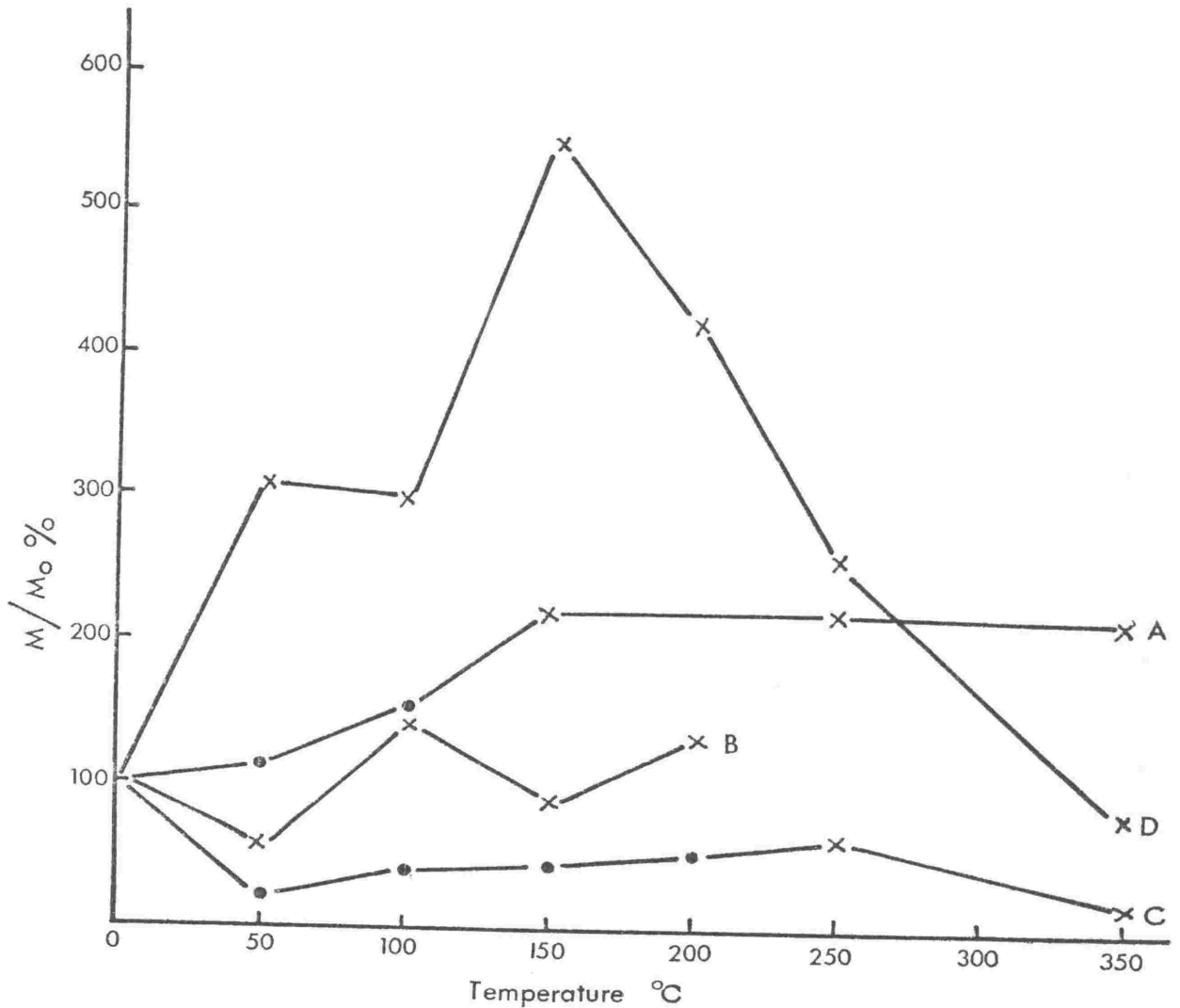
Fig. 4: Thermal demagnetisation curves of four cores from Site 83. (M is remaining intensity, M_0 is initial intensity). Core B broke after running at 200°C. Crosses represent reversed direction of magnetisation; dots represent normal direction.
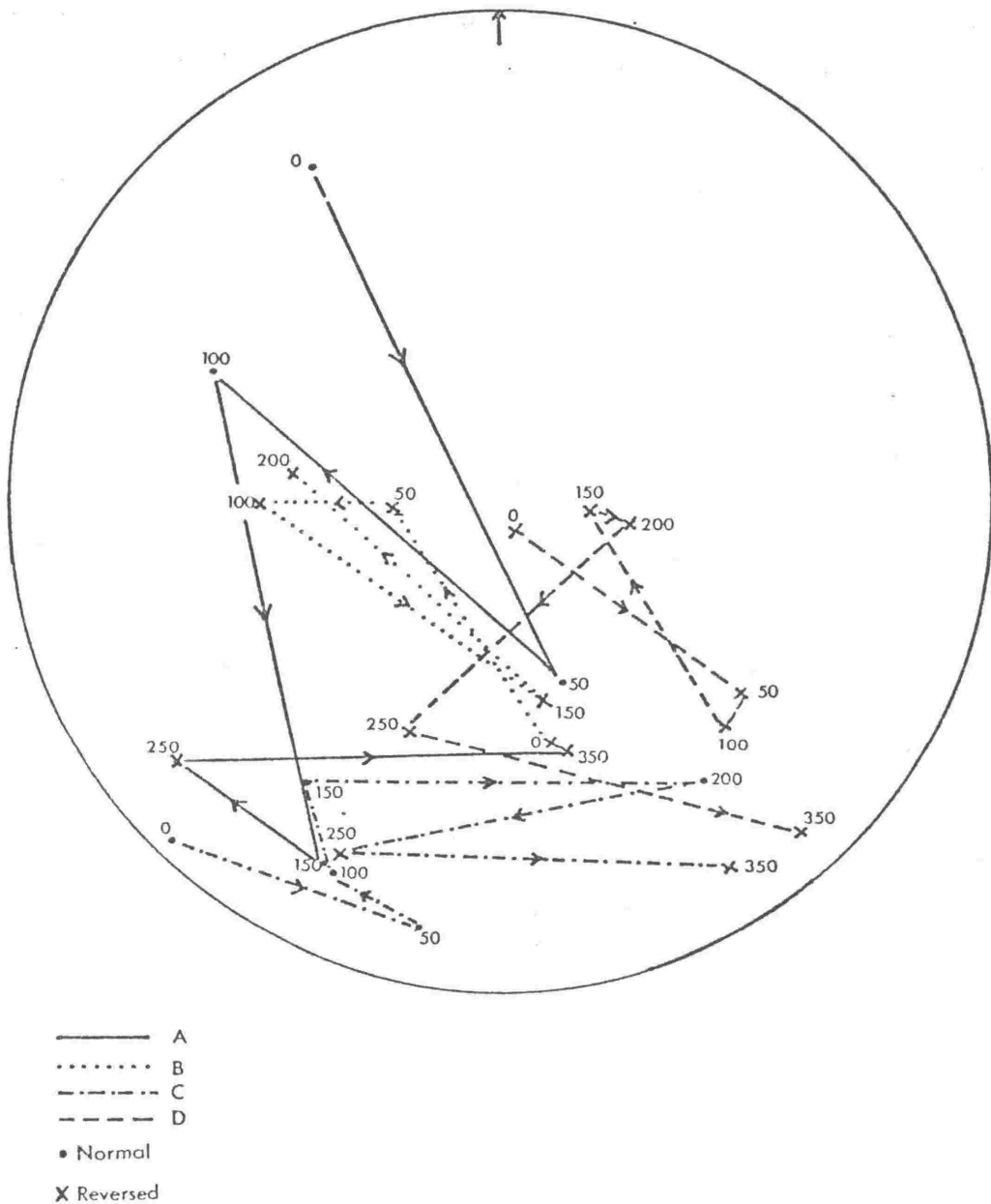
Fig. 5: Changes in direction of magnetisation during thermal
demagnetising of four cores from site 83. Crosses
represent reversed directions of magnetisation; dots
represent normal directions. Numbers are temperatures
of demagnetisation in degrees Celsius.
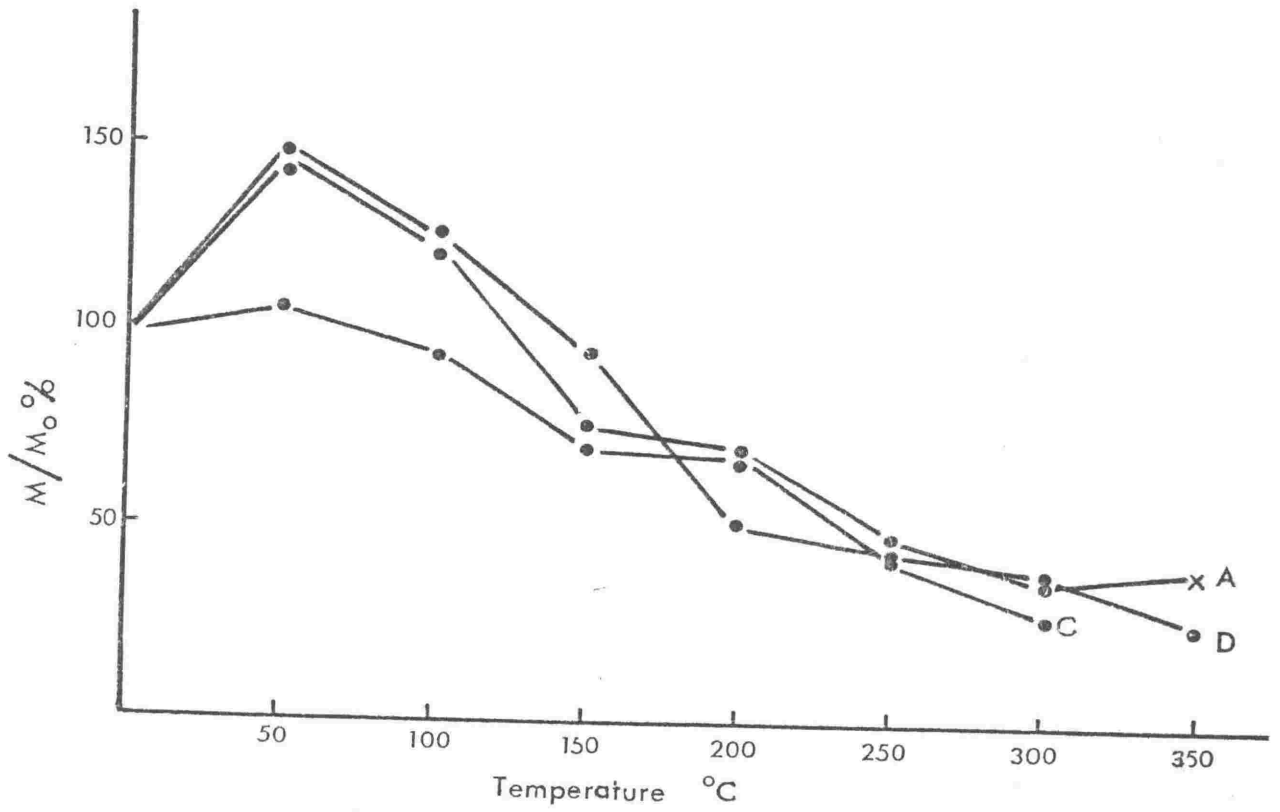
Fig. 6: Thermal demagnetisation curves of three cores from site 73. Core C broke after running at 300°C. Crosses represent reversed direction of magnetisation, dots represent normal direction.

slight increase in relative intensity. With the equipment available and the by now very low intensities being measured (of the order of $0.5x10^{-7}$ emu/cc), it was thought unrealistic to take these samples to higher temperatures. The declination and inclination of cores from site 73 (Fig. 7) varied greatly and were closest prior to cleaning where they also had the strongest intensity of all sites ($0.5x10^{-6}$ emu/cc). It was concluded that the cores from this site had a very strong viscous component. These cores were taken from a site within the Rewa Pumice Member of the Kaimatira Pumice Sand. Cores from site 7, 10m above 73, and site 82, 14m above 73, gave a normal direction of magnetisation after cleaning at $350^{\circ}C$ but as these sites are also in the Rewa Pumice sediment they too may have a strong viscous component, and no confidence can be attached to the direction of magnetisation. Christoffel (pers. comm. 1973) also reports strong unstable components in tephras. These components may be due to rapid deposition or mineralogy.

Results from single cores taken from other sites (Fig. 8) show similar patterns to site 83 with relative intensity increasing prior to direction of magnetisation generally reversing between 250 and $300^{\circ}C$.

On the results of these experiments all samples were thermally demagnetised at $350^{\circ}C$ in an attempt to remove unstable viscous components.

Results and discussion

From the previous discussion, sites near the Rewa Pumice are considered to have a strong viscous normal component and on the basis of the cleaning experiments, are most likely reversed. Thus polarities are considered to be reversed in the whole sequence up to a point between site 84 and site 9, 40 m beneath the Potaka Pumice (Fig. 9).
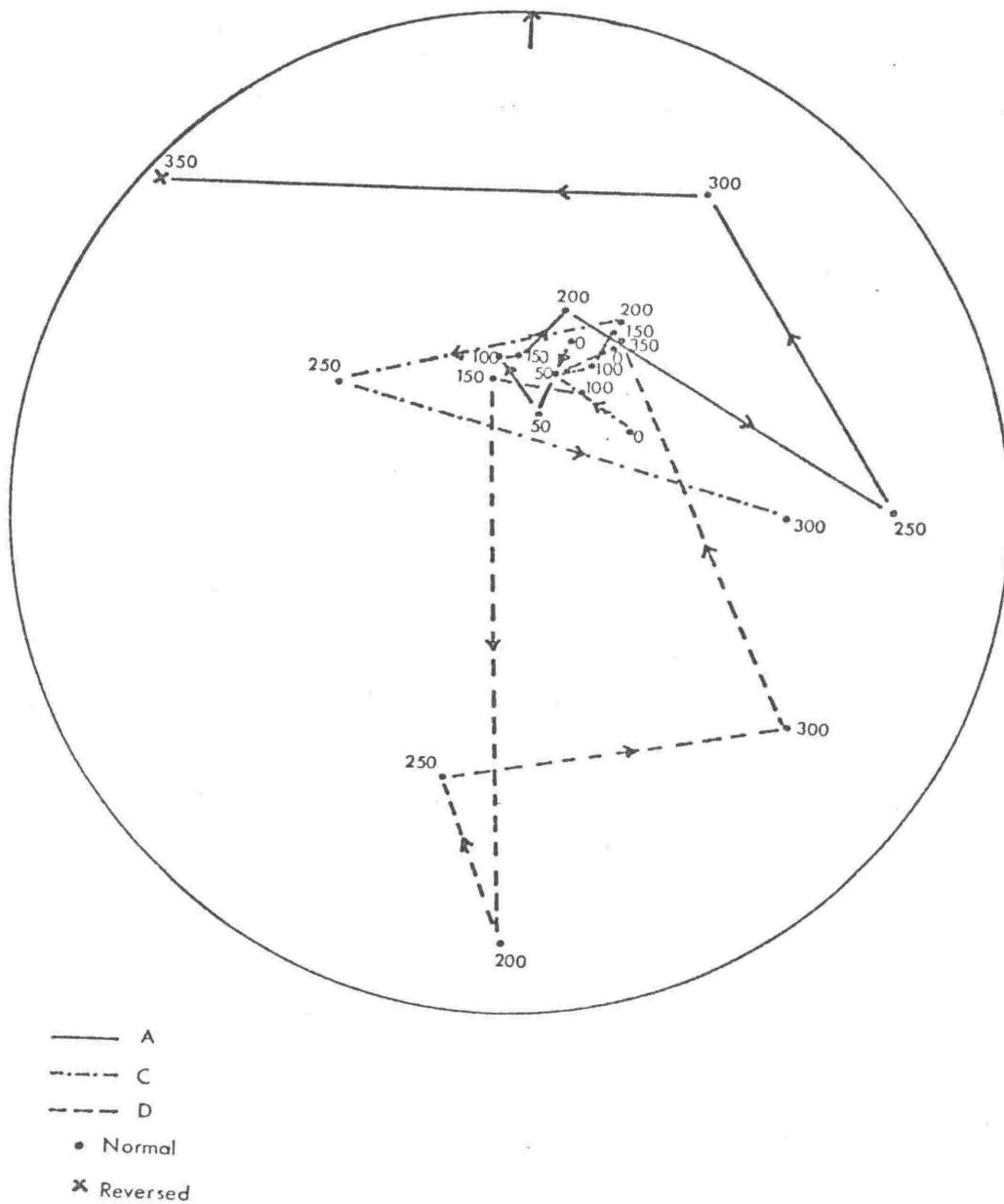
Fig. 7: Changes in direction of magnetisation during thermal
demagnetising of three cores from site 73. Crosses
represent reversed direction of magnetisation; dots
represent normal direction. Numbers are temperatures
of demagnetisation in degrees Celsius.
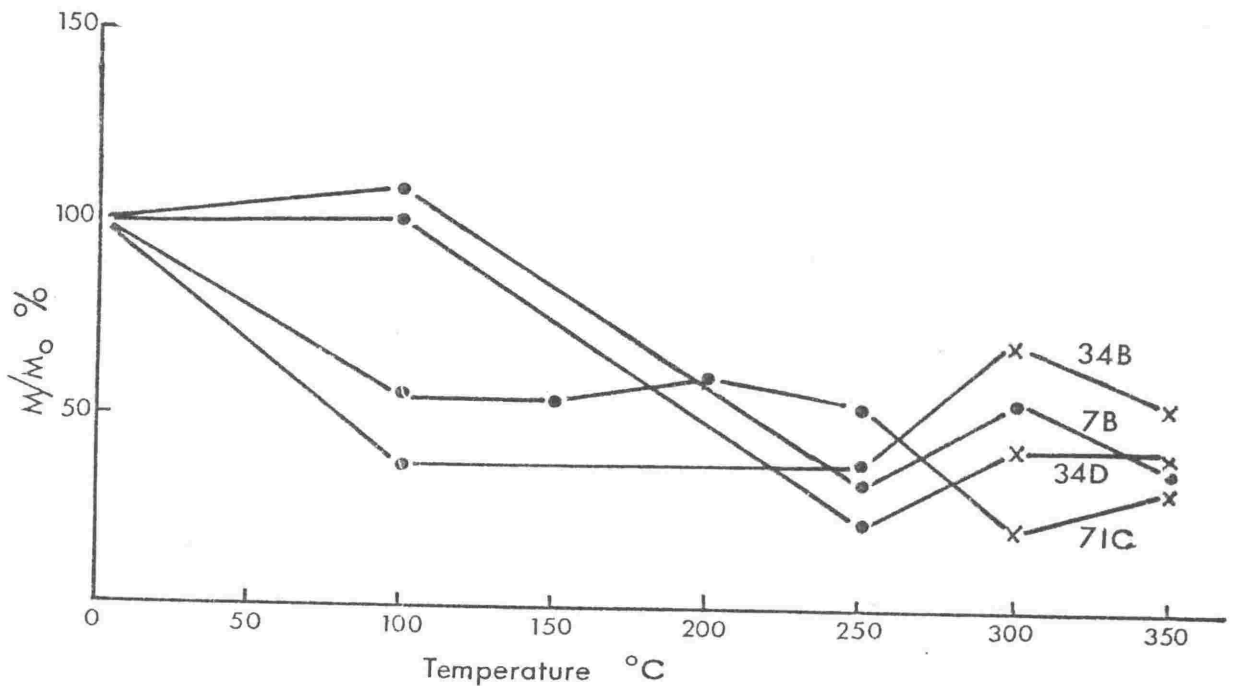
Fig. 8: Typical thermal demagnetisation curves. Dots represent normal direction of magnetisation; crosses represent reversed direction.
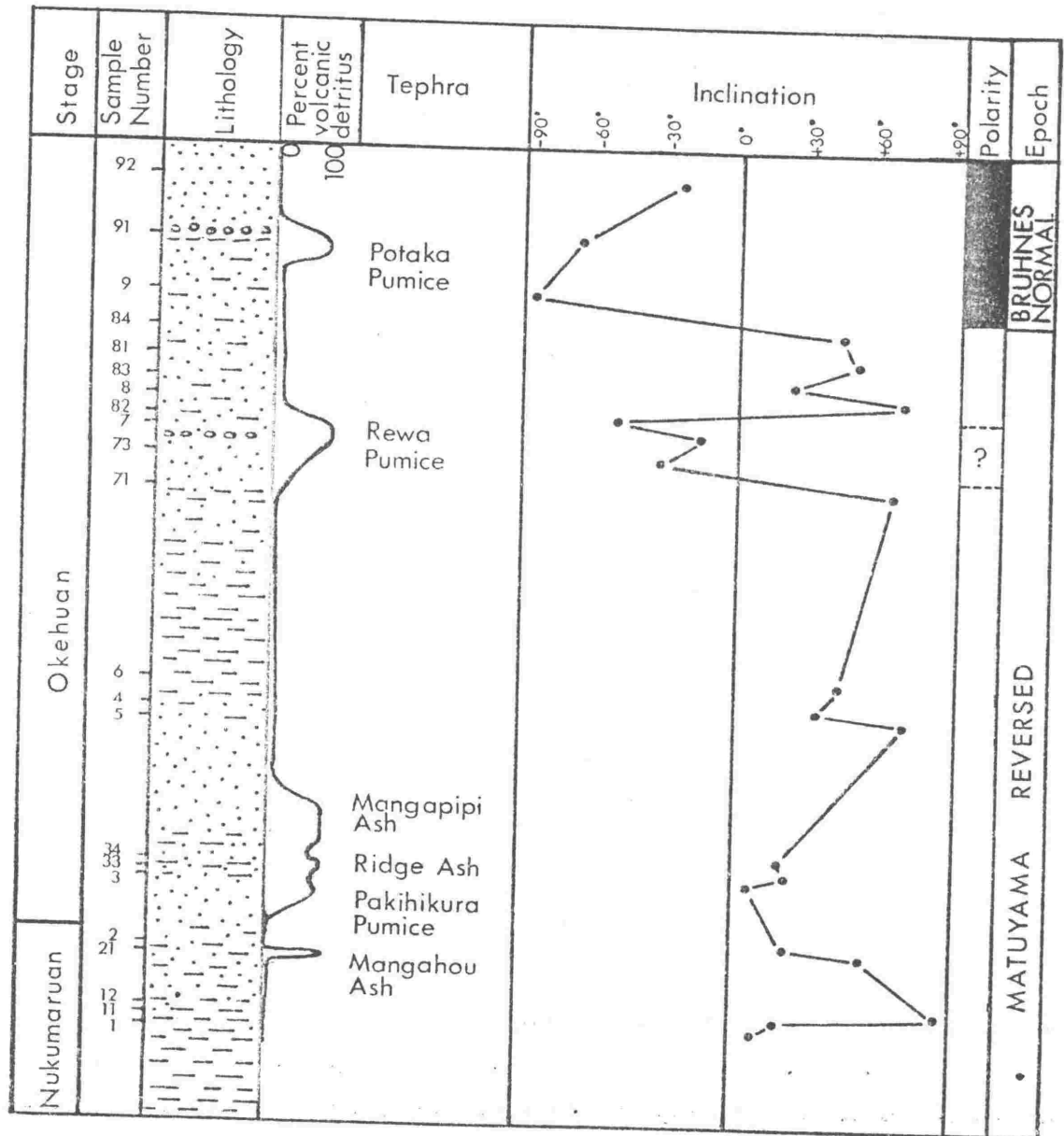
Fig. 9: Palaeomagnetic stratigraphy of the upper Nukumaruan and
lower Okehuan sediments of the Rangitikei River Valley.

Eight tephras have been identified in deep-sea cores east of New Zealand (Ninkovich, 1968, and pers. comm. to Kohn, 1973). The lowest is 1.13m.y. old, based on palaeomagnetic dates and assuming a constant rate of sedimentation. As the Mangahou Ash (Fig. 9) is the first of a sequence of eruptions recorded in the Wanganui Basin it is suggested that this may be the equivalent of this 1.13m.y. tephra. If this is so then the normal direction of polarity at the top of the sequence may be assigned to either the Jaramillo event of the Matuyama reversed epoch or to the Bruhnes normal epoch.

The third deep-sea tephra (Ninkovich, 1968) coincides with the upper Jaramillo reversal, and contains biotite. The only biotite bearing tephra in the palaeomagnetic sequence studied here is in the Mangapipi Ash (Fig. 9). Palaeomagnetic samples could not be taken within or close to this unit as the sediment is too unconsolidated and consequently the Jaramillo event, if present beneath the Mangapipi Ash could not be confirmed. The suggested correlation with the deep-sea tephras support a late Matuyama age for this part of the section. The Bruhnes-Matuyama boundary is considered to lie between sites 84 and 9, approximately 40m beneath the Potaka Pumice.

This conclusion is supported by fission-track dates on the tephras (Chapter 3).

CHAPTER 3

FISSION-TRACK DATING OF PLEISTOCENE TEPHRAS

Introduction

Many beds of volcanic glass and pumice (Fig. 10) are included in the Pleistocene marine sediments of the Wanganui Basin. Most contain little or no non-volcanic detritus and it is concluded that they were deposited soon after eruption either directly by airfall on to the sea, or indirectly by rivers flowing into the sea. Regardless of the mode of transport, these layers form excellent time planes and are treated as tephras.

In the Wanganui Basin they have so far been recognised in the Pleistocene sediments only, and are best exposed in the Rangitikei River section, where the oldest is lower Nukumaruan and the youngest is upper Castlecliffian.

Glass shards from the tephras were dated using the fission-track method to provide a chronology for the basin, as well as permitting intra-basinal correlation, correlation with dated tephras elsewhere in New Zealand and with dated ignimbrites in the volcanic source area. Certain ignimbrites in the source area cannot be dated directly because of alteration of the glass, but on the basis of stratigraphy and petrography in the Wanganui Basin and the source area, tentative ages can now be proposed.

Fission-track method

Silk and Barnes (1959) using the scanning electron microscope, noted damage trails in natural terrestrial materials, and Price and Walker (1962) developed an etching technique whereby these trails could be enlarged and viewed through an optical microscope. The conclusion that the damage trails had been formed by spontaneous fission of ^{238}U gave a new geochronological tool particularly useful in bridging the gap between the limits of ^{14}C and K/A techniques. Fission-tracks should provide an estimate of the age of a mineral (or glass) since solidification, provided that the mineral has not subsequently been raised through a temperature

Fig. 10: Tephra horizon in the Kaimatira Pumice Sand,
          at N138/583910.

high enough to anneal the tracks. The amount of uranium in the mineral must have remained constant and there must be sufficient uranium to produce enough tracks to count in a reasonable time.

Some authors (Lakatos and Miller, 1972), believe that the tracks can be annealed by hydration of glass but their conclusions were based on experiments of short duration (less than a year). Their extrapolation of these data to geological time is considered dubious. The glasses from the Wanganui tephra contain up to six percent water, but their fission-track ages are consistent with ages determined at some horizons by methods other than fission-track dating. Hydration, if it has occurred, evidently has not affected the dates.

Fleischer and Price (1964a) outlined the basic theory and technique for fission-track dating of glasses. Fundamentally, their technique consists of determining the ratio of the density of spontaneous fission-tracks to the density of tracks caused by induced fission of ^{235}U by thermal neutrons (low energy) in a nuclear reactor.

Age determinations are based on the following equation:-

$$\text{Age} = 6.168 \; \frac{\rho_s}{\rho_i} n \times 10^{-8} \text{ years}$$

where ρ_s = number of spontaneous counts per unit area

ρ_i = number of induced counts per unit area

n = time-integrated flux of neutrons.

The decay constant used throughout for spontaneous fission of ^{238}U was $\lambda_f = 6.85 \pm 0.2 \times 10^{-17} \text{yr}^{-1}$ (Fleischer and Price, 1964b, Kleeman and Lovering, 1971).

Techniques

1) Tephra sample was sieved to remove material finer than 63μm, and coarser than 500μm. Quartz, feldspar, lithic fragments and mafic minerals were removed with the Frantz Isodynamic separator.

2) The volcanic glass was cleaned in an ultrasonic bath for one minute, and then air dried.

3) Flat glass shards were separated from pumiceous glass on the magnetic separator.

Settings on the separator for steps 1 and 3 varied from sample to sample.

4) The shard sample was split as follows:-

    a) approximately 65mgm weight was wrapped in aluminium foil in preparation for irradiation to determine ρ_i.

    b) The rest of the sample was retained to determine ρ_s.

5) Standards (NBS and a glass from Dr J. Kleeman of Armidale University, Australia containing 0.823 and 0.355 ppm uranium respectively) were sandwiched between Lexan plastic which was to serve as a track recorder; all were then wrapped in aluminium foil, placed in aluminium cans and sent for irradiation. These standards monitor neutron flux and are used to determine the thermal neutron dose.

6) On return from the reactor the irradiated shards were mounted by embedding in plastic (Epofix or Epiglass are suitable) in teflon moulds, and polished to an optical finish. The non-irradiated part of the sample was treated in the same manner.

7) Both mounts were etched in 48% HF at room temperature for 8-15 secs. The optimum etching time varies from sample to sample, therefore initial etching was for 8 secs. If the tracks were too small the sample was etched again. It is imperative that both mounts be etched together.
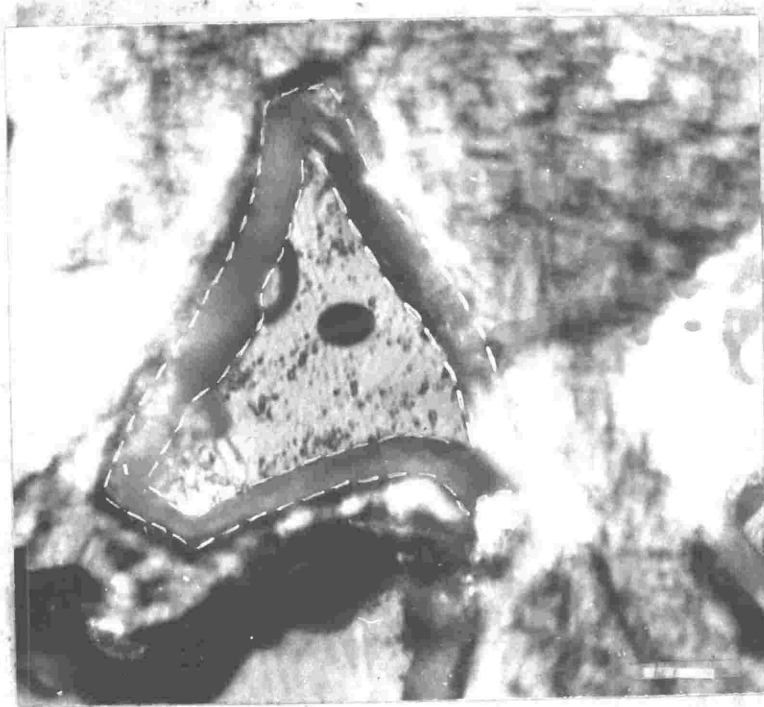
Fig. 11A: Spontaneous fission-track in glass shard. Area between
dotted lines represent glass removed during etching.
Bar scale is 20 μm
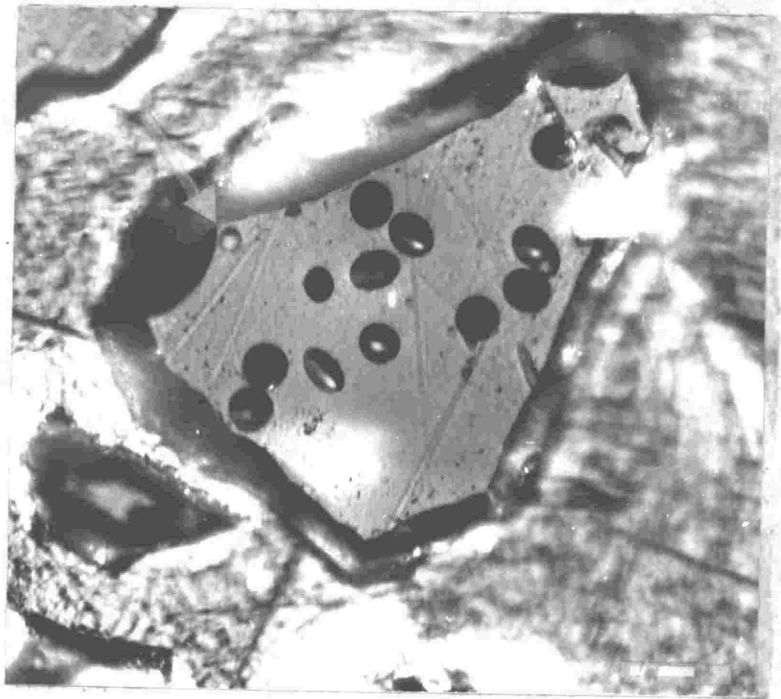
Fig. 11B: Induced fission-tracks in glass shard. Arrow points
to bubble. Bar scale is 20 μm

The mounts were left in ammonia solution to neutralise any remaining HF.

8) ρ_s and ρ_i were determined by counting tracks (Figs. 11A and 11B) and normalising the area counted to one square centimetre. This was done under reflected light, at a magnification of X450, using a point counter. To determine the area covered the basic principles of modal analysis were used. The east west movement of the mechanical stage was at 0.1mm intervals and the north south 0.2mm. Thus 5000 counts on glass shards (those that fell under the cross hairs) is equivalent to 1 cm^2.

9) The Lexan plastic was etched in 6N NaOH for 15 mins at 70°C.

10) Tracks in the Lexan were counted by mounting the plastic on a glass slide and viewing with transmitted light at a magnification of X480. In this case a grid was used to determine the area covered.

In the samples used in this study some of the Lexan samples appear to have annealled. Consequently the Kleeman glass standards were polished and etched in 48% HF at 23°C for 6secs. Tracks were then counted in the same manner as the Lexan in order to determine the dose.

11) The precision of the dates was calculated from the sums of errors determined from the number of spontaneous and induced tracks counted and from the tracks in the Lexan or glass standards. The uncertainties of the exact value of the spontaneous fission decay constant of ^{238}U and in the uranium determinations on the glass standards were not included.

Checks on the validity of the technique

1) Ages determined on several samples by two operators are in agreement, (Table 3). Kohn and the writer counted the same surfaces of induced and spontaneous tracks on three samples. The dose was determined by the writer only.

2) Ages determined by counting different surfaces are in agreement (Table 4). This was done by regrinding, polishing and etching new surfaces.

29.

Sample	Neutron dose ($\times 10^{14}$ n.cm^{-2})	Spontaneous tracks				Induced tracks				Age m.y.B.P.	
		counted		cm^{-2}		counted		cm^{-2}			
		DS	BK	DS	BK	DS	BK	DS	BK	DS	BK
Missing Tuff	34.40	232	112	611	622	3842	1878	47619	46328	2.72	2.85
Rangitawa Pumice	23.16	96	23	120	115	6365	1815	45334	45286	0.38	0.36
Cape Kidnappers sample 226	23.16	13	11	43	39	1485	1520	18525	18961	0.33	0.29

Table 3: Results of counts on three tephras by two operators (DS and BK). Dose was determined by DS only.

Sample	Neutron dose ($\times 10^{14}$ n.cm^{-2})	Spontaneous tracks		Induced tracks		Age m.y.B.P.
		counted	cm^{-2}	counted	cm^{-2}	
P105 run 1	19.95	129	496	2310	57879	1.06
P105 run 2	19.95	161	503	2223	55736	1.11

Table 4: Repeat counts on sample P105 by regrinding and repolishing the sample.

3) The validity of the dates determined using this method was checked on several samples that had been dated by other methods:-

a) ash layer D from core RC9-113 and RC12-215 dated at 0.31 and 0.32m.y. B.P. respectively (Ninkovich, 1968, and Kohn, 1973) by interpolation between dated palaeomagnetic reversals assuming a constant sedimentation rate. The fission track date obtained by the writer is $0.32^{\pm}0.05$m.y.B.P., (Table 5).

b) ash layer from deep-sea core RC12-215 dated at 1.07m.y.B.P. (Kohn, 1973). The fission-track date by the writer is $1.02^{\pm}0.16$m.y.B.P., (Table 5).

c) the Spooner Tuff, dated by Lienert, Christoffel and Vella (1972) on the basis of palaeomagnetic stratigraphy should be older than 2.43 and younger than 2.82m.y.B.P. (using the palaeomagnetic scale of Opdyke, 1972). The fission-track date on this sample is $2.62^{\pm}0.16$m.y.B.P., (Table 5).

d) The Bruhnes-Matuyama palaeomagnetic boundary (0.69m.y.) was determined by the writer (Chapter 2) to lie between the Potaka Pumice and the Rewa Pumice. The fission-track dates on these tephras are 0.61 and 0.74m.y.B.P. respectively.

e) Ages are all stratigraphically consistent with one another.

f) Ninkovich (1968) identified five tephra layers in cores east of New Zealand dated at 0.27, 0.31, 0.67, 0.73 and 0.86m.y.B.P. Three additional tephras from unpublished data occur at 0.29, 1.07 and 1.13m.y. B.P., (Core RC12-215). Although these cores penetrated sediments with a maximum age of 3m.y.B.P. no older tephra were recorded. Thus it appears that a series of large eruptions began in New Zealand a little over one million years ago, which is in accord with the dates determined in this thesis.

Sample	Etch time (secs)	Spontaneous tracks		Induced tracks		Neutron dose ($\times 10^{14}$ n.cm^{-2})	Fission-track age m.y.B.P.	Age determined by other techniques m.y.B.P.
		counted	cm^{-2}	counted	cm^{-2}			
RC12-215 2.8-2.95 metres	10	43	113	7109	50660	23.38	0.32$\pm$0.05	0.32
RC12-215 9.19-9.23 metres	13	44	220	2595	32248	24.09	1.02$\pm$0.16	1.07
Spooner Tuff	12	427	763	8742	61680	34.40	2.62$\pm$0.16	2.43 to 2.82

Table 5: Fission-track ages of samples dated by other techniques.

Dates on tephras in the Rangitikei River section

A thick sequence (2433m) of marine to estuarine Pleistocene sediments are well exposed in the Rangitikei River valley. The palaeontological control is good (Te Punga, 1953) and the tephras there were the first to be dated and are treated as a standard sequence for the Wanganui Basin.

Only thick tephras were dated (Fig. 12, Table 6); many minor eruptions were recorded but not dated.

The oldest known tephra in the Wanganui Basin is within the Ohingaiti Sand near the base of the Nukumaruan Stage with an age of 1.50±0.21m.y.B.P. A complete lack of tephra horizons within the sediments indicates that no significant eruptions occurred until the deposition of the Mangahou Ash at 1.26±0.17m.y.B.P. The most significant phase of volcanic activity recorded in the Wanganui Basin began 1.06±0.16m.y.B.P. ago, and lasted until 0.88±0.13m.y.B.P. This activity produced the detritus that formed the sediments of the Makirikiri Tuff Formation (Fleming, 1953), which forms the base of the Okehuan Stage. The next major phase of eruptions began at approximately 0.74±0.09m.y.B.P. and lasted until 0.61±0.06m.y.B.P. and formed the sediments of the Kaimatira Pumice Sand Formation (Fleming, 1953). In the Rangitikei River Valley the next eruptions are recorded by pumice in the Waitapu Shellbed (Te Punga, 1953), dated at 0.52±0.08m.y.B.P., and in the Waiomio Shell Conglomerate (Te Punga, 1953) dated at 0.45±0.09 m.y.B.P. The youngest tephra recorded in the sequence is the Rangitawa Pumice (Te Punga, 1953) which is dated at 0.38±0.04m.y.B.P. Sediments of the Hawera Series unconformably overlie this tephra.

Correlation of tephras within the Wanganui Basin

1) The Ohingaiti Ash

This tephra has been recorded in only one outcrop in the Wanganui Basin, but the Ohingaiti Sand / which it occurs can be traced to the Wanganui coast

Rangitawa Pumice 0.38

Waiomio Shell Bed 0.45

Waitapu Shell Conglomerate 0.52

Potaka Pumice 0.61

Rewa Pumice 0.74

Mangapipi Ash 0.88
Ridge Ash 1.04
Pakihikura Pumice 1.06
Mangahou Ash 1.26

Ohingaiti Ash 1.50

Castle-cliffian

Okehuan

Nukumaruan

Hautawan

Pleistocene

500m

0

Scale
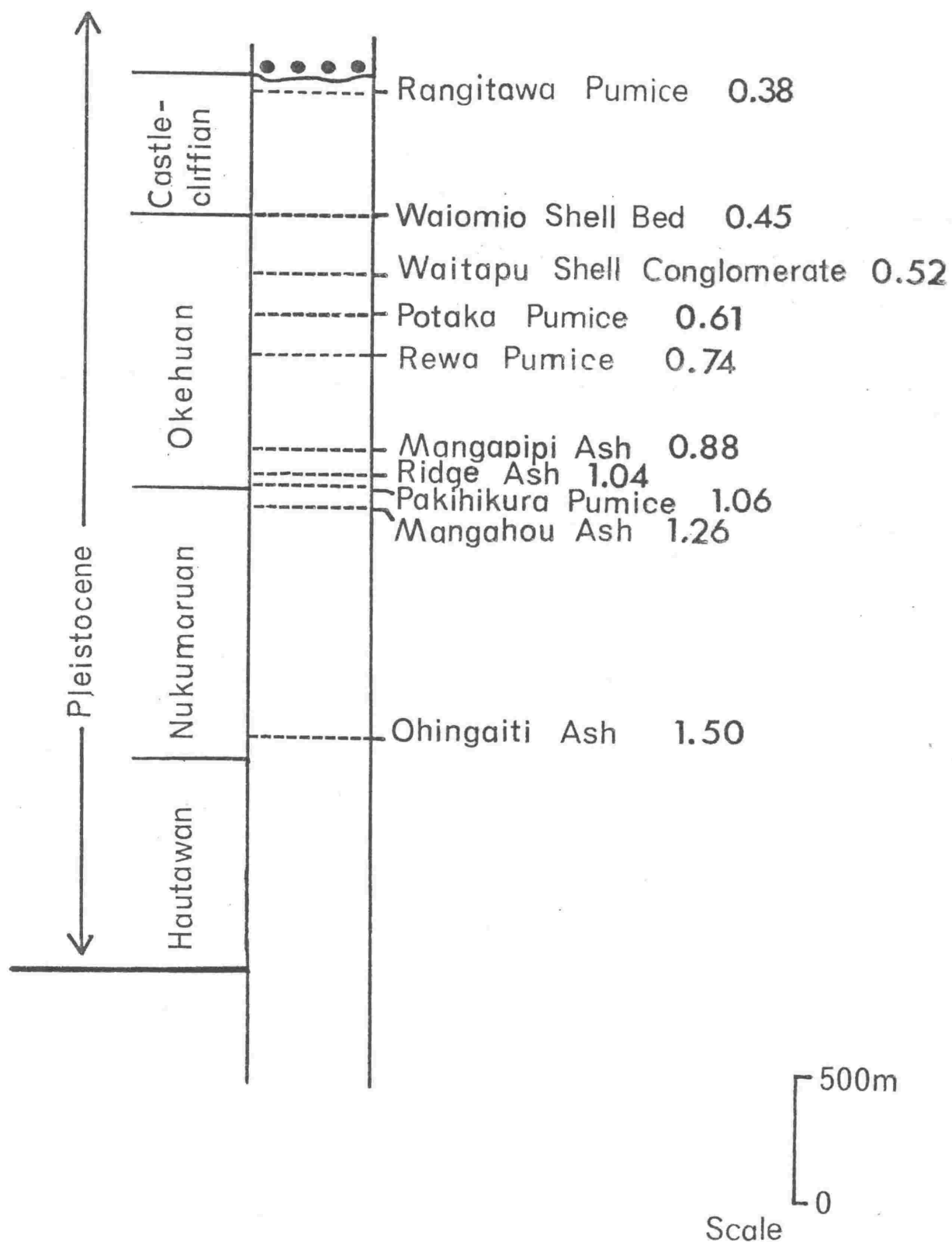
Fig. 12: Tephra and pumice rich horizons in the Rangitikei Valley section. Ages in million of years before present.

Sample	Etch time (secs)	Spontaneous tracks		Induced tracks		Thermal neutron dose $(x10^{14}n. cm^{-2})$	Age m.y.B.P.
		counted	cm^{-2}	counted	cm^{-2} $(=\rho_s cm^{-2})$		
Rangitawa Pumice	10	96	120	3842	45344	23.16	0.38 ± 0.04
Waiomio Shell Bed	12	25	114	9880	35886	23.16	0.45 ± 0.09
Waitapu Shell Conglomerate	12	44	169	3710	46206	23.16	0.52 ± 0.08
Potaka Pumice	10	100	156	5156	36672	23.38	0.61 ± 0.06
Rewa Pumice	11	77	154	4241	30182	23.38	0.74 ± 0.09
Mangapipi Ash	12	48	267	3647	45321	24.14	0.88 ± 0.13
Ridge Ash	8	49	245	3414	33895	23.38	1.04 ± 0.15
Pakihikura Pumice	10	44	220	2060	25530	19.95	1.06 ± 0.16
Mangahou Ash	12	56	280	2586	32045	23.38	1.26 ± 0.17
Ohingaiti Ash	12	51	196	2789	27694	34.4	1.50 ± 0.21

$\lambda_f = 6.85 \times 10^{-17} y^{-1}$

Table 6: Fission-track dates on tephras from the Rangitikei River section.

in the west and to the Mesozoic ranges in the east, (Table 7).

The name Ohingaiti Ash is here proposed for the grey, rhyolitic ash 1.5m thick, 90m above the base of the Ohingaiti Sand in the Rangitikei River (N139/169918), 4km south of Ohingaiti Township.

2) Mangahou Ash

The Mangahou Siltstone on the Wanganui coast contains a considerable amount of glass, and was correlated by Fleming (1953) with the tephra in the Rangitikei Valley, 20m beneath the base of the sediments of the Ohekuan Stage, (Table 7). For this reason the term Mangahou Ash is proposed for the tephra exposed in the Rangitikei valley. The type locality is on Pakihikura Road (N139/142846) where it occurs as a white rhyolitic ash, 0.5m thick interbedded with grey-brown silts and sands.

This is most probably the same horizon as that recorded beneath the Makirikiri Tuff in several sections and in the Stantiall Oil Well by Superior (1943).

3) Makirikiri Tuff Formation

These sediments occur at the base of the Okehuan Stage. The formation can be traced across the basin and is readily recognisable because it is the first major influx of volcanic detritus. Superior (1943) and Te Punga (1953) respectively called this unit the Basal Ash and Pakihikura Pumice. Piyasin (1966) in the east of the basin, included these tephras in the Mangatarata Formation; Rich (1959) mappedthem as part of the Tua Paka Formation in the region of Palmerston North (Fig. 13). As the sediments are readily traced across the basin the name Makirikiri Tuff is here extended to include all the above named correlatives.

At the Rangitikei River at least three tephra members are recognised in the Makirikiri Tuff Formation. They were dated at 1.06, 1.04 and

Stage	Wanganui Subdivision	Age m.y.B.P.	Rangitikei Valley
Castlecliffian		0.38	Rangitawa Pumice
	Upper Castlecliff Shellbed		Glycimeris Shellband
	(several formations)		
	Seafield Sand		Toms Conglomerate
	Upper Kai-iwi Siltstone		
	Kupe	0.45	Waiomio Shell Bed
Okehuan	Upper Westmere Si.St.		
	Lower Westmere Si.St.		
	Omapu Shellbed ?	0.52	Waitapu Shell Conglomerate
	Lower Kai-iwi Si.St.		
	Kaimatira Pumice Sand	0.61	Potaka Pumice
		0.74	Rewa Pumice
	Upper Okehu Si.St.		
	Okehu Shell Grit		
	Lower Okehu Si.St.		
		0.88	Mangapipi Ash
	Makirikiri Tuff	1.04	Ridge Ash
		1.06	Pakihikura Pumice
Nukumaruan	Upper Maxwell		
	Mangahou Si.St.	1.26	Mangahou Ash
	Ohingaiti S.St.	1.50	Ohingaiti Ash

Table 7: Intrabasinal correlation. Dates of horizons in the Rangitikei
River correlated to the Formations in the Wanganui Subdivision
(correlations based on Fleming, 1953 and 1957).

FLEMING (1953)		SUPERIOR (1953)		TE PUNGA (1953)	PIYASIN (1966)	RICH (1959)
West of Whangaehu	East of Whangaehu	West of Rangitikei	East of Rangitikei	Rangitikei	Woodville	Palmerston North
Kaimatira Pumice Sand Formation	Kaimatira Pumice Sand Formation	Castlecliff Formation →	Castlecliff Formation →	Potaka Pumice	Mangatarata Formation	Tua Paka Formation
Upper Okehu Siltstone Formation	Okehu Siltstone Formation	Coutts Creek Horizon	Kimbolton Ash	Upper Rangitikei Formation →		
Okehu Shell Grit Formation		Castlecliff Formation →	Coutts Creek Horizon			
Lower Okehu Siltstone Formation						
Maldrikiri Tuff / Butlers Shell Formation / Conglomerate Formation	Maldrikiri Tuff Formation	Basal Ash	Basal Ash	Pakihikura Pumice		

Fig. 13: Nomenclature of lower Okehuan sediments used by various geologists. That of Fleming (1953) is adopted in the present study.

0.88m.y.B.P. (Table 6). The name Pakihikura Pumice is here restricted to
the lowest tephra which is 0.5m thick. It is best exposed on the road 200m
south of Pakihikura Creek, (N139/136839). The Ridge Ash occurs as a unit
approximately 4.5m thick, 27m above the Pakihikura Pumice outcrop on the south-
east side of the road. The Mangapipi Ash is a tephra unit some 22m thick with
the best exposure at Mangapipi Creek (N139/131828). Although it is
considered here as one unit it is composed of at least two tephra beds
separated by very ashy sands and lenses of lignite.

The Pakihikura Pumice and the Ridge Ash cannot be distinguished in the
field without stratigraphic control. The Mangapipi Ash however, has a tephra
bed in its upper portion that contains biotite as a constituent of its
ferromagnesian mineral assemblage.

Three samples of the Makirikiri Tuff Formation tephras from other
areas in the Wanganui Basin were also dated in this study, (Table 8).
Samples from the Wanganui area (loc. 3, N137/484959; loc. 9, N138/656949)
were dated at 1.04 ± 0.13 and 0.96 ± 0.14m.y.B.P. respectively and may represent
either the Pakihikura Pumice or the Ridge Ash Members. The third sample,
from the extreme east of the basin, in the Oroua Valley north of Apiti
(N139/442855) is the lowest tephra in a well exposed sequence, presumably
the Pakihikura Pumice, and was dated at 1.09 ± 0.07m.y.B.P.

4) Kaimatira Pumice Sand Formation

The sediments of this formation represent the second major phase
of volcanic activity recognised in the Wanganui Basin sediments. The
formation has never been formally correlated across the basin.
Superior (1943) mapped the Coutts Creek Horizon, (correlated by
Fleming (1953) with the Kaimatira Pumice Sand Formation) from Wanganui
to Hunterville, but not to the Rangitikei River or across it. On
the east side of this river they mapped the Kimbolton Ash which they
considered to be younger than the Coutts Creek Horizon (Fig. 13). The

| Sample | Etch (secs) | Spontaneous tracks | | Induced tracks | | Thermal neutron dose $(\times 10^{14} \text{n.cm}^{-2})$ | Age m.y.B.P. |
		counted	cm^{-2}	counted	cm^{-2} $(=\rho_s \text{cm}^{-2})$		
M3	12	65	325	3184	45161	23.38	1.04 ±0.13
M9	10	47	294	2657	44283	23.38	0.96 ±0.14
P105	12	290	500	4533	56163	19.95	1.09 ±0.07

Table 8. Fission-track dates on tephras from the Makirikiri Tuff Formation.

Potaka Pumice (Te Punga, 1953) at the Rangitikei River is the same as the
Kimbolton Ash.

In the Rangitikei Valley two tephra units are present; the older
of the two which is 0.74 ± 0.09m.y.B.P. is exposed in the road cut just south
of Rewa village (N144/125797). It is a pumice conglomerate up to 1.5m
thick bounded above and below by pumiceous sands. This unit is here called
the Rewa Pumice Member. It is also recognisable in the Oroua River valley
(N144/297272). The younger tephra (0.61 ± 0.06m.y.B.P.) exposed at the top
of Rewa Hill, 115m above the Rewa Pumice, is the horizon mapped by Te Punga
(1953) as the Potaka Pumice, the name here adopted for this tephra member.
At its type locality it consists of 18m of thin to medium bedded fine sand
to gravel. It is readily recognisable in the field by conspicuous hornblende
phenocrysts. Towards the west it is rarely represented by pure tephra, but
rather by coarse, medium sorted, ashy, hornblende rich sand. This facies
is represented at Kaimatira Bluff and in the upper cross-bedded unit of the
Kaimatira Pumice Sand at the coast. Titanomagnetite trace element analyses
(Table 9) from several exposures of the hornblende rich sands west of the
Rangitikei River and from the tephra member east of the Rangitikei also
support this correlation, i.e. that the hornblende rich Kaimatira Pumice
Sand is the correlative of the Potaka Pumice.

Superior (1943) mapped the Kimbolton Ash in the region of Finnis
Road, Pohangina (N144/253585), but fission-track dates from this sequence
indicate a much younger age. Two tephras from this locality (Table 11)
are dated at 0.32 ± 0.07 and 0.28 ± 0.05m.y.B.P. The ferromagnesian assemblage
of the younger is 95% biotite, 5% hypersthene, and the older, 80% hypersthene,
10% hornblende and 10% biotite. Neither of them resembles the Potaka Pumice.

On the ridges between the Oroua and Pohangina Rivers the only
exposure of the upper Kaimatira Pumice Sand tephra found was on Zig Zag Road
(N144/293652) where the hornblende rich Potaka Pumice was identified.

Sample	Grid Ref.	Ti %	Mn %	V ppm	Cr ppm	Co ppm	Ni ppm	Facies
K141	N144/016776	5.8	.443	3149	252	70	98	Hornblende sands
K72	N144/216794	6.7	.536	3287	284	71	98	Tephra
K71F	N144/132795	9.1	.106	3201	356	42	116	Tephra
K90	N139/302820	8.8	.380	3682	243	60	91	Tephra
K51	N144/131795	6.2	.509	3258	371	69	104	Tephra
K148A	N139/710892	6.95	.740	3343	355	92	104	Hornblende sands
K21B	N138/567928	6.60	.504	3524	431	70	101	Hornblende sands

Table 9: Partial chemical analyses of titanomagnetites from the Potaka Pumice. (Analyst B. P. Kohn).

Sample	Grid Ref.	Ti %	Mn %	V ppm	Cr ppm	Co ppm	Ni ppm	Facies
K30D	N144/125797	8.7	.594	1033	111	63	53	Rewa Pumice
K76	N138/844853	8.3	.575	963	76	47	47	?Kaukatea Ash
K148D	N138/710892	8.95	.500	1439	119	118	339	Kaukatea Ash

Table 10: Partial chemical analyses of titanomagnetites from the Rewa Pumice and Kaukatea Ash. (Analyst B. P. Kohn).

Sample	Etch time (secs)	Spontaneous tracks		Induced tracks		Thermal neutron dose $(x10^{14} n.cm^{-2})$	Age m.y. B.P.
		counted	cm^{-2}	counted	cm^{-2} $(-\rho_s cm^{-2})$		
Upper	18	34	85	2557	42532	23.00	0.28 $\pm$0.05
Lower	13	23	115	5228	52165	23.38	0.32 $\pm$0.07

Table 11. Fission-track dates on tephra from Finnis Road, Pohangina.

Sample	Etch time (secs)	Spontaneous tracks		Induced tracks		Thermal neutron dose $(x10^{14} n.cm^{-2})$	Age m.y. B.P.
		counted	cm^{-2}	counted	cm^{-2} $(-\rho_s cm^2)$		
Kaukatea Ash	12	50	125	2507	31663	23.38	0.57 $\pm$0.08

Table 12: Fission track date on tephra from Kaukatea Road.

Volcaniclastic sediments mapped by Rich (1959) as the equivalent of the Kaimatira, east of Tua Paka Farm (N149/222367) are also incorrectly correlated. A tephra at the top of the section is younger than 100ky B.P. Completion of the dating of this sample by the fission-track method has been deferred because it will be extremely time consuming.

Thus, the Kaimatira Pumice Sand Formation can be traced from the coast (N137/418930) to the ridge between the Oroua and Pohangina Valleys (N144/376673) where it is lost before being recognised in the Pohangina River Valley again. It includes two tephra members, the Rewa Pumice (0.74m.y.B.P.) and the Potaka Pumice (0.61m.y.B.P.). West of the Rangitikei these members do not always occur as tephra beds but a lithofacies correlative of the Potaka Pumice can be identified in the upper portions.

5) Kaukatea Ash

The Kaukatea Ash is a tephra unit 4m thick exposed in the high valley sides of Kaukatea Stream, (N138/710892), overlying a massive siltstone approximately 15m thick containing the fossil <u>Chlamys gemmulata</u>. This in turn overlies hornblende rich pumiceous sands identical to the dominant western lithofacies of the Potaka Pumice. Fleming (1953) mapped these sediments as part of the Undifferentiated Kai-iwi Group. The outcrop is in fact 5km south of the base of the Kai-iwi Group (the Kaimatira Pumice Sand) and his map suggests that the Kaukatea Ash (though not named by him) is near the top of the Group. However, on the basis of the hornblende and the trace elements of the titanomagnetites (Sample 148A, Table 9), the present writer feels that the hornblende rich sands are the equivalent of the Kaimatira Pumice Sand. On these grounds, the massive siltstone is most likely to be the equivalent of the Lower Kai-iwi Siltstone, (Fleming, 1953). The stratigraphic position of the Kaukatea Ash is thus postulated to be at the top of the Lower Kai-iwi Siltstone. The implied southward displacement

of the upper Kaimatira Pumice Sand relative to the basal Kaimatira may be
due to a series of east west faults mapped in the region but not traced
extensively.

The type locality of the Kaukatea Ash is on the southern side of the
Kaukatea Stream Valley (N138/710892). It has been dated at 0.57 ± 0.08
m.y.B.P., (Table 12) a date consistent with the present stratigraphic
interpretation.

6) Waitapu Shell Conglomerate

The Waitapu Shell Conglomerate is a pumice rich horizon in the
Rangitikei Valley (N144/026749) but as yet has not been recognised elsewhere
in the basin. The fission-track age of its glass is 0.52 ± 0.08 m.y.B.P.
(Table 6). As the pumice is undoubtedly epiclastic the age of the conglomerate
is slightly younger but is probably within the error limits of the fission-
track age.

7) Waiomio Shell Bed

The Waiomio Shell Bed is another pumice rich conglomerate with an age
on the glass of 0.45 ± 0.09 m.y.B.P. The remarks about the age on the Waitapu
Shell Conglomerate apply here also. Fleming (1957) placed this horizon
in the Waikopiroensis Zone which forms the base of the Castlecliffian Stage
and thus is a correlative of the Kupe Formation of the Wanganui Subdivision
(Fleming, 1957), (Table 7).

8) Rangitawa Pumice

The Rangitawa Pumice was first recognised by Te Punga (1953) in the
Rangitawa Stream, (N143/958627), a small tributary of the Rangitikei River.
It has not been recognised anywhere else in the basin. The member is
unconformably overlain by conglomerates of the Haweran Series and the age
of the pumice of 0.38 ± 0.04 m.y.B.P. gives a maximum age for the beginning of
this series.

Rates of sediment accumulation

The sedimentary sequence is thickest in the Rangitikei River section and thinnest along the present Wanganui coast. The time represented by the Okehuan Stage is 0.61m.y. At the Rangitikei the thickness of this stage is 800m indicating a sedimentation rate of 1.31m/ky. At the present coast the maximum thickness is 117m, indicating a rate of sedimentation of 0.19m/ky. (Thicknesses based on Te Punga (1953) and Fleming (1953)).

In the Rangitikei Valley the thickness from the Pakihikura Pumice to the Ohingaiti Ash is 743m with an age span of 0.44m.y., indicating a rate of sediment accumulation of 1.69m/ky. Assuming the same rate for the lowest 90m of the Nukumaruan, and for the Hautawan, ages of 1.55 and 1.87m.y.B.P. are obtained respectively for the beginning of these stages (thicknesses based on Superior, 1943). The age on the base of the Pleistocene (i.e. base of Hautawan) is in good agreement with the age near 1.79m.y. from palaeomagnetic stratigraphy in the Wairarapa (Kennett et al, 1971), and with the estimated age of the base of the Calabrian in Southern Italy (Selli, 1967).

Ages of Pleistocene time-stratigraphic units in the Wanganui Basin

The ages of the boundaries of time stratigraphic units are summarised as follows:

	m.y.B.P.
Hawera Series	< 0.38
Castlecliffian Stage	0.45
Okehuan Stage	1.06
Nukumaruan Stage	1.55
Hautawan Stage	1.87

Correlation of Cape Kidnappers Section, Hawke's Bay

The section on the south side of Hawke Bay, westward from Cape Kidnappers (Fig. 14) is well exposed and contains many tephra beds. Fleming (1957) suggested that the Maraetotara Sand which unconformably
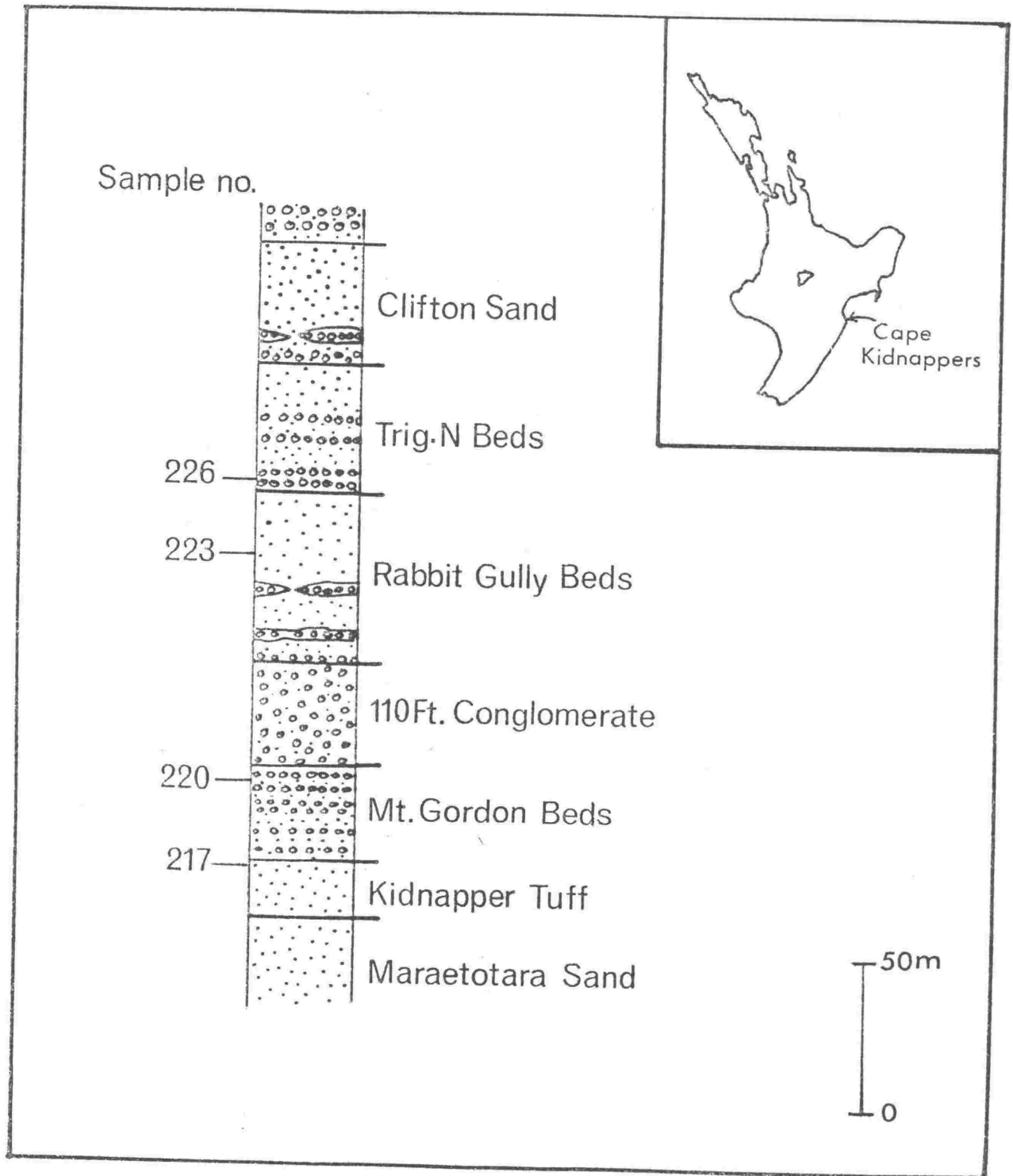
Fig. 14: Stratigraphic sequence of Pleistocene sediments at Cape Kidnappers (after Kingma, 1971).

overlies Waitotaran strata, is young Castlecliffian i.e. from this thesis less than 0.45m.y.B.P.

Four fission-track dates from glasses in this section have been determined, (Table 13). The upper beds of the basal tephra (Sample 217) contains biotite and this fact, together with the age of 0.85 ± 0.10m.y B.P. identifies it with the upper tephra of the Mangapipi Ash Member of the Makirikiri Tuff Formation.

Thus the fission-track dates indicate an Okehuan age for the section from Maraetotara Sands to the top of the Mt Gordon Beds where an age of 0.47 ± 0.09m.y. was determined, (sample 220). Although this date is within the error limits of the Waiomio Shell Bed and the Waitapu Shell Conglomerate it does not contain biotite as part of its ferromagnesian mineral assemblage as do these two horisons in the Wanganui Basin.

The younger ages determined for the Cape Kidnappers section are 0.36 ± 0.08 and 0.32 ± 0.07m.y.B.P.

To identify and correlate the individual tephra layers more work must be carried out using ferromagnesian mineral assemblages and other identifying properties together with the fission-track dates.

Correlation of tephras in deep-sea sediments

Ninkovich (1968) determined ages of rhyolitic tephra in deep-sea cores from the Pacific Ocean 1000km to the east of New Zealand. It is supposed that the tephras originated from the central volcanic district of New Zealand. Ninkovich estimated the ages of the tephras by interpolation between dated palaeomagnetic reversals, and between the Matuyama-Bruhnes reversal and the core tops, assuming a constant sedimentation rate in the intervals. Ninkovich's published ages, and additional ages not yet published (pers. comm. to B. P. Kohn, 1973) are compared with the tephra dates from the Wanganui Basin in table 14.

Sample Number	Horizon	Etch time (secs)	Spontaneous tracks		Induced tracks		Thermal neutron dose $(\times 10^{14} n, cm^{-2})$	Age m.y. B.P.
			counted	cm^{-2}	counted	cm^{-2} $(-\rho_a cm^{-2})$		
226	Second tephra in the Trig N Beds	8	24	41	1482	18483	23.16	0.32 ±0.07
223	20m below the top of Rabbit Gully Beds	13	22	55	1739	21683	23.16	0.36 ±0.08
220	Top tephra in the Mt Gordon Beds	13	27	104	2543	31683	23.16	0.47 ±0.09
217	Uppermost tephra in the Kid-napper Tuff	10	71	168	2285	28391	23.16	0.85 ±0.10
$\lambda_f = 6.85 \times 10^{-17} y^{-1}$								

Table 13: Fission-track dates on the tephra at Cape Kidnappers, Hawke's Bay.

Wanganui Basin	Age m.y.B.P.	Deep-sea cores (Ninkovich, 1968, and pers. comm. to Kohn, 1973)	
		core RC9-113	core RC12-215
Upper Finnis Rd	0.28	0.27	0.27 0.29
Lower Finnis Rd	0.32 ←	→ 0.31	0.32
Rangitawa Pumice	0.38		
Waiomio Shell Bed	0.45		
Waitapu Shell Conglomerate	0.52		
Kaukatea Ash	0.57		
Potaka Pumice	0.61 ←	→ 0.67	0.64
Rewa Pumice	0.74	0.73	0.77
Mangapipi Ash	0.88 ←	→ 0.86	0.87
Ridge Ash	1.04		
Pakihikura Pumice	1.06 ←		→ 1.07
Mangahou Ash	1.26 ←		→ 1.13

Table 14. Tentative correlation of Wanganui Basin tephras with deep-sea tephras. (All ages in m.y.B.P.).

The deep-sea tephra dated by Ninkovich at 0.86m.y.B.P. contains biotite, like the upper unit of the Kidnapper Tuff and the Mangapipi Ash.

Kohn (1973) correlates the Lower Ahuroa Ignimbrite with the tephra dated at 0.64 and 0.67m.y.B.P. in the deep-sea cores. As is discussed below, the Lower Ahuroa Ignimbrite is most likely the correlative of the Potaka Pumice, thus the Potaka Pumice is correlated with the 0.64 and 0.67 m.y.B.P. deep-sea tephra.

The horizon dated at 0.31m.y.B.P. by Ninkovich has been identified as the distal ash of the Whakamaru Ignimbrite (Kohn, 1973). This contains hypersthene, hornblende to a lesser extent and a small percentage of biotite. The same mafic mineral assemblage is found in the lower ash on Finnis Road (N144/253585) dated at 0.32 ± 0.07m.y.B.P.

Source ignimbrites of tephras from the Wanganui Basin

Ignimbrites are correlated with the Wanganui Basin tephras on the basis of fission-track dates, their ferromagnesian mineral assemblages, and in some cases magnetite trace element compositions.

The oldest tephra in the Wanganui Basin is the Ohingaiti Ash dated at 1.50m.y.B.P. Kohn (1973) dated the Tridymite Rhyolite from Coromandel at 1.50m.y.B.P. and the two are correlated because of their comparable age and the lack of other ignimbrites or distal tephras of similar age.

The Mangahou Ash (1.26m.y.B.P.), the Pakihikura Pumice (1.06m.y.B.P.) and the Ridge Ash (1.04m.y.B.P.) are most likely correlatives of ignimbrites in the King Country, such as the older members of the Pakamaunau Group - the Rangitoto Ignimbrites, (not dated by Kohn (1973)). These include the Pumice Lapilli Ignimbrite, Ngaroma Lenticulite, and the Crystal Lithic Lapilli Ignimbrite, (Blank, 1965), which all have reversed polarities, determined during this study, (Table 15) and are consequently older than 0.69m.y.B.P. Furthermore, they are overlain by the Ongatiti Ignimbrite which is also

King Country Ignimbrite	Declination	Inclination	Intensity (emu.co)
Ongatiti Ignimbrite	164.82	79.67	0.147×10^{-3}
Pumice Lapilli Ignimbrite	208.66	45.89	0.401×10^{-3}
Ngaroma Lenticulite	184.67	56.79	0.146×10^{-3}
Crystal Lithic Lapilli Ignimbrite	163.48	81.17	0.410×10^{-3}

Table 15. Palaeomagnetic determinations on cores from King Country Ignimbrites. Positive inclination indicates reversed polarity.

reversed (Table 15), and dated by Kohn (1973) at 0.75m.y.B.P. As the Rangitoto Ignimbrites are the oldest known in the central volcanic district, they are likely to be correlatives of the first major tephra influx into the Wanganui Basin, (Table 16).

The Mangapipi Ash Member, 22m thick in the Rangitikei Valley is considered to represent several eruptions. At least two different mineral assemblages occur in different horizons within it. One tephra in the lower part contains abundant lithic fragments, while another tephra in the upper part, dated at 0.88m.y.B.P. contains biotite and hypersthene. Kohn (1973) dated the Aongatete and Waiteariki Ignimbrites from Coromandel at 0.86 and 0.84m.y.B.P. respectively and showed from trace element analyses of their titanomagnetites that neither could be correlated with the 0.86m.y.B.P. tephra of Ninkovich (1968). Thus at least three ignimbrites are believed to have erupted at this time and the Mangapipi Ash may contain the distal deposits of them all.

The Rewa Pumice is dated at 0.74m.y.B.P. On the basis of trace element data from its titanomagnetite (Table 10) it cannot be correlated with any ignimbrite noted by Kohn (1973, p. 160). It may be the distal tephra of a pumice breccia that because of poor consolidation, has been completely eroded from the central North Island volcanic district, or may be buried.

A very pumiceous horizon (not dated), 20m beneath the Rewa Pumice in the Rangitikei sequence may be the equivalent of the Ongatiti Ignimbrite dated at 0.75m.y.B.P., (Kohn, 1973).

Abundance of hornblende and trace element composition of the titanomagnetite of the Lower Ahuroa Ignimbrite dated at 0.65m.y.B.P. (Kohn, 1973) are similar to those in the Potaka Pumice (Table 9).

The Kaukatea Ash (0.57m.y.B.P.) and the pumice of the Waitapu Shell Conglomerate and the Waiomio Shell Bed are possibly correlatives of some

Age m.y B.P.	Tephra or tephra bearing horizon	Mineral assemblage of tephra	Ignimbrite(s)	Age (Kohn, 1973) m.y.B.P.
0.28	Upper Finnis Rd tephra	3		
0.32	Lower Finnis Rd tephra	3	Whakamaru	0.33
0.38	Rangitawa Pumice	2	Atiamuri	> 0.33 < 0.58
0.45	Waiomio Shell Bed	3		
0.52	Waitapu Shell Conglomerate	3	Paeroa Range Group	> 0.33 ≤ 0.58
0.57	Kaukatea Ash	3		
0.61	Potaka Pumice	2	Lower Ahuroa	0.65
0.74	Rewa Pumice	2		
0.88	Mangapipi Ash	3 2	Unknown Waiteariki Aongatete	0.84 0.86
1.04	Ridge Ash	2		
1.06	Pakihikura Pumice	2	Rangitoto (R)	> 0.75
1.26	Mangahou Ash	2		
1.50	Ohingaiti Ash	1	Tridymite Rhyolite	1.50

Table 16: Tentative correlation of Wanganui Basin horizons with ignimbrites of North Island.

(R) signifies reversed magnetic polarity determined during this study.

+ Ferromagnesian assemblage

1 = hypersthene

2 = hypersthene + hornblende

3 = hypersthene + hornblende + biotite

of the Paeroa Range Group Ignimbrites (Martin, 1961). Kohn (1973) dated
the oldest of this Group, the Te Kopia Ignimbrite at 0.58m.y.B.P. but this
has a different titanomagnetite chemistry to the Kaukatea Ash (Table 9).
The Waitapu Shell Conglomerate pumice has a mafic mineral content of 85%
biotite similar to the ignimbrite capping the highest part of the scarp at
the type section of the Paeroa Range Group, (Martin, 1961). As the Waiomio
Shell Bed also contains abundant biotite, and all the ages on these deposits
fall within the range estimated by Kohn (1973) for these ignimbrites (0.33
to 0.58m.y.B.P.) they are considered to be correlatives. The tentative
correlation of the Waitapu Shell Conglomerate with the topmost Paeroa
Ignimbrite suggests an age of 0.48m.y.B.P. for the latter.

The Rangitawa Pumice, 0.38m.y.B.P., contains hypersthene, hornblende,
and augite but not biotite. It may be the equivalent of the Atiamuri
Ignimbrite which is not dated but is considered by Kohn (1973) to be
younger than the Paeroa Ignimbrite. The Waiotapu, Whakamaru, Te Whaiti
and Rangitaiki Ignimbrites can be discounted as correlatives as they all
contain biotite.

In the lower tephra at Finnis Road (0.32m.y.B.P.) hypersthene is the
dominant ferromagnesian mineral with biotite and hornblende subordinate, as
in the Whakamaru Ignimbrite (0.33m.y.B.P., Kohn, 1973).

In the upper tephra at Finnis Road, about 8g D.S. 50m above the lower, biotite is
the dominant mafic. The age determined on this unit is 0.28m.y.B.P.
As yet no correlative of this is known.

PART II

DETAILED SEDIMENTOLOGY OF SOME LOWER OKEHUAN SEDIMENTS

CHAPTER 1

GENERAL INTRODUCTION

The purpose of this study was to interpret sediment source, mode and direction of sediment transport, mode of deposition and post depositional changes within a portion of the Quaternary sediments of the Wanganui Basin.

A sequence of sediments was required that could be traced across the entire basin and that was defined at top and bottom by reliable time planes. The sequence chosen comprises the five formations of the lower Okehuan Stage that were defined by Fleming (1953) at the west side of the basin as the Makirikiri Tuff, Lower Okehu Siltstone, Okehu Shell Grit, Upper Okehu Siltstone and the Kaimatira Pumice Sand Formations. The lower four comprise the Okehu Group, while the fifth is the lowest formation of the Kai-iwi Group. The two volcaniclastic formations afforded the required time planes (Fig. 15).

Previous Work

Of the many geological reports on the Wanganui Basin those most pertinent to the present study are the unpublished report by the Superior Oil Company (referenced in the text as Superior, 1943), unpublished theses by Rich (1959) and Piyasin (1966) and publications by Fleming (1953) and Te Punga (1953). The only mapping extending across the entire basin is that of Superior. Maps of the other authors cover smaller areas within the basin (Fig. 16).

Nomenclature and correlation of the formations

The lithostratigraphic nomenclature of Fleming (1953) has been extended across the Wanganui Basin, corresponding units being synonimised. Correlation of the volcaniclastic formations has been discussed in Part I, and the main conclusions are briefly reviewed: the Makirikiri Tuff and its westward equivalent the Butlers Shell Conglomerate include the Basal Ash of Superior (1943) and the Pakihikura Pumice of Te Punga (1953), the
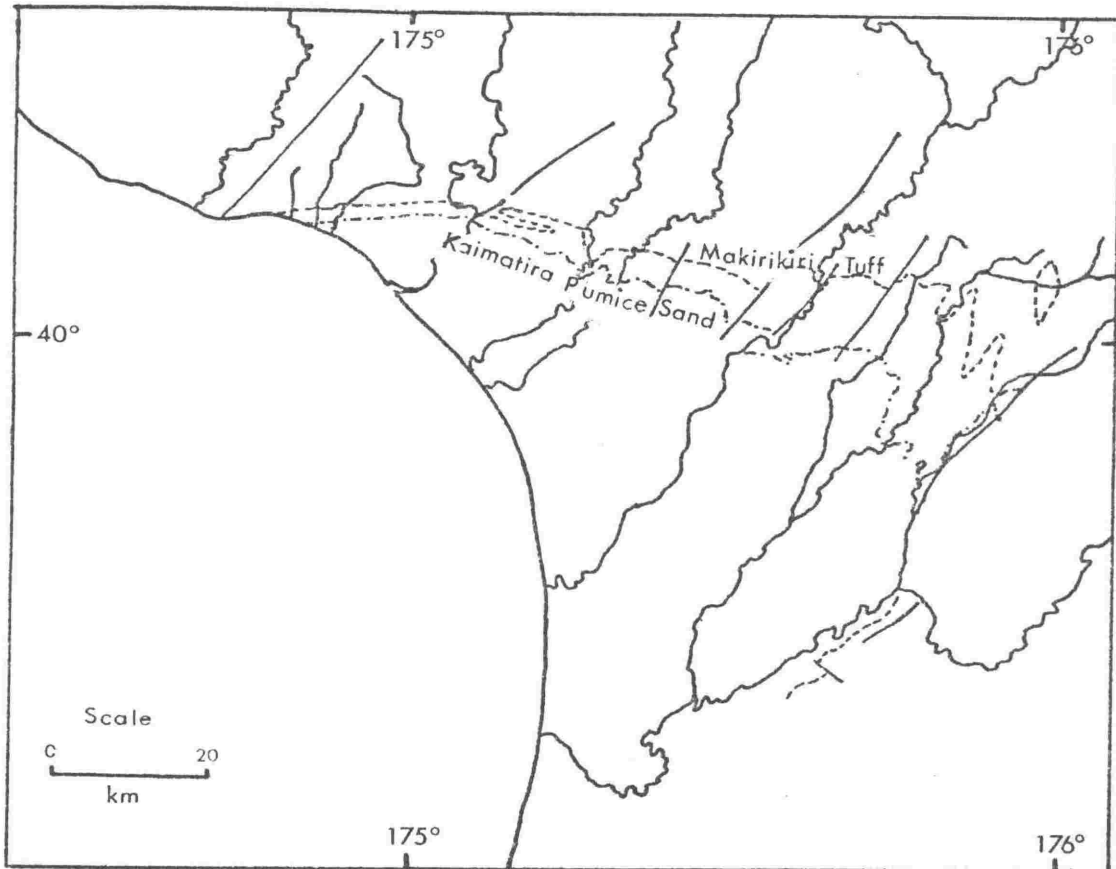
Fig. 15: Map tracing the outcrop of the Makirikiri Tuff and Kaimatira Pumice Sand Formations. Plain lines are faults.
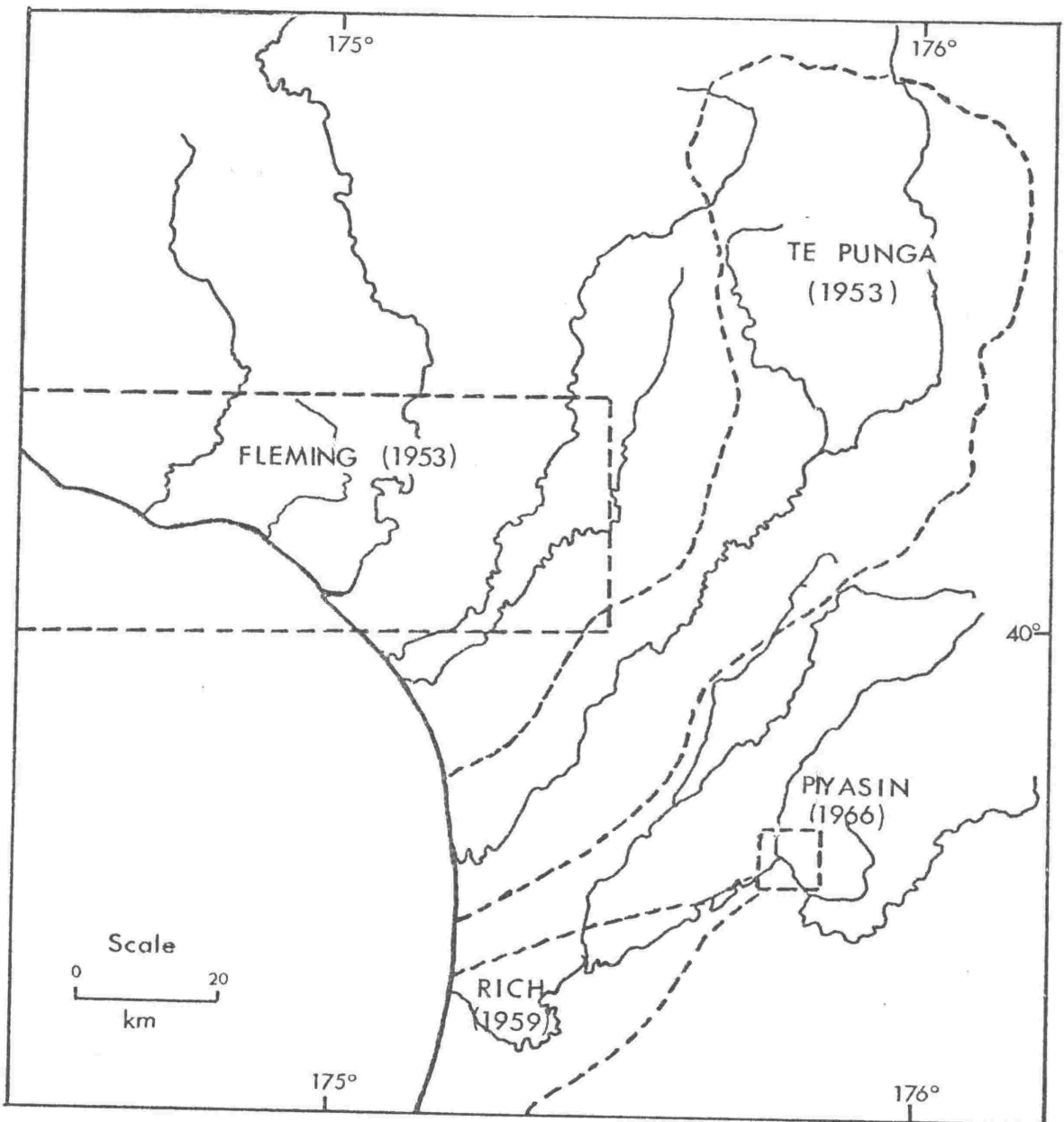
Fig. 16: Map showing the areas covered by geologists (other than
          Superior (1943)) whose literature is pertinent to the
          present study.

lower part of the Mangatarata Formation of Piyasin (1966) and the lower
Tua Paka Formation of Rich (1959). The Kaimatira Pumice Sand is equivalent
to the Coutts Creek Horizon (Superior), west of the Rangitikei; east of
the Rangitikei it includes the Kimbolton Ash (Superior) and also the
Potaka Pumice (Te Punga) everywhere except on the ridge just west of the
village of Pohangina. The upper Tua Paka of Rich is not the equivalent
of the Kaimatira Pumice Sand,being much younger.

Between the two volcaniclastic formations Fleming mapped the Okehu
Siltstone Formation in the east of the Subdivision and the Lower Okehu
Siltstone, Okehu Shell Grit and the Upper Okehu Siltstone Formations at
the coast. The Okehu Siltstone becomes sandier in the region of the
Pohangina River. It is readily distinguished from the bounding formations,
being composed of grey thin-bedded monotonous sandy silt without any
volcanic detritus.

General palaeogeographic results from earlier studies

Superior (1943) suggested that these Okehuan sediments were the first
of a phase of more rapid infilling of the basin with a series of dominantly
non-marine and estuarine sediments.

Fleming (1953) concluded that the Butlers Shell Conglomerate was
deposited unconformably on Nukumaruan sediments as sandy shell banks of
the intertidal zone that interfingered with intertidal silts. He
recognised the volcanic detritus in the formation and correlated it with
the Makirikiri Tuff. The latter formation contains little faunal evidence
of marine conditions and he considered it to be a delta of pumiceous
alluvium. Carbonaceous layers in the Makirikiri Tuff were attributed by
Fleming to nearby vegetation but the writer here considers that they may
represent material charred during eruptions and brought down from the
central volcanic region.

At the coast, Fleming recognised an erosion interval between the Butlers Shell Conglomerate and the Lower Okehu Siltstone, and another between the Okehu Shell Grit and the Upper Okehu Siltstone. These intervals are not evident towards the east. He considered that the deposition of each siltstone formation was initiated by a marine trans- gression, with the silts themselves being deposited offshore. East of the Whangaehu River, the siltstones are practically barren of fossils and Fleming made no attempt at interpreting the palaeogeography.

He considered the Okehu Shell Grit to have been deposited in an intertidal and subtidal environment on the wave planed sediments of the Lower Okehu Siltstone.

The Kaimatira Pumice Sand, he suggested, was deposited in various sub-environments of the shallow water zone with sediment supplied from the central North Island volcanic region. He suggested that facies lacking fossils might be due either to very high sediment accumulation rates or to low salinities. In the present study sedimentary structures are described which tend to confirm a rapid rate of sediment accumulation. Penecontempor- aneous deformation structures, formed where sediment was accumulating very rapidly, were also noted by Fleming and are described in detail in the present study.

Te Punga (1953) recognised that sedimentation was continuous in the Rangitikei Valley area. He suggested that the two volcaniclastic units were deposited in very shallow waters and the intervening siltstone was deposited offshore at depths greater than five fathoms. Fossil assemblages at certain horizons in the Makirikiri Tuff he considered typical of intertidal estuarine conditions, e.g. the Mangapipi Fossil Beds, whereas those at certain horizons in the Kaimatira Pumice Sand he considered to be typical of open coastal beach, e.g. a shell horizon 13m below the Potaka Pumice.

Rich (1959) correlated the lower portion of the Tua Paka Formation with the Makirikiri Tuff Formation; no evidence has been found in the

present study to dispute this even though the upper portion to the east
of Tua Paka Farm is now known not to be the equivalent of the Kaimatira
Pumice Sand (fission-track date, Part I). Rich suggested that the sediments
were deposited in environments varying from shallow marine through
estuarine or littoral, to fresh water. His conclusions were based on faunal
evidence and on interpretation of sedimentary structures such as ripple
marks and intraformational conglomerates.

On the basis of faunal evidence Piyasin (1966) considered the
sediments of the Mangatarata Formation to have been deposited in the
littoral zone.

Extent of field work

Field work was carried out mostly during the summers 1970-71 and 1971-72.
Stratigraphic sections were examined and measured in the river valleys and
along road sections paralleling the rivers. Exposures are infrequent on
the interfluves but those that exist were examined. Appendix 2 contains
detailed descriptions of the sections and Appendix 3 gives localities.

General results regarding stratigraphy

Stratigraphic columns are presented in figure 17 (fold out, back
pocket). The most striking feature they show is the variation in sediment
thickness, with a minimum of approximately 60m along the present Wanganui
coast and a maximum of 500m in the region of the Rangitikei River.
Correlations of horizons between columns are based on fission-track dates
and the petrography of the tephra units. The percentages of volcanic
detritus marked at the sides of the columns are based on field estimates
and clearly distinguish the three primary formations. Sequences within
each section are referred to in more detail later.

The area of minimum sediment accumulation was along the Wanganui
coast where erosional breaks are recognised between the formations. The

area of maximum accumulation was in the centre of the basin where no major breaks were recorded. As all the sediments were deposited in shallow marine to estuarine environments the centre of the basin must have been subsiding continuously during deposition of the sequence examined.

CHAPTER 2

SEDIMENTARY STRUCTURES

Sedimentary structures or associations of structures can be used to interpret depositional and post-depositional processes. In the present study area diverse structures abound in the volcaniclastic and shell conglomerate formations but only plane parallel lamination occurs in the Okehu Siltstone Formation.

Most of the structures in the volcaniclastic formations are comparable to those found by other authors in shallow water marine to intertidal deposits. Structures in the extreme eastern fringe of the basin are more suggestive of fluvial deposition. These conclusions are in agreement with the palaeontological evidence of Superior (1943), Fleming (1953) and Te Punga (1953).

Another conclusion obtained from the sedimentary structures is the very high rate of sediment deposition by currents carrying volcanic detritus from the central volcanic region of North Island.

Primary structures

A) Cross-stratification

I) Small scale structures*

i) Ripple marks

In the Makirikiri Tuff and the Kaimatira Pumice Sand the ripples are composed of moderately sorted coarse silt to fine sand. Due to the unconsolidated nature of the sediment, bedding plane surfaces are seldom exposed. Thus the plan form of the ripple can be determined at very few sites only.

No ripple marks were recorded in the Okehu Siltstone Formation; nor do they occur in the Makirikiri Tuff Formation in the northeast of the area where these sediments tend to be coarser and are more poorly sorted.

* Based on the classification of Allen (1968).

At localities where rippled surfaces were exposed at least three measurements were made of each of the following parameters: amplitude, height and ripple symmetry; averages were then computed (Table 17). Ripple index (Tanner, 1967) was computed and plotted against ripple symmetry index (Fig. 18). The ripple symmetry is high (RSI approaches 1.0) and the data all plot in the area delineated by Tanner (1967) as ripples produced by wave action.

From the relationship of Tanner (1959), wavelength against water depth, one can conclude that the ripples in the Wanganui basin were formed in water depths less than 12metres. A few horizons (site nos. 97 and 192) have ripples with a ripple index less than 5 which Tanner (1959) suggests were formed at depths less than 300mm.

Rhomboid ripples were noted at one locality only (Loc. 37, N139/302837). Hoyt and Henry (1963), in reviewing the form and origin of these structures, suggested that they are a valuable indicator of a littoral environment. They also suggested that the angle of slope of the beach where rhomboid ripples form is related to the grain size of the sediment. Thus at locality 37 where the ripples are formed of fine sand, the angle of slope of the beach was between 2° and 5°. Shepard (1963) also concluded that the average slope of a beach face in this grade material is 3°.

ii) Ripple-drift cross-lamination

This form of small scale bedding occurs very frequently, in fine to medium sand grades of the more tuffaceous parts of the volcaniclastic formations, particularly the Kaimatira Pumice Sand.

Types A, B and C of Jopling and Walker (1968) were all recognised. Most cosets of ripple-drift cross-lamination are continuous over the length of each exposure (up to 200m). Frequently this type of bedding shows

Site No.	Length mms (s)	Height mms (h)	RI s/h	a	b	RSI a/b
7	123	21	5.9	82	62	1.50
8	63	11	5.7	34	29	1.17
37	113	21	5.4	71	42	1.69
	151	15	10.1	81	70	1.16
	135	12	11.3	80	55	1.45
	163	22	7.4	91	72	1.26
52	305	36	8.5	161	145	1.11
	121	21	5.8	61	60	1.02
57	121	20	6.1	63	58	1.09
64	163	30	5.4	90	73	1.23
65	151	29	5.2	76	75	1.01
	170	19	8.9	85	85	1.00
67	105	18	5.8	55	50	1.10
71	110	20	5.5	55	55	1.00
	135	27	5.0	71	66	1.08
	102	19	5.4	53	49	1.08
83	76	14	5.4	40	36	1.11
93	131	15	8.7	76	55	1.38
97	131	19	6.9	76	55	1.38
	93	21	4.4	52	41	1.27
	103	19	5.4	63	40	1.58
122	131	15	8.7	77	54	1.43
	196	25	7.8	116	81	1.43
	129	21	6.1	75	64	1.17
	126	24	5.3	73	53	1.38
133	137	23	6.0	70	67	1.04
145	158	24	6.6	81	77	1.05
148	134	22	6.1	69	65	1.06
149	112	21	5.3	57	55	1.04
157	41	5	8.2	21	20	1.05
	52	7	7.4	27	25	1.08
191	98	18	5.4	50	48	1.04
	109	15	7.3	55	54	1.02
192	112	31	3.6	58	54	1.07
	124	33	3.8	64	58	1.10
	123	26	4.7	63	58	1.09
193	124	21	5.9	63	59	1.07

Table 17: Ripple mark parameters. Each value is an average of N va
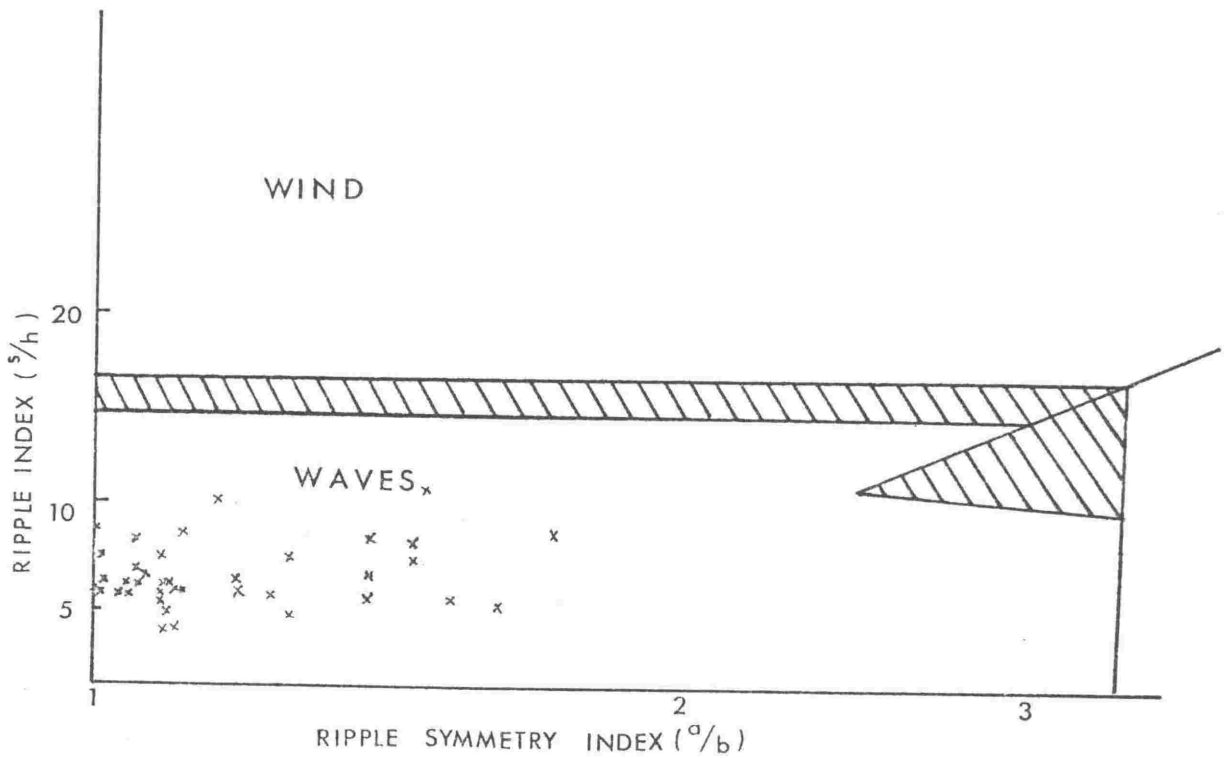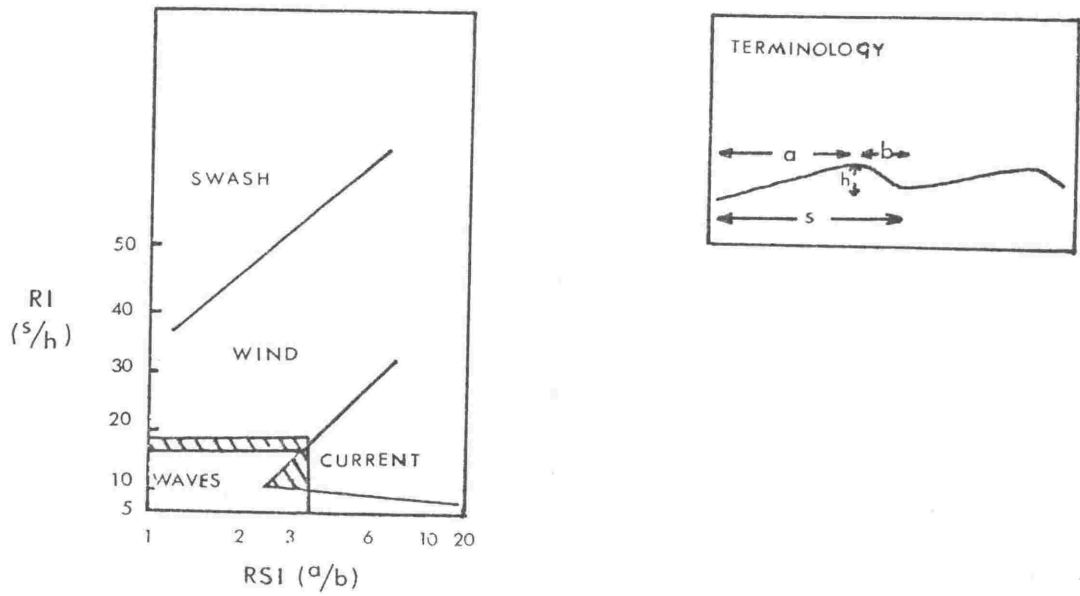
Fig. 18: Plot of ripple index (s/h) against ripple symmetry (a/b).
Terminology is explained in the upper right inset;
classification of Tanner (1967) is shown in the upper
left inset.

bipolarity of current direction, i.e. the foresets dip in opposing directions, suggesting that they were formed by ebb and flow of tidal currents (Reineck, 1963).

The formation of ripple-drift cross-lamination requires excess sediment supply from above (McKee 1965, Sanders 1963, Jopling and Walker, 1968).

The most common form of ripple-drift cross-lamination in the Wanganui Basin is type A (Fig. 19), which Jopling and Walker (loc. cit.) suggested is formed when the ratio of suspended to traction load is relatively low, i.e. deposition is dominantly from traction.

Figure 20 illustrates type B, which Jopling and Walker suggested are formed when the ratio of suspension to traction load is high enough to preserve the stoss side.

As the ripple-drift cross-lamination in the Wanganui Basin sediments is always associated with the more tuffaceous volcaniclastic material, it is proposed that they were formed by sediment carried to the sea by flood waters from the central volcanic region of North Island following volcanic activity (J. W. Cole, pers. comm.). Rapid erosion and runoff is to be expected because the source area would have been depleted in vegetation as observed in recent nuees ardentes eruptions e.g. that of Mt Lamington, Papua (Taylor, 1958). It should be emphasised that the eruptions represented in the sediments here are probably of a much greater magnitude than any that have been recorded in historic times. Lignite lenses of charred vegetation at the bases of highly volcaniclastic layers give direct evidence of the burning of vegetation in the source areas.

Commonly associated with the ripple-drift cross-lamination are wavy beds, (Reineck and Wunderlich, 1968), (Fig. 21). They are often associated with cyclic sequences (Fig. 22); the thickness of each cycle varies from 60mm to 200mm with a mode around 110mm (Fig. 23) and the
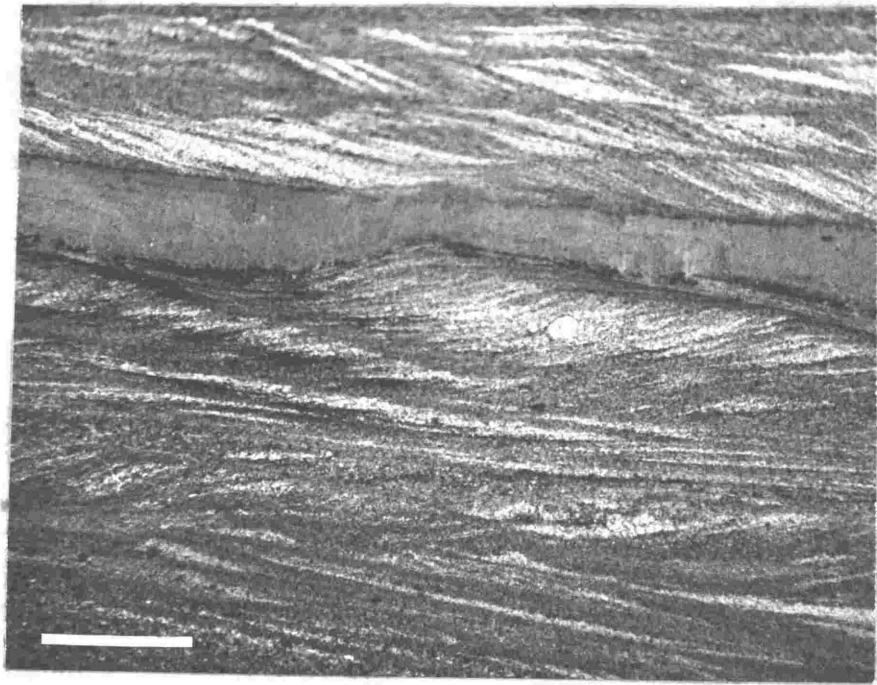
Fig. 19: Type A ripple-drift cross-stratification, (Jopling and Walker, 1968). Bar scale 30mm.
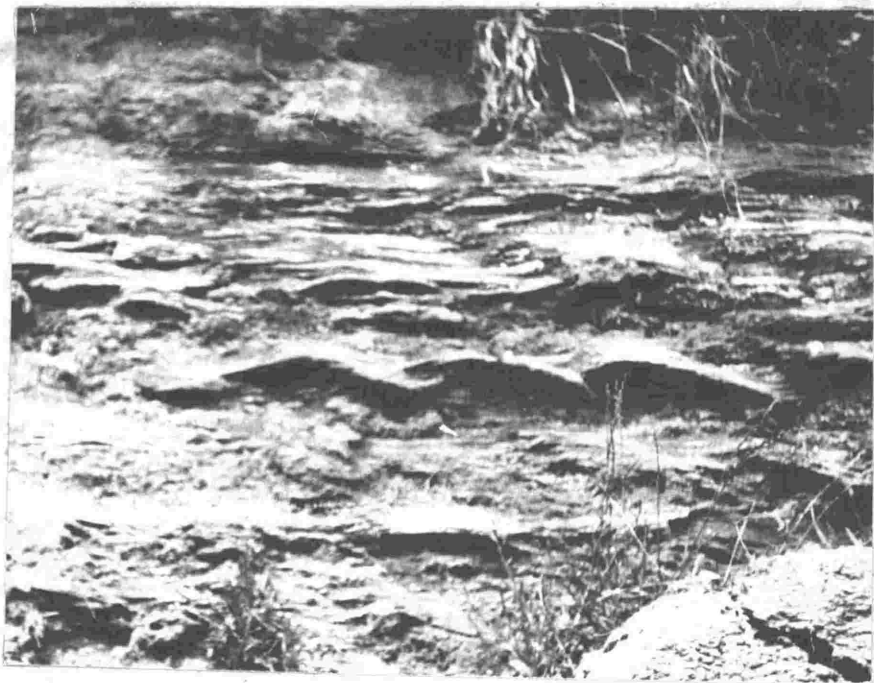
Fig. 20: Type B ripple-drift cross-stratification, (Jopling and Walker, 1968).
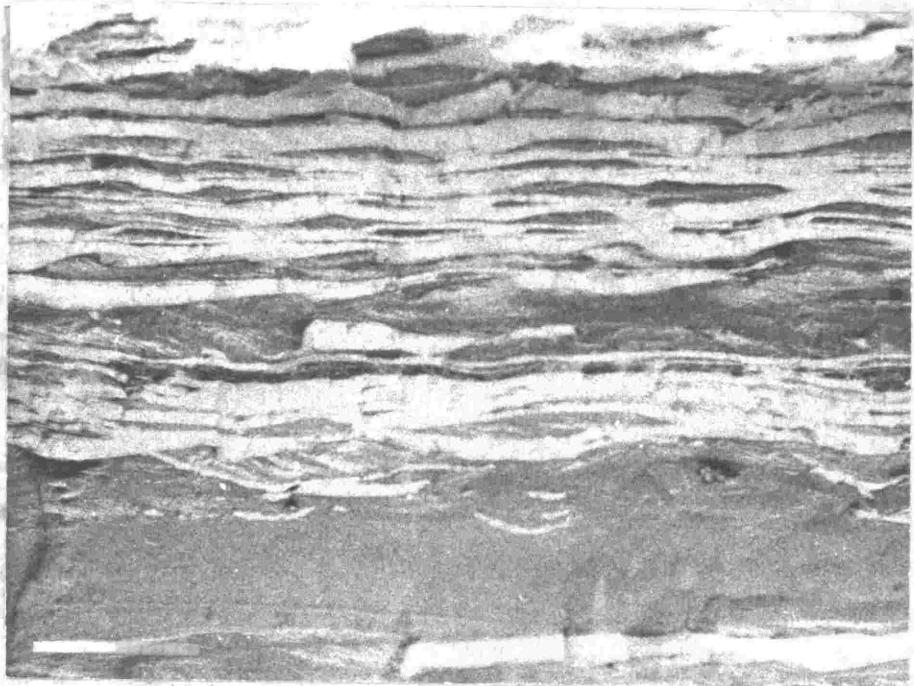
Fig. 21: Wavy and flaser bedding in the Kaimatira Pumice
          Sand. Bar scale 100mm.

one
cycle
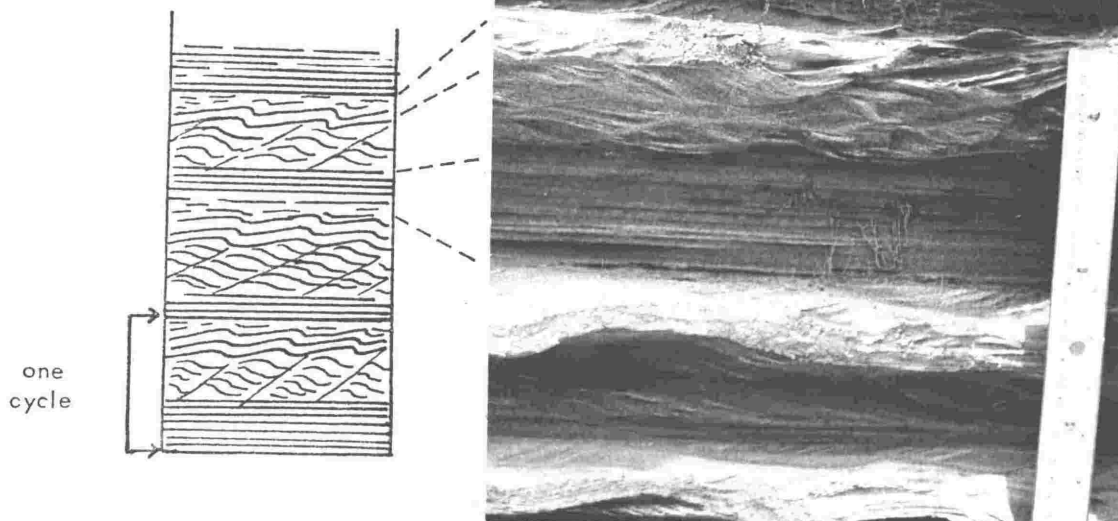
Fig. 22:   Details of cycles with structures showing some similarities
to Bouma units B, C and D of turbidity currents.
Ruler 300mm.
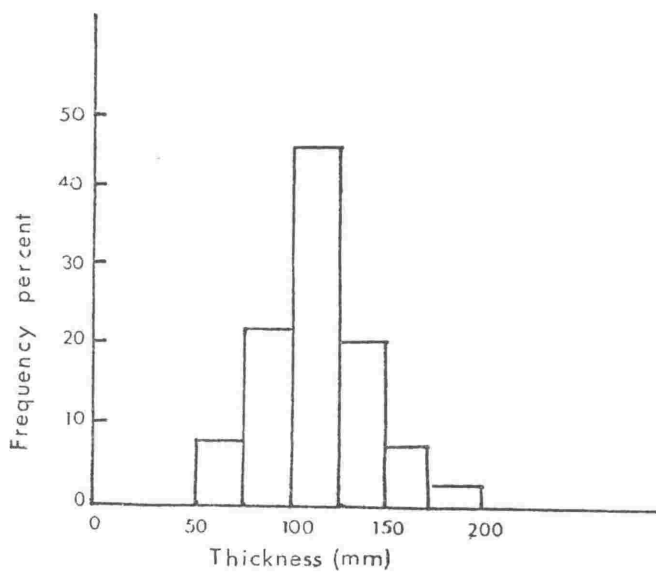
Fig. 23:   Frequency plot of thickness of cycles.

contact between the top of one cycle and the bottom of the next is always sharp. In each cycle grain size and sorting decrease upwards e.g. at locality 8(N138/623907) the base of a unit has mean grain size of 4.69 phi and a standard deviation of 1.13 and the upper portion has a mean grain size of 5.06 phi, and a standard deviation of 1.67. This variation in grain size parameters is typical of the cycles, though some of them are composed of coarser material.

Three major structures are associated with the cycles (Fig. 22); plane parallel lamination is generally present at the base of each cycle, ripple-drift cross-lamination type A in the middle sometimes grading up to type B, and wavy bedding in the upper part, which occasionally displays incipient plane parallel lamination in its upper portions.

The graded bedding and the units in these cycles are similar to the B, C and D units of turbidites (Bouma, 1962), and may represent a similar decrease in flow regime. As with turbidity currents no dune phase is present; the lower plane parallel lamination may represent the lower part of the upper flow regime, (Fig. 24). Jopling and Walker (1968) noted that type A ripple-drift is formed when traction plays a more dominant part than suspension in sediment transport. Thus any dunes that may have been formed would have been reworked as the traction load as flow decreased. As the finer material is dropped from suspension, type B ripple-drift cross-stratification sometimes formed.

The moderately sorted nature of the lower sequence showing plane parallel lamination suggests that the flow conditions changed more slowly than might be expected in a turbidity current; i.e. that the material was moved as a traction carpet for a sufficient time for the fines to be winnowed out.

The upwards decrease in grain size is explained by the fact that the coarser grains are dominantly transported as the traction load, with

water surface

Ripples
(a)

Plane bed
(d)

Dunes with ripples superposed
(b)

Antidunes
(e)

Dunes
(c)

Chutes and pools
(f)
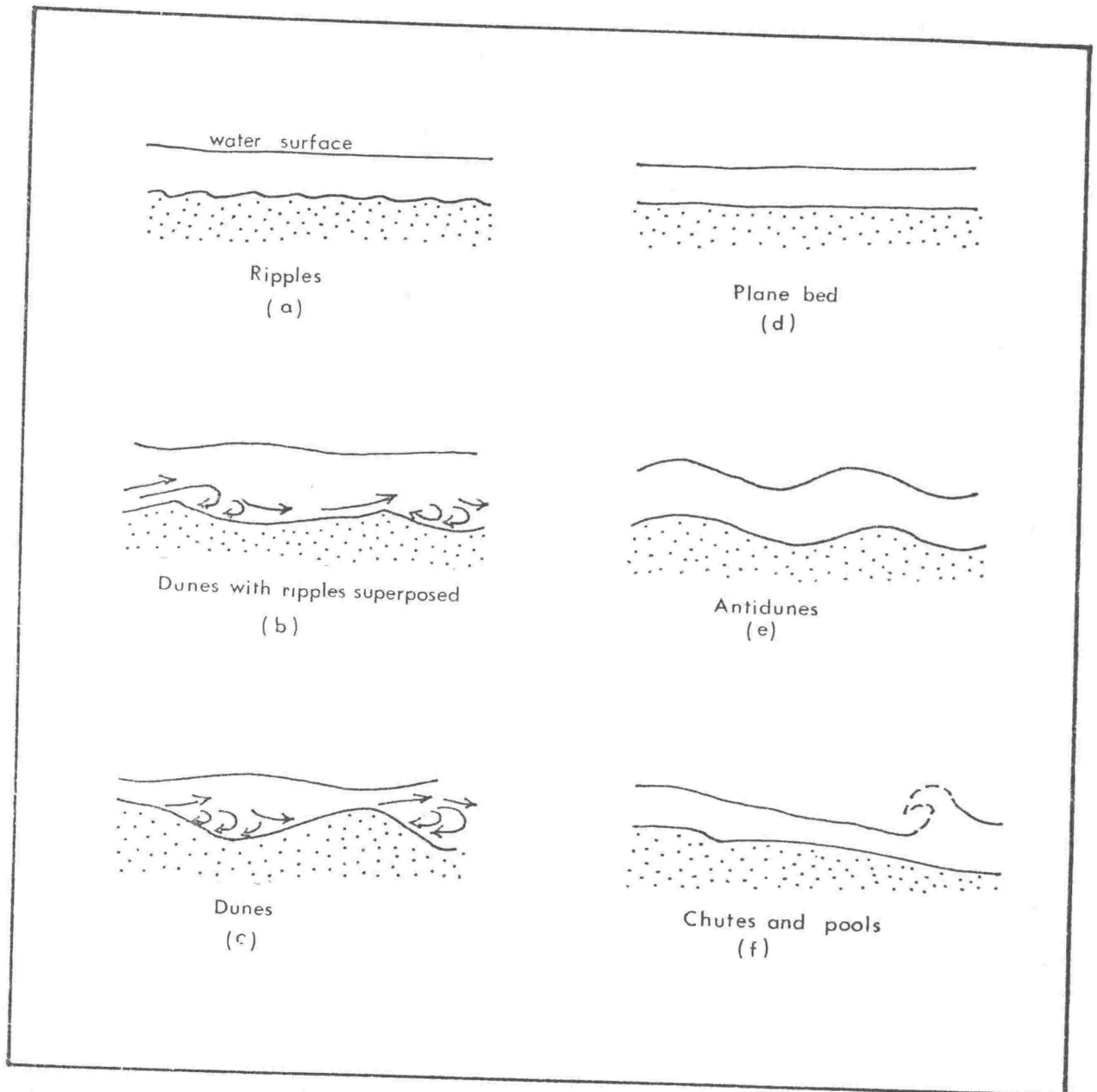
Fig. 24: Diagram to illustrate the concept of flow regime, (after
          Simons and Richardson, 1961). The sequence (a) to (f)
          represents the idealised sequence observed in flume
          studies as the stream power is increased. Forms (a) to
          (c) define the lower flow regime, and forms (d) to (f)
          the upper flow regime.

the finer grains remaining in suspension until the flow velocity decreased so that they too could become part of the traction load.

The cycles all occur in the more tuffaceous of the volcaniclastic sequences and in some of the tephra beds. In the latter, the contact between the cycles is not so sharp and the size grading not so strong; these are interpreted as representing oscillatory flow conditions within a current carrying only volcanic detritus that had been extremely recently erupted and may have been blanketing the central volcanic region.

In the general case, however, the type of sediment, flow conditions deduced above and the cyclic nature of the sediments suggest that each cycle was formed by sediment laden flood waters coming down from the volcanic region of central North Island. It is possible that each cycle represents one flood.

The association of relatively fine grained wavy beds and coarser grained beds with ripple-drift cross-lamination is common in sequences other than the cyclic type described above. The contacts between the drifted and the wavy material are always sharp and the two types of sediment do not appear to be genetically related. The sands contain the greater proportion of volcanic debris. The wavy beds represent the normal type of quiet sedimentation, while the ripple drifted sands were again introduced during floods.

iii) Flaser bedding

Flaser bedding (Fig. 25) defined as cross-stratification with intercalated flasers by Reineck and Wunderlich (1968) is very common in sequences west of the Oroua Valley. All types of flaser bedding were identified within the study area. Reineck (1960) interpreted silt flasers to represent rapid fluctuations in mode of sediment deposition with the

flasers formed during quiet periods. This interpretation is consistent in the present study but there are instances where flaser bedding is associated with horizons that progressively grade upwards from coarse sands to fine silts, a feature not dissimilar to the graded cyclic sequences described earlier. These silt flasers are often eroded by the overlying coarse sands (Fig. 26), such that each upwards graded unit is here interpreted as the deposit of one flood where the flasers represent the tail-end suspension deposit of a heavily laden current.

Most of the flaser bedding, however, is identical to that described by Reineck, who suggested that it is characteristic of tidal deposits. The bipolarity of the ripple-drift cross-lamination is also consistent with a tidal environment.

II) Large scale structures

Large scale cross-stratification is also confined to the volcaniclastic formations. They are best developed in the Makirikiri Tuff, where they are more common than their small scale counterparts. Several types, differentiated texturally and geometrically are described.

i) Structures in sand

a) The first group (Fig. 27) described are those formed in medium to coarse sands with more than 75% volcanic detritus. They are similar geometrically to a small scale kappa or lambda (Fig. 28) cross-stratification of Allen (1963) and they are tentatively considered to represent climbing dunes. Little reference is found in the literature to such structures but Blatt, Middleton and Murray (1972, p. 132) state that "Dunes may migrate up the backs of other dunes....". As the Wanganui Basin forms have such a high percentage of volcanic material they may have formed very rapidly in upper lower flow regime conditions with suspension
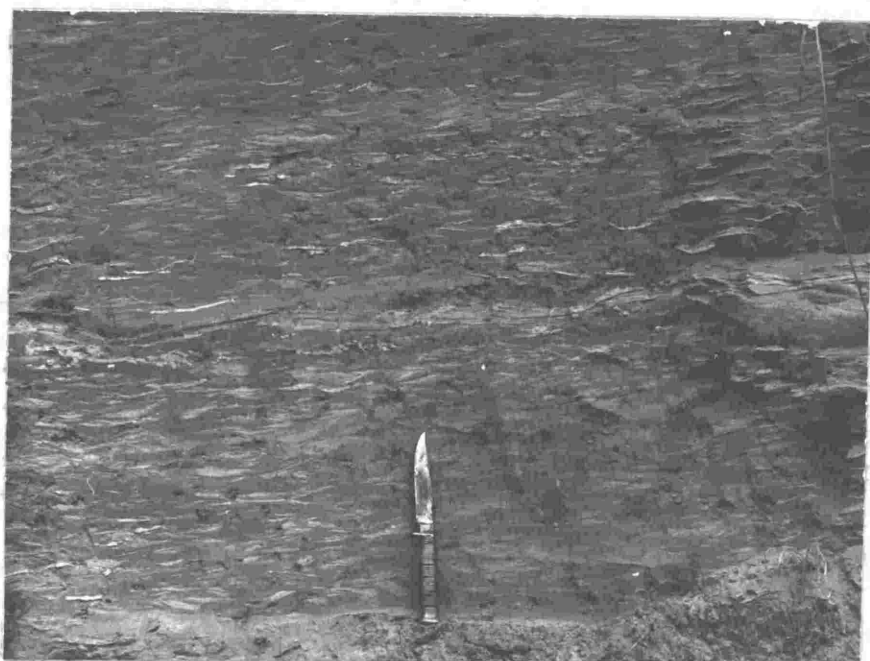
Fig. 25: Flaser bedding in the Kaimatira Pumice Sand. Knife is 240mm long.

Fig. 26: Graded bedding and erosion of silt flasers. Bar scale 50mm.
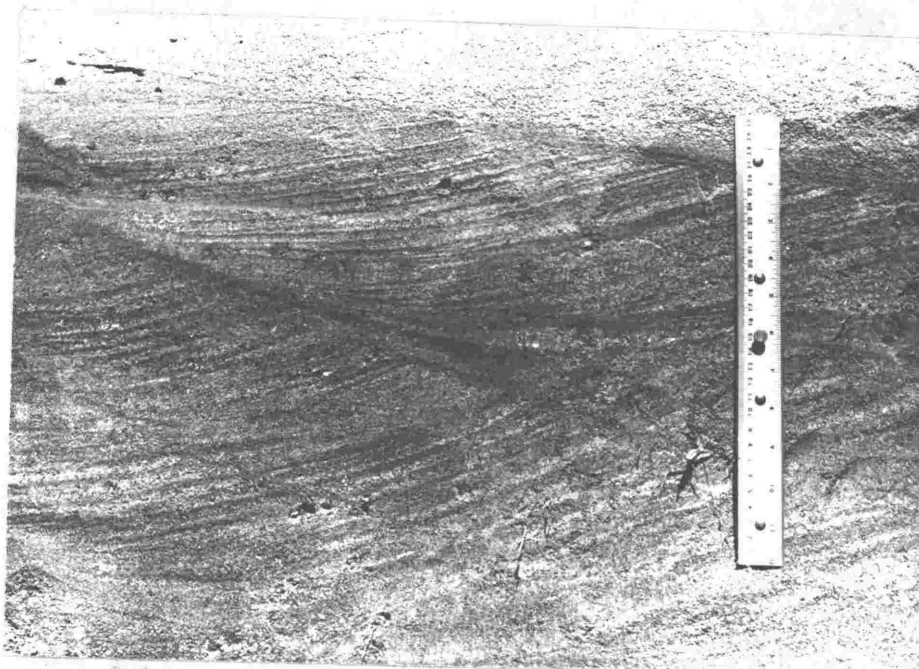
Fig. 27:   Large scale cross-stratification in medium to coarse
           sands. Ruler is 300mm long.
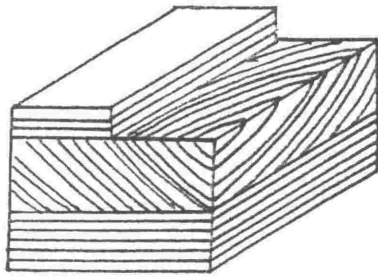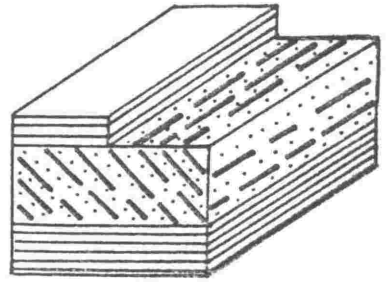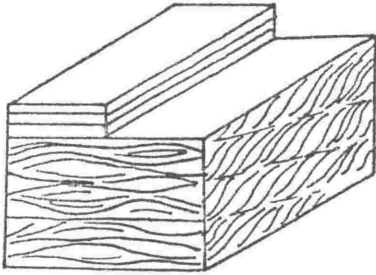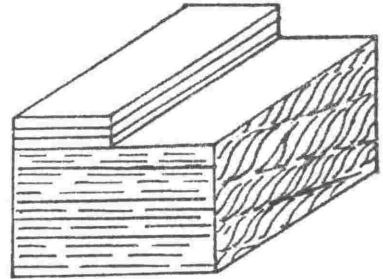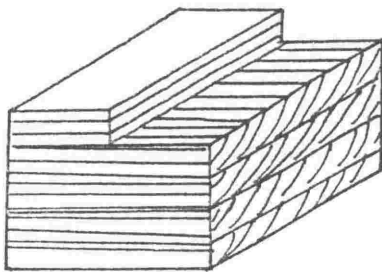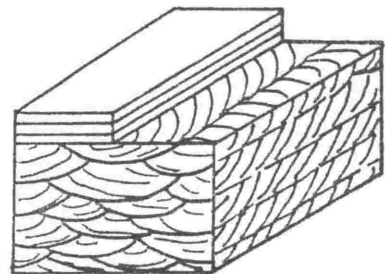
Fig. 28: Partial reproduction of classification of cross-stratification of bedding forms (Allen, 1963) described in the text.

to traction ratio fairly low, as stoss sides are seldom preserved. (As Type A ripple-drift cross-lamination).

Suitable conditions for the preservation of this structure exist in channels in tidal estuaries, tidal sand banks and the sandy floors of tide swept seas, (Allen, 1970).

b) The omikron and pi forms (Fig. 28) of Allen (1963) are also common in medium to coarse sand. These may represent migrating, not climbing dunes. The geometric form is similar to mega ripples or dunes of the North Sea (Reineck, 1963). The cross lamination is dominantly ebb orientated but always has a bimodal character. Reineck (1963) found that such mega ripples were confined to areas of higher current velocity and were moving parallel to the tidal currents, in depths less than 20 metres, in agreement with the depths of similar forms reported by Allen (1970, p. 176).

ii) Cross-stratification in pebbly or shelly sands and conglomerates

a) Low angle (dip less than 15°) planar cross-stratification is typically associated with alternating very thinly bedded shell conglomerates and silts. The shells are worn and often broken. The sets are 80-300mm thick and all have bimodal vectors, (Fig. 29). It is suggested that they were formed as offshore gravel banks within the reach of tidal influence. Such features are illustrated by Allen (1970) as parts of tidal current ridges.

b) Single sets with a set thickness 1.0-5.0 metres and a foreset dip averaging 20° (Fig. 30) are associated with the same lithology as the above. They occur in the Kaimatira Pumice Sand Formation only, in the region west of the Rangitikei River. At one locality (Loc. 8, N138/624907) the structures (Fig. 31) are well exposed and have an overall
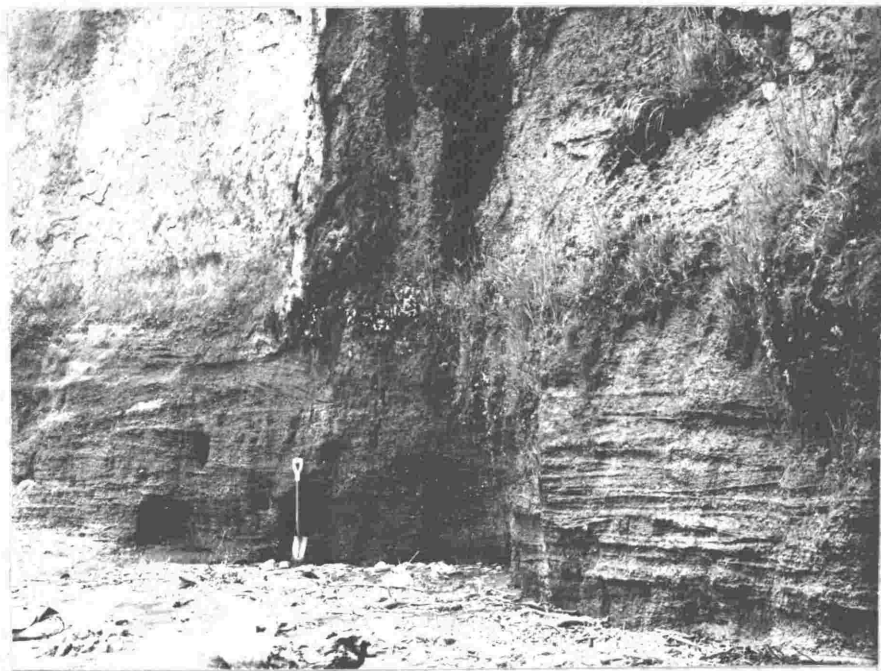
Fig. 29:   Large scale cross-stratification in the Okehu Shell Grit.
Spade one metre long.
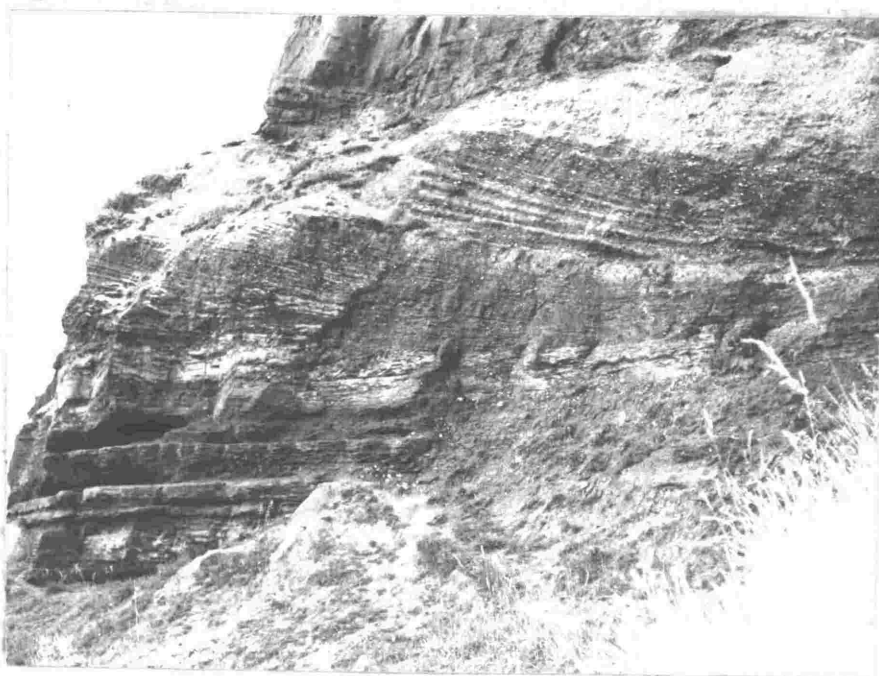
Fig. 30:   Large scale cross-stratification in the Kaimatira Pumice Sand.
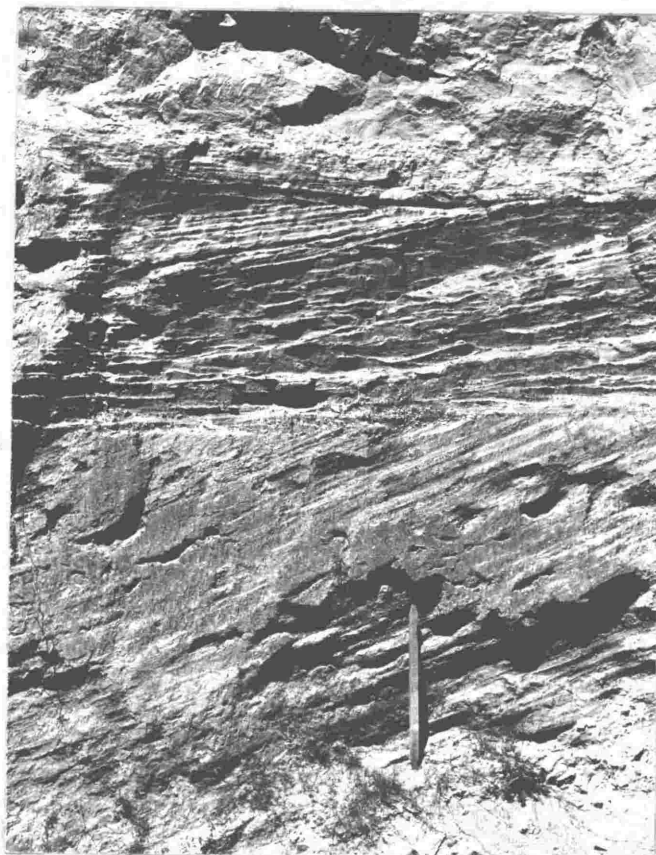
Fig. 31:   Large scale cross-stratification in the Kaimatira
           Pumice Sand Formation, (N138/624907). Post one
           metre high.

lensoid form with a unimodal dip direction. The forms approximate the epsilon and alpha (Fig. 28) cross-stratification of Allen (1963) but differ in their heterogeneous lithology and having an erosional contact. Allen (1963) suggested that the solitary units of homogeneous lithology represent banks in rivers, estuaries, beaches and in the shallows just off beaches. Such banks have also been described by Hülsemann (1955) in sediments from the North Sea and from the Molasse in Switzerland. It is probable that in the Wanganui Basin this cross-stratification represents banks in sheltered waters where shells accumulated and were repeatedly covered by a protecting layer of fine sediment.

iii) The third type is also texturally heterogeneous having alternating layers of silt and pebbly conglomerate (sometimes shelly). The sets are grouped and have a trough form, none being greater than 0.5m thick, (Fig. 32). The sets can be traced for at least 50 metres in most exposures and have uneven lower and upper contacts. It somewhat resembles the pi form (Fig. 28) of Allen (1963). Knight (1929) believed that each set of this type could be related to the cutting and filling of a channel under water. Coarse shelly beds with identical structures occur in the bottoms of migrating channels in the Haringvliet estuary, Holland (Oomkens and Terwindt, 1960).

Directional measurements of this type of cross-stratification were not used in the Wanganui Basin palaeocurrent analysis as the significance of the dip of the foresets is uncertain. In similar deposits in the Haringvliet, Holland, Oomkens and Terwindt (1960) found the dip direction of the foresets paralleling the estuary, but Augustinus and Riezebos (1971) considered that the channels are filled laterally and the foresets would thus give a palaeocurrent direction normal to channel flow.
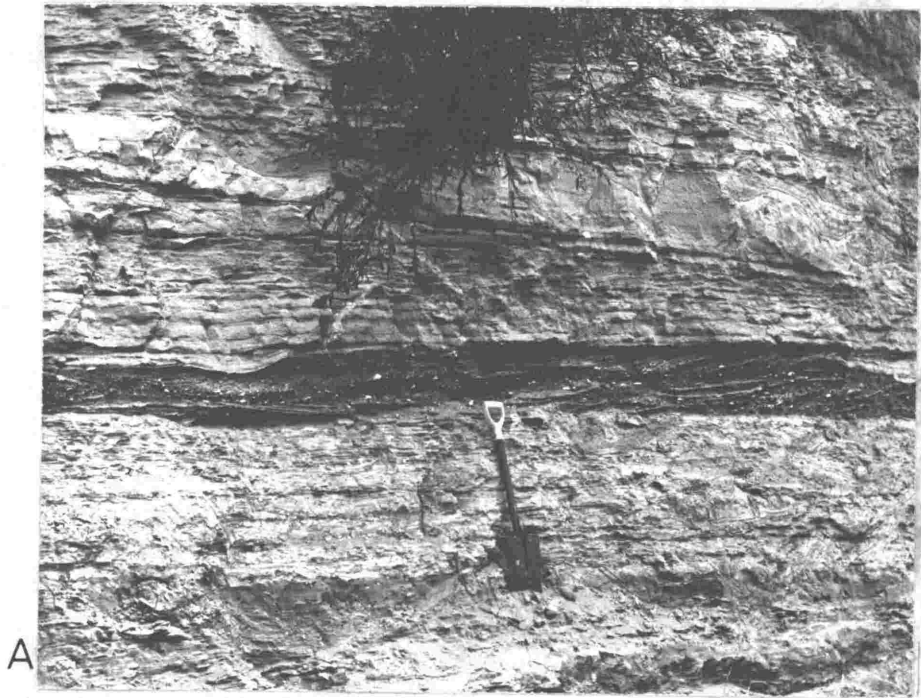
Fig. 32, A and B: Large scale cross-stratification interpreted as
channel lag deposits.   Spade one metre long.

iv) "mega flaser" structures

Large scale flaser structures (Fig. 33) were recorded at several localities. Van der Linden (1963) used the term to describe similar structures in the Molasse of Switzerland.

The sands are moderately well sorted, but contain scattered pebbles and broken shell fragments. The cosets have an overall lensoid form up to 20 metres in length. The individual sets, up to one metre high, have erosional upper contacts. The flasers generally have a sharp, unconformable, sometimes rippled lower contact with the underlying sands. The upper contact of the flasers varies from gradational to sharp, and sometimes shows the effects of loading (Fig. 34). The very irregular form of the flame structures that resulted from this loading suggests that the silts were very wet when the overlying sand was being deposited.

On the evidence of associations with other structures Van der Linden (1963) suggested that the mega flasers in the Molasse, were formed in deeper water, offshore from a bay, but it is suggested here that those in the Wanganui Basin may represent beach deposits.

The sand is fine, moderately well sorted, has less than one percent silt, and contains a few pebbles and broken shells, suggestive of beach deposits. The mega flasers are considered to have been formed by migration of a ridge and hollow sequence on the back beach. A low ridge is frequently developed by storms above the high tide level, and behind these ridges is a depression, often containing water and trapping fine sediment which is frequently rippled. The fine sediment in such a depression may be preserved as flaser structures if the storm beach migrates landwards, depositing sediment conformably on the wet silt, sometimes producing loading structures. By progressive shoreward and landward migration of the ridge on a prograding beach a sequence of mega flasers may develop. The lensoid nature of these cosets also tends to confirm this model.

Fig. 33: Mega flaser structures in the Kaimatira Pumice Sand.
Spade one metre long.
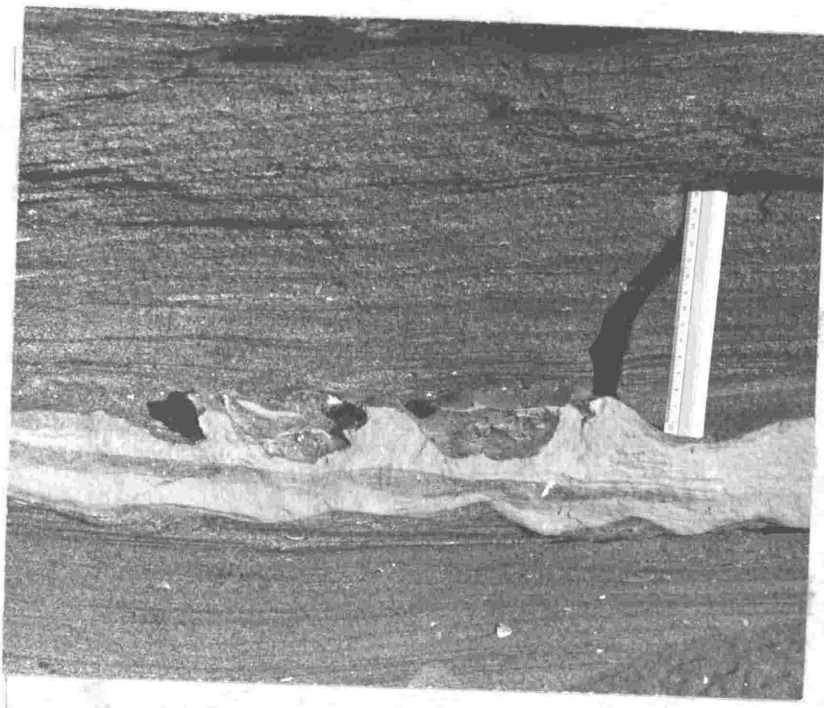
Fig. 34: Loading of the silt flasers. Ruler 150mm long.

B) Plane parallel lamination

Thin bedded parallel and sub-parallel units are common in all formations.

a) Okehu Siltstone

Silt and clay laminae of the Okehu Siltstone Formation were probably deposited from suspension, as Inman (1949) and Sundborg (1956) have shown that such fine material is usually transported in this manner. Alternation of laminae of different size grades could record alternation of supply, or differential settling of sediment from suspension following periods of high turbulence.

b) Makirikiri Tuff and Kaimatira Pumice Sand

From the evidence of other structures discussed above, the two volcaniclastic formations were deposited in shallow water, certainly within the range of wave or tidal action. Tidal flats subject to oscillating currents are often covered by ripple marks, but if sedimentation rate is low, the ripples may be destroyed and the sediment accumulates with slightly uneven horizontal laminae (Van Straaten, 1961, McKee, 1965). This case probably applies to those parts of the Wanganui Basin in which the proportion of volcaniclastic material is relatively low, implying a lower sedimentation rate.

However where the percentage of volcanic detritus is high, implying a high sedimentation rate, the plane parallel lamination has been interpreted as deposition under upper flow regime conditions. Such sequences are also characterized by moderate sorting and segregation of grains according to composition on alternate laminae. Thus they combine the plane parallel lamination of upper flow regime with the better sorting of lower flow regime deposits. Michaelis and Dixon (1969) suggest that this may occur in shallow water where oscillating wave-generated currents produce higher flow regime conditions as well as effective segregation of

sediment according to size and density. Formation of heavy mineral laminae on beaches is an example of this effective sorting.

Under these conditions, then, the sediment is deposited within the influence of wave motion which is approximately one half the wave length, which in turn is a function of exposure of the area and fetch. Keunen (1950) cites two examples: a 40m.p.h. wind blowing across 30 miles of open sea causes appreciable water movement at a bottom 18 feet deep, whereas the same wind with a 300 mile fetch would affect bottom sediments in 70 feet of water. But the depths under which upper flow regime conditions would occur are but a fraction of these.

C) Intraformational breccias and conglomerates

Intraformational breccias and conglomerates occur near the base of beds of tuffaceous medium to fine sand. The clasts are silt blocks that are generally subrectangular with a small degree of rounding on the ends, indicating at least some abrasion during transport. The apparent long axes of the clasts are mostly between 10mm and 300mm with a few up to 500mm in length.

The fabric displays either of two forms:

a) a preferred orientation of the clasts which may parallel the base of the beds and show some imbrication (Fig. 35);

b) random orientation of clasts.

At some localities erosion of the silt beds is evident and the texture and lithology of the clasts is identical to this rock type. Thus the breccias were formed by penecontemporaneous fragmentation of the underlying silt beds by currents strong enough to transport the blocks. Sternberg (1972) concluded that the current velocities required for sediment erosion and transport in a marine environment are the same as those required in fluvial systems, (e.g. Simons et al. 1961). Using
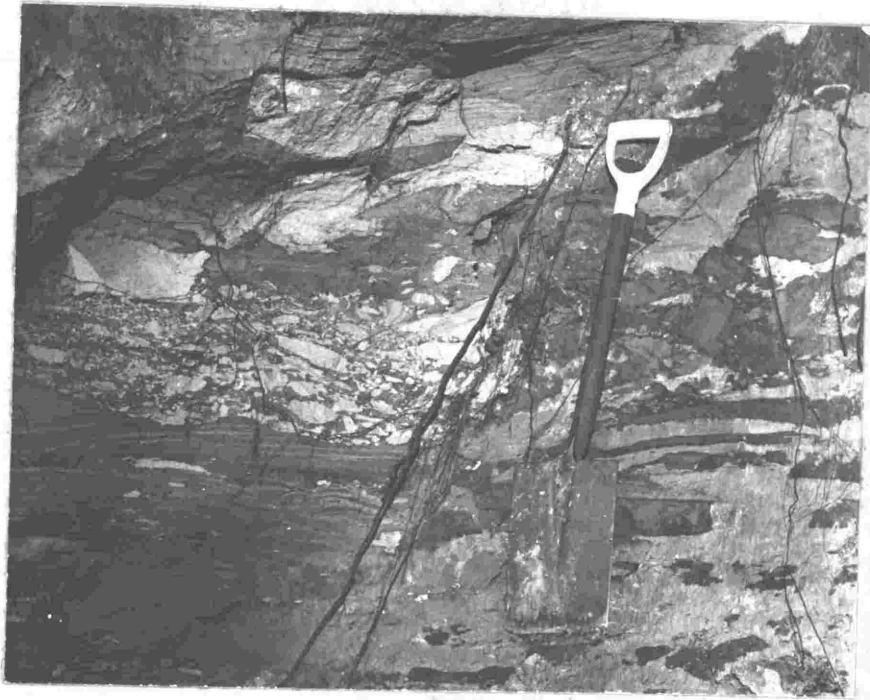
Fig. 35:   Sub-horizontally orientated blocks of siltstone in
           ashy sands. Spade one metre long.

Shield's diagram (in Blatt, Middleton and Murray, p. 91) the shear stress T_0 for the initiation of movement of a particle 10mm in diameter is 100dynes/cm^2. The shear velocity $U* = \sqrt{T_0/\rho}$ is therefore 10cm per sec., where ρ is the density of the fluid medium.

D) Erosional features

Channels and erosion surfaces are prominent features within the Makirikiri Tuff and Kaimatira Pumice Sand Formations. Two types are represented:

a) those with an irregular base and unsorted fill,

b) those with a smooth even basal contact and stratified fill (Fig. 36).

a) In the first type the fill is invariably composed of very poorly sorted subrounded pebbles, cobbles and boulders. The long axes of the boulders range up to 1.5m. The clasts are mostly greywacke, with volcanic rocks (andesite, rhyolite and pumice) totalling as much as 20%. The matrix is silty, very coarse sand, composed mainly of lithic fragments. The general appearance of the fill is chaotic.

The beds into which the channels are cut are cross-stratified medium sands which display bimodal vectors associated with the tidal zone. The beds immediately above the channel are sands with abundant Amphidesma, a bivalve characteristic of the tidal zone. It is safe to conclude that these channels were cut in inter-tidal or slightly sub-tidal waters.

Velocities greater than 3m per sec one metre above the sediment water interface, (Hjulström, 1939) would be required to transport the coarse debris infilling the channels. The presence of the volcanic detritus and the very poor sorting suggest that these deposits may be the related to a flow that had a laharic origin.

Conglomerate channels of similar form and textural composition are present in the north east of the area, (in the region of the township of
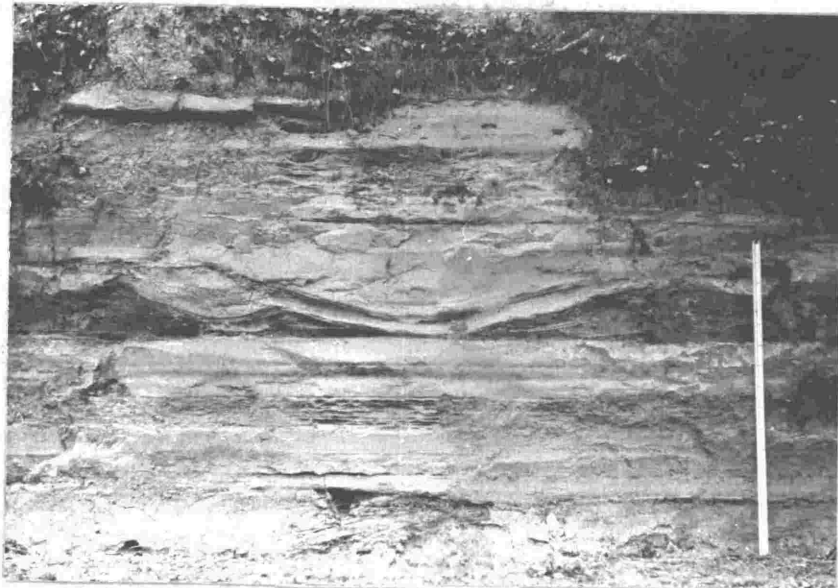
Fig. 36: Channel cut and fill in the Kaimatira Pumice Sand
Formation. Interpreted as forming in a tidal flat
environment. Scale 1.5m.

Apiti), but do not contain any volcanic detritus. The clasts are subangular, with long axes up to 0.2m, set in a poorly sorted silty sand matrix and at two localities are imbricate. Irregularly interbedded with the conglomerates are silts and lignites containing no positive evidence of a marine environment. In only one section was a fining upwards sequence recognised. Thus the presence of the poorly sorted conglomerate fill in channels with an irregular base, imbrication and the interfingering silts and lignites suggest that these deposits in the north-eastern part of the basin are the product of a braided river.

b) The second type of channels vary in depth from 90mm to 5m, and in all cases the fill is finer than the deposits into which they are cut. The layering of the fill follows the outline of the channel, becoming less concave upwards until it is horizontal. From the above characteristics and associations with vectorially bimodal cross-stratification it is suggested that these channels were probably formed in a tidal flat.

Secondary structures

Secondary structures are as numerous and varied as the primary structures. Various types of contorted bedding were noted and all are considered to be penecontemporaneous. They are described in the following descriptive groups:

A   Convolute bedding

B   Crumpled bedding

C   Slump ball structures

A)   Convolute lamination is a term first used by Ten Haaf (1956). Beds displaying such features have upper and lower surfaces that are generally almost planar, while internally the bed displays a complex pattern of broad synclines and sharp anticlines. Ten Haaf limited the term to contortions in

which the laminae were largely continuous and without faulting. He suggested that they were formed within turbidite deposits. However, Dott and Howard (1962) described convolute laminations in the Dinwoody Formation of west Wyoming and north east Utah - sediments which they concluded were deposited in shallow agitated waters in nearshore marine and non-marine environments, similar to those that are inferred in the present study area. Sanders (1965) and Dzulynski and Walton (1965) put forward evidence that these structures were formed by plastic deformation of the bed at the same time as the sediment was being deposited rapidly from suspension.

Many examples that clearly come within the form definition of Ten Haaf occur in the western side of the Wanganui Basin and are all associated with medium to fine sand with a high percentage of volcanic detritus, (Fig. 37). The units extend laterally up to 100 metres (the length of the longest exposure). All are associated with other features indicating a high sedimentation rate, e.g. ripple-drift cross-lamination. Rapid sedimentation and the rapid expulsion of pore water is a likely cause of these structures. At several localities pumice pebbles up to 25mm in diameter were seen in the nodes of the anticlines suggesting that they were "floated" to this position by the escaping water. Only one case of significant preferred orientation of fold axes was seen.

As well as the classical forms of convoluted laminae forms with less regular geometric outline were recognised, (Fig. 38). These are found in the most pumiceous of the volcaniclastic sequences where medium sand overlies coarse sand.

Some instances of truncation of anticlinal crests were found. (The term corrugated bedding introduced for this by Schrock (1948) is considered redundant.) Anketell et al (1969) proved by experiment that these truncations could be produced during liquefaction without erosion, and
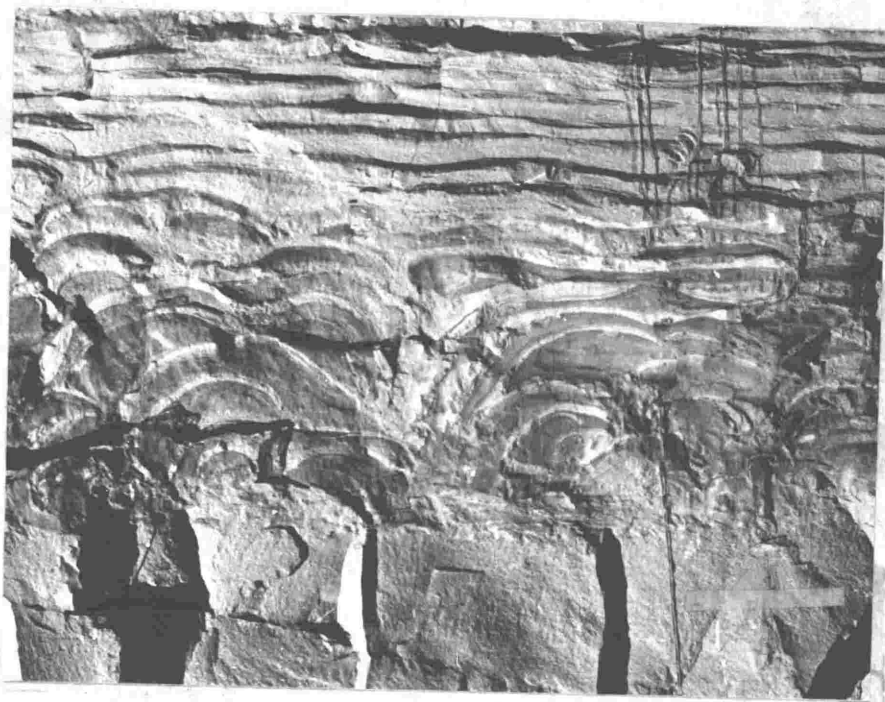
Fig. 37: Convolute laminations in the Kaimatira Pumice Sand Formation.
Note sharp anticlinal peaks and broad flat synclines,
geometrically typical of the definition by Ten Haaf (1956).
Bar scale 0.5m.
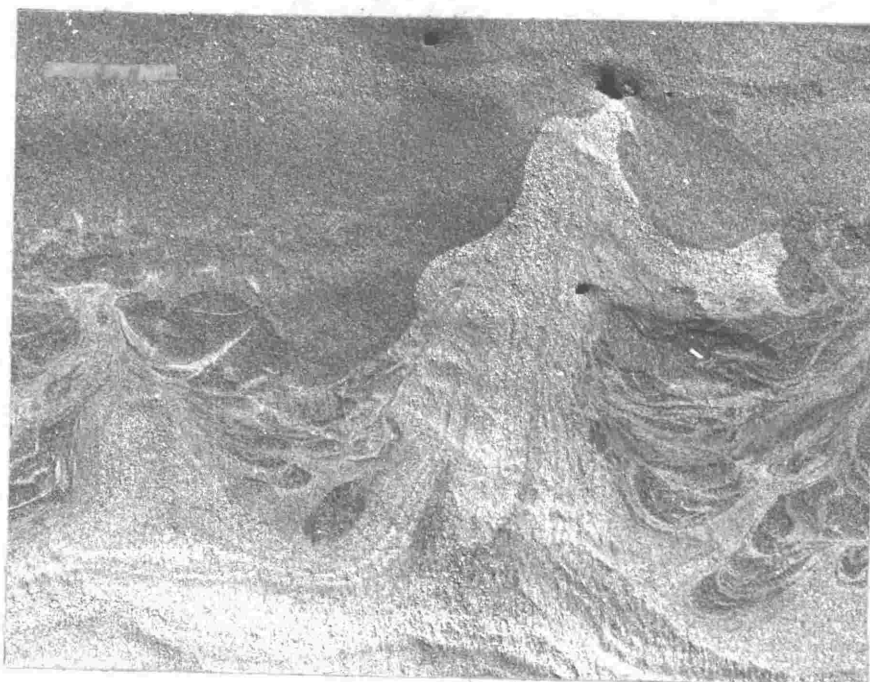
Fig. 38: Convolute laminations in very coarse pumice sands.
Bar scale 0.1m.

that in unstable water-saturated layers, the sediment extruded with the
escaping pore waters settled back on the bed surface to form a thin
veneer unconformably overlying the distorted bedding.

Some examples of truncated anticlinal crests in the Wanganui
Basin no doubt formed in that way, but others were evidently formed
differently. At some localities current scour appears to be the cause of
the truncation especially in cases where the convoluted bed has an upper
contact with conglomerates.

B) Crumpled bedding

The term crumpled bedding was used by Allen (1960) to describe
deformed and sometimes faulted synsedimentary structures. In the Wanganui
Basin sediments these structures are usually between 0.2 to 2.5 metres in
height and do not occur where there is any appreciable amount of volcanic
detritus. The sediments are finer and less friable than those of the
convolute laminae. Faulting, where present, must have happened after the
main phase of plastic deformation, though thickening of the layers indicates
that the sediment was still in a semi-plastic state (Fig. 39 and 40).

Some forms of crumpled bedding are greater than 1m high (Fig. 41) and
exhibit a general preferred orientation of fold axes. The directions of the
fold axes differed by as much as 90° from flow directions deduced from
foreset orientation of primary cross-stratification in the overlying
sediments. These structures are interpreted as slump features indicating
palaeoslope rather than palaeocurrent direction. A gradient of no more
than 4° is needed for slumping to occur on a submarine slope (Lewis, 1971),
and such gradients may be likely in shallow marine environments.

Other structures that fall geometrically under the heading crumpled
bedding but are genetically related to some forms of convolute lamination
are described here. They are the ruptured structures described by Davies
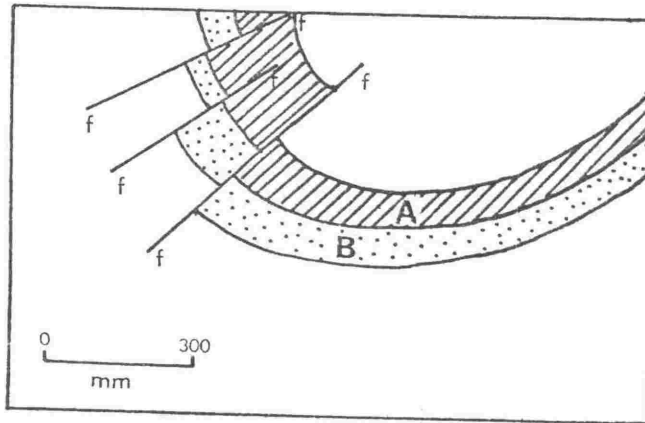
Fig. 39: Crumpled bedding (Allen, 1960) at locality 90,
N139/302820. Note thickening of units A and B.

Fig. 40: Complex form of crumpled bedding. The core of this
contains many small faults similar to those in the
above figure.
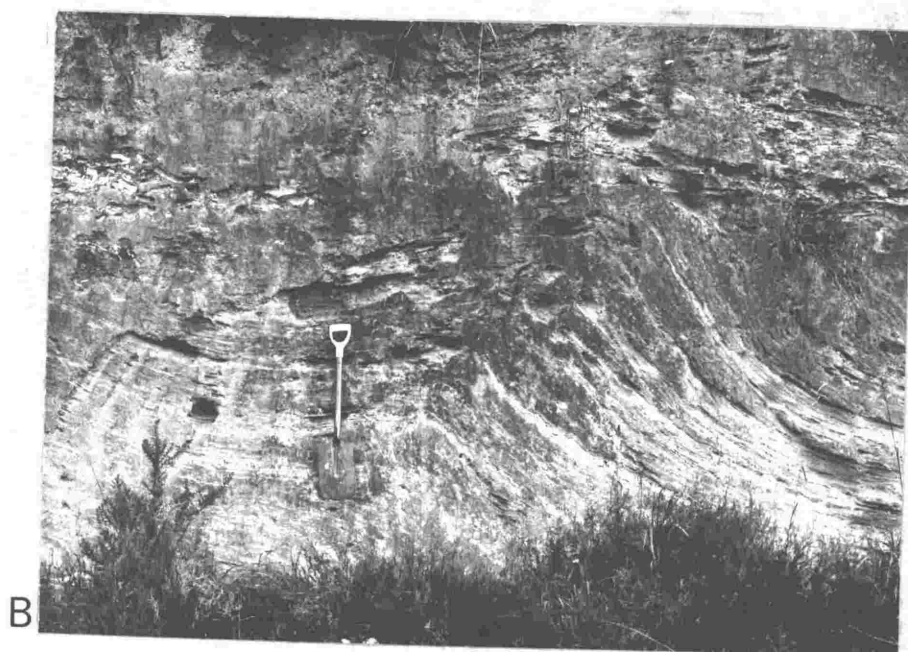
Fig. 41A and B: Large scale crumpled bedding interpreted as slump
features in the Kaimatira Pumice Sand Formation.

(1965). In these structures the anticlines appear to have been broken by
the upward expulsion of the sediment slurry. Again, such structures
typically occur in the more tuffaceous volcaniclastic sediments.

In figure 42, upward injection of material from bed 'a' resulted
in the rupture of bed 'b'. Small slivers of bed 'b' were "floated" away
and incorporated in bed 'c' which must have been mobile at the time.

Similar structures were described by Anketell et al (1969)
in water saturated layered sequences in sedimentation tanks. They noted
that deformation occurred once the layers reached a critical thickness,
which raises the total weight of the column beyond the limits of its
bearing capacity. In other experiments they triggered the deformation by
a slight shock which in nature may equate with earthquake waves. After the
initial shock they observed the upward intrusion between downsinking lobes.

Using sediment from the study area, studies similar to those of
Anketell et al were carried out in small tanks (300mm square). Sand was
evenly sedimented to a thickness not greater than 10mm followed by a
similar layer of silt. The process was repeated but even with 200mm of
sediment no rupturing occurred. In other cases the sand silt layers were
built up to 100mm depth and the tank was tapped lightly. Intrusion followed
with the pore water of the sands escaping upwards and rupturing the silts.
Some fragments of the silt layer then sank back beneath their original
stratigraphic position. These crude experiments suggest that the escape
of pore water and rupturing was triggered by shock rather than by excessive
overburden.

C) Slump Ball Structures

Slump ball structures, rounded masses of contorted sandstone
isolated in clay, (Keunen, 1949), are a type of load structure formed
where sandstone penetrates underlying plastic clay. Such structures
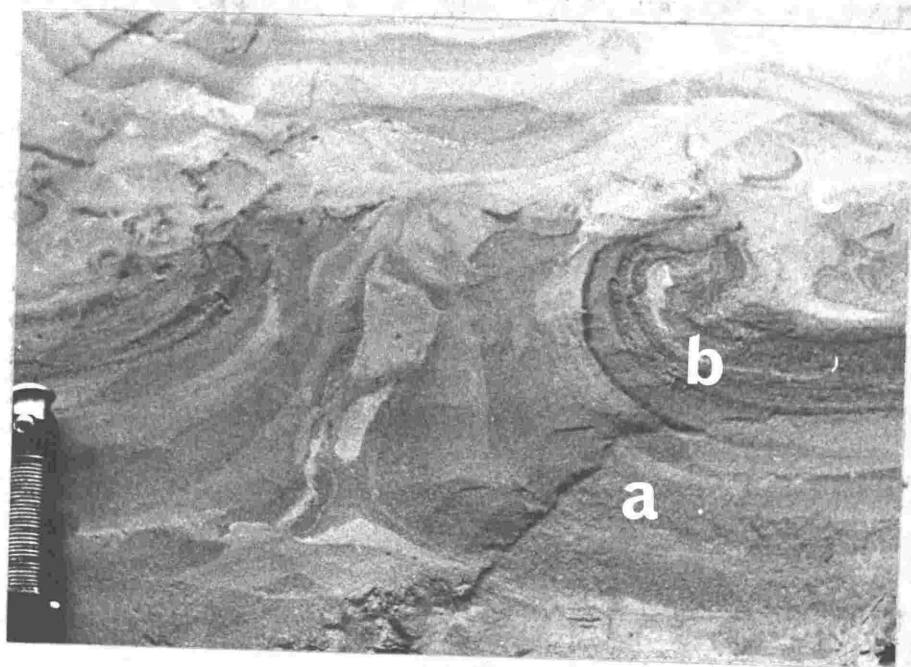
Fig. 42: Ruptured structure in the Kaimatira Pumice Sand
Formation. Knife handle 100mm.

(Fig. 43) are rare in the Wanganui Basin probably because of the general absence of clay sized material.

Associations of sedimentary structures

At several localities sequences of structures and textural relationships were recorded and are interpreted below:

1) Locality 157 (N144/288513) on the eastern side of the basin exhibits features interpreted as upper tidal environments (Fig. 44).

The basal unit of rippled and flaser bedded well sorted medium to coarse sands is followed by a silt unit that has a high percentage of carbonaceous material in its upper portion where dark grey root structures are developed normal to bedding. This silt is interpreted as a palaeosol. Overlying marine ashy sands display vectorially bimodal ripple-drift cross-lamination and were probably deposited in an intertidal environment, while volcanic activity in central North Island provided abundant sediment. This was followed by a bed of rippled silts and fine sands. Above this unit thinly bedded silts and very fine sands which show the development of small channels with a fill of clayey silt and also, on different bedding planes, of straight linear ripples with their strikes varying up to 45° from each other, are typical of a tidal environment.

2) Offshore from Oregon beaches, Clifton, Hunter and Phillips (1971) recognised a series of zones of sedimentary structures paralleling the coast and roughly correlated with zones of changing wave conditions (Fig. 45). Though the preservation potential of such structures is low they might be expected to survive in a subsiding basin in which sedimentation was rapid, such as the Wanganui Basin. Two sites were located where some of these facies recognised by Clifton et al, together with other depth indicators, occur in vertical sequence and are tentatively interpreted as minor marine transgressions.
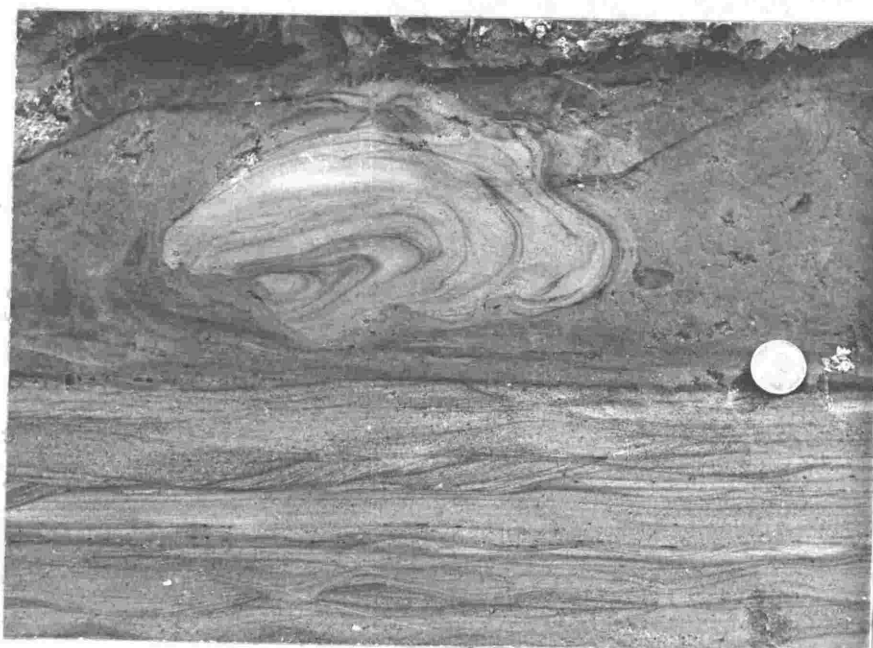
Fig. 43: Slump ball structure in the Makirikiri Tuff Formation.
Coin 25mm diameter.

STRUCTURES

Plane parallel
lamination

Ripples with strikes
varying by up to 45° on
different beds
Channels

Ripples

Bimodal—bipolar
ripple—drift cross—
lamination

Root charnels

1m

Flaser bedding
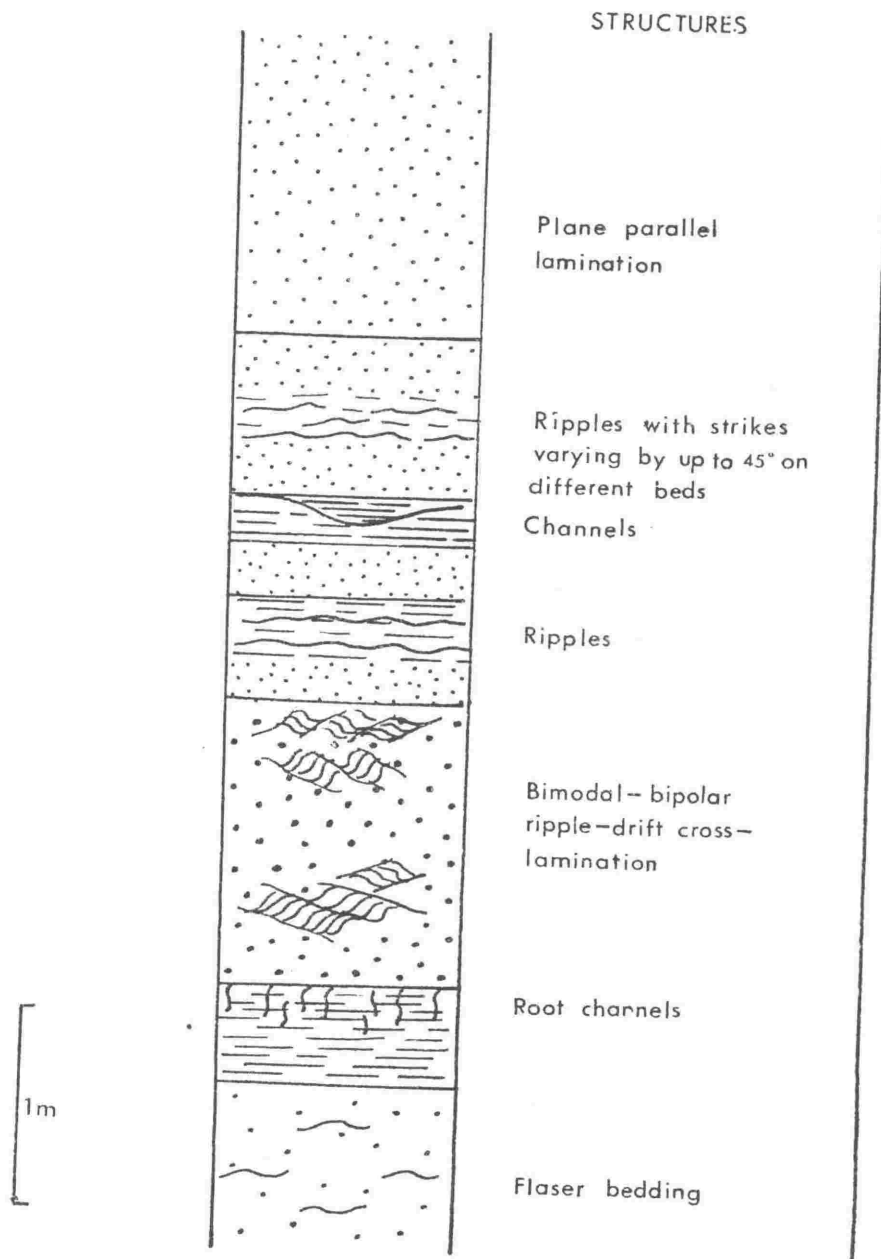
Fig. 44: Stratigraphic section through a sequence interpreted
as dominantly intertidal. (Loc. 157, N144/288513).

offshore →| ←——————— near shore ——————→

Sea surface

— —1.7m

Sea floor — —3.3m

| Structural Zone | Asymmetrical ripples | Lunate megaripples | Outer planar | Inner rough | Inner planar |

0   30m
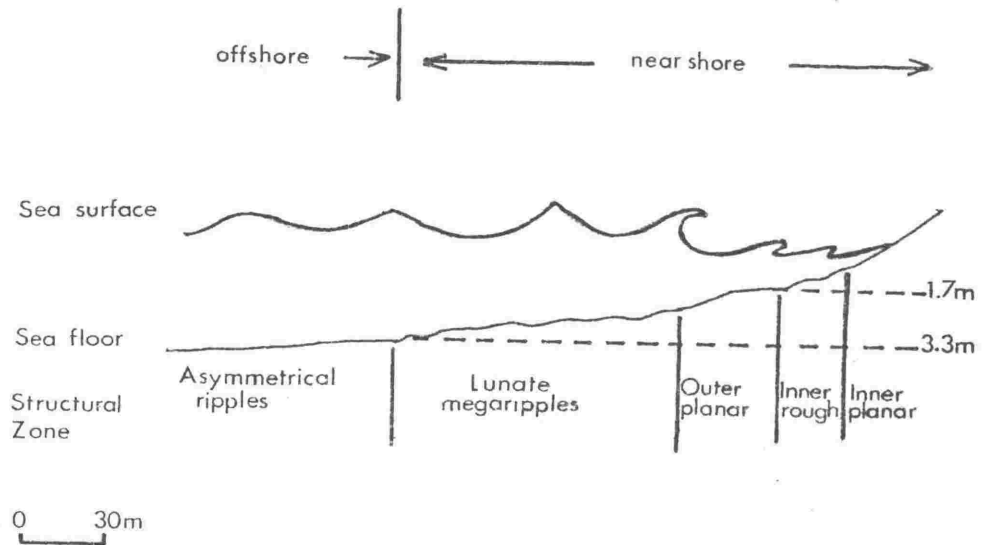
Fig. 45: Zones of wave action and sedimentary structures on the
Oregon coast, (after Clifton, Hunter and Phillips, 1971).

The first example is illustrated in figure 46. The lowest unit is flaser bedded, moderately sorted medium to coarse sands with some vectorially bimodal ripple-drift cross-lamination. The next is a well sorted medium sand with only vectorially bimodal ripple-drift cross-lamination. Those two units probably represent the intertidal or immediately sub-tidal zone. The third unit has gradational contact with the second and consists of plane parallel laminated well sorted medium sands, with rhomboid ripples on top. As previously mentioned the latter structures are typical of beach deposits and probably represent the upper portion of the swash zone.

The fourth unit is composed of medium to coarse friable sands showing large scale trough cross-stratification incorporating a sequence of horizontal plane parallel lamination, symmetrical ripples and ripple-drift cross-lamination within each. Foresets indicate a direction away from the palaeoshore (determined from the rhomboid ripples). The ridges of the large scale stratification parallel the palaeoshore; thus this unit has some of the attributes of the inner rough facies of Clifton et al (1971).

The fifth unit has a sharp basal contact, and appears to possess properties of both the inner and outer facies. The chord and height of the trough cross-stratification and the texture of the sediments suggest outer rough facies, but dominantly bimodal foreset vectors suggest the inner rough facies adjacent to a steep beach.

There is an upward gradational contact into the sixth unit which equates with the outer rough facies in all aspects described by Clifton et al.

Although other interpretations may be put on these structures the sequence is mostly consistent with that described by Clifton et al. The few inconsistencies may be due to differing supply and texture of the sediment and to local current patterns.

	SEDIMENTARY STRUCTURE	TEXTURE	CURRENT DIRECTION	ENVIRONMENT
	Large (2.0m) trough cross-beds	Very coarse gravelly pumiceous sands and conglom-erates	Landward	Outer rough
	Large trough cross-beds. Intraformational breccias. Flasers	Very coarse pebbly sands	Bimodal dominantly seaward	Current attributes of inner rough; otherwise outer rough.
	Lge cross beds	m-c sand	Seaward	Inner rough
	Ripples,plane parallel lamin-ation.Rhomboid ripples	Well sor-ted m. sand	Seaward	Inner planar-beach swash zone
	Herringbone Flasers Some ripple-drift	Mod.well-well sor-ted m.-c. sand with silt flasers	Bimodal	Intertidal

Fig. 46: Section (loc.37, N139/302837) showing vertical sequence of shallow marine sub-environments based on studies of Clifton et al (1971).

A second sequence interpreted as a minor transgression is illustrated in figure 47. Very thin bedded, very fine to fine, moderately sorted sands, at the base, appear to belong to the inner planar facies. An erosion surface marks the contact with the overlying unit which is dominantly medium to coarse pebbly sand with vectorially bimodal large scale cross-stratification more than 0.5m high. Some symmetrical ripples and ripple-drift cross-stratification are present, and also a channel filled with poorly sorted conglomerate. These features are characteristic of the inner rough zone off steep beaches with the additional channel component. The overlying unit consists of massive fine sands and silts with lenses of coarse sand containing <u>Amphidesma</u> and displaying large scale trough cross-stratification with a set thickness greater than 1.5m, and unimodal foreset dip directions. This unit is interpreted as outer planar with intercalated outer rough facies.

A sharp contact at the top is followed by alternating fine and medium sands with plane parallel lamination and some ripples. This zone may be the equivalent of the inner offshore facies; the plane parallel lamination may represent sites of reworking of sediment with sufficient sediment introduction to preserve only a few ripples.

The highest beds exposed are massive silts and very fine sands which contain <u>Chlamys gemmulata</u> and are considered to represent an offshore environment.

Discussion

Major features indicative of a shallow water environment influenced by tidal action are considered in a comprehensive review by Raaf and Boersma (1971) who list the following six points:

1) cross-stratification with bimodal vectors

2) juxtaposition of large and small scale structures
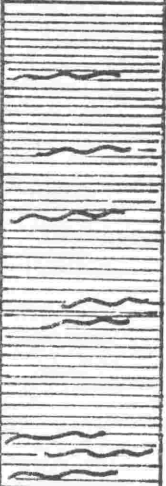
	SEDIMENTARY STRUCTURE	TEXTURE	CURRENT DIRECTION	ENVIRONMENT
	Convolute lamination	Very fine sandy silt	-	-
	Massive	Silt and very fine with _Chlamys gemmulata_ abundant	-	Offshore
	Laminated to very thin bedded with some symmetrical ripples	Very fine sand	Bimodal	Inner Offshore
	Massive with lenses of large scale trough cross beds	Fine sand and silt with lenses of coarse sand and gravels containing _Amphidesma_	Unimodal	Outer planar with inter-bedded outer rough
	Large scale trough cross-beds with a channel	Medium to coarse pebbly sands. Channel fill is poorly sorted conglomerate	Bimodal	Inner rough
	V.thin bedded	Very fine to fine sand	-	Inner planar

Fig. 47: Stratigraphic sequence at locality 148 (N138/710892) and interpretation based on the study of Clifton, Hunter and Phillips, (1971).

3) poorly developed sequential regularity and occasional fining
   upwards sequences

4) secondary phenomena related to the bidirectional and intermittent
   character of tidal currents

5) fairly common occurrence of flaser and/or lenticular bedding

6) slight to intensive bioturbation suddenly disappearing without being
   related to a change in character of the sediments.

Raaf and Boersma (loc. cit.) concluded that the distinction of
sub-environments of the tidal zone can only be positively identified for
ancient clastic deposits in a few examples.

The first five features listed by Raaf and Boersma (1971) occur in
the Makirikiri Tuff and Kaimatira Pumice Sand Formations. The bimodality
of the cross-stratification is emphasised later in the palaeocurrent analysis.
Juxtaposition of large and small-scale cross-stratification occurs most
commonly in the lower portions of the Makirikiri Tuff sediments and points
to highly variable hydrodynamic conditions both in space and in time.

The sixth point listed by Raaf and Boersma (1971) relates to
bioturbation of the sediments. In this thesis, except in the shell
conglomerates, macrofossils are infrequent in the western side of the
basin and absent in the east. Trace fossils too are generally rare. Te
Punga (1953) in the Rangitikei sequence, recognised small, thin shelled
specimens of <u>Chione (Austrovenus) stutchburyi</u> (Gray) and suggested that
they may have been stunted in growth by the excessive quantities of volcanic
detritus or by a greatly reduced salinity of the water.

Ripple-drift cross-lamination is not generally found in the shallow
water to tidal flat environments. Its abundance in the Wanganui Basin
volcaniclastics is explained by the extremely rapid supply of sediment
from the central North Island region.

The recent study by Clifton et al (1971) is a major contribution to the understanding and interpretation of near shore sediments. Two sequences have been described above which are very consistent with their findings.

To the north east of the basin the sediments exhibit characteristics that indicate a more fluvial environment, more particularly that of braided streams. This is suggested by the strong erosion surfaces underlying the poorly sorted conglomerates. Some of the conglomerates have obvious imbricate texture. The finer material is dominantly large scale cross-bedded and has associated lignitic lenses, that may have been formed by organic detritus trapped in the quiet water area.

Conclusions

The main conclusions gained from the study of sedimentary structures are:

1) the Okehu Siltstone Formation was deposited from suspension in water depths greater than the volcaniclastic formations,

2) the Makirikiri Tuff and the Kaimatira Pumice Sand Formations were deposited in shallow waters subject to tidal and wave section everywhere except the north east where fluvial deposition appears to have been dominant. The abundance of ripple-drift cross-lamination and water expulsion structures, especially in the more volcanic horizons, suggests very high rates of sedimentation during and after eruptive phases.

CHAPTER 3

GRAIN SIZE PARAMETERS

Introduction

Grain size distribution of any sediment is determined by the size range of materials that were available, and by the processes that acted upon the sediment during transport and deposition. The statistics of the size distributions have been used by many geologists to provide information about the palaeoenvironment. Folk (1961) has summarized the state of knowledge on the geological meaning of standard grain size statistics - mean, standard deviation, skewness and kurtosis. The first three are thought to be environmentally sensitive and have been used by many workers to distinguish processes.

The mean size indicates the average competence of the depositing medium; the standard deviation or the dispersion about central tendency reflects the degree of sorting, while skewness is a measure of the asymmetry of the distribution such that positive skewness indicates an excess of material in the fine fraction. The geological meaning of kurtosis is not fully understood.

Friedman (1961) was able to distinguish dune, beach and river sands on the basis of their textural characteristics. According to Passega (1957, 1964) a plot of the coarsest one percentile (C) against the median (M) can distinguish several modes of transport. He contended that the value of C is representative of the maximum competence of the transporting agent, and M is the statistic characteristic of the total range of particle sizes undergoing transport. C approaches the value of M if the coarse half of the sediment is very well sorted. Therefore the relative displacement measured parallel to the M axis, of the plotted points from the limit C = M is an index of the sorting in the coarse half of the sample. Basic types of CM patterns are shown in the inset to figure 51.

Textural maturity (Folk, 1951) provides a descriptive scale that gives some indication as to the effectiveness and the operative time of the agents acting during transport and deposition. Thus immature sediments may have been deposited where currents were weak and no reworking took place, or they may have been deposited where they were rapidly covered by another sequence. The more mature sediments are those that have been subjected to severe or long-continued abrasion and sorting, such as on beaches, where grains are constantly being moved. Folk (1951) defines textural maturity as the degree to which sand is free of interstitial clay and is well sorted and well rounded.

Procedures

Most samples examined were friable and easily disaggregated; those that were not were crushed with a rubber bung. Finer grained samples were disaggregated by soaking in water. For each sand sample 25-35gms was sieved for ten minutes in a Ro-Tap shaker with screens at half phi intervals. Silt and clay fractions were analyzed by pipette method using a battery of six settling columns as designed by the New Zealand Oceanographic Institute, (Van der Linden, 1968). Size analyses for both procedures had good reproducibility, (Fig. 48 and 49).

Results

All results are tabulated in Appendix 4. The sediments examined fall into three textural populations, (Fig. 50), sandy gravel, sand and silt, with little overlap between the two latter. The sandy gravel is mostly of Mesozoic greywacke clasts, although at a few places in the west volcanic clasts and shell debris are a major component. The sand is mostly of volcanic detritus and when present dominates all other detritus. The silt is only partly volcanic. Evidently the different
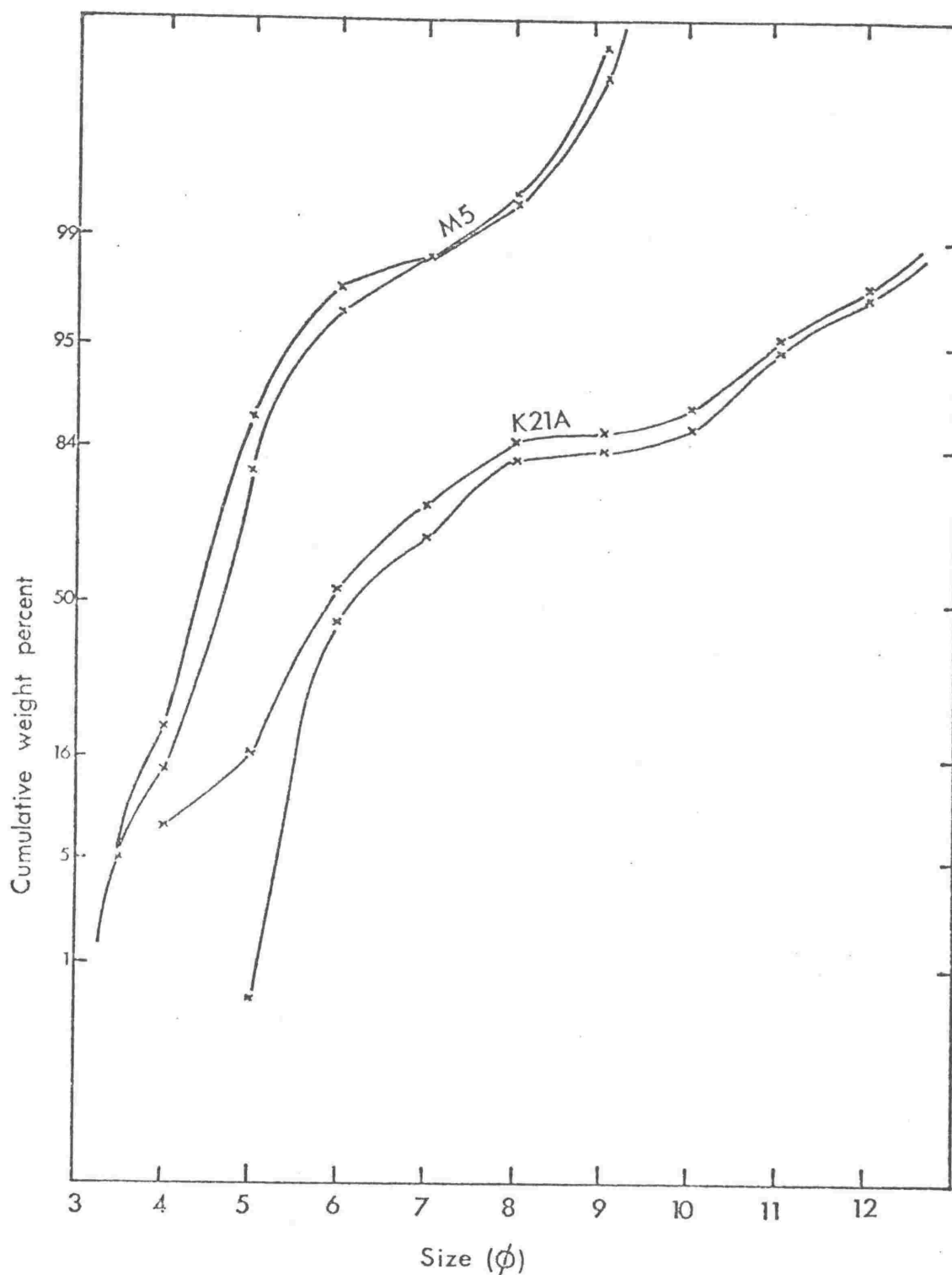
Fig. 48:   Size distribution curves for two pipette analyses, of
samples M5 and K21A to show reproducibility.
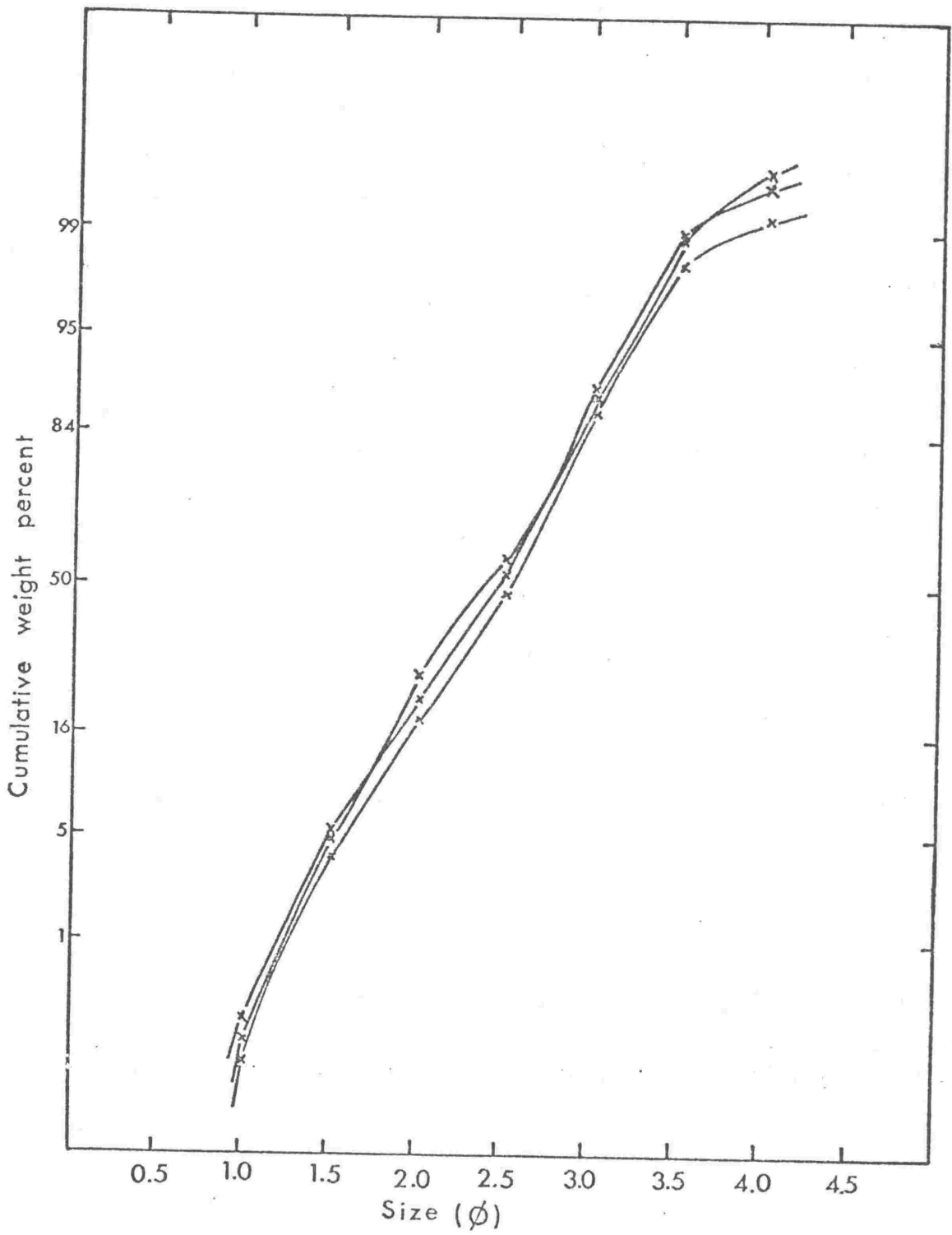
Fig. 49:   Size distribution curves for three sieve analyses of
          sample K30D to show reproducibility.

grain size populations to some extent reflect the different sources of supply.

Clays, muds and muddy gravels are lacking. Folk et al (1970) noted that sand and clay mixtures are rare in nature and that most samples from near shore environments tended to be 97-100% sand regardless of the source. Most of the volcaniclastic sands of the Wanganui Basin are over 90% sand (Fig. 50) even though there is evidence from the silt populations that finer material was being introduced. The postulated environment of these sands is near shore and presumably the silt was removed.

Relation between mean size and sorting

Mean size is plotted against sorting (standard deviation) for all samples, (Fig. 52). The best sorted material is that with a grain size from 2.5 to 3 phi. This relationship is not unusual. Inman (1949) first explained it by using Shields' and Hjulström's diagrams which show that fine sand is the most easily removed sediment. At the point where fine sand is deposited a slight increase in velocity leads to erosion and there is a very delicate balance between erosion and deposition, leading to good sorting of a sediment that is transported by the lowest velocity currents, and then deposited elsewhere.

Passega (1972) suggested that all fine sands of highly mobile basins are very poorly sorted regardless of environment of deposition, but in the Wanganui Basin, which was very mobile, all fine sand is moderately well or well sorted.

Relations of grain size to sedimentary structures

The gravels, sands and silts can be divided according to the sedimentary structures (which reflect the processes acting on the sediments) and to some extent lithology, with which they are associated.

Fig. 50: Textural classification of sediments analyzed. (Classification of Folk et al, 1970).

o Large scale cross-stratified gravelly sands and gravels.

• Large scale cross-stratified shelly gravelly sands, and gravels

▲ Large scale cross-stratified sands.

▢ Plane parallel laminated sands.

■ Bipolar-bimodal ripple-drifted sands.

△ Ripple-drifted sands and coarse silts.

× Plane parallel laminated volcaniclastic silts.

. Plane parallel laminated non-volcaniclastic silts (i.e. Okehu Siltstone)

Gravel

Percent gravel

80

30

5

0.01

Mud 9:1   1:1   1:9 Sand

Mud : Sand ratio

3 ⊙
5 ✕

10 □
5 ▲

Sand

All others

90

Percent sand

50

10

Clay   2 1   1 2   Silt

Clay : silt ratio
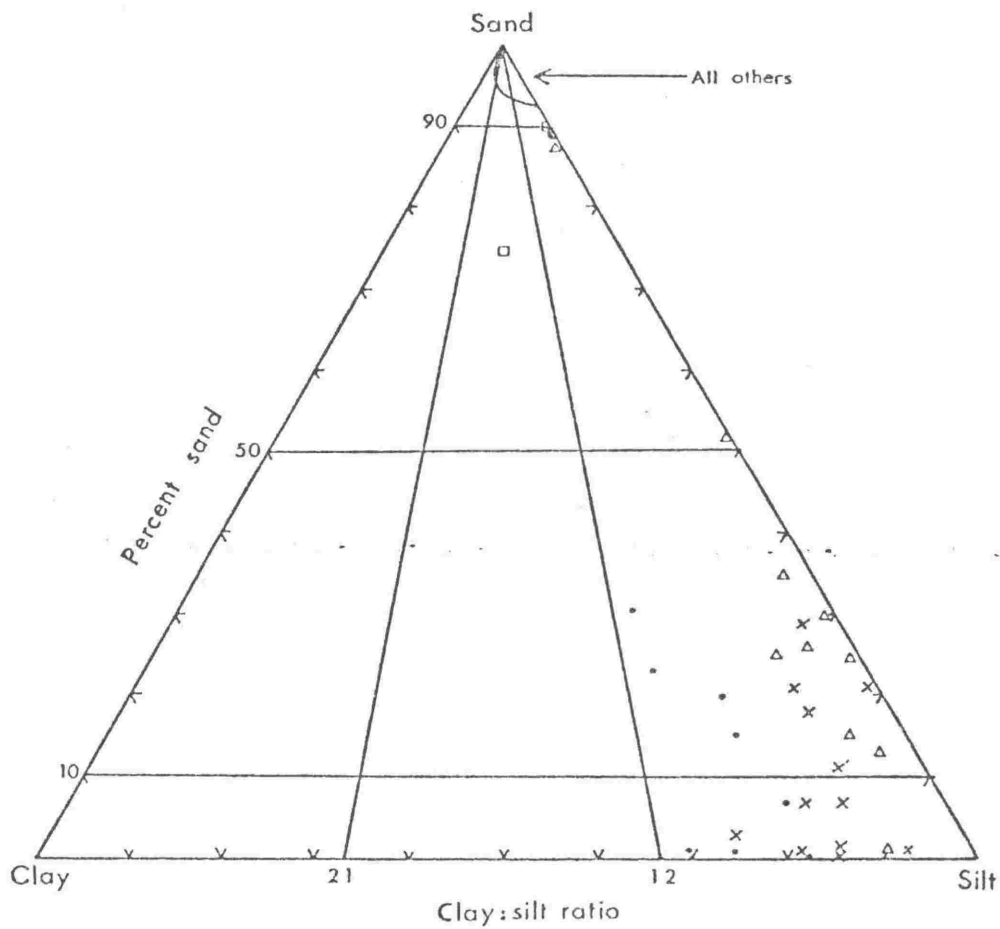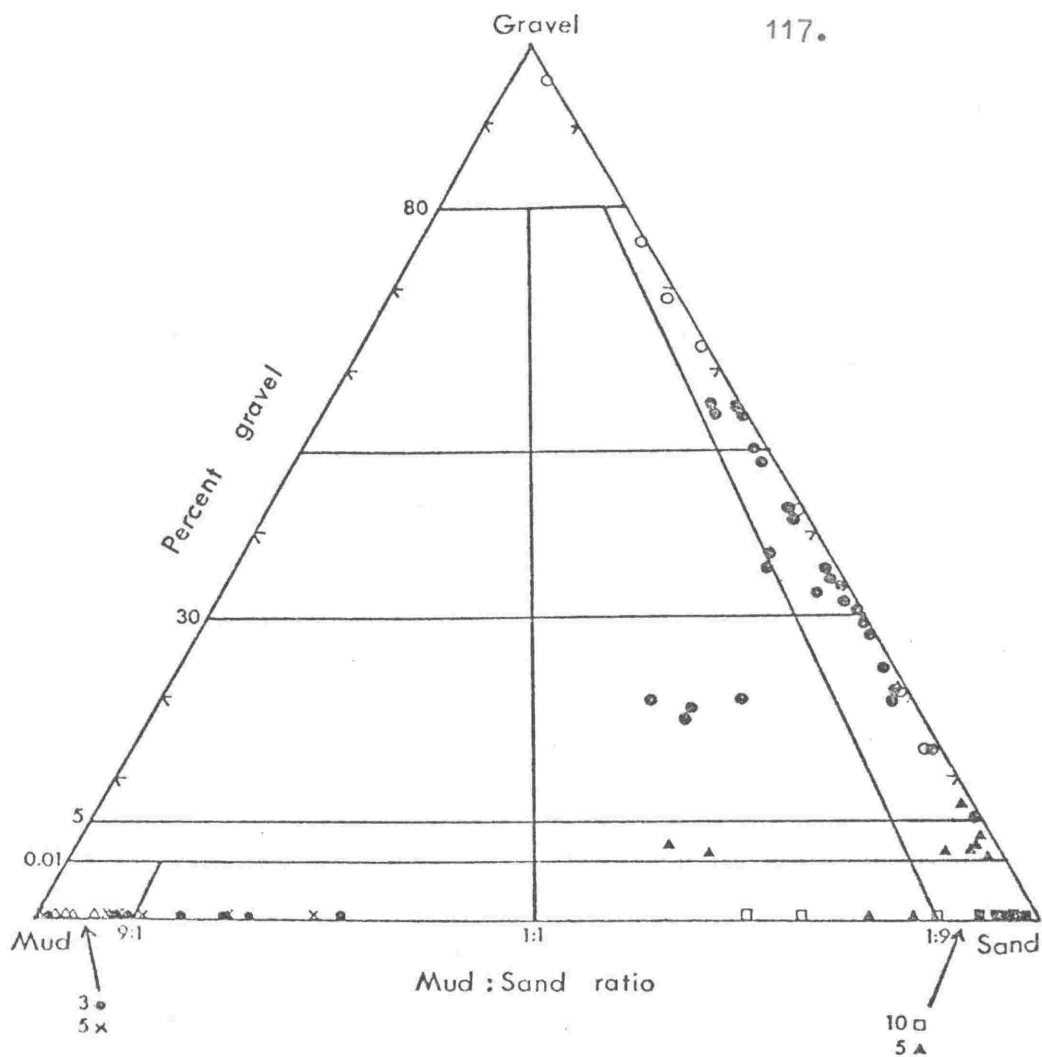
Fig. 51: Plot of C against M for all samples.

o   Large scale cross-stratified gravelly sands and gravels.

•   Large scale cross-stratified shelly gravelly sands and gravels.

▲   Large scale cross-stratified sands.

▫   Plane parallel laminated sands.

▪   Bipolar-bimodal ripple-drifted sands.

△   Ripple-drifted sands and coarse silts.

×   Plane parallel laminated volcaniclastic silts.

·   Plane parallel laminated non-volcaniclastic silts (i.e. Okehu Siltstone).

C-M patterns of sediments deposited in different environments (Passega, 1957, 1964)

M = Median (φ)

C = Coarsest one percentile (φ)
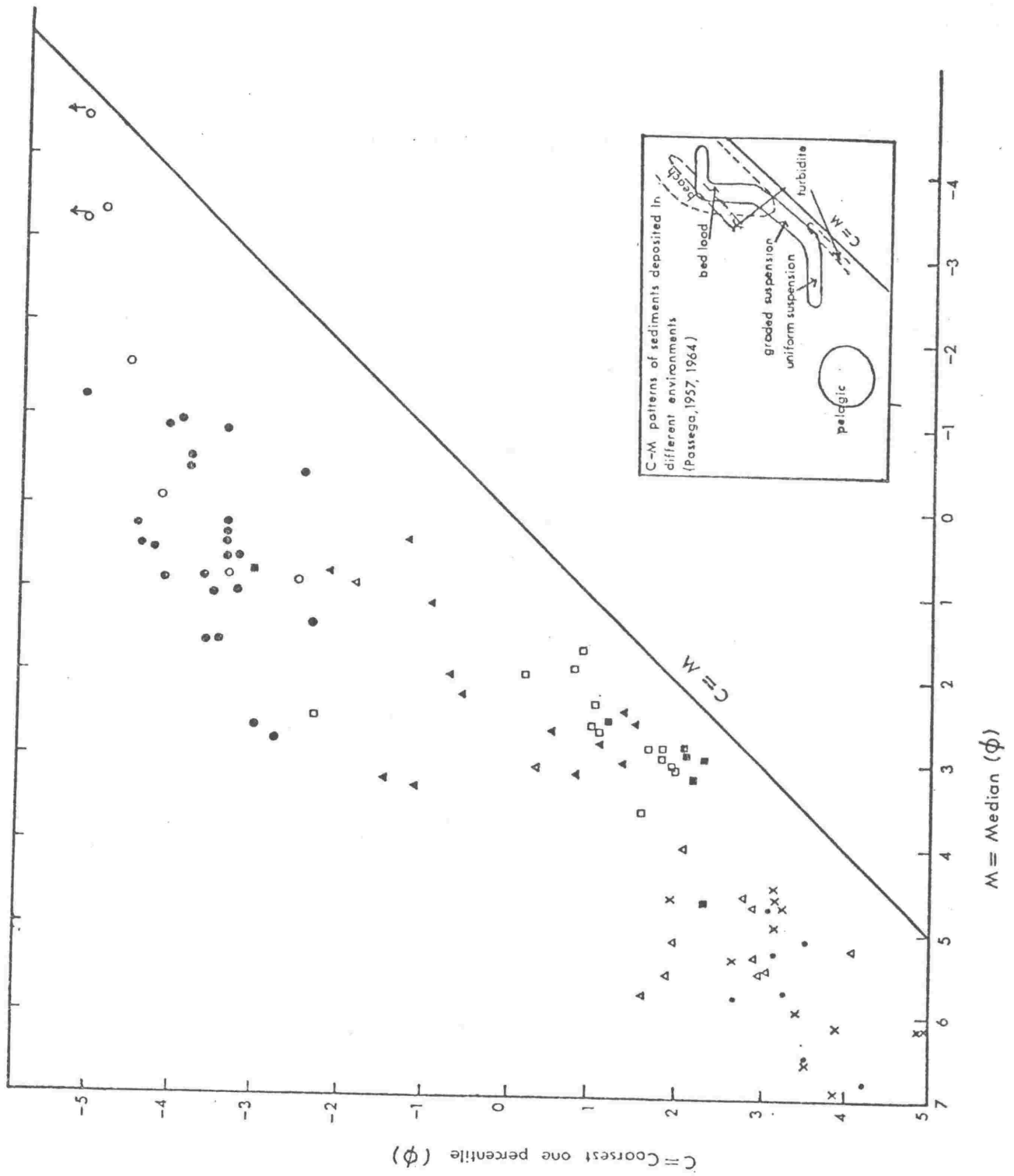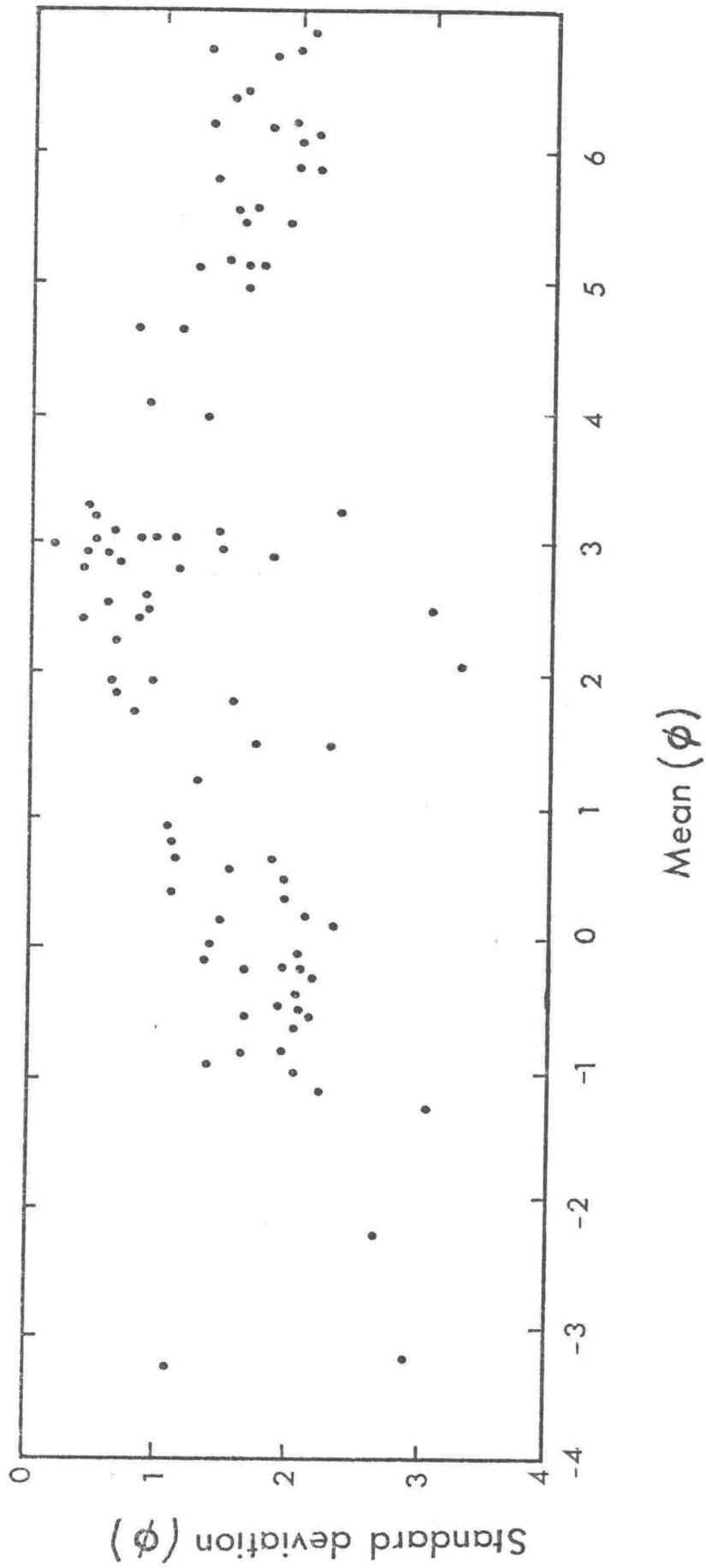
Fig. 52: Mean versus standard deviation, illustrating best sorting in the fine sand fraction.

a) Okehu siltstone-plane parallel lamination

The plane parallel laminated Okehu Siltstone are very poorly
to poorly sorted and have positive skewness, (Fig. 53, Table 18 and 19),
indicating no reworking, in agreement with an environment offshore and
below wave base.

The only significant lateral variation in mean grain size is in the
far east of the basin at the Pohangina River where this formation consists
of silty very fine sand.

Some degree of bimodality in all samples, from 4.0 to 6.0 phi
may reflect differences in grain size of different laminae. As it
does not necessarily fall on the 4.0 phi boundary it is probably not due
to the change in technique from sieving to pipetting.

An analysis of the C-M plot (Fig. 51) indicates deposition from
suspension not by traction currents. All but one sample conform to the
statement by Passega (1957) that the maximum value of C in such sediments
is seldom greater than 2 phi, and that the maximum value of M is seldom
greater than 3.3 phi.

b) Plane parallel laminated volcaniclastic silts

This lithology includes some large flasers, and partings within
the large scale cross-stratification. These beds usually display no
sedimentary structures other than incipient plane parallel lamination. The
latter may again explain the break in all curves at 5 to 6 phi, (Fig. 54).
The sediments are all poorly sorted with a positive skew, (Fig. 54,
Tables 18 and 19). The C-M plot (Fig. 51) indicates deposition from
suspension. They are also all texturally immature. These attributes
support the conclusion drawn from the associated bed forms that these
sediments are the tailings deposited after coarser sediments, all probably
deposited in one sedimentation event. Frequent gradational contact between
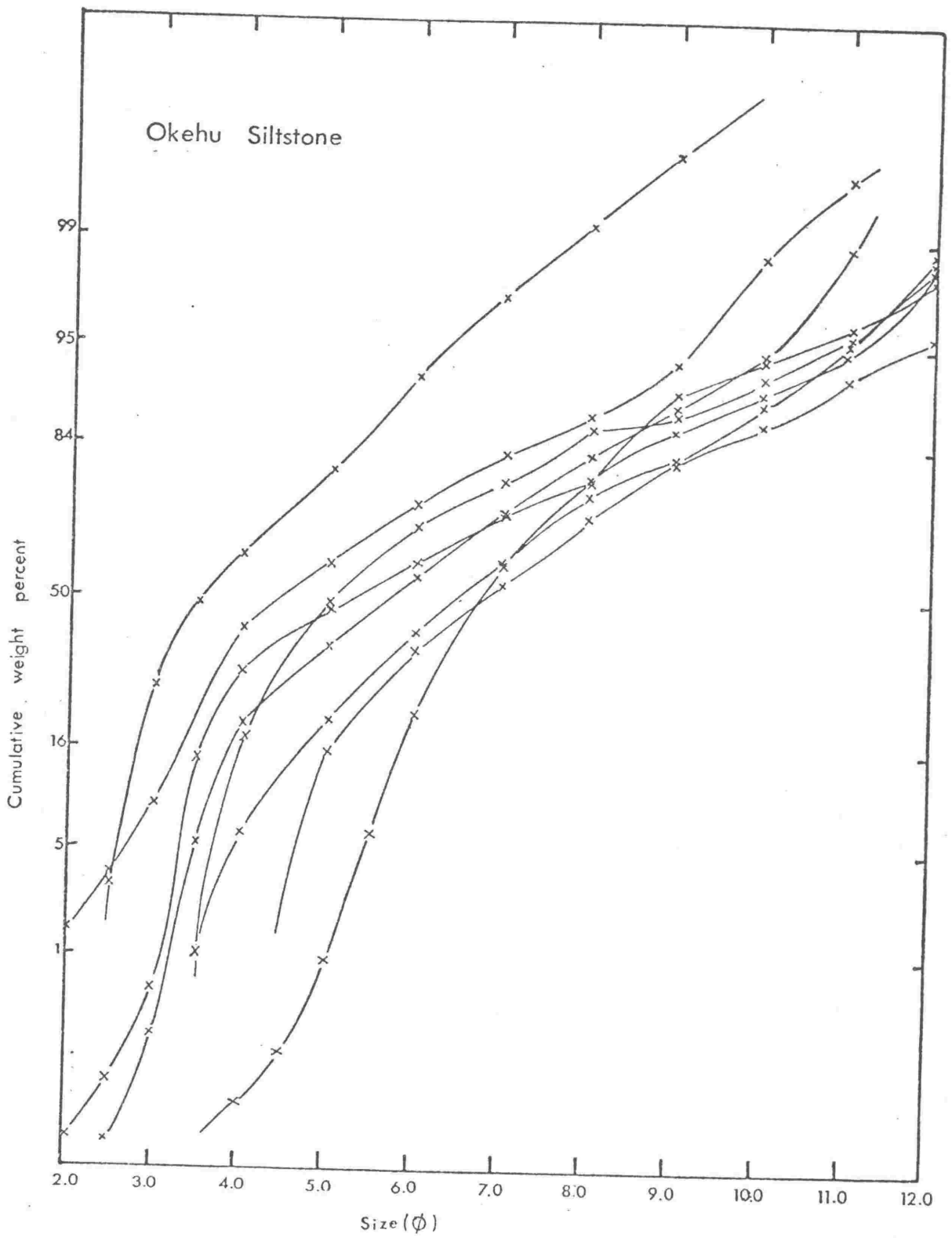
Fig. 53: Size distribution of Okehu Siltstone.

	very well sorted	well sorted	moderately well sorted	moderately sorted	poorly sorted	very poorly sorted	extra poorly sorted
Thin bedded laminated non-volcaniclastic silts	0	0	0	0	2	6	0
Thin bedded laminated volcaniclastic silts	0	1	0	1	7	1	0
Bimodal bipolar ripple-drift cross-lamination	1	3	2	0	0	0	0
Ripple-drift cross-lamination	0	0	0	1	11	0	0
Plane parallel laminated sands	0	1	4	1	4	1	0
Large scale cross-stratified sands	0	1	2	3	7	1	0
Low angle bipolar cross-stratified shelly gravels	0	0	0	1	9	10	0
Large scale cross-stratified gravels	0	0	0	0	4	3	0
Total %	1.1	6.8	9.1	8.0	50.0	25.0	0.0

Table 18: Distribution of standard deviation within the various groups defined by lithology and structure.

	Strongly fine skewed	Fine skewed	Near symmetrical	Coarse skewed	Strongly coarse skewed
Thin bedded laminated non-pyroclastic silts	4	4	0	0	0
Thin bedded laminated pyroclastic silts	4	2	4	0	0
Bipolar bimodal small scale cross-stratification	2	1	2	1	0
Ripple-drift (Type A) cross-lamination	4	4	4	0	0
Plane parallel laminated sands	5	4	3	0	1
Large scale cross-stratified sands	2	4	6	2	0
Low angle bipolar cross-stratified shelly gravels	3	5	5	5	2
Large scale cross-stratification gravels	5	0	0	1	1
Total %	32	27	27	10	4

Table 19: Distribution of skewness within various groups defined by lithology and structure.

125.
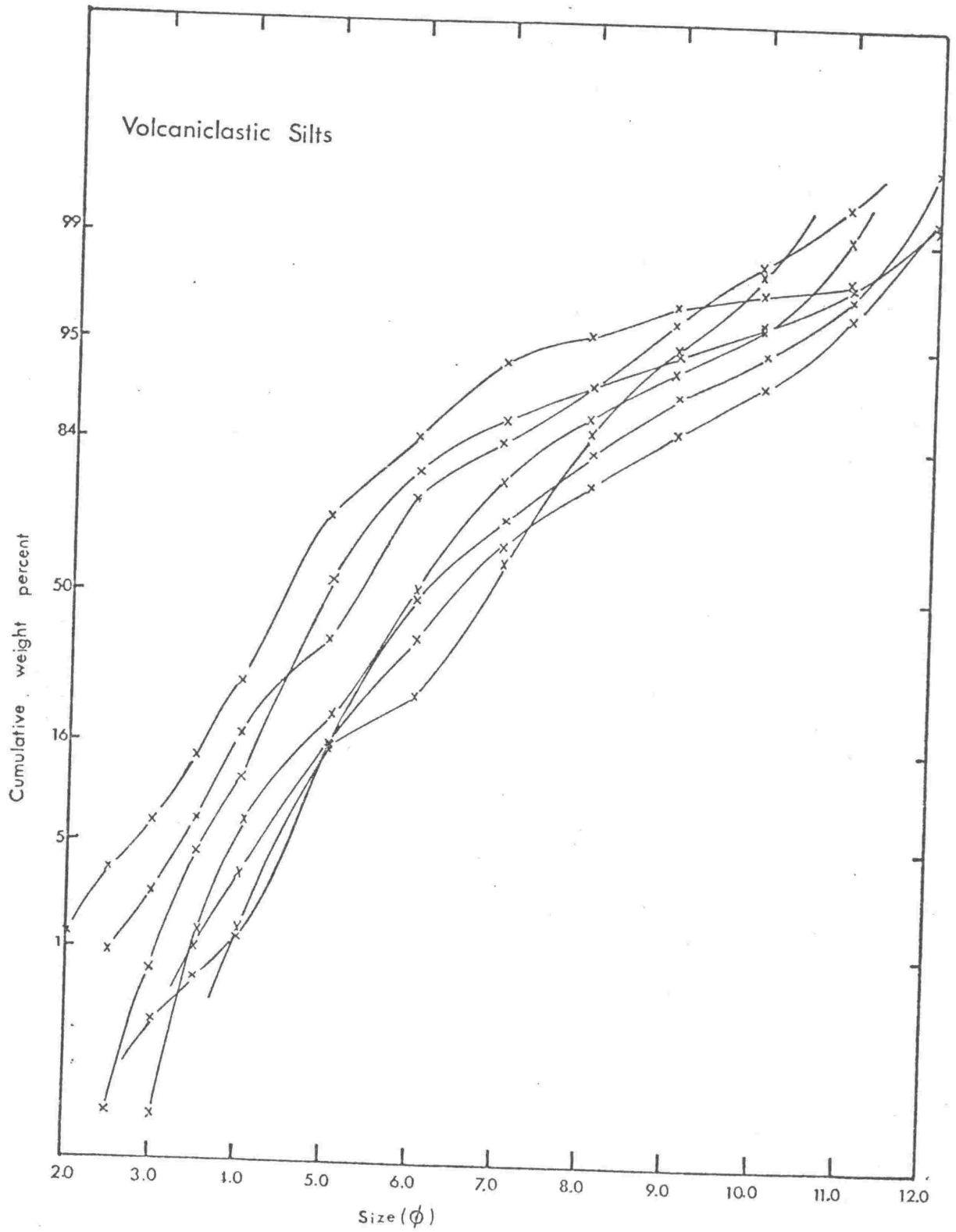
Fig. 54: Size distribution of volcaniclastic silts.

the silt flasers and the underlying sands also support this conclusion.

c) Bipolar-bimodal ripple-drift cross-stratified sands

Statistics of all samples are remarkably similar. The samples are in the medium to fine sand range, are moderately sorted with a slight positive skew in all but one case (Tables 18 and 19, Fig. 55), and all but one are classified as texturally mature. These statistics support the interpretations made from sedimentary structures that the sediments were deposited in a tidal environment, where there was continual reworking. Though finer than the beach samples analysed by Friedman (1961), they have a similar standard deviation. The statistics, when plotted similarly to Friedman however, show no environmental distinctness.

Mean size varies from 2.47 to 3.23 phi and thus can be moved by water flowing at a velocity of 20cm/sec one metre above the sediment-water contact, (Hjulström, 1939). As explained previously fine sand lends itself to better sorting as it lies in the region on Hjulström's diagram where there is a very delicate balance between erosion and deposition.

All samples but one plot very close to the C = M line of Passega (Fig. 51) which again only emphasises the good sorting. By the Passega plot the sediments are characterised as deposits from a graded suspension.

d) Ripple-drift cross-laminated sediments - mostly type A.

The samples vary from coarse sand to fine silt. Consistent with the inferred mode of origin of the sedimentary structures, sorting is poor (Fig. 56, Tables 18 and 19) indicating that the sediment was deposited rapidly and probably was covered rapidly preventing reworking.

Samples were taken from the top and bottom of one of the graded units described in chapter 2. The bottom sample was a ripple-drifted sand, type A, and the upper was a type B. The size statistics (mean 4.69phi
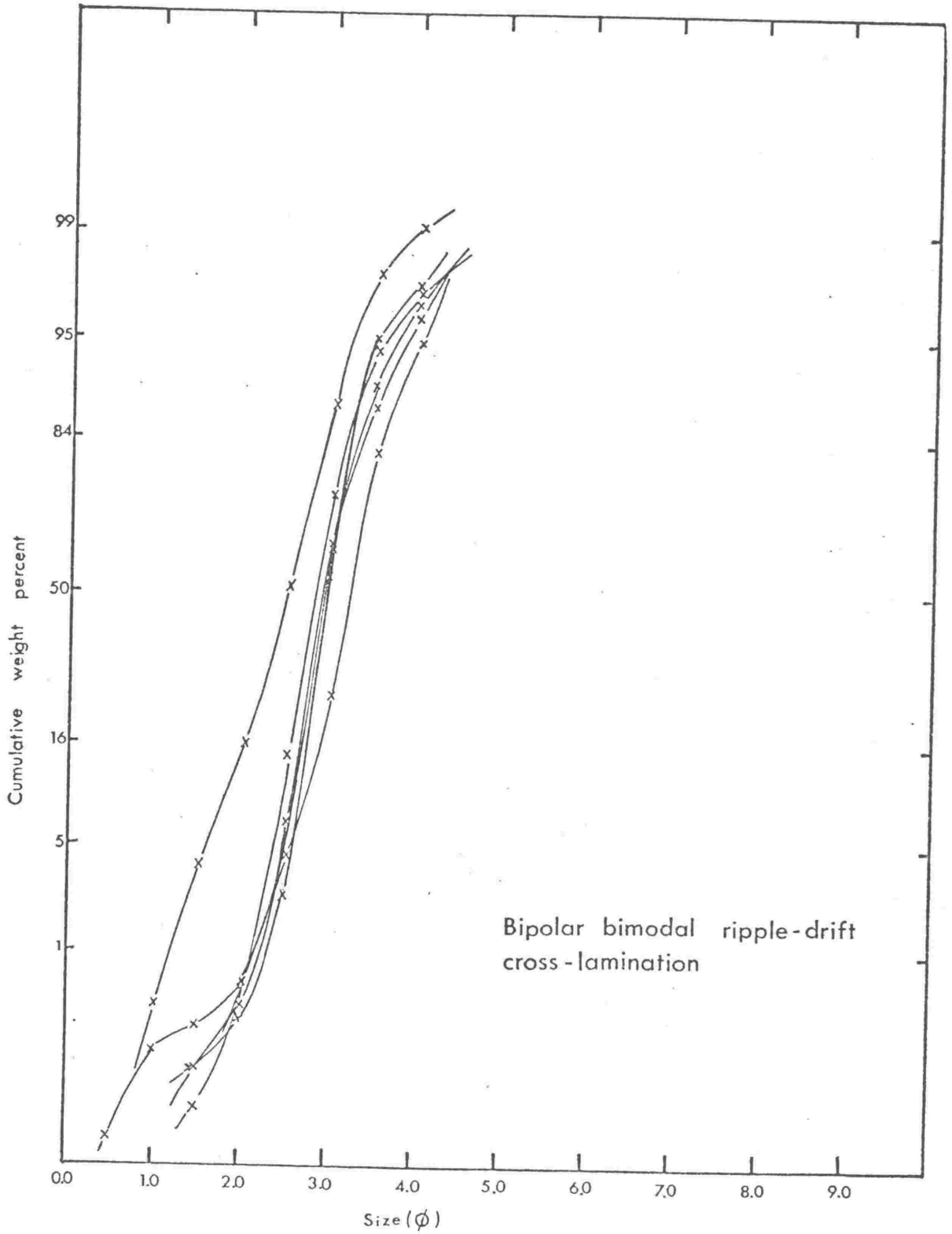
Fig. 55: Size distribution of bipolar bimodal ripple-drift cross-laminated sands.
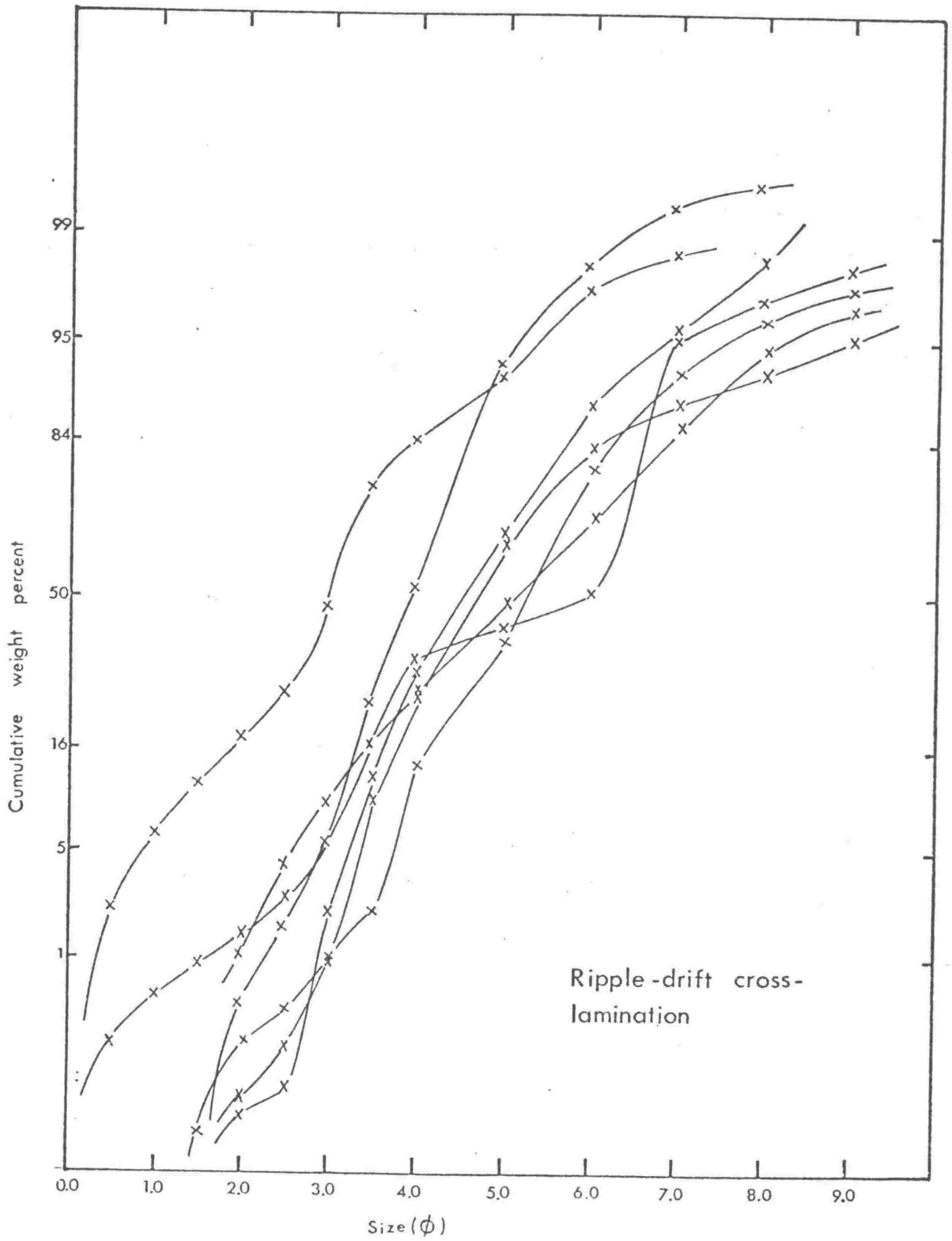
Fig. 56: Size distribution of ripple-drift cross-laminated sediment.

and standard deviation 1.13phi for the lower and mean 5.06phi and standard deviation 1.67phi for the upper) reveal an upward decrease in both. These graded units were each ascribed to one flood deposit in which the flow regime progressively decreased.

The C-M plots (Fig. 51) for the sediment displaying this structure are somewhat scattered but are mostly in the field of suspension, which previous workers have indicated is necessary for the formation of type A ripple-drift cross-lamination. Both the tephras and the volcaniclastic sands often show this type of structure. The former are texturally immature while the latter are submature. The immaturity of the tephras reflects rapid deposition of a very "youthful" material that has undergone little or no reworking during transport.

The mean grain size range suggests current velocities between 17 and 30 cm/sec one metre above the sediment water interface (Hjulström, 1939).

e) Plane parallel laminated sands

Mean grain size varies from 1.6 to 3.1phi, (Fig. 57). The change in slope in some of the cumulative curves may again be due to the alternating laminae of different grain size. All samples are texturally submature except one tephra that is immature and one other sample that is mature, (Tables 18 and 19).

The C-M plots (Fig. 51) are uniform and have C values proportional to M, which Passega (1957) suggested may indicate deposition from graded suspension. For the sizes involved the minimum velocity of the current required to transport this sand is 16cm/sec one metre above the sediment water interface, (Hjulström, 1939). Using Shields' diagram the shear velocity for the sediments in question ranges from 1.3 to 2.2 cm/sec.
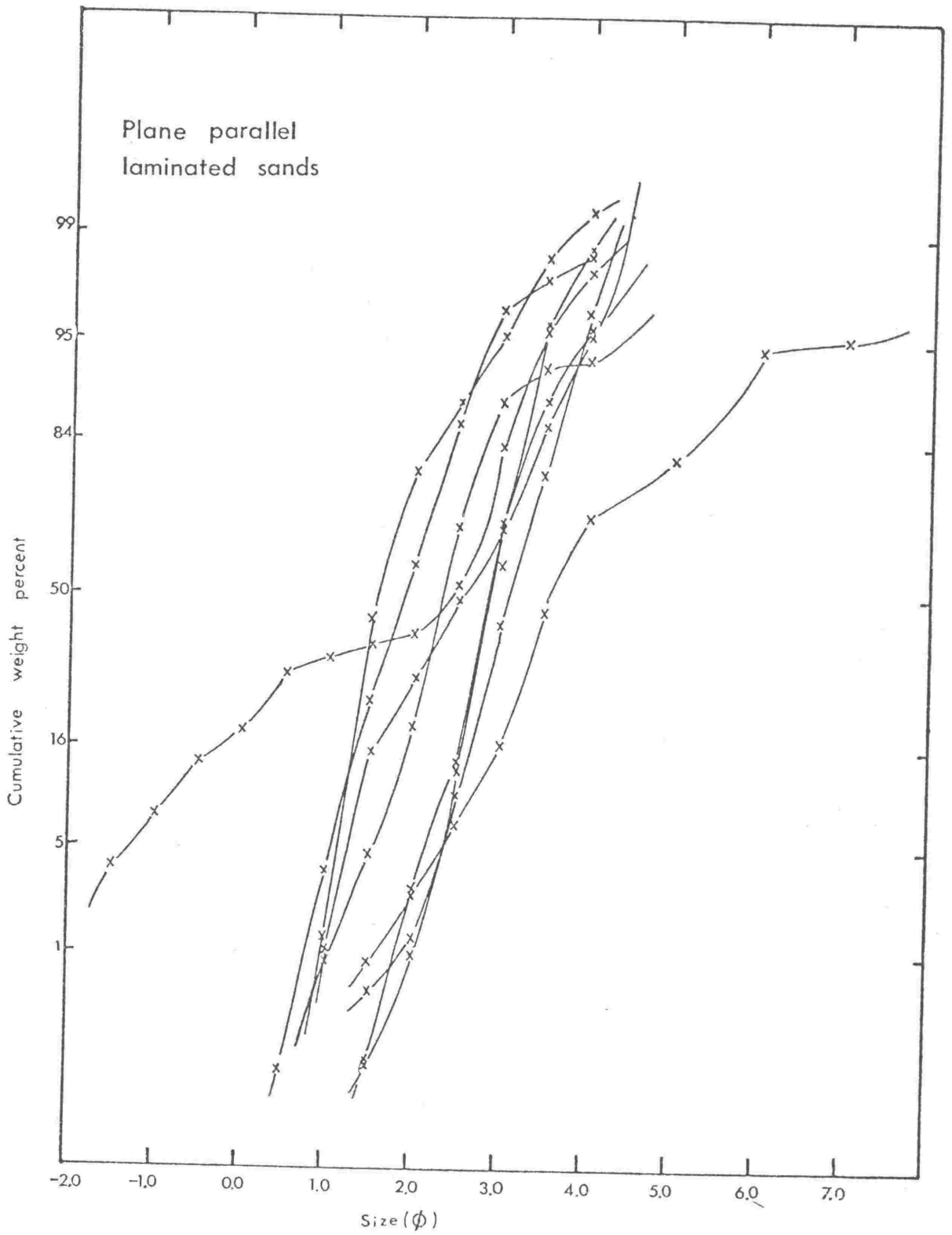
Fig. 57: Size distribution of plane parallel laminated sands.

f) Large scale cross-stratified sands

All samples from the large scale cross-stratified sands are
submature, mean grain size varies from very fine to coarse sand, sorting
is poor and skewness varies from -0.24 to +0.33, (Fig. 58, tables 18 and 19).
The size data are consistent with the deposition inferred from the sedimentary
structure, i.e. upper lower flow regime, high velocity, high sediment load
and little or no reworking. Forty percent of these samples are from tephra
horizons which again emphasises the rapid deposition and lack of reworking
of this lithology.

The range of grain sizes indicates flow velocities varying from
20-30cm/sec one metre above the sediment water interface, (Hjulström, 1939).

g) Greywacke conglomerates

All gravels composed of greywacke clasts are poorly sorted and
have a positive skew, (Fig. 59, tables 18 and 19). None of them contained
more than one percent silt. From faunal ecology (Fleming, 1953) and the
type of large scale cross-stratification associated with most gravels,
these horizons in the west probably represent intertidal gravel bars;
those in the east are more likely deposits of a braided stream, (Chapter
2). Both would have been in an environment where silt was removed by
continual reworking processes.

h) Large scale cross-stratification.— Shell conglomerates and coarse sands

All shell conglomerates and coarse sands are poorly sorted but
contain little or no silt and skewness varies from -0.70 to 0.49, (Fig.
60, tables 18 and 19). They are probably deposits of shallow sand banks,
the absence of silt fraction being due to continuous winnowing by wave
action. The shells are mostly broken and rounded indicating reworking.
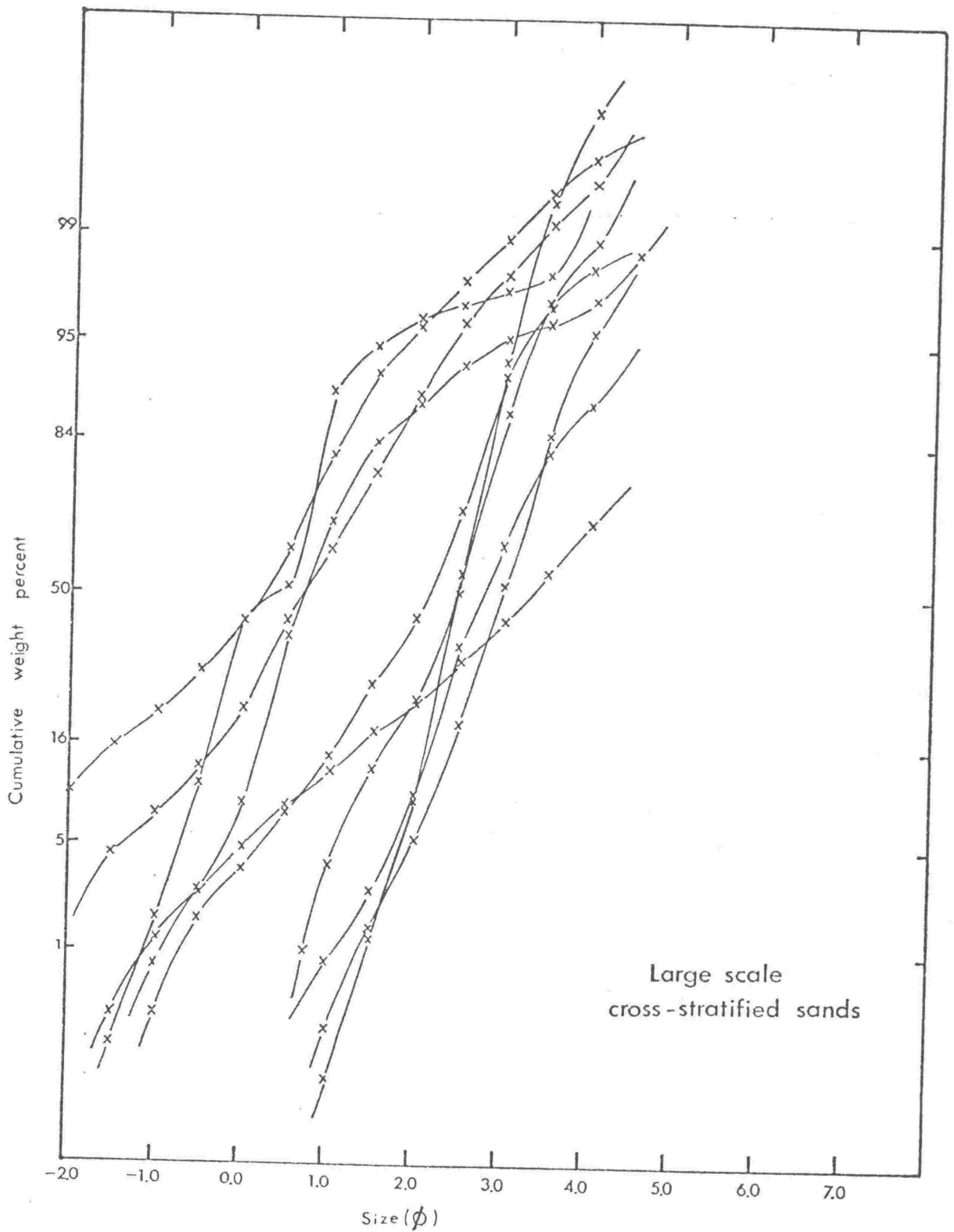
Fig. 58: Size distribution of large scale cross-stratified sands.

Greywacke conglomerates

Cumulative weight percent

Size (ϕ)
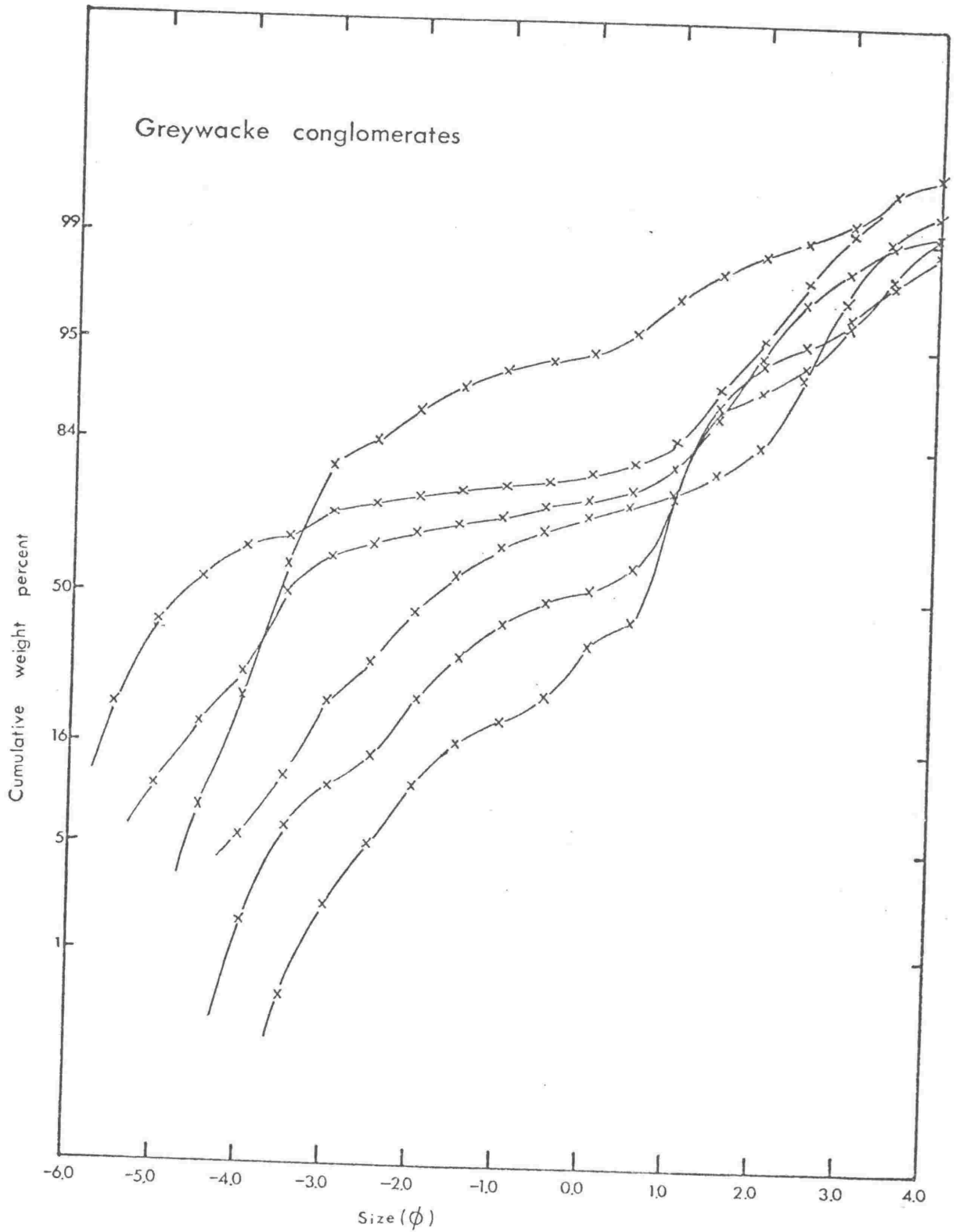
Fig. 59: Size distribution of greywacke conglomerates.
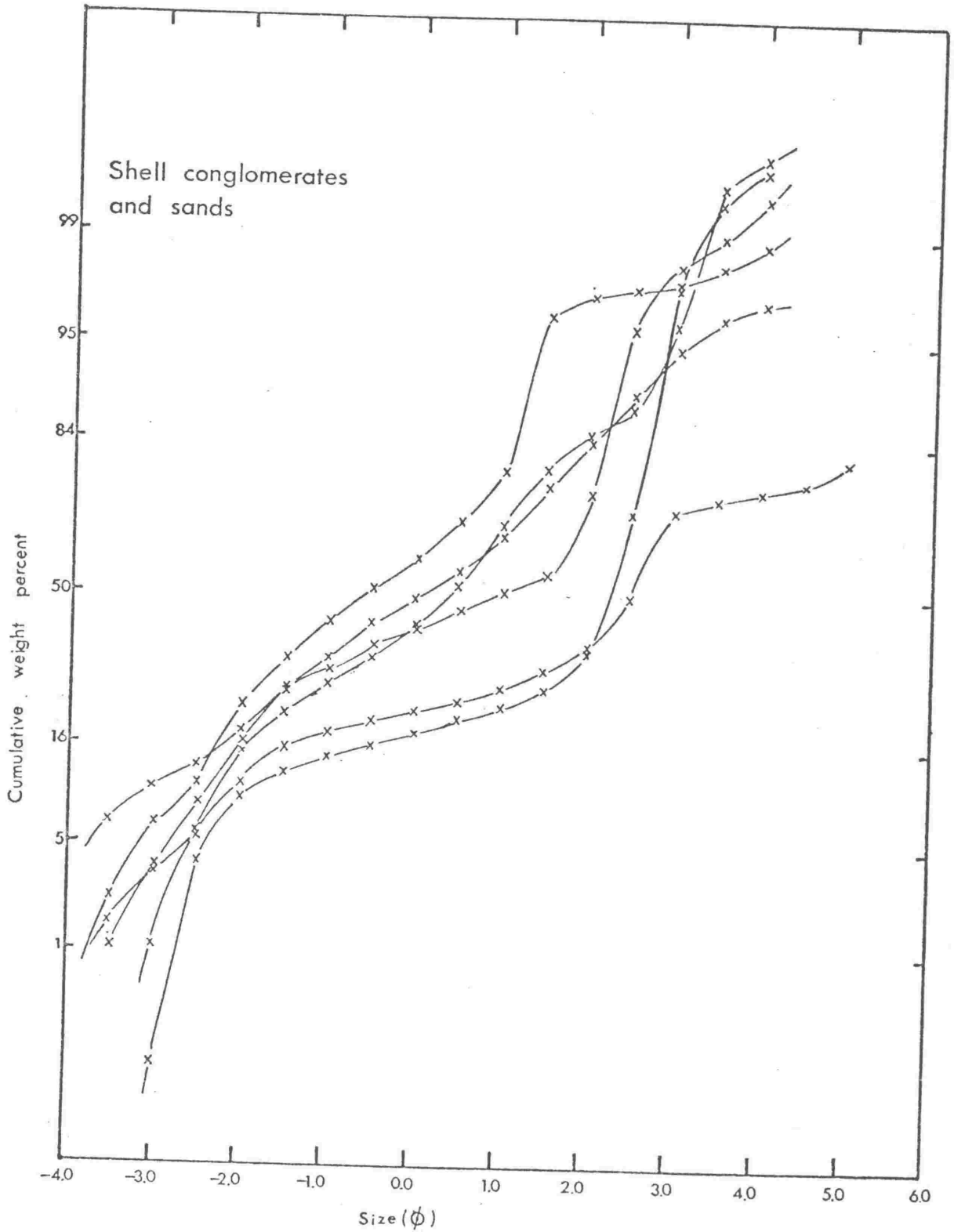
Fig. 60: Size distribution of shell conglomerates and sands.

Summary of conclusions from grain size statistics

Most of the sediments examined are poorly sorted (Table 18) owing to:

a) immature source material

b) brief transport and rapid burial

The best sorted are those that form the bimodal-bipolar ripple-drift cross-stratification, indicating continual reworking by wave action.

The majority of the samples are positively skewed which is in agreement with the poor sorting indicating little winnowing activity which can be attributed to lack of reworking or rapid burial.

These conclusions about the environment from textural evidence are in agreement with those inferred from the sedimentary structures.

Mineralogy of Sands

The striking feature of the sands is their range in composition from pure tephra to non-volcanic detritus. Their grain compositions are discussed below in approximate order of abundance:

1. Glass

Glass occurs as mostly angular bubble wall shards and pumice fragments smaller than -1 phi. It is usually colourless, and rarely slightly brown. The refractive indices are less than 1.504 indicating rhyolitic composition (Challis, 1962), confirmed by X-ray fluorescence analysis of the tephra.

It is not certain whether the tephras in the Wanganui Basin were airfall or whether they were transported by rivers flowing south. The latter seems most likely for gravel size detritus, and most tephra layers show at least some signs of reworking by marine currents, even though shards are still angular. However, in laboratory abrasion tests shards tumbled alone in a mill for the equivalent distance of 35km showed no signs of abrasion, (Van der Lingen, 1968). Those shards which exhibit some rounding are in horizons either where there is more than 50% non-volcanic detritus, or where there is coarse sand and gravel. In the former the rounding may be attributed to reworking for long periods before it was buried. In the latter it may be attributed to rapid abrasion by the pebbles (Van der Lingen, 1968).

2. Quartz

In the tephra the quartz is euhedral to subhedral with no signs of rounding, strain free, monocrystalline and free of inclusions, and is typical of quartz from a volcanic source.

In other sediments a second type of quartz was recognised, more rounded and commonly containing dust inclusions as does the quartz of the Mesozoic greywackes.

3. Feldspar

Grain mounts were etched and stained to distinguish potassic and calcic feldspar using a method slightly modified form that described by Bailey and Stevens (1960), (Appendix 5).

In all grain mounts examined plagioclase was dominant ranging in composition from An_{10} to An_{45}. Two types of plagioclase grains were distinguished, a subrounded form showing alteration and a clear angular to euhedral form with glass occasionally attached to the edges. Thin sections of the Mesozoic greywackes from the central axial range of North Island mostly contain altered plagioclase. Grains of altered plagioclase in the Pleistocene sediments therefore were presumably derived from the greywacke directly or recycled through Tertiary sediments.

The clear euhedral grains of plagioclase feldspar are probably volcanic in origin. The composition of these, restricted to An_{28}-An_{38} is consistent with a derivation from acid volcanic rocks of central North Island, (Ewart, 1969).

Potassic feldspar grains, including microcline are all subrounded. The microcline only is fresh, the rest generally sericitized. Both types occur in the greywackes of the axial ranges.

4. Orthopyroxene

Grains of orthopyroxene smaller than 0 phi occur throughout the Makirikiri Tuff and the Kaimatira Pumice Sand Formations. No orthopyroxenes or other volcanic detritus were recorded in the Okehu Siltstone. In the tephra horizons the grains are mostly euhedral and evidently volcanic in origin.

The orthopyroxenes have many inclusions of magnetite, apatite and glass. Optic axial angles ($2V_\alpha$), determined on the universal stage were between 55° and 60°. Maximum refractive index of grains from different

stratigraphic horizons varied from 1.712 to 1.720. These properties indicate a composition between Mg_{53} and Mg_{65}. Two samples from the Kaimatira Pumice Sand were analyzed by X-ray fluorescence and structure formulae calculated after removal of excess P_2O_5 and CaO, (Table 20). Though these chemical analyses indicate a composition of Mg_{50} to Mg_{51} inspection reveals up to 0.5% TiO_2 which may represent titanomagnetite which had not been extracted adequately from the orthopyroxenes during preparation. Allowing for this the composition would be slightly more magnesium rich, and thus in agreement with the optical properties.

Some of the hypersthene grains (and some clinopyroxenes) have multiple pyramidal terminations, (Fig. 61), similar to those noted by Ross et al (1929), Edelman and Doeglas (1932) and Hutton (1959). Coarse grains tend to have blunt pyramids whereas finer grains have very slender needle like pyramids that are often two or three times as long as the grain body itself. The only explanation appears to be that it is due to solution along planes of weakness, (Edelman and Doeglas, 1932). Because of their highly fragile nature solution must have taken place after deposition in the sedimentary horizons.

5. Clinopyroxene

Clinopyroxenes occur as subrounded, subhedral to anhedral grains finer than 0 phi. Optic axial angles ($2V_\gamma$) vary from $55°$-$60°$ with an intermediate refractive index of 1.710-1.720, which taken together indicate a composition of ferrosalite (Deer, Howie and Zussman, 1963, V.2, p. 1, fig. 1, p.132, fig. 41).

As they occur in the tephra horizons they are considered to be volcanic in origin. Greywackes of the axial range rarely contain augite.

	K8 original wt.	K8 wt.corrected for apatite	K148 original wt.	K148 wt.corrected for apatite
SiO_2	50.33	50.89	49.97	50.89
TiO_2	0.41	0.41	0.54	0.55
Al_2O_3	0.78	0.78	0.88	0.90
FeO	30.89	28.11	30.44	27.90
MnO	1.14	1.15	1.17	1.14
MgO	16.56	16.74	16.22	16.52
CaO	2.29	1.88	2.50	2.05
Na_2O	0.04	0.04	0.03	0.03
K_2O	0.04	0.04	0.05	0.05
P_2O_5	0.33	0.00	0.38	0.00

α	1.692 ± 0.002	α	1.698 ± 0.002
γ	1.712 ± 0.002	γ	1.714 ± 0.002
$2V_\alpha$	$55-60°$	$2V_\alpha$	$55-60°$

Number of ions on the basis of six oxygens

Si	1.967		1.964
Ti	0.012		0.016
Al	0.036		0.041
Fe	0.909		0.901
Mn	0.038		0.037
Mg	0.964		0.951
Ca	0.079		0.085
Na	0.004		0.002
K	0.002		0.003

$$\frac{100\ Mg}{Mg+Fe+Mn} = 50.47 \qquad = 50.34$$

Table 20: Chemical analyses of orthopyroxenes from the Kaimatira Pumice Sand Formation.
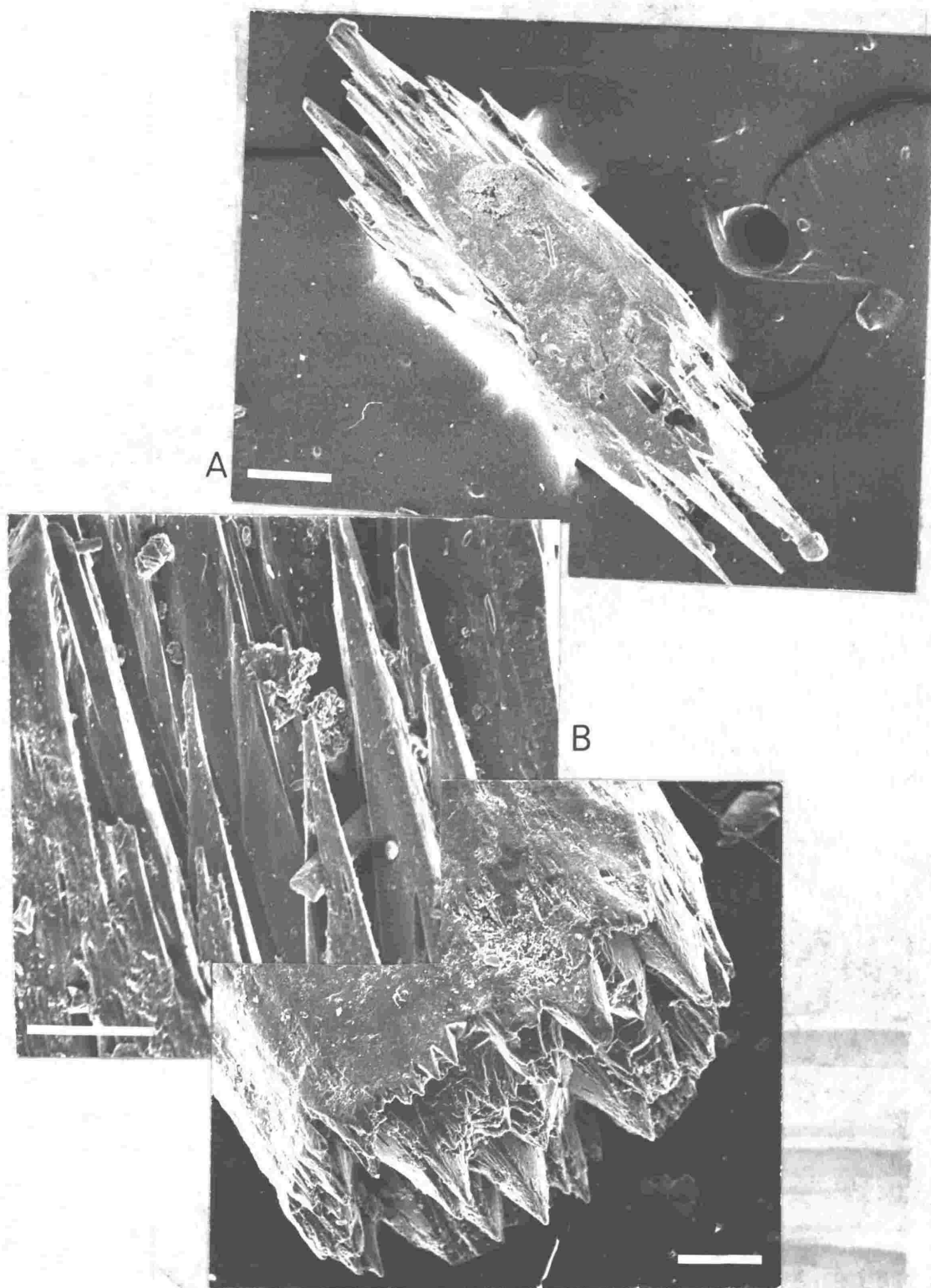
Fig. 61: Scanning electron microscope photographs of pyramidal
terminations on hypersthene grains. (Photos: P. N. Webb,
N.Z. Geol. Survey). Bar scale A = 30μm, B = 5μm, C = 10μm.

6. Green-brown hornblende

Green-brown hornblende occurs in most strata and is most common (up to 60% of the ferromagnesian assemblage) in the Potaka Pumice Member of the Kaimatira Pumice Sand Formation and least common in the Okehu Siltstone. The grains are euhedral and are unrounded in the tephra but exhibit some rounding in other strata. They range in size from 0 phi down, have $2V_\alpha$ between 70° and 80°, and a pleochroic scheme as follows:

α = light green to light brown

β = yellow green

γ = dark green to brown green

The association of the euhedral grains with the tephra horizons indicates a volcanic source. The rare grains in the Okehu Siltstone were probably derived by reworking of the underlying volcaniclastic layers.

7. Lamprobolite

Lamprobolite (not kaersutite, as electron microprobe scans revealed no TiO_2), occurs rarely and is mostly smaller than 3 phi. Although its characteristic lathe like habit is still recognisable the grains are all considerably rounded. As this mineral is usually associated with andesites and basalts, the grains may have been from the early Egmont volcanics.

8. Actinolite

Actinolite occurs in many horizons but most commonly in the Butlers Shell Conglomerate where it is associated with the metamorphic minerals garnet and chlorite. Its lathe like form is still recognisable but it generally shows varying degrees of rounding. The grain size ranges from 3 phi down. This mineral undoubtedly is derived from the metamorphic rocks of South Island.

9. Garnet

Garnet occurs in the 3-4 phi fraction of most sediments but the highest percentage occurs in the Butlers Shell Conglomerate. Grains vary from angular to rounded and often have prismatic and bubble like inclusions. The colour varies from pale pink to orange-pink.

Ten grains from the Butlers Shell Conglomerate were analyzed on the electron microprobe by Dr C. P. Wood (N.Z. Geol. Survey) and the results are listed in table 21A. End member compositions were calculated, based on the assumption that all the iron was in the ferrous state, table 21B. Results (Fig. 62) indicate a similar composition to that of garnets in the greenschist facies of South Island (Browne and Wood, 1972).

From this small sample it is concluded that the garnets from the Butlers Shell Conglomerate were derived from metamorphic rocks. The garnets in other formations are likely to have the same source.

10. Zircon

Zircon occurs in variable amounts in the fractions finer than 3 phi. It is widely distributed both areally and stratigraphically. The grains are usually euhedral but some horizons are well rounded. The euhedral grains are clear and colourless. Some of the rounded grains are pale pink; the rounding and the pale pink colour (Ledent et al, 1964) indicate that they are older than the clear euhedral grains. The surfaces of the rounded grains are minutely pitted and etched like frosted quartz grains; this may be due to solution etching.

All zircon grains have prismatic inclusions, randomly orientated, with a refractive index lower than zircon, which may be apatite. They also contain needle-like and dust inclusions.

Provenance of the zircon is difficult to determine because, besides being a stable heavy mineral that may have been recycled, it is known from a variety of sources including some ignimbrites of central North Island,

Sample	1	2	3	4	5	6	7	8	9	10
SiO_2	36.7	37.9	37.6	36.0	37.1	37.7	37.3	37.8	37.6	37.5
Al_2O_3	21.0	21.2	20.3	20.9	20.9	20.6	21.2	20.8	19.9	21.1
FeO	34.4	29.6	30.8	33.9	28.8	31.4	30.1	23.1	35.0	22.4
MgO	3.4	2.0	1.9	1.6	0.6	1.0	0.8	0.4	1.3	0.4
CaO	2.4	6.0	6.4	3.7	8.6	7.2	4.5	9.5	4.6	8.8
MnO	1.8	3.1	3.7	3.8	4.1	2.7	6.7	8.8	3.2	10.1
Total	99.7	99.8	100.7	99.9	100.1	100.6	100.6	100.4	101.6	100.3

Table 21A: Chemical analyses of garnets from the Butlers Shell Conglomerate

	1	2	3	4	5	6	7	8	9	10
Alm.	75.8	67.3	74.8	74.8	63.9	69.6	68.3	51.4	75.3	50.2
Pyr.	13.4	8.1	6.3	6.3	2.4	3.9	3.2	1.6	5.0	1.6
Gross.	6.8	17.5	10.5	10.5	24.5	20.4	13.1	27.1	12.7	25.3
Spess.	4.0	7.1	8.5	8.5	9.2	6.1	15.4	19.9	7.0	22.9

Table 21B: End member compositions of above garnets

Analyst – C. P. Wood (N.Z. Geol. Surv.)
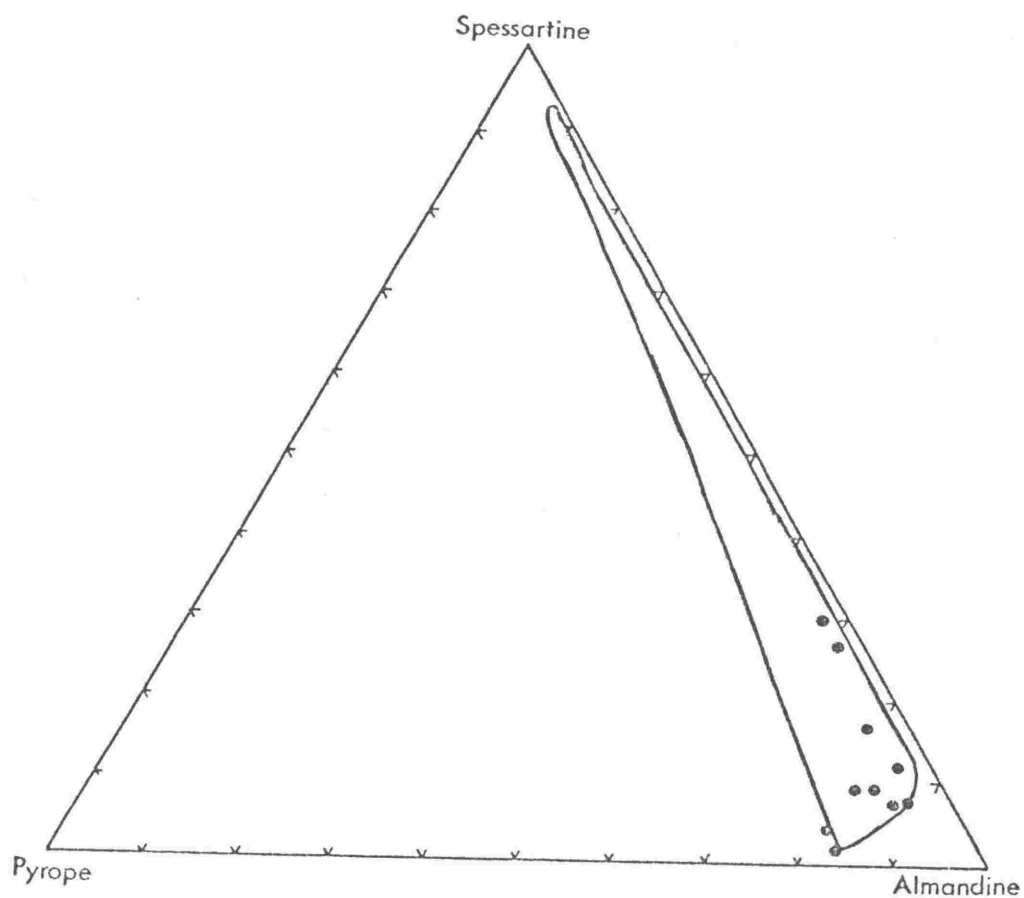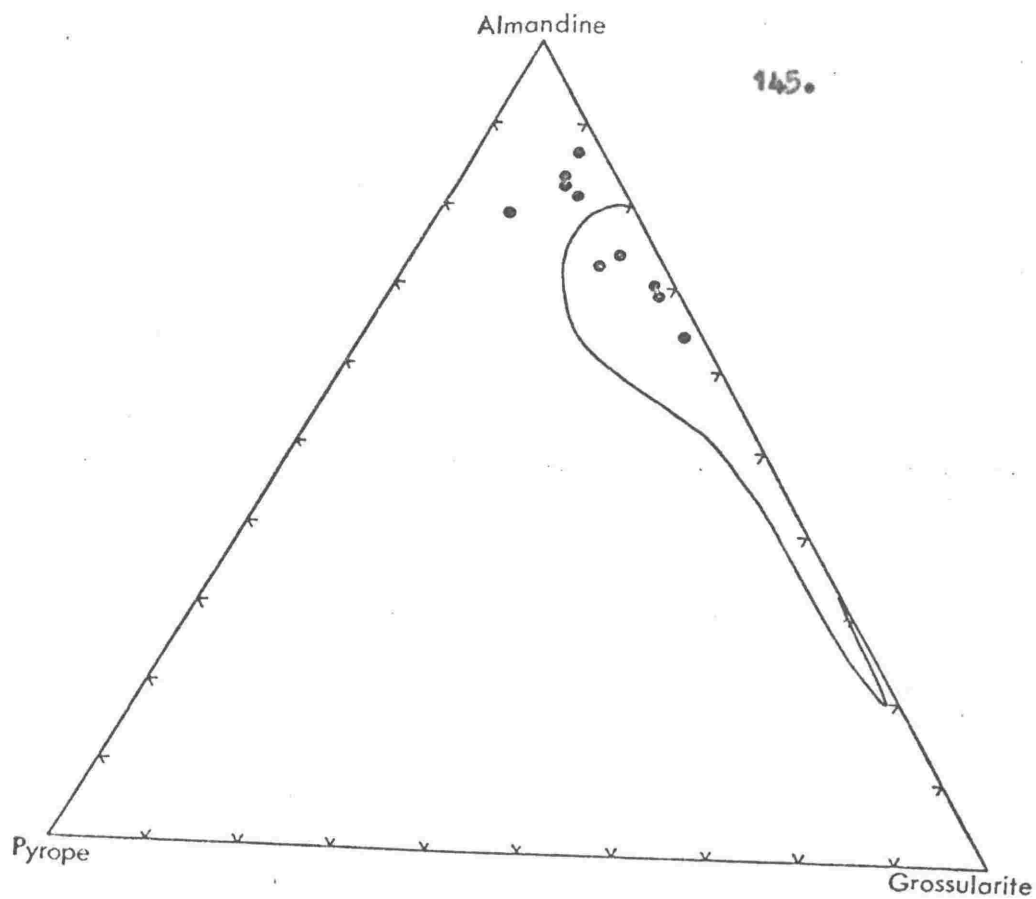
Fig. 62: Ternary diagrams, Almandine-Pyrope-Grossularite and Almandine-Pyrope-Spessartine. Solid line encloses field of garnets from New Zealand schists, (after Browne and Wood, 1972).

and is a rare constituent in the tephra horizons.

11. Epidote

Epidote is common in the 3-4 phi fraction in the Butlers Shell Conglomerate but is generally scarce in other sediments. The grains are always well rounded. The source area may either be the Mesozoic greywackes or the metamorphic rocks of South Island.

12. Biotite

Biotite occurs rarely in the fraction finer than 2 phi. Particularly in the Okehu Siltstone it shows incipient alteration to chlorite. It is a common mineral in a tephra bed of the Mangapipi Ash Member of the Makirikiri Tuff in the Rangitikei River section.

13. Chlorite

Chlorite occurs throughout the sediments in the 2-4 phi fraction, and is the dominant mafic in the Okehu Siltstone, where some show alteration from biotite. Again the source may be the axial greywackes or metamorphic rocks or, a small percentage, through alteration of biotite.

14. Other translucent grains

Monazite, tourmaline, cassiterite and rutile are very rare. Since they are all very stable heavy minerals they may have been recycled many times. Their abundance is masked by the unusual abundance of more unstable heavy minerals from central North Island.

15. Opaque minerals

The opaque minerals too are dominated by those derived from the central volcanic region. Magnetite is most abundant; ilmenite is common.

16. Rock fragments

Most rock fragments were difficult to identify positively as they are composed of silt and smaller size material. They occur in all formations,

those in the tephras probably represent material ejected with the volcanic detritus.

In the volcaniclastic sequences the rock fragments are all argillite or very finely crystalline volcanic. In the Okehu Siltstone, however, muscovite schist is the most common constituent and this points to a source in South Island. Chloritized argillites also occur, presumably from very low grade metamorphic rocks of North or South Island.

Distribution of heavy minerals within different size grades

Heavy minerals were separated using bromoform and standard techniques. Weight percentages of heavy minerals were determined for several samples on a one phi interval, (Fig. 63). In mature sands the finer fraction usually has the highest percentage, this being the normal size range of most stable heavy minerals. The immaturity of Wanganui Basin sediments is emphasised by the abundance of heavy grains in the coarser grades and by the inconsistent variation in the percentages within the size grades.

Percentages of the various heavy minerals in each one phi class was then determined using the field of view method and counting 300 mineral grains, (Fig. 64). In all cases studied the dominant mafic of the coarser fractions (0-2 phi) is hypersthene, other minerals being augite, hornblende and opaques. As the proportion of hypersthene, augite and hornblende decreases towards the finer grades, that of other minerals such as garnet and chlorite correspondingly increases. The proportion of opaque minerals also increases towards the finer grades; some very fine opaque grains may have been released on breakdown of the hypersthene.

These results confirm that two classes of sediment with different origins were supplied to the basin. Hypersthene, hornblende and augite - unstable heavy minerals (Pettijohn, 1957), were introduced with the immature volcanic detritus. The more stable heavy minerals, restricted to the finer
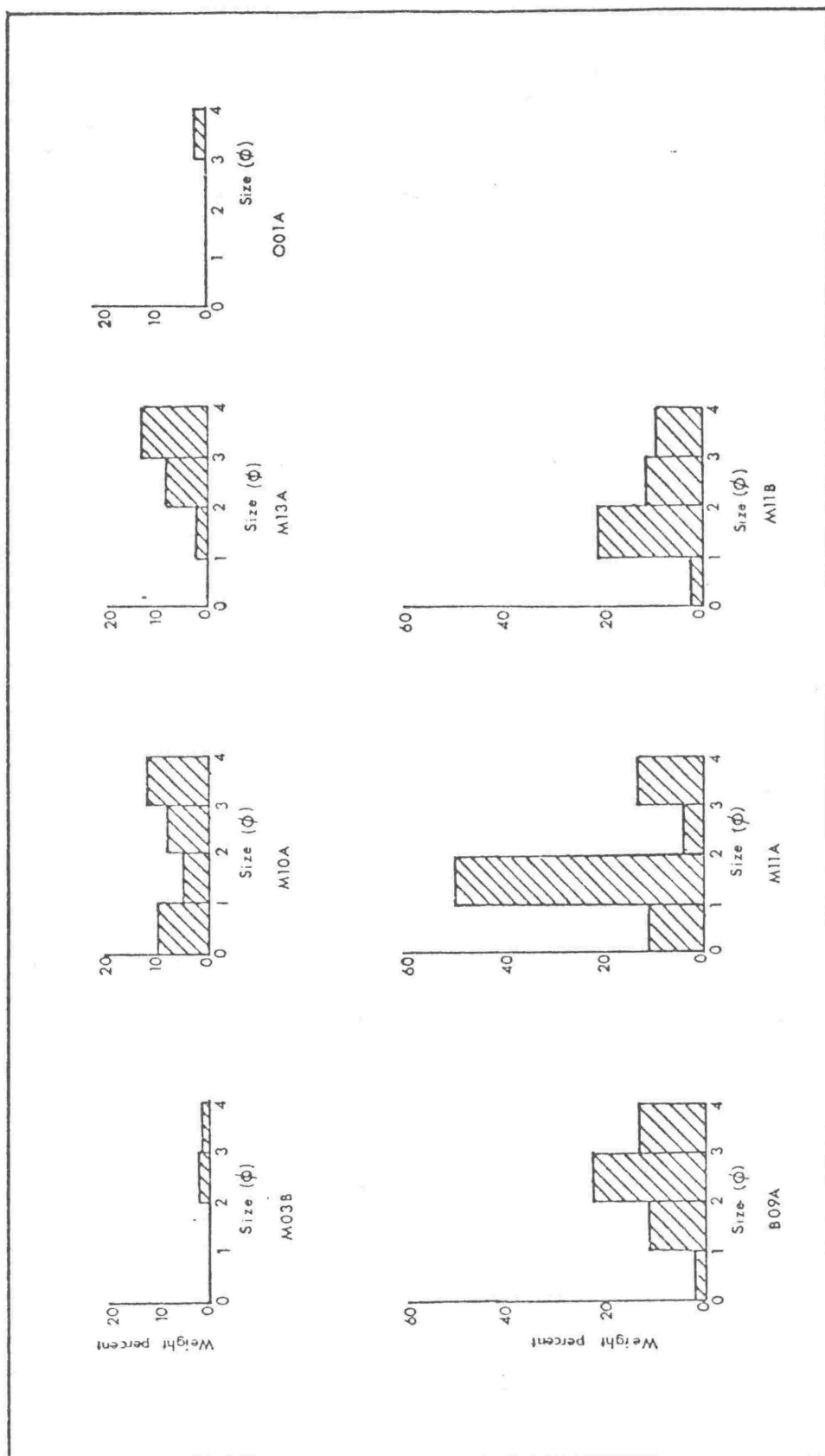
Fig. 63: Variations in weight percentages of heavy minerals, on a one phi division in sands.

Legend:

Hypersthene	
Augite	
Hornblende	
Opaque	
Garnet	
Biotite	b
Chlorite	c
Zircon	z
Epidote	e

M12A

M11B

M10A
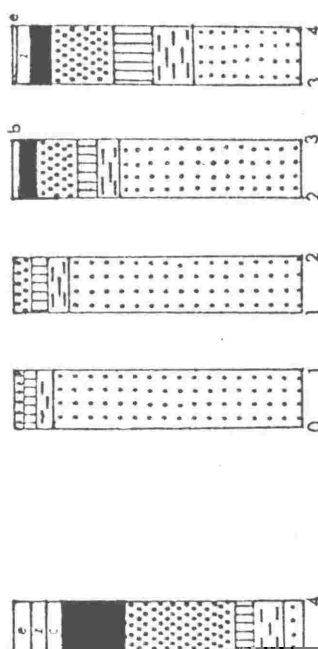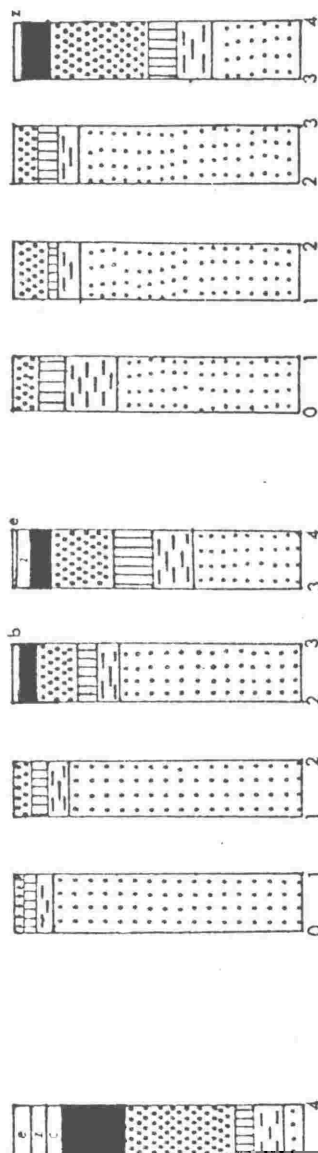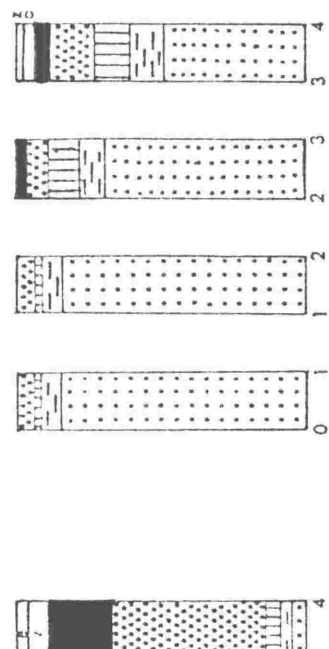
vy mineral composition in sand samples with a one phi division.
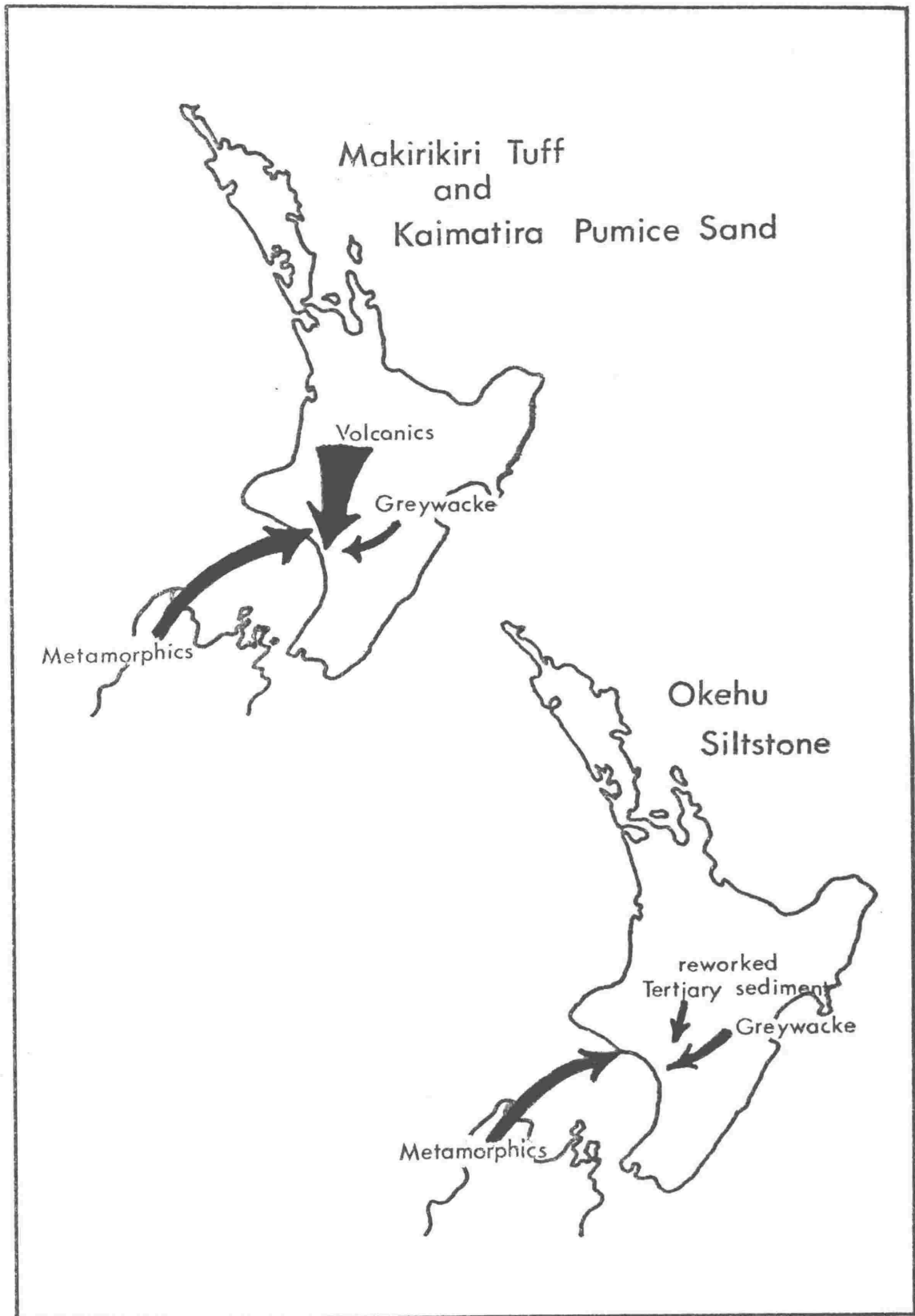
Fig. 65: Probable sources of sediment. Thickness of arrow
represents relative percentage of detritus.

sizes mostly originated from the main range greywacke or low grade
metamorphic rocks. Some such as rounded pink zircon have been recycled and
may have entered the basin directly from the Mesozoic greywackes or from
the Tertiary sediments.

Regional distribution of heavy minerals

Samples representative of a wide area were analyzed and 300 non-
opaque grains of the 3 to 4 phi fraction counted using the field of view
method, (Table 22). No areal or vertical trends could be detected within
formations. The chief factor controlling heavy mineral distribution is
variation in input of volcanic detritus and the influence of this is so
great that it may be masking any other significant trends.

General conclusions from the petrography of sands

1. Dominant source for the Makirikiri Tuff and Kaimatira Pumice Sand
Formations is the volcanic regions of central North Island, (Fig. 65)
as evidenced by euhedral grains of quartz, feldspar, hypersthene,
hornblende and augite, together with the abundance of glass.

2. When volcanic influx was lower or non-existent, (Fig. 65) as in the
case of the Okehu Siltstone, other minerals, e.g. chlorite and epidote
point to sediment source in the Mesozoic greywackes or Tertiary sediments
of North Island, or the low grade metamorphic rocks of South Island. The
latter source also supplied garnets to the basin.

3. Hornblende, though present with hypersthene, is a diagnostic mineral
for the Potaka Pumice Member of the Kaimatira Pumice Sand Formation. It is
clearly visible with the naked eye in this horizon.

Sample	Hypersthene	Augite	Green-brown hornblende	Red-brown hornblende	Actinolite	Zircon	Monazite	Rutile	Epidote	Garnet	Chlorite	Biotite
BO1A	a	c	c	s	s	s	r	r	c	C	s	s
BO1B	C	s	c	r	s	s			c	c	s	s
BO1C	c	c	c			c			c	a	c	s
*MO3	A		c									
M10A	A	c	c			s				c		
M11B	A	C	C			c			s	c		s
M12A	A	C	C			c					c	c
M22	A	r							s	c		
M27	A	r	c	r	r	r			s	r		
*M29	A		c									
*M29/2	A		c									
M32	A	r	s	r	r	r	r		r	r	r	
M35	a	r	c						s	r		
M37	a	c	c	r	s				s	r		
M47	A	c	s			r						
*M65	A											C
M82	A	c	c	r	r	r		r	s	c	r	r
M84	a	r	a	r		c			c	c	s	r
M105B	A		s	r		s	r		s	c	s	r
K02	a	a	a			s			s	c	s	
*K51	a		C			r						
K71A	A	s	c	r	r	r			s	c	s	r
K71D	C	s	c	r	r	r		r	s	c	s	
*K72	a		A									
K76	A	s	s	r	r				s	s		
*K135	a		A			r						
K140	a	r	c	r	r	c			c	s		

Table 22: Heavy mineral composition of the 3-4 phi fraction of sands.
Asterisk marks tephra samples. M = Makirikiri Tuff,
K = Kaimatira Pumice Sand.

Key: A = 50%   c = 5-9%
        a = 30-50%   s = 1-4%
        C = 10-30%   r = rare

Clast Lithology

Most clasts in the conglomerate horizons are greywacke. Others are ignimbrite, andesite, vein quartz and argillite. Petrographic descriptions of typical clasts are described in Appendix 6. Variation in relative abundance of greywacke and volcanic pebbles provides evidence about local transport and is thus plotted with the palaeocurrent and sediment transport data (Chapter 5).

The greywackes are similar to those of the Mesozoic sediments of the central axial ranges and are assumed to have come mostly from this source, with a few possibly from central North Island e.g. the Rangitoto Range. Ignimbrite pebbles are most common in the Butlers Shell Conglomerate and the basal conglomerates of the Makirikiri Tuff Formation. The ignimbrite sheets from which they may have been derived could not be determined from the lithology. Andesite clasts were not introduced into the basin until the deposition of the Kaimatira Pumice Sand Formation where ignimbrite pebbles are rare.

Thus the conglomerates positively confirm two sediment sources for the Makirikiri Tuff and the Kaimatira Pumice Sand, i.e. greywacke and volcanic terrains.

The Okehu Shell Grit clasts, contain apart from shell, only altered greywacke and argillite, suggesting a source solely in the central axial ranges.

Petrography and chemistry of the tephras

Some properties of the tephra horizons have already been mentioned. These include the description of the glass shards with a refractive index of less than 1.504, indicating a rhyolitic composition, and the heavy minerals which are listed with the heavy minerals of sands, (Table 22). The dominant mafic mineral is hypersthene except in the Potaka Pumice

where hornblende generally exceeds 50% of the ferromagnesian mineral assemblage. Augite and zircon occur rarely in some of the tephras.

Major element analysis

Samples of fresh glass from various tephra layers were analysed using a Sieman's X-ray fluorescence spectrometer. No significant differences in the bulk composition were found. All glasses have a silica content of 69-72% (Table 23).

Magnetite trace element composition

An attempt was made to use quantitative analyses of trace elements in the magnetites extracted from tephra (Kohn, 1973) to confirm correlation of different exposure of the Kaimatira Pumice Sand Formation throughout the basin. The elements that have proved most successful for distinguishing tephra in the central volcanic district of North Island are V, Co, Ti, and Mn (Kohn, 1973). Results are listed in tables 24 and 25. Those in table 24 are all from the Potaka Pumice Member of the Kaimatira Pumice Sand and all have similar proportions of those elements. The next four (Table 25) are from other horizons, one (K30D) from the Rewa Pumice, the next two (K76 and K148D) from a fine grained tephra above the Potaka Pumice, west of the Rangitikei River. The last sample (140C) is from a much younger tephra (0.32m.y.B.P.) on Finnis Road. All four of these samples are distinct from the Potaka Pumice but are similar to one another even though they are from tephras of three different ages.

It follows that similarity of trace element composition cannot be used alone to positively identify tephra in the Wanganui Basin. However the results support the correlation of the Potaka Pumice across the basin and it is possible that comprehensive analyses of all the tephras in the Wanganui Basin might eventually prove the trace element composition of titanomagnetites from different tephras to be distinctive.

	SiO_2	TiO_2	Al_2O_3	Fe_2O_3	MnO	MgO	CaO	Na_2O	Loss	Total
M38	69.12	0.24	13.85	2.40	0.07	0.28	1.09	2.58	6.80	99.48
M46	69.19	0.24	13.60	1.87	0.08	0.19	1.99	2.63	6.11	99.13
M48	71.61	0.15	12.95	1.76	0.05	0.22	1.01	2.05	5.95	99.77
M53	70.27	0.27	13.17	2.62	0.07	0.24	1.01	2.99	5.46	99.89
M23	68.82	0.19	12.19	2.20	0.08	0.17	1.01	2.72	8.49	99.67
M16C	70.34	0.15	12.23	2.04	0.11	0.08	0.77	3.48	6.96	99.98
M16Lo	69.47	0.21	12.94	2.31	0.08	0.18	1.21	3.46	6.37	100.13
K21C	69.70	0.21	12.56	2.00	0.06	0.46	1.05	2.93	6.47	99.42
K30D	69.62	0.26	12.56	2.79	0.07	0.33	1.90	2.94	5.22	99.64
K51	72.29	0.13	11.76	1.31	0.04	0.16	1.01	2.51	4.96	98.17
K67	69.10	0.29	12.62	2.35	0.05	0.79	1.26	2.96	6.81	99.81
K148D	70.16	0.18	12.66	1.83	0.06	0.30	1.30	3.50	7.18	101.12

Table 23: Major element analyses of glass from tephra beds. Sample numbers with prefix M are from the Makirikiri Tuff Formation; those with prefix K are from the Kaimatira Pumice Sand Formation.

Sample	Grid Ref.	Ti %	Mn %	V ppm	Cr ppm	Co ppm	Ni ppm	Facies
K141	N144/016776	5.8	.443	3149	252	70	98	Hornblende sands
K72	N144/216794	6.7	.536	3287	284	71	98	Tephra
K71F	N144/132795	9.1	.106	3201	356	42	116	Tephra
K90	N139/302820	8.8	.380	3682	243	60	91	Tephra
K51	N144/131795	6.2	.509	3258	371	69	104	Tephra
K148A	N139/710892	6.95	.740	3343	355	92	104	Hornblende sands
K21B	N138/567928	6.60	.504	3524	431	70	101	Hornblende sands

Table 24: Partial chemical analyses of titanomagnetites from the Potaka
Pumice. (Analyst B. P. Kohn)

Sample	Grid Ref.	Ti %	Mn %	V ppm	Cr ppm	Co ppm	Ni ppm	Tephra
K30D	N144/125797	8.7	.594	1033	111	63	53	Rewa Pumice
K76	N138/844853	8.3	.575	963	76	47	47	?Kaukatea Ash
K148D	N138/710892	8.95	.500	1439	119	118	339	Kaukatea Ash
140C	N144/253585	9.00	.715	1604	214	60	56	Lower ash on Finnis Rd

Table 25: Partial chemical analyses of titanomagnetites from other tephras.
(Analyst B. P. Kohn).

Lignites

A few lignites overlie identifiable palaeosols and one example is described in chapter 2. However the great majority of the lignites are associated with tephra layers. They vary in thickness from a few millimetres to 0.5 metre and are generally lensoid in form. There is no indication of seat earth or root structures in the sediment immediately beneath them. The recognisable plant structures are compressed and many are distinctly charred. Owing to the poor preservation only one specimen could be identified by B.P.J. Malloy (Botany Division, D.S.I.R., Christchurch). This specimen was from locality 153(N149/215380) and is Leptospermum sp., probably L. ericoides or kanuka, which implies dry seasonal conditions (B.P.J. Malloy, pers. comm.).

The lignite lenses lie in the lower portions of the tephras. Up to seven lenses have been observed separated by tephra layers up to 0.5 m thick. They are presumed to represent vegetation charred during nuees ardentes eruptions in the central North Island. These nuees were probably the pumice breccia type as burned wood has never been found in New Zealand associated with ignimbrites. The charred vegetation was probably transported to the Wanganui Basin by flood waters after the eruptions. The transport of charred vegetation by mud flows was observed following eruptions at Mt Lamington, Papua, 1951 (Taylor, 1958).

The upper parts of each major tephra unit, with no lignite may be up to 1.5m thick and may represent the major eruption of the phase represented by the whole tephra sequence. The lack of lignite in the higher parts of the sections may be because the major eruption was an ignimbrite or because vegetation in the area of the eruption had already been destroyed by the initial nuees of the phase.

It is assumed that the lignites represent strand or near strand deposits.

Palaeocurrent analysis from cross-stratified sediment

Introduction

The Makirikiri Tuff and Kaimatira Pumice Sand Formations of the
Wanganui Basin are mostly deposits of a shallow water shoreline environment.
Evidence for this was described in previous chapters, and includes the
presence of intertidal to subtidal molluscan fauna, detrital lignites which
are presumed to represent strand line deposits, and rare palaeosol horizons
indicating occasional emergence. Evidence for tidal environment from
sedimentary structures includes channels, symmetrical ripples, flaser
bedding and abundant bipolar-bimodal cross-stratification.

Sediment transport directions for such shoreline deposits may be
influenced by longshore drift, tidal and wind-driven currents, and the
outflow of rivers. These influences can be expected to change and interact
in a complex fashion over small distances and short periods of time.
Nevertheless a study of palaeocurrent directions for these formations was
considered worthwhile to document the degree of complexity of palaeocurrent
systems in a positively identified tidal environment, and to estimate its
usefulness in a sediment transport study.

Several directional studies have been undertaken on recent inter-tidal
environments as accessibility is relatively easy. However, there are very
few detailed studies of subtidal current transport systems, using foreset
dip directions of cross-stratification as the current indicator. One of
these was by Reineck (1963) in the south-eastern region of the North Sea.
He determined direction of sediment transport from cross-stratification
in box cores and found different current patterns in different geographical
environments:-

a) in the intertidal zone sediment transport was diagonal to the coast,
paralleling the tidal current.

b) Between barrier islands (East Frisian Islands) and the mainland
sediment transport was in two directions; 1, parallel to the tidal
current, and 2, at right angles to the tidal current away from the
mainland.

c) On the immediate open shelf beyond the islands directions again paralleled
the tidal current, but farther out to sea there was no dominant sediment
transport direction.

d) Off the mouths of rivers current directions were seaward and landward
due to tidal currents. In addition, there were currents paralleling the
coast, which were also bipolar.   The resulting pattern is quadrimodal.

These complex patterns of sediment transport in near shore environments
have been observed on a single time plane. An additional problem for the
geologist is that shoreline sedimentary environments are ephemeral; small
scale fluctuations in the sea level may cause large lateral changes in the
position of the shoreline with associated facies changes. Sedimentary
sequences, which have accumulated over thousands of years (Makirikiri Tuff -
200ky, Kaimatira Pumice Sand - 130ky) are likely to retain an extremely
complex pattern. Perhaps, for this reason, few palaeocurrent studies have
been undertaken on shallow water deposits. Tanner (1955) and Selley (1967)
both confirmed this complex nature of palaeocurrents in fossil shoreline
deposits.

Development of a palaeocurrent model is difficult for tidally
influenced marine environments. Potter and Pettijohn (1963) noted "the
model concept supposes the maintenance of a particular set of conditions
which produces a particular basin-wide pattern of sedimentation, during a
significant interval of time". During Okehuan times the coastline was
probably slightly inland of the present outcrop of the two formations
studied (Fig. 66), with dominant sediment source in the central volcanic

district to the north and the axial ranges to the east, as today. A
model is thus proposed (Fig. 67), based on current systems operating
today along the Wanganui coast (Lewis, pers. comm., 1973).

Data collection

In most cases azimuths were measured on at least three sets of
large or small-scale cross-stratification. A total of 244 such groups
were measured. Readings in each group were confined to one structure. As
the sediments are unconsolidated it was possible to cut back exposures with
a spade to determine the direction of maximum dip. However, error in
measuring each direction was probably of the order of $\pm 5^{\circ}$.

Other directional features, such as channel orientation and pebble
imbrication were measured, but were too few to be useful in the final
analysis.

Mathematical analysis

Vector means (Curray, 1956) were computed for each group and the
standard deviation was calculated about the mean as if the data were linear
(Barrett, 1970). Vector magnitude computed as a percent, and confidence
intervals, were also determined, (Appendix 7).

In analysing the data at each locality it was evident that a large
proportion were bimodal. For these cases separate vector means were
computed for each mode. At sites where bimodality was obvious, the numbers
of directions were taken roughly in proportion to the numbers of cross beds
trending in each direction. For this reason, individual readings were used
when directions were grouped on a grid (Figs 68, 69, 70, 71) so that the
relative abundance of different directions is preserved on the rose diagram.
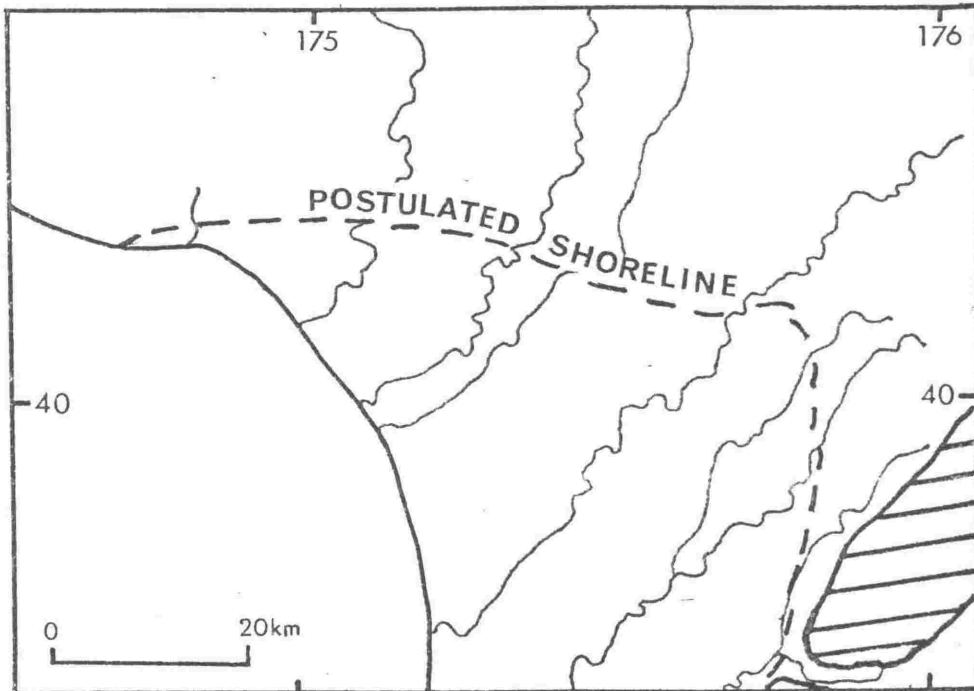
Fig. 66: Position of the postulated shoreline during the deposition of the Makirikiri Tuff and Kaimatira Pumice Sand Formations.
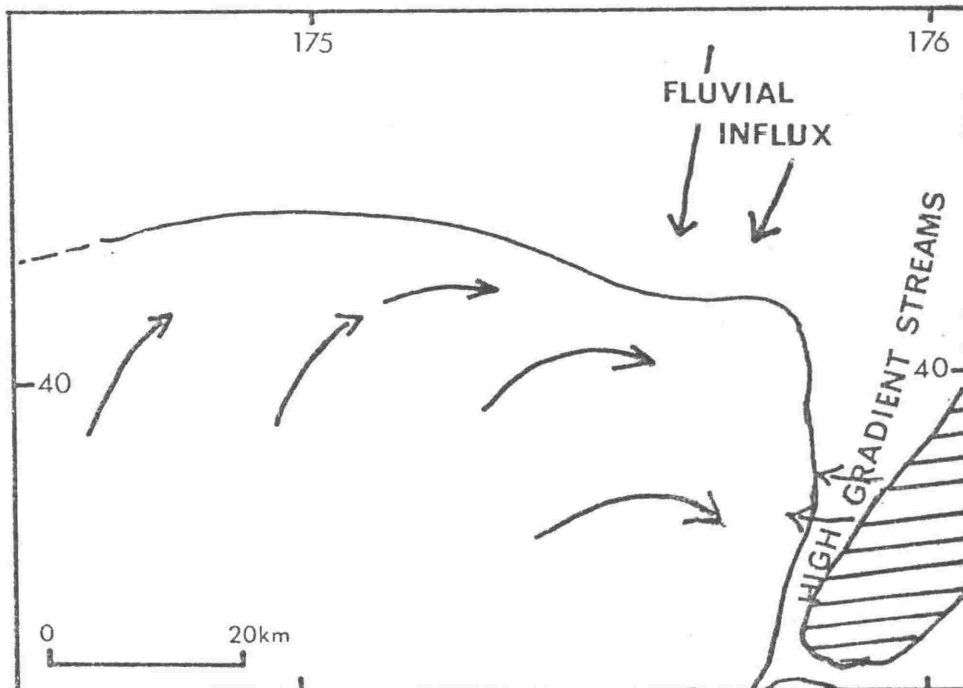
Fig. 67: Palaeocurrent model postulated for the time of deposition of the Makirikiri Tuff and Kaimatira Pumice Sand Formations.

Fig. 68: Palaeocurrent pattern revealed by foreset dips of
large-scale cross-stratification in the Makirikiri
Tuff Formation. Grid numbers refer to the
NZ 1:250,000 maps.

Makirikiri Tuff

Grouped data

43 readings

Suggested pattern
of dominant
sediment transport

10 readings

N

0   10km
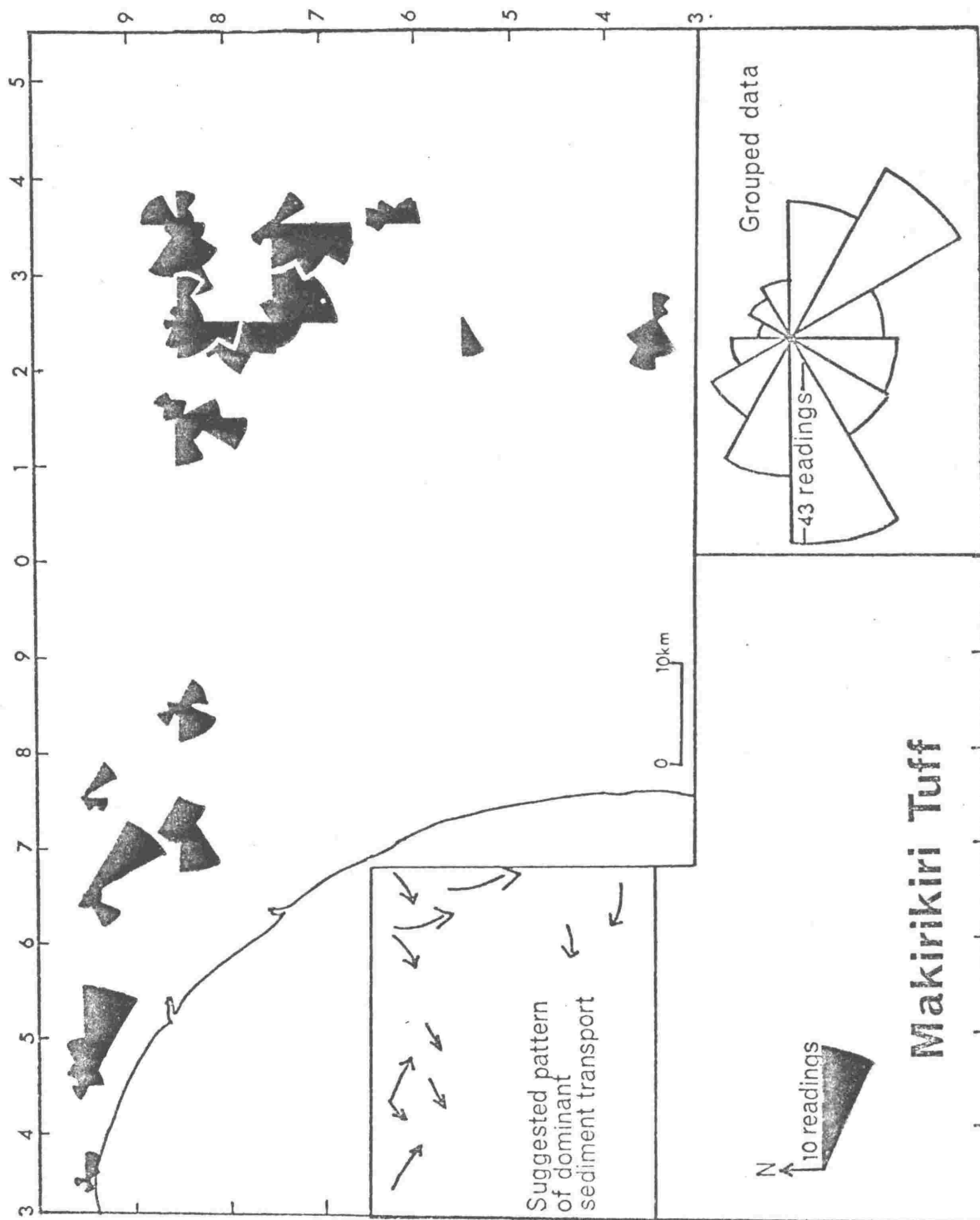
Fig. 69: Palaeocurrent pattern revealed by foreset dips of
          small-scale cross-stratification in the Makirikiri
          Tuff Formation. Grid numbers refer to the
          NZ 1:250,000 maps.
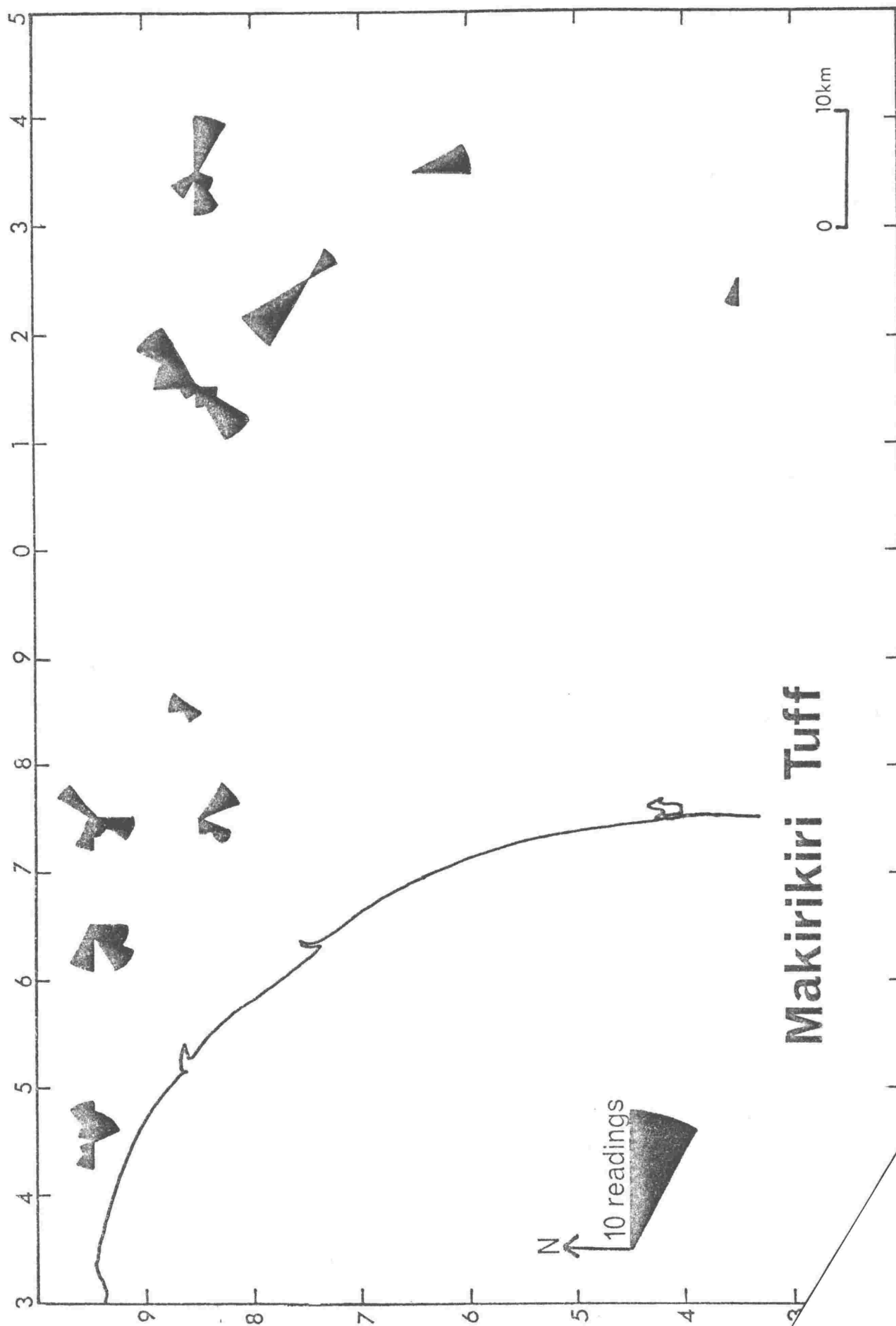
Makirikiri Tuff

Fig. 70: Palaeocurrent pattern revealed by foreset dips of large-scale cross-stratification, in the Kaimatira Pumice Sand Formation. Grid numbers refer to the NZ 1:250,000 maps.

Kaimatira Pumice Sand

Grouped data

10 readings

N

36 readings

0 10km

Suggested pattern
of dominant
sediment transport
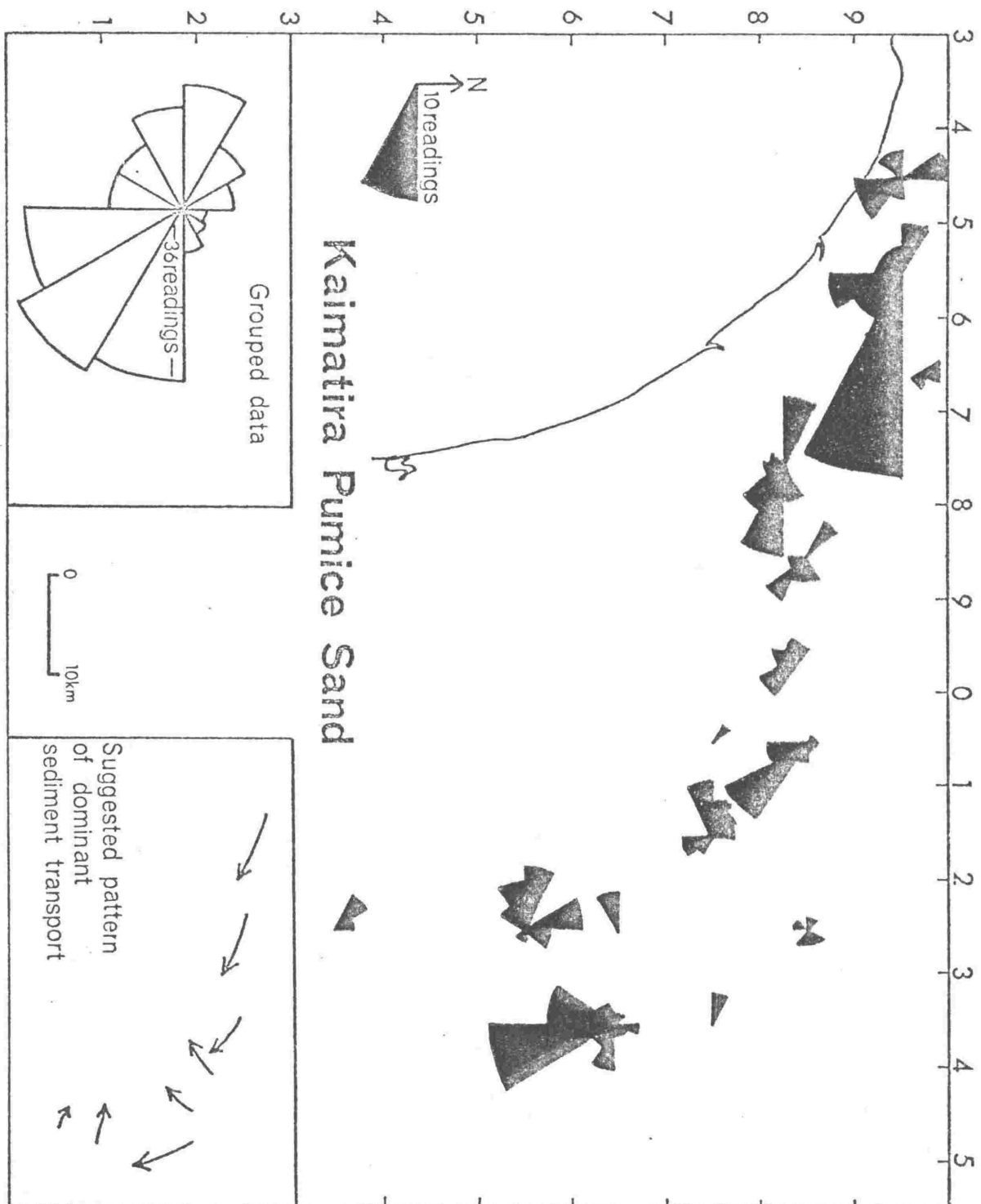
Fig. 71: Palaeocurrent pattern revealed by foreset dips of small-
scale cross-stratification in the Kaimatira Pumice Sand
Formation. Grid numbers refer to NZ 1:250,000 maps.

Kaimatira Pumice Sand
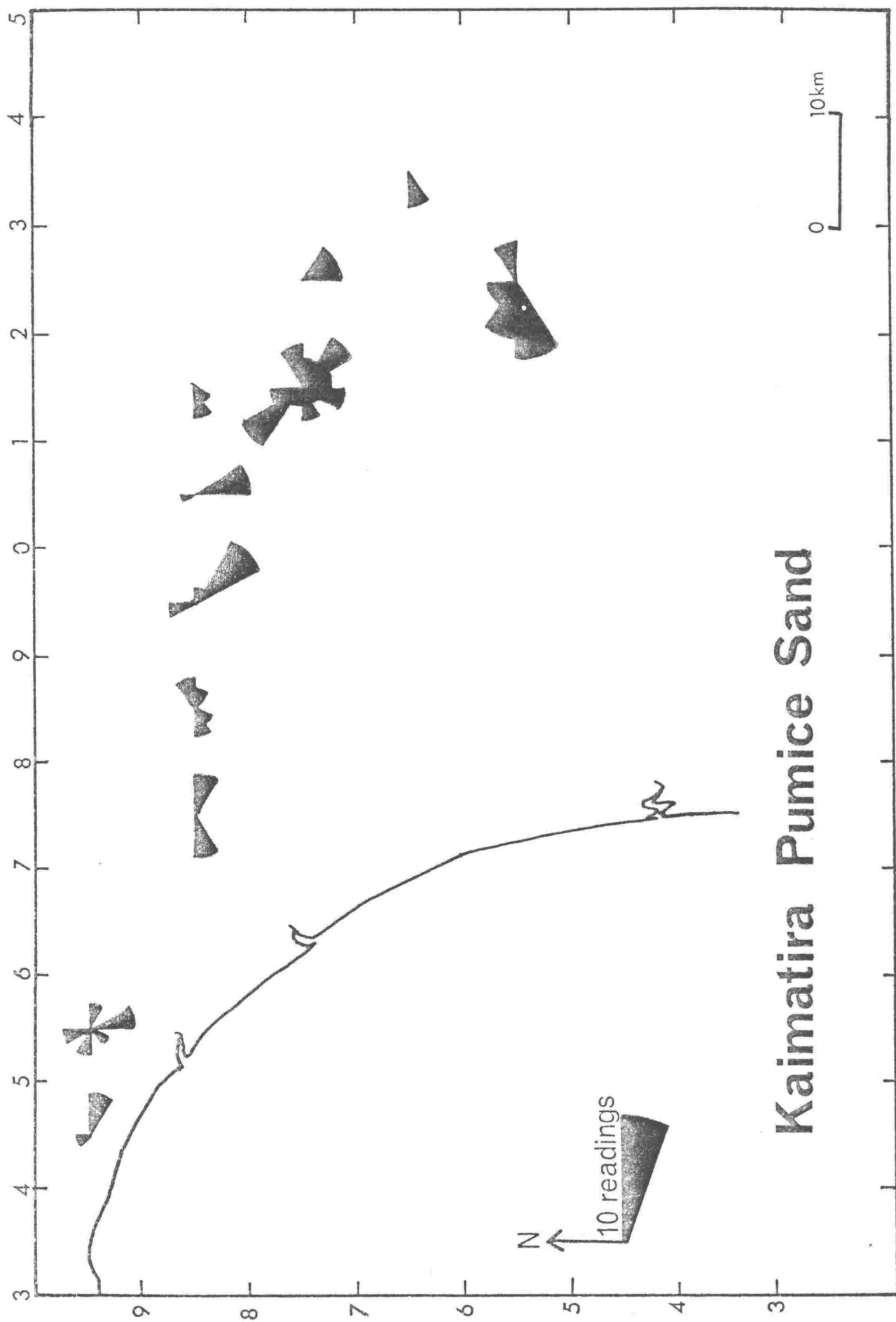
Results and discussion

Regional variation

Individual cross bed directions were grouped on the New Zealand four mile to the inch map, i.e. the edge of each grid square represents 10,000 yards.

1) foreset directions of large scale structures in the Makirikiri Tuff Formation are bimodal with the dominant mode seaward but at an angle to the postulated coast, (Fig. 68). On the south eastern fringe of the basin the dominant mode is seaward and normal to the postulated shoreline.

2) Small scale cross-stratification shows no regional trends (Fig. 69) and may therefore be controlled by local topography rather than a regional current system, or may have varied more over small intervals of time.

3) Large scale cross-stratification for the Kaimatira Pumice Sand is also bimodal but dominantly directed at an angle away from the postulated shoreline, (Fig. 70).

4) Small scale cross-stratification again shows no regional trends although a few modes in the centre of the basin show some parallelism with the large scale structures, (Fig. 71).

Reliability of large and small scale cross-stratification as direction indicators

Allen (1967), commenting on the hierarchy of sedimentary structures as flow indicators, concluded that large scale structures were truer indicators of flow direction over a large area than small scale structures. The larger structures are the product of higher flow regime conditions where greater bed roughness and more turbulent flow with more cross currents would tend to produce a greater variation in direction over a small area, but over a large area are more representative of regional flow. Small scale structures, on the other hand, are formed during more uniform flow conditions, showing

little variability over a small area, but great diversity over a large area.

However small scale structures with their low internal variability because of their size, are easier to measure, whereas estimation of true direction of large scale structures is more difficult to determine accurately.

For groups where more than four readings had been taken some assessment of reliability can be gauged by examining variation in standard deviations, (Fig. 72). The small scale bedding has a smaller mean deviation than the large, (15° and 20°) respectively. The modal class for the small scale structures is 5° to 9°; the large scale is bimodal, the dominant class being 15° to 19°, and the subordinate 5° to 9°. Insufficient data were recorded in the present study to discern the meaning of the two modes but it is here suggested that the lower values, being the same as the small scale mode, may in fact be the standard deviation for the smaller of the large scale cross-stratification.

In general, however, the results indicate greater reliability of means determined from small scale structures. As mentioned previously, the greater variation in direction within large scale cosets may represent either a real variation or variation due to sampling.

A similar pattern is indicated when confidence intervals/are plotted (95% level) for groups where four or more readings were taken, (Fig. 73). Of the small scale groups 91% have confidence intervals less than 30°, whereas of the large scale groups only 77% have confidence intervals less than 30°.

<u>Variation in current direction with time</u>

Variations in current direction in stratigraphic sequence are plotted in figure 74. Results indicate:

1) Small-scale cross-stratification is more frequently bimodal than large. In all but one section 50% or more cosets of small scale structures are bimodal.
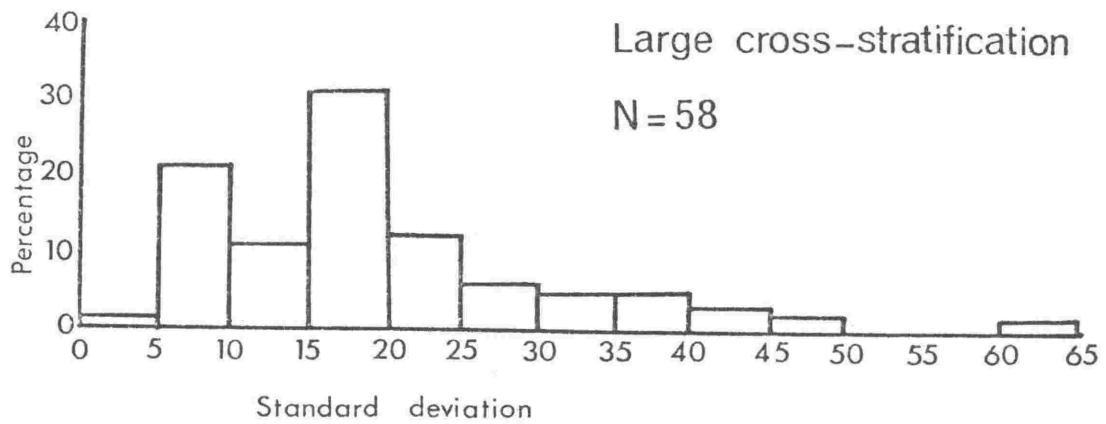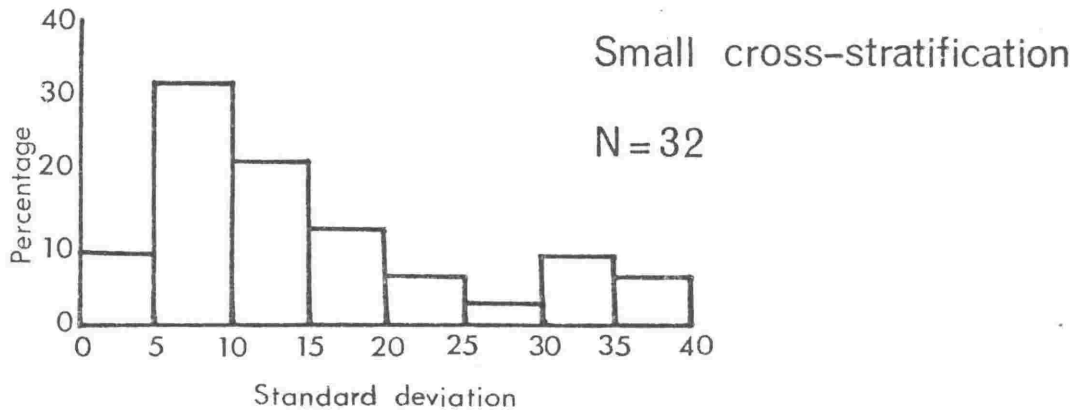
Fig. 72: Standard deviation for groups of data with more than four readings per group.
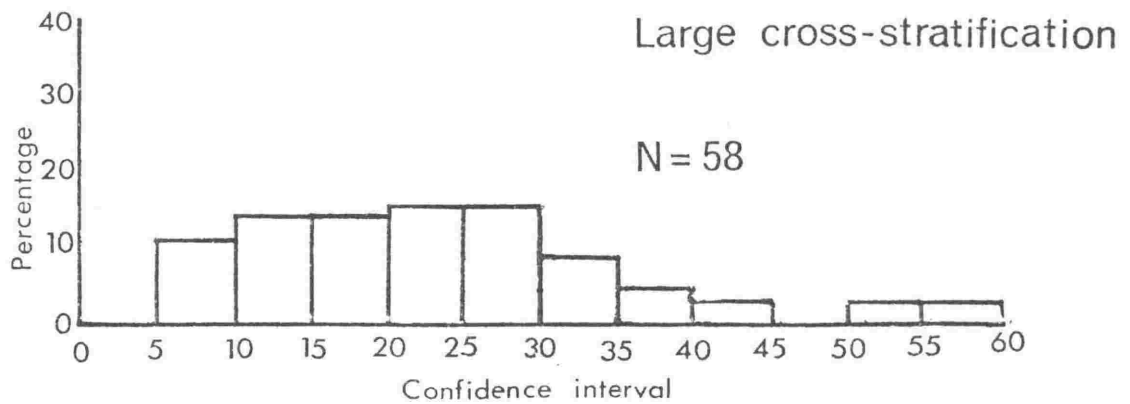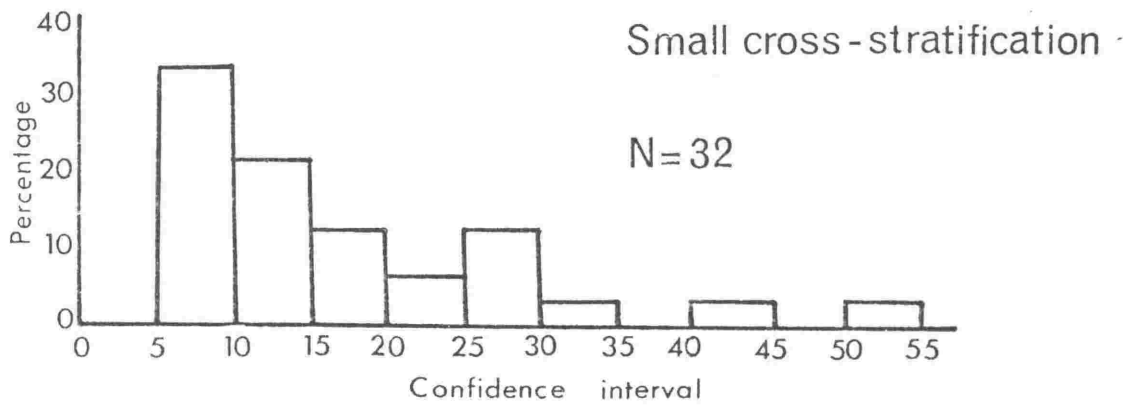
Fig. 73: Confidence interval for groups of data with more than four readings per group.
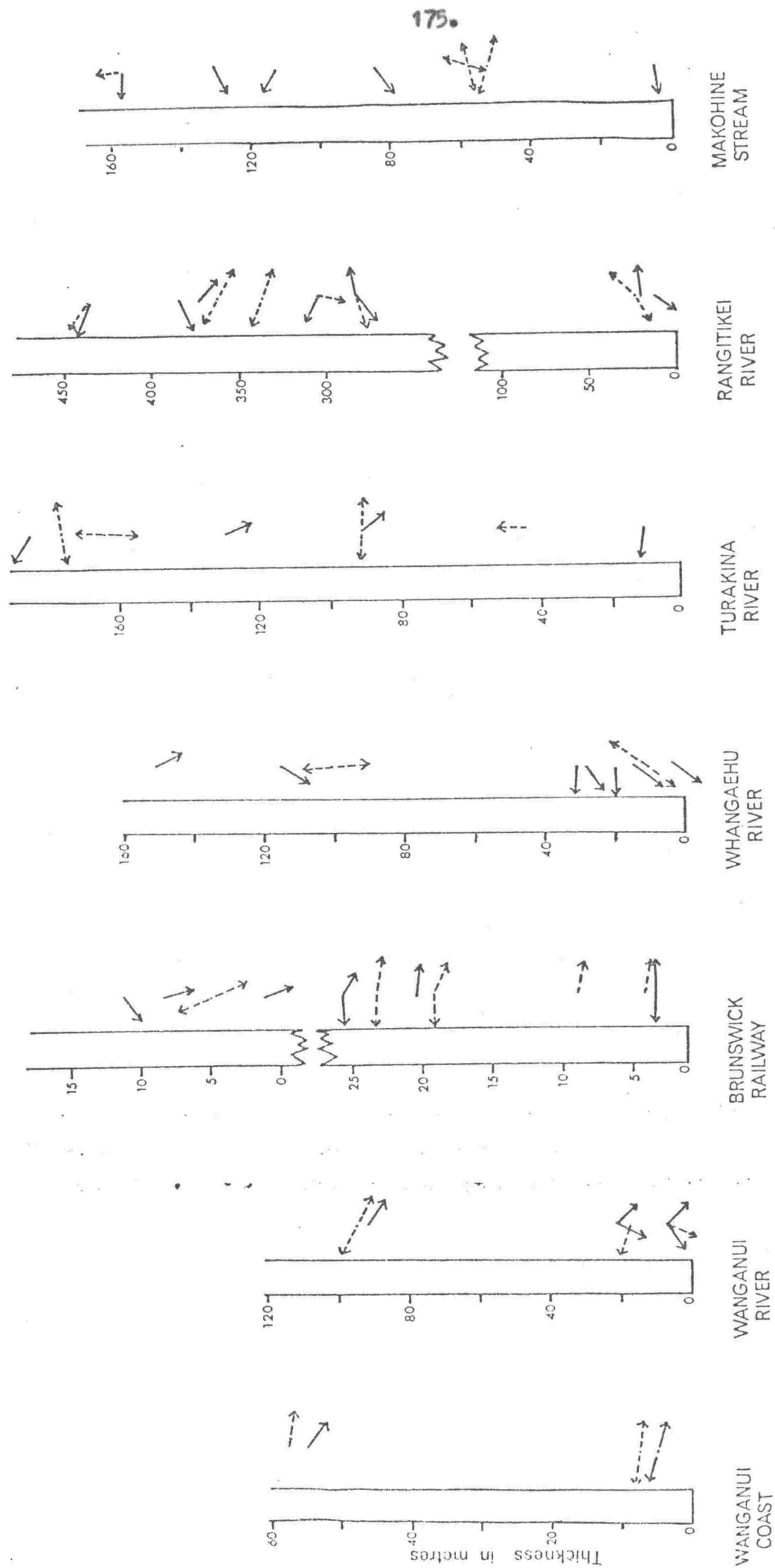
Fig. 74: Stratigraphic variations in palaeocurrent direction. Solid arrows represent large scale cross stratification, broken lines represent small scale cross stratification.

2) There is no consistency in the proportion of bimodal large scale-cross-stratification. The percentage of bimodal cosets varies from 0 to 66% in any one section.

3) Variations in current direction from small scale cross-stratification over stratigraphic intervals of thirty metres or more are usually large (up to 90°), and erratic, although at one locality (section 65, N137/580911), measured directions range through only 10° in a thirty metre interval. However, sampling was not usually as close as in this sequence.

4) Large cross-stratification directions normally fall within a 45° sector in all sections whether closely sampled or not. Only the Turakina, and rare sites in the upper parts of the Whangaehu, Wanganui and Rangitikei sections show any larger variation.

5) Small and large scale cross-stratification are not usually coincident even at one site where measurement on the two structures were taken within a few metres of one another; the directions vary by as much as 90°. This is not always the case, as the directions taken along the present Wanganui coast are coincident.

Conclusions

1) Small scale cross-stratification yields more reliable local current directions than large scale cross-stratification for individual cosets. However, directions from small scale structure are more variable stratigraphically (i.e. with time) than large scale structures.

The lack of any clear pattern in the regional trend of small scale structures is real, and not due to errors in measurement. It is probably due to wide variation in current directions from place to place and from time to time.

Although vector means of large scale cosets can be less reliably determined than those for small scale cosets, stratigraphic variation is considerably less. Thus, in these ancient shallow water deposits, large

scale cross-stratification is a more reliable directional indicator of regional sediment transport. This is in accord with Allen's (1967) theoretical arguments.

2) The regional palaeocurrent pattern revealed from the large scale cross-stratification is complex. The bimodality of the directions emphasising the shallow water marine origin of these sediments is most likely due to tidal currents.

By removing the secondary mode, a simplified flow pattern is revealed, (inset to figures 68 and 70). For the area from Wanganui to Hunterville the dominant flow is to the south east, i.e. at an acute angle to the postulated shoreline. From the Rangitikei River to the Pohangina River, flow varies from south east to west. From Pohangina to Palmerston North flow is dominantly westward, seaward, normal to the postulated shoreline, away from the axial ranges, and may have been influenced by high velocity streams flowing into the sea at this point.

Although the pattern is complex, the dominant pattern of sediment transport appears to have been seaward but subparallel to the coast, not dissimilar to current pattern along the Wanganui coast at the moment, (K. B. Lewis, pers. comm.).

The large secondary modes in the north eastern area may have been caused by fluvial influx.

Sediment transport determined from conglomerate parameters

Plumley (1948) in one of the earliest studies of gravel transport, made quantitative analyses on detritus transported by streams draining the Black Hills, South Dakota. He concluded that selective transport accounts for 75% of the size decrease, the rest being attributed to abrasion and breakage. He also found that the rate of change of roundness with

distance is proportional to some power of the distance and to the difference between the roundness and a limiting value of the roundness. Sphericity increases slightly with distance but is somewhat erratic. The initial lithological composition of the clasts is directly related to the source area of the gravel as might be expected.

On the basis of these conclusions, mean size, roundness and lithology were determined for clasts in the conglomerate horizons of the Makirikiri Tuff and Kaimatira Pumice Sand, to determine direction of sediment transport on a regional scale.

Methods

Pettijohn (1957) showed that the mean diameter of clasts in gravel is directly proportional to the diameter of the largest clasts. Because of this, Pelletier (1958) argued that the average of the ten largest clasts should be a rapid but reliable way of detecting changes in mean size of gravels, and hence indicate transport direction. To this end, the mean diameters of the ten largest greywacke clasts were measured for conglomerate horizons. In addition the lithology and roundness of 100 randomly selected clasts was determined.

Results and discussion

Mean size of the ten largest clasts (Fig. 75) shows a very obvious high along the eastern margin of the basin which was rimmed by Mesozoic greywackes of the central axial range at the time of deposition. The mean size is highest in the south east where the postulated shore line comes closest to the Ranges (Fig. 66); most of these sediments are very shallow marine and the conglomerates may be the product of high gradient streams entering the sea and dumping their load at this point. The conglomerates in the north east have been mostly interpreted as deposits of a braided stream or shallow
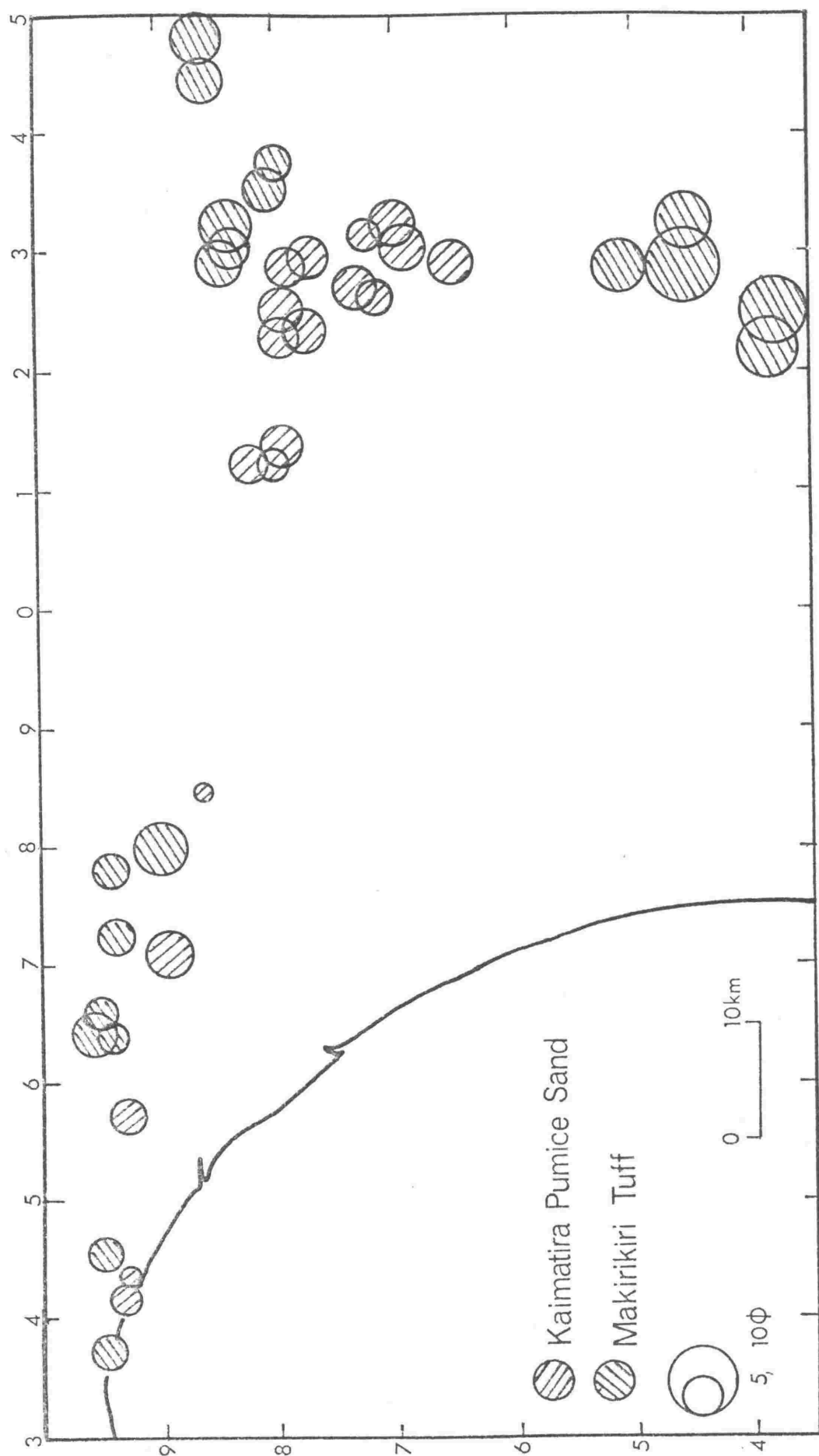
Fig. 75: Size variation of the ten largest greywacke clasts in conglomerate beds.
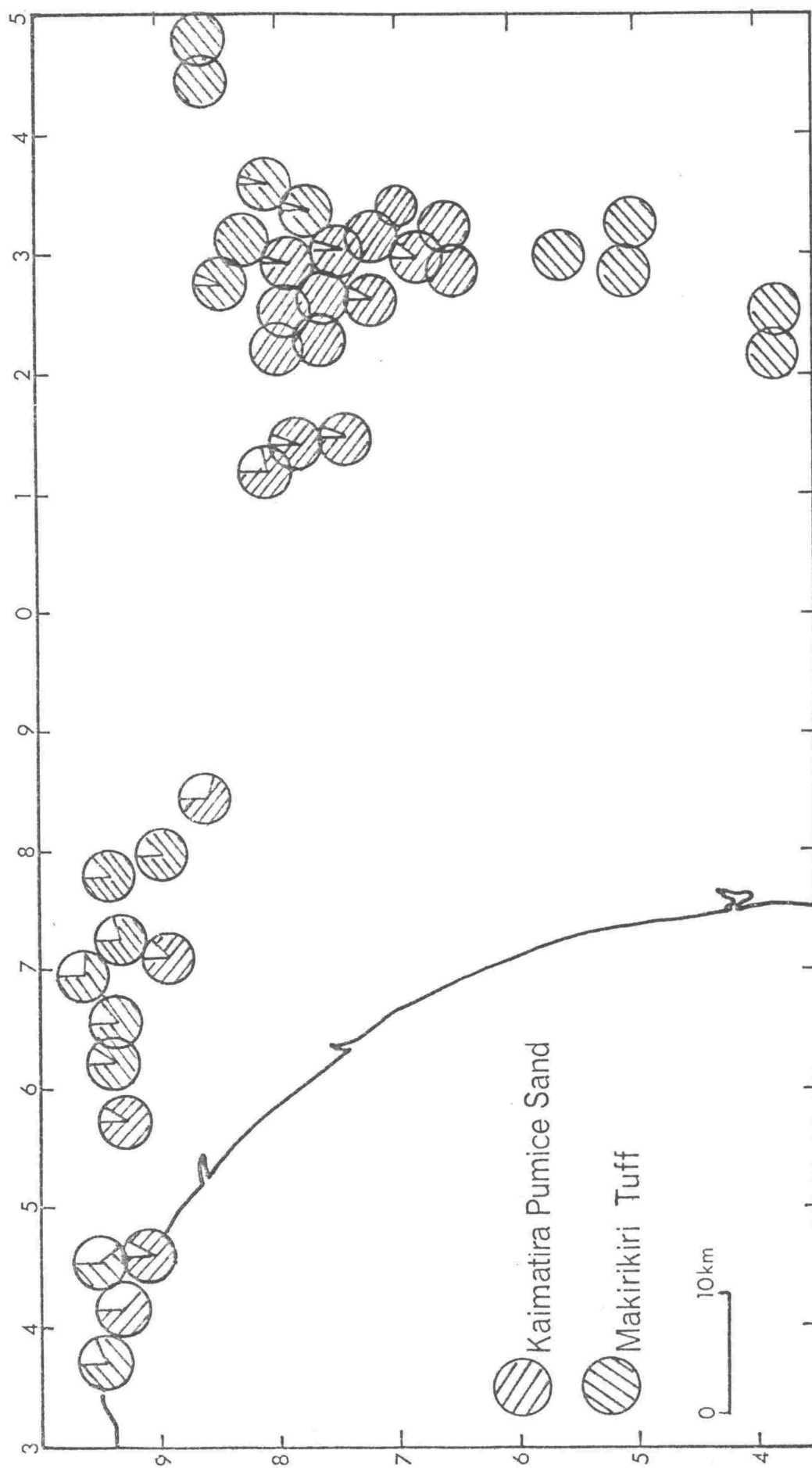
Fig. 76: Variation in conglomerate composition. Shaded area represents percent greywacke.

Fig. 77: Variation in roundness (using the scale of Krumbein, 1941) of greywacke clasts.

marine environment (Chapter 2). Their mean size is lower and, assuming similar source controls, particularly spacing of jointing and induration, they appear to have been transported further. Very rare volcanic clasts are associated with these greywackes (Fig. 76) indicating that at least some of the detritus was being transported from as far afield as the central volcanic district.

In the west of the basin from Wanganui to Hunterville the mean size of the ten largest clasts is smaller. There is also a slight overall increase in the roundness of the greywacke clasts (Fig. 77) compared to those from the eastern side of the basin. In addition there is a greater percentage of volcanic clasts in the conglomerates, up to 80% in some beds, consistent with a source area to the north in the central volcanic district. Further, one site where clast size is larger than average in this area is a channel deposit of very poorly sorted detritus of greywacke and volcanic origin with no stratification and may represent a distal laharic deposit, such that this size increase reflects only very local change in flow conditions.

Conclusions

From the foregoing discussion it is evident that there are two sources of sediment in this area - one sedimentary and the other volcanic. The high percentage of greywacke, relatively large size and subrounded to subangular nature of the conglomerates clasts in the eastern edge of the basin suggests a source to the east in the Mesozoic greywackes. To the west of the basin, there is an increase in volcanic clasts, a slight increase in roundness and a decrease in size of the greywacke clasts compared to those in the west. The volcanic detritus is probably derived from the north and it is concluded that so too is the greywacke of the western area. As the

palaeocurrents indicate a dominant eastward drift of sediment, this too confirms the northerly source of greywacke in this region. Sources of this greywacke could be highlands such as the present Rangitoto Ranges.

PART III

PALAEOSALINITIES FROM CARBON AND OXYGEN ISOTOPE ANALYSIS

OF CARBONATE SHELLS IN THREE QUATERNARY FORMATIONS

WANGANUI BASIN, NEW ZEALAND

INTRODUCTION

McCrea (1950), Urey et al (1951) and Epstein et al (1953) experimentally determined the relationship between the oxygen isotope compositions of water and calcium carbonate precipitated in equilibrium with the water, and the temperature of the water. The relationship is expressed by the following equation, (Epstein et al, 1955):

$$T(^\circ C) = 16.5 - 4.3 \, (\delta^{18}O_{carbonate} - A) + 0.14 \, (\delta^{18}O_{carbonate} - A)^2$$

where A is a correction factor for the $\delta^{18}O$ of the water relative to mean ocean water, and is equal to zero for standard mean ocean water (SMOW). When the isotopic ratio of the carbonate is analysed, T may be calculated if A is known.

Epstein (1953) deduced that the ^{18}O content of sea water would increase with salinity. Salinity and ^{18}O content are both increased by evaporation, and fresh water precipitated from the atmosphere is therefore always depleted in ^{18}O relative to SMOW. When fresh water and sea water, mix the salinity and ^{18}O content of the latter decrease simultaneously. Along the coast where fresh water run-off from the land is significant, any near-shore water is likely to be depleted in this way (Epstein and Mayeda, 1955) and the oxygen isotope ratios of shells precipitated in such waters will therefore also vary with salinity.

The carbon isotope ratio ($^{13}C/^{12}C$) may also indicate where fresh-water has mixed with ocean water (Clayton and Degens, 1959; Keith and Weber, 1964; Keith et al, 1964) because the intermixed fresh-water contains carbon derived from land plants which are depleted in ^{13}C due to biological fractionation. Palaeosalinity maps based on carbon isotope ratios were found to be in agreement with palaeontological and other geological evidence, (e.g. Allen and Keith, 1965, and Keith et al, 1964).

Keith and Weber (1964) derived the following equation to discriminate between marine and fresh-water limestone of Jurassic and younger age:

$$Z = a \, (\delta^{13}C + 50) + b \, (\delta^{18}O + 50)$$

The terms a and b are 2.048 and 0.498 respectively. Their results showed that "limestone with a value of Z greater than 120 would be classed as marine, those with Z lower than 120 as fresh water and those with Z near 120 as indeterminate."

Mook (1971) investigated the problem more thoroughly, by analysing oxygen and carbon isotopes in carbonate shells of present day bivalves from the North Sea and inflowing rivers, thus covering a range of fully marine, mixed and fresh-water conditions. In a series of traverses he found a gradual increase in $\delta^{13}C$ and $\delta^{18}O$ towards the ocean. His plot of the results provides a potential standard for determining more precise palaeosalinities than those given by Keith and Weber (loc. cit.).

ANALYSES OF WANGANUI BASIN FOSSILS

When Devereux (1968) determined oxygen isotope palaeotemperatures from New Zealand fossils, he chose only fossils that could be assumed to have lived in undiluted ocean water so that he could assume A=0 in the equation of Epstein et al (loc. cit.). The Wanganui Basin Quaternary fossils were unsuited to this purpose because they mostly belong to inshore environments (Fleming, 1953; Te Punga, 1953) where ocean water was likely to have been diluted by fresh-water.

The diagram of Mook (loc. cit.) showing $\delta^{18}O$ plotted against $\delta^{13}C$, now provides a possible standard whereby:

a) samples precipitated in diluted ocean water may be identified and if necessary rejected for palaeotemperature work.

b) relative salinities may be determined.

c) if a sufficient range in salinities are present in one horizon temperatures may be determined graphically.

The first requirement is to determine whether Mook's results can be reproduced using stratigraphically lateral sequences of fossils representative of a range of salinities. The following account is concerned specifically with this problem, using fossils from selected horizons in the Wanganui Basin. The results are applied to the solution of palaeogeography, but not at this stage to the determinations of palaeotemperatures.

Three Pleistocene fossil horizons were chosen that had previously been studied in detail across an extensive area in the Wanganui Basin. They were the Taimui Shellbed, the Tewkesbury Formation and the Waipuru Shellbed described by Fleming (1953), (Fig. 78). All shells analysed were bivalves, Venericardia purpurata (Deshayes) being chosen wherever represented by well preserved shell; Chlamys gemmulata (Reeve), Maorimactra acuminella Finlay, Tawera subsulcata (Suter) or Dosinia (Austrodosinia) aff. horrida Marwick being chosen from other sites.

Procedures

All samples analysed were from shells that showed no signs of chalky or weathered surfaces. Each sample was cleaned ultrasonically in distilled water for 2 to 3 minutes, dried, and ground under carbon tetrachloride to a fine powder. After drying again, the powder was soaked in sodium hypochlorite for 48 hours to remove any organic components, (Emiliani, 1966, Devereux, 1968). Finally it was again dried and sieved through a 65 μ cloth mesh, the fine fraction being retained for the isotopic study, (Walters et al, 1972). To evolve carbon dioxide, 20 mgm of sample was reacted under vacuum
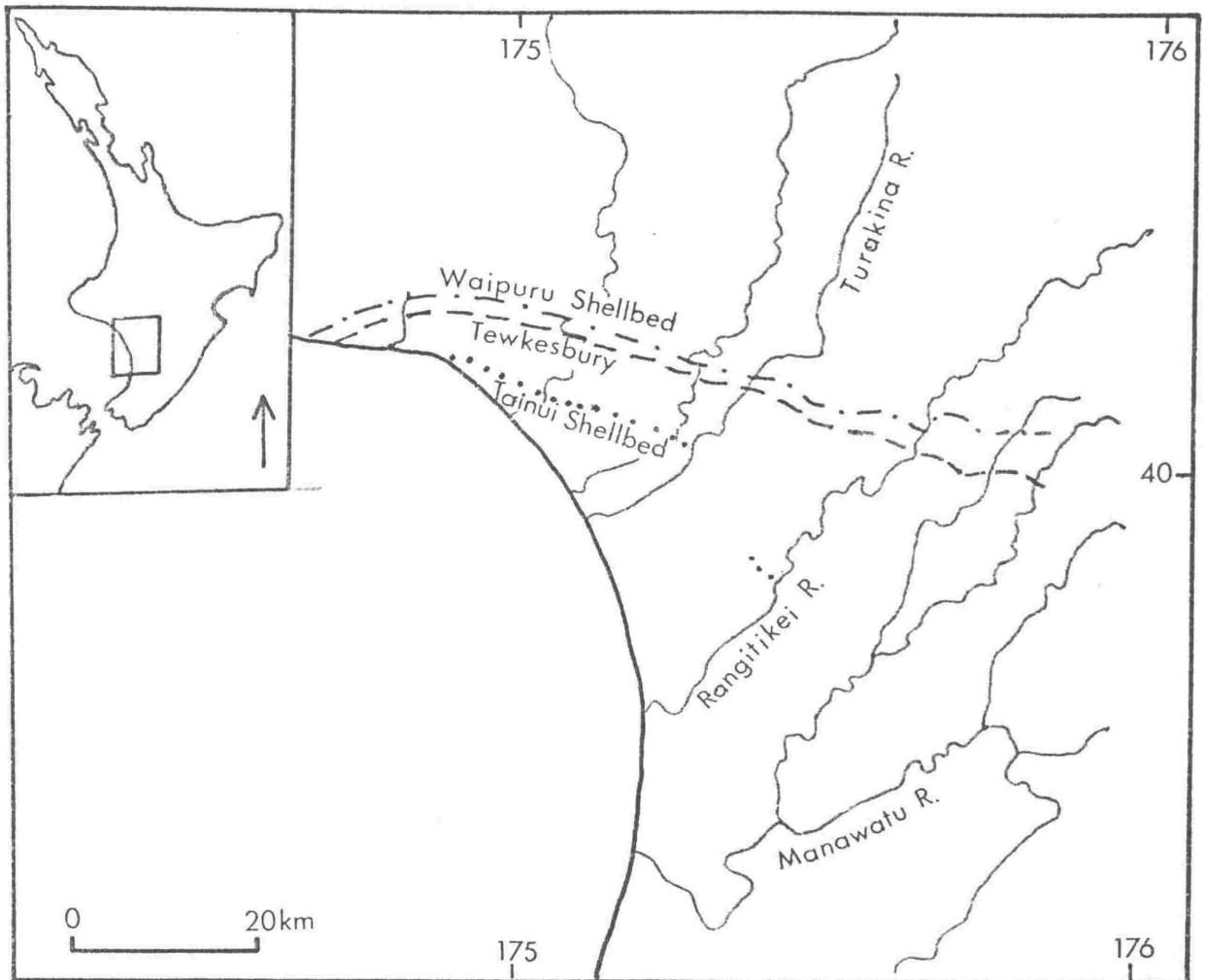
Fig. 78: Sketch map to show the distribution of the Waipuru Shellbed, the Tewkesbury Formation and the Tainui Shellbed.

with 100% phosphoric acid at 25°C for at least 48 hours.

Oxygen and carbon isotope ratios of the carbon dioxide were measured on Nuclide Analysis 60°, 6" (15cm) double collector mass spectrometer. The machine standard was Te Kuiti Limestone (TKL). A carbonate from the Tewkesbury Formation (number 165V1) was run as a standard sample with each set of analyses, (table 27). The standard deviation for each analysis was approximately 0.2°/oo. Many samples were run twice and the results were within the standard deviation of each other.

Ratios determined against the TKL standard were later computed to the international standard PDB and are given on the delta notation:

$$\delta^{18}O_{sample} \ (°/oo) = \frac{{}^{18}O/{}^{16}O_{sample} - {}^{18}O/{}^{16}O_{standard}}{{}^{18}O/{}^{16}O_{standard}} \times 1000$$

$$\delta^{13}C_{sample} \ (°/oo) = \frac{{}^{13}C/{}^{12}C_{sample} - {}^{13}C/{}^{12}C_{standard}}{{}^{13}C/{}^{12}C_{standard}} \times 1000$$

Results and discussion

a) Waipuru Shellbed

The Waipuru Shellbed can be traced from the Wanganui coast (N137/430982) to Marshalls Road (N139/287895), (Fig. 78). From palaeoecology, Fleming (1953) inferred deposition in fully saline water offshore at a depth of 10 to 20 fathoms in the centre and east of the basin, and in shallower water to the west.

The Z values (Table 26) are all greater than 120 indicating fully marine conditions according to Keith and Weber (1964). Most results plot within or near the area delineated as marine by Mook (1971), (Fig. 79). Except in the extreme east at Marshalls Road, the $\delta^{13}C$ values are higher

Sample no.	Locality	Species	$\delta^{13}C$ (°/oo) w.r.t. PDB	$\delta^{18}O$ (°/oo) w.r.t. PDB	Z value
164	N137/471987 (Kai-iwi)	Venericardia purpurata	1.89	1.16	131.75
163	N138/872941 (Mangatipona Rd)	"	2.60	1.49	133.97
162	N139/048890	"	1.85	1.57	131.84
166	N138/930933	"	1.67	1.35	131.39
170	N138/810948 (Whangaehu Valley)	"	2.03	1.41	132.16
181	N139/186896 (Turakina Valley)	"	1.68	1.01	131.24
GS4123	N137/497983 (Brunswick Rd)	"	1.11	0.89	130.01
211	N138/658988 (Parakino Rd)	"	1.19	1.45	130.46
214	N139/287895 (Marshall Rd)	Chlamys gemmulata	0.67	0.64	128.99
160	N139/123876 (Hwy 1)	"	1.51	0.72	130.56
GS4132	N138/658969 (Parapara Rd)	Venericardia purpurata	1.37	0.99	130.60
GS4011	N137/470978 (Rangitatau Rd)	"	1.61	1.53	131.36

Table 26: Isotope ratios of fossil shells from the Waipuru Shellbed.
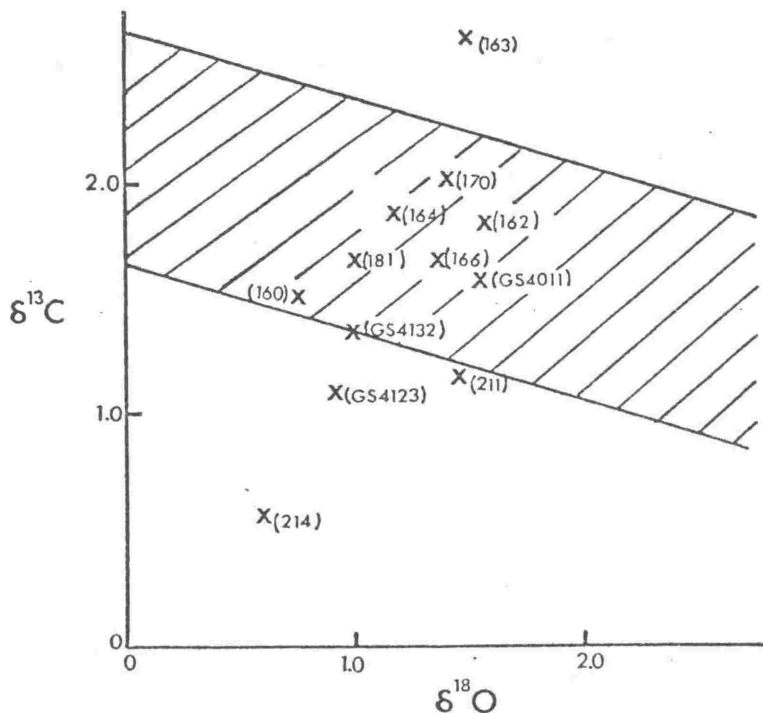
Fig. 79: Carbon and oxygen isotope ratios for mollusc shells from the Waipuru Shellbed.. Sample numbers in brackets. Shaded area represents composition of calcium carbonate precipitated in equilibrium with ocean water as a function of temperature.
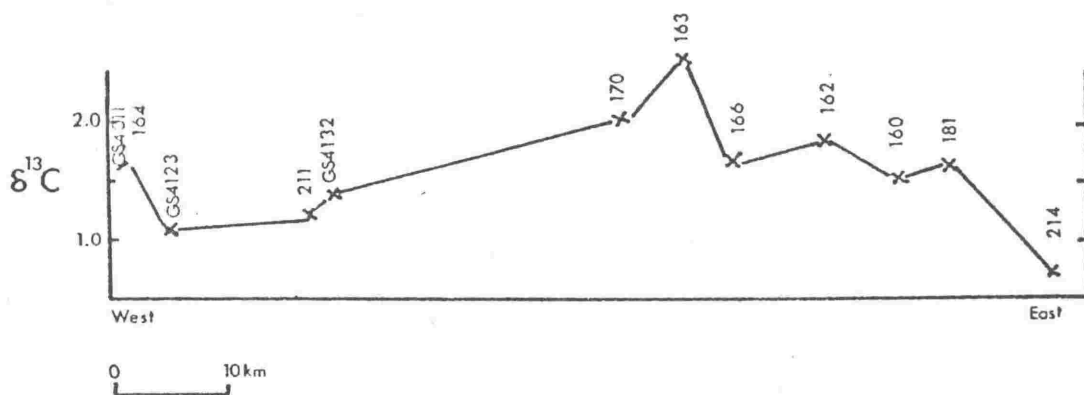
Fig. 80: Variation in carbon isotope ratio of mollusc shells across the basin of deposition. Sample numbers as in figure 79.

in the centre and east of the basin than in the west (Fig. 80). As
dilution of sea water by fresh water and sea depth both tend to be functions
of distance from shore, salinity can be expected to decrease with decrease
in depth for open oceans. Thus the eastern shore line at the time was
probably close to the present position of Marshalls Road.

The reduced $\delta^{13}C$ values in the west of the basin, also suggest a slight
reduction of salinity and are in agreement with the shallowing inferred by
Fleming (1953).

b) Tewkesbury Formation

The Tewkesbury Formation immediately overlies the Waipuru Shellbed and
can be traced from the coast (N137/338955) to the eastern side of the
Rangitikei River, (N139/154891), (Fig. 78). Fleming (1953) noted that the
assemblages in the western outcrops are characteristic of "inter-tidal and
shallow-water sand and mud-flats, in semi-enclosed estuaries and inlets,"
whereas those at the centre of the basin," indicate deposition in saline
offshore waters of moderate depth."

According to the equation of Keith and Weber (loc. cit.) only one sample
(Table 27) was deposited in a non-marine environment, yet values of $\delta^{13}C$
plotted against $\delta^{18}O$ (Fig. 81) mostly lie outside the fully marine field,
in agreement with the palaeoecological results. The large scatter (Fig. 81)
is to be expected of such inshore environments where fresh-water input
varies from place to place and also from time to time.

Again the $\delta^{13}C$ values (Fig. 82) are higher in the central and eastern
portion of the basin than in the west, indicating fully marine salinity
in the region of the present Rangitikei River. Although the trend of
variation is the same as in the Waipuru Shellbed, the value of carbon and
oxygen isotope ratios are less. Thus, the results show that the basin did
not alter significantly in form during deposition of the two formations,
but did shallow substantially before deposition of the Tewkesbury Formation.

Sample no.	Locality	Species	$\delta^{13}C_{PDB}$	$\delta^{18}O_{PDB}$	Z value
175	N137/497980	_Tawera subsulcata_	1.10	0.89	130.28
165 (V1)	N138/911920	_Venericardia purpurata_	1.40	1.02	130.67
			1.46	1.21	130.89
		(repeat runs)	1.57	1.29	131.16
			1.49	1.16	130.93
			1.32	1.08	130.54
			1.56	1.17	131.07
			1.55	1.14	131.04
165 (V2)	N138/911920	_Venericardia purpurata_	1.60	1.20	131.17
165 (C1)	N138/911920	_Chlamys gemmulata_	1.37	1.18	130.70
GS3092	N139/043892	_Venericardia purpurata_	1.09	1.19	130.12
GS4129	N137/338955	"	1.20	1.57	130.54
161	N139/050884	"	1.73	1.74	131.74
210	N137/655968	_Dosinia (Austrodosinia)_ aff. _horrida_	+0.38	0.71	103.53
180	N139/155892	_Maorimactra acuminella_	0.52	0.70	128.74
172	N138/806939	"	0.59	1.59	129.29

Table 27: Isotope ratios of shells from the Tewkesbury Formation.
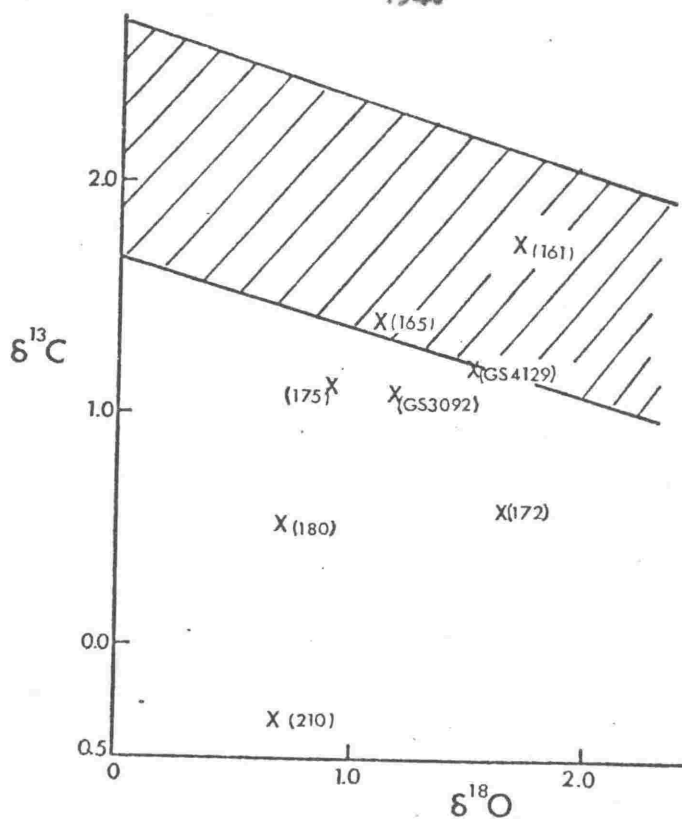
Fig. 81: Carbon and oxygen isotope ratios for mollusc shells from the Tewkosbury Formation. Sample numbers in brackets. Shaded area represents composition of calcium carbonate precipitated in equilibrium with seawater as a function of temperature.
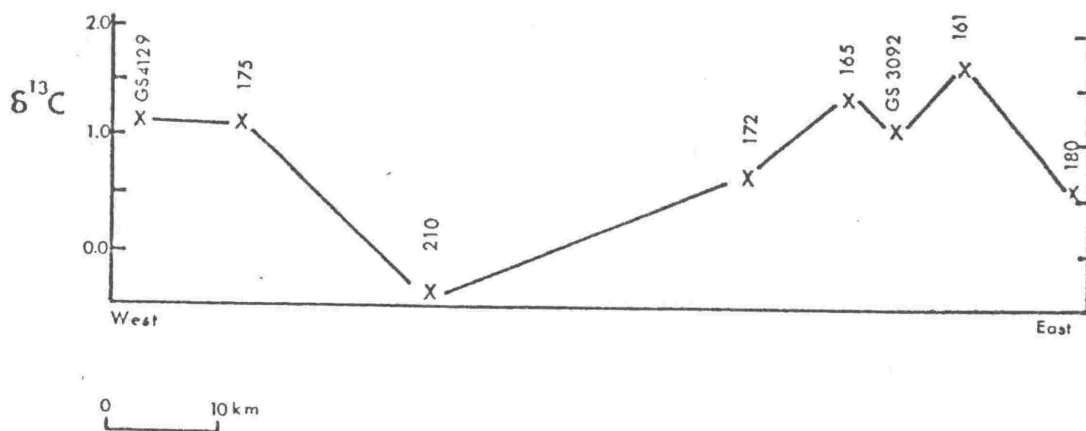
Fig. 82: Variation in carbon isotope ratio of mollusc shells across the basin of deposition. Sample numbers as figure 81.

c) Tainui Shellbed

The Tainui Formation can be traced (Fig. 78) from the Wanganui coast (N137/479893) to Onepui Bridge at the Rangitikei River, (N143/890696). Palaeoecology (Fleming, 1953) indicates deposition in waters that shallowed from west to east. Fluctuating depths greater than 20 fathoms were inferred for the sites west of Wanganui, and rapidly fluctuating shallow depths near an estuarine shoreline for the Rangitikei area.

From the Z values of Keith and Weber (1964), (Table 28), all the samples are marine, but in the plot of $\delta^{13}C$ against $\delta^{18}O$ the sample from the Rangitikei River (no. 156) falls outside the fully marine field (Fig. 83).

In rough agreement with the palaeoecology, $\delta^{13}C$ decreases irregularly (Fig. 84) towards the east with a low in the region of the Whangaehu River, which may indicate a local concentration of fresh water supply.

CONCLUSIONS

The carbon and oxygen isotope ratios of the Pleistocene shells are sensitive indicators of palaeosalinity.

The Z values calculated from the equation of Keith and Weber (1964) indicate fully marine conditions in all but one case, but plots of $\delta^{13}C$ against $\delta^{18}O$ permit a more refined distinction of fresh water intermixing and show that some samples grew in water of reduced salinity. The indicated salinities are substantially in agreement with the palaeontological evidence of Fleming (1953).

Sample no.	Locality	Species	$\delta^{13}C$ w.r.t. PDB	$\delta^{18}O$ w.r.t. PDB	Z value
GS4241	N138/741812	Chlamys gemmulata	1.51	1.85	131.48
GS4144	N138/677852	"	1.39	1.50	130.90
172/1	N137/475897	Venericardia purpurata	2.02	2.18	132.53
172/2	N138/588870	"	2.09	1.75	132.45
209	N138/757838	"	1.92	1.97	132.21
159	N143/980696	"	1.11	0.74	129.94

Table 28: Isotope ratios of shells from the Tainui Shell Bed.
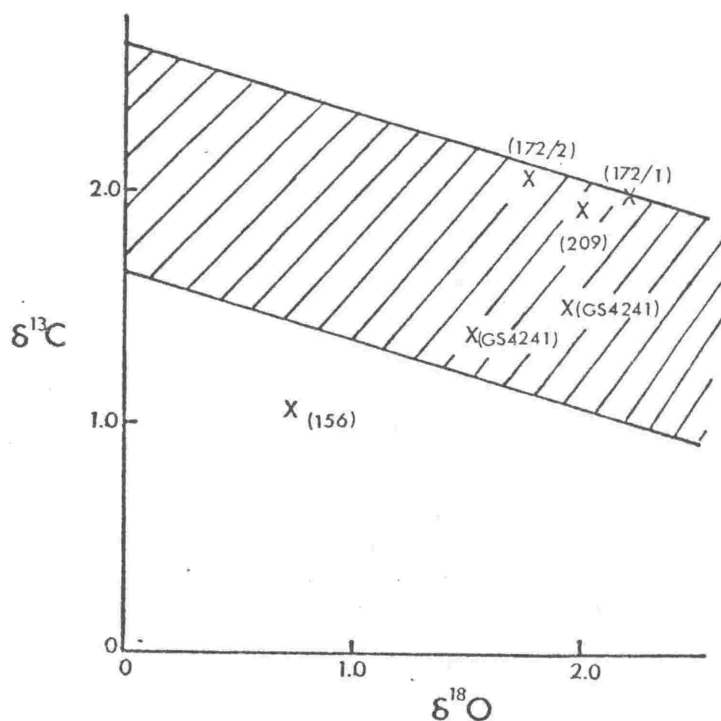
Fig. 83: Carbon and oxygen isotope ratios for mollusc shells from the Tainui Shellbed. Sample numbers in brackets. Shaded area represents composition of calcium carbonate precipitated in equilibrium with seawater as a function of temperature.
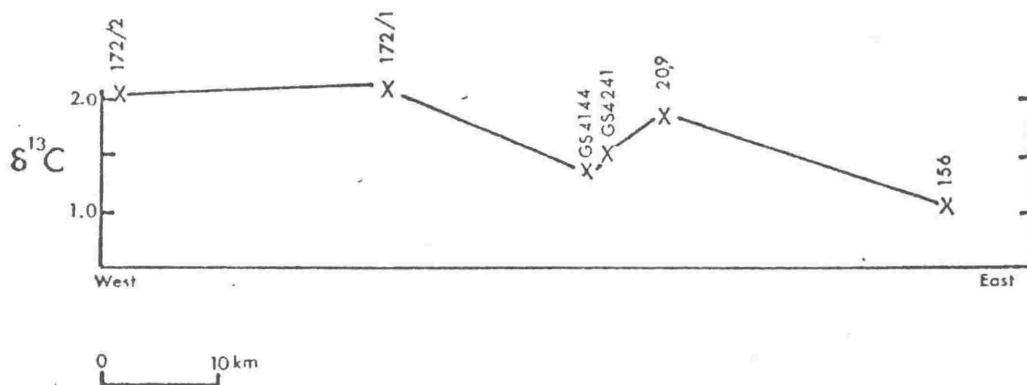
Fig. 84: Variation in carbon isotope ratios of mollusc shells across the basin of deposition. Sample numbers as figure 83.

REFERENCES CITED

ALLEN, J.R.L., 1960, The Nam Tor sandstones: a "turbidite facies" of the
    Namurian Deltas of Derbyshire, England: Jour. Sed. Petr., v. 30,
    p. 193-208.

ALLEN, J.R.L., 1963, The classification of cross-stratified units with
    notes on their origin: Sedimentology, v. 2, p93-114.

ALLEN, J.R.L., 1967, Notes on some fundamentals of palaeocurrent analysis,
    with reference to preservation potential and sources of variance:
    Sedimentology, v.9, p.75-88.

ALLEN, J.R.L., 1968, Current Ripples: North Holland, Amsterdam, 433p.

ALLEN, J.R.L., 1970, Physical Processes of Sedimentation, Unwin Univ. Books,
    248p.

ALLEN, P., AND KEITH, M. L., 1965, Carbon isotope ratios and palaeosalinities
    of Purbeck-Wealden Carbonates: Nature, v. 208, p.1278-1280.

ANKETELL, J. M., CEGLA, J., AND DZULYNSKI, ST., 1969, Unconformable surfaces
    formed in the absence of current erosion: Geol. Rom., v.8, p.41-46.

AUGUSTINUS, P.G.E.F, AND RIEZEBOS, H.Th., 1971, Some sedimentological
    aspects of the fluvioglacial outwash plain near Soesterberg:
    Geol. en Mijn., v.50, 341-348.

BAILEY, E. H., AND STEVENS, R. E., 1960, Selective staining of K-feldspar
    and plagioclase on rock slabs and thin sections: Am. Min., v.45,
    p.1020-1025.

BARRETT, P. J., 1970, Palaeocurrent analysis of the mainly fluviatile
    Permian and Triassic Beacon rocks, Beardmore Glacier area,
    Antarctica: Jour. Sed. Petr., v.40, p.395-411.

BEU, A. G., 1969, Index macrofossils and New Zealand Pliocene and lower
    Pleistocene time-stratigraphy: New Zealand Jour. Geol. Geophys.,
    v.12, p.643-658.

BLANK, H.R.Jr., 1965, Ash-flow deposits of the central King Country,
    New Zealand: New Zealand Jour. Geol. Geophys., v.8, p.588-607.

BLATT, H., MIDDLETON, G.V.M., AND MURRAY, R., 1972, Origin of sedimentary
    rocks: Prentice-Hall Inc., New Jersey, 634p.

BOUMA, A. H., 1962, Sedimentology of some flysch deposits, Elsevier Pub. Co., 168p.

BROWNE, P.R.L., AND WOOD, C. P., 1972, Garnet-bearing sands from the East Coast, North Island, New Zealand: New Zealand Jour. Geol. Geophys., v.15, p.649-660.

CHALLIS, G. A., 1962, in WELLMAN, H. W., Holocene of the North Island of New Zealand: a coastal reconnaissance: Trans. Royal Soc. New Zealand, v. 1, p.29-99.

CLAYTON, R. N., AND DEGENS, E. T., 1959, Use of carbon isotope analysis of carbonates for differentiating fresh-water and marine sediments: Amer. Assoc. Petr. Geol. Bull., v. 43, p.890-897.

CLIFTON, H. E., HUNTER, R. E., AND PHILLIPS, R. L., 1971, Depositional structures and processes in the non-barred high-energy nearshore: Jour. Sed. Petr., v.41, p.651-670.

COLE, J. W., AND KOHN, B. P., 1972, Pyroclastic nomenclature in New Zealand: New Zealand Jour. Geol. Geophys., v.15, p.686-687.

COPE, R. N., AND REED, J. J., 1967, The Cretaceous palaeogeography of the Taranaki - Cook Strait area: Proc. Australas. Inst. Min. Metall., v.222, p.63-72.

CRAWFORD, J. C., 1869, Essay on the geology of the North Island of New Zealand: Trans. New Zealand Inst., v.1, p.305-328.

CRAWFORD, J. C., 1870, On alluvial gold in the Province of Wellington: Trans. New Zealand Inst., v.2, p.353.

CURRAY, J. R., 1956, The analysis of two dimensional orientation data: J. Geol., v.64, p.117-131.

DAVIES, H. G., 1965, Convolute lamination and other structures from the Lower Coal Measures of Yorkshire: Sedimentology, v.5, p.305-326.

DEER, W. A., HOWIE, R. A., AND ZUSSMAN, J., 1963, Rock forming minerals: Longmans Green and Co. Ltd., London, v.2, 379p.

DEVEREUX, I., 1968, Oxygen isotope studies: Unpublished Ph.D. thesis, Victoria Univ., Wellington, 117p.

DOELL, R. R., AND COX, A., 1965, Measurement of the remanent magnetization of igneous rocks: U.S. Geological Survey Bull., 1203-A, 32p.

DOTT, R. H. Jr., AND HOWARD, J. K., 1962, Convolute lamination in non-graded sequences, J. . Geol., v.70, p.114-121.

DZULYNSKI, ST., AND WALTON, R. K., 1965, Sedimentary features of flysch and greywackes: Elsevier, Amsterdam, 274p.

EDELMAN, C. H., AND DOEGLAS, D. J., 1932, Reliktstrukturen Detritischer Pyroxene und Amphibole: Tschermaks mineralogische und petrographische Mitteilungen, v.42, p.482-490.

EMILIANI, C., 1966, Palaeotemperature analysis of Caribbean cores P6304-8 and P6304-9 and a generalised temperature curve for the past 425,000 years: J . Geol. , v.74, p.109-126.

EPSTEIN, S., BUCHSBAUM, R., LOWENSTAM, H. A., AND UREY, H. C., 1953, Revised carbonate-water isotopic temperature scale: Geol. Soc. Am. Bull., v.64, p.1315-1326.

EPSTEIN, S., AND MAYEDA, T., 1955, Variations on the O^{18}/O^{16} ratios in natural waters: Geochim. Cosmochim. Acta, v.4, p.213-224.

EWART, A., 1969, Petrochemistry and feldspar crystallisation in the silicic volcanic rocks, central North Island, New Zealand: Lithos, v.2, p.371-388.

FINLAY, H. J., 1939, New Zealand foraminifera: key species in stratigraphy - No.1: Royal Soc. New Zealand, Trans., v.68, p.504-533.

FINLAY, H. J., AND MARWICK, J., 1947, New divisions of the New Zealand upper Cretaceous and Tertiary: New Zealand Jour. of Science and Technology, v.28, p.228-236.

FLEISCHER, R. L., AND PRICE, P. B., 1964a, Techniques for geological dating of minerals by chemical etching of fission fragment tracks: Geochim. Cosmochim. Acta, v.28, p.1705-1714.

FLEISCHER, R. L., AND PRICE, P. B., 1964b, Decay constant for spontaneous fission of U-238: Phys. Rev., v.133B, p.63-64.

FLEMING, C. A., 1953, The geology of the Wanganui subdivision: New Zealand Geol. Surv. Bull., n.s. 52, 362p.

FLEMING, C. A., 1957, The genus _Pecten_ in New Zealand: New Zealand Geol. Surv. Pal. Bull., No.26, 69p., 15 plates.

FLEMING, C. A., 1962, New Zealand biogeography - a palaeontologist's
approach: Tuatara, v.10, p.53-108.

FOLK, R. L., 1951, Stages of textural maturity in sedimentary rocks:
Jour. Sed. Petr., v.21, p.127-130.

FOLK, R. L., 1961. Petrology of sedimentary rocks: Hemphill's Austin,
Texas, 154p.

FOLK, R. L., AND WARD, W. C., 1957, Brazos river bar: a study in the
significance of grain size parameters: Jour. Sed. Petr., v.27,
p.3-26.

FOLK, R. L., ANDREWS, P. B., AND LEWIS, D. W., 1970, Detrital sedimentary
rock classification and nomenclature for use in New Zealand:
New Zealand Jour. Geol. Geophys., v.13, p.937-968.

FOSTER, J. H., 1966, A palaeomagnetic spinner magnetometer using fluxgate
gradiometer: Earth and Planet. Science Letters, v.1, p.463-466.

FRIEDMAN, G. M., 1961, Distinction between dune, beach and river sands
from their textural characteristics: Jour. Sed. Petr., v.31,
p.514-529.

HJULSTRÖM, F., 1939, Transportation of detritus by running water: in
TRASK, P. D., Ed., Recent Marine Sediments, p.5-31, S.E.P.M.
Spec. Pub. no. 4.

HOYT, J. H., AND HENRY, V. J. Jr., 1963, Rhomboid ripple marks, indicator of
current direction and environment: Jour. Sed. Petr. , v.33,

HÜLSEMANN, J., 1955, Grossrippeln und Schrägschichtungs-Gefüge im Nordsee-
Watt und in der Molasse: Senck. Leth., v.36, p.347-357.

HUTTON, C. O., 1959, Mineralogy of beach sands between Halfmoon and Monterey
Bays, California: California Div. Mines., Special Report 59, 32p.

INMAN, D. L., 1949, Sorting of sediments in the light of fluid mechanics:
Jour. Sed. Petr. , v.19, p.51-70.

JOPLING, A. V., AND WALKER, R. G., 1968, Morphology and origin of ripple
drift cross-lamination, with examples from the Pleistocene of
Massachusetts: Jour. Sed. Petr. , ~~v.33, p.473-479.~~ v 38, 971-984

KEITH, M. L., ANDERSON, G. M. AND EICHLER, R., 1964, Carbon and oxygen
isotopic composition of mollusk shells from marine and fresh-water
environments: Geochim. Cosmochim. Acta, v.28, p.1757-1786.

KEITH, M. L., AND WEBER, J. N., 1964, Carbon and oxygen isotope composition
of selected limestones and fossils: Geochim. Cosmochim. Acta,
v.28, p.1787-1816.

KENNETT, J. P., WATKINS, N. D., AND VELLA, P., 1971, Paleomagnetic chronology
of Pliocene-early Pleistocene climates and the Plio-Pleistocene
boundary in New Zealand: Science, v.171, p.276-279.

KEUNEN, Ph.H., 1949, Slumping in the Carboniferous rocks of Pembrokeshire:
Geol. Soc. Lond. Quart. Jour., v.104, p.365-385.

KEUNEN, Ph.H., 1950, Marine Geology: John Wiley and Sons Inc., New York,
568p.

KINGMA, J. T., 1971, Geology of the Te Aute Subdivision: New Zealand Geol.
Surv. Bull., n.s.70, 173p.

KLEEMAN, J. D., AND LOVERING, J. F., 1971, A determination of the decay
constant for spontaneous fission of natural uranium using fission-
track accumulation: Geochim. Cosmochim. Acta, v.35, p.637-640.

KNIGHT, S. H., 1929, The Fountain and the Casper Formations of the Laramie
Basin: Univ. Wyoming Spec. Publ. Sci., v.1, p.1-82.

KOHN, B. P., 1973, Some studies of New Zealand Quaternary pyroclastic
rocks: Unpublished Ph.D. thesis, Victoria Univ., Wellington.

KRUMBEIN, W. C., 1941, Measurement and geological significance of shape
and roundness of sedimentary particles: Jour. Sed. Petr.,
v.11, p.64-72.

LAKATOS, S. AND MILLER, D. S., 1972, Fission-track stability in volcanic
glass of different water contents: Jour. Geophys. Res., v.77,
p.6990-6993.

LEDENT, D., PATTERSON, C., AND TILTON, G. R., 1964, Ages of zircon and
feldspar concentrates from North American beach and river sands:
J. Geol., v.72, p.112-122.

LEWIS, K. B., 1971, Slumping on a continental slope inclined at $1^{\circ}-4^{\circ}$:
Sedimentology, v.16, p.97-110.

LIENERT, B. R., 1971, Construction of a spinner magnetometer and
palaeomagnetic measurements on a Pliocene-Miocene sedimentary
section: Unpublished M.Sc. thesis, Victoria Univ., Wellington.

LIENERT, B. R., CHRISTOFFEL, D. A., AND VELLA, P., 1972, Geomagnetic dates
on a New Zealand upper Miocene-Pliocene section: Earth and
Planet. Science Letters, v.16, p.195-199.

MARTIN, R. C., 1961, Stratigraphy and structural outline of the Taupo
    Volcanic Zone: New Zealand Jour. Geol. Geophys., v.4, 449-478.

McCREA, J. M., 1950, On the isotopic chemistry of carbonates and a
    paleotemperature scale: Jour. Chem. Phys., v.18, 849-857.

McKEE, E. D., 1965, Experiments on ripple lamination: in MIDDLETON, G. V.,
    ed., Primary sedimentary structures and their hydrodynamic
    interpretation, S.E.P.M. Spec. Pub. no.12., p.66-83.

MICHAELIS, E. R., AND DIXON, G., 1969, Interpretation of depositional
    processes from sedimentary structures in the Cardium Sand:
    Canadian Petr. Geol. Bull., v.17, p.410-443.

MOOK, W. C., 1971, Palaeotemperatures and chlorinities from stable carbon
    and oxygen isotopes in shell carbonate: Palaeogeog., Palaeoclim.
    Palaeoecol., v.9, p.245-263.

MORGAN, P. G., 1924, in WITHERS, T. H., The fossil cirripedes of New
    Zealand: New Zealand Geol. Surv. Pal. Bull. No.10, 47p.

NINKOVICH, D., 1968, Pleistocene volcanic eruptions in New Zealand recorded
    in deep-sea sediments: Earth and Planet. Science Letters, v. 4,
    p.89-102.

OOMKENS, E., AND TERWINDT, J.H.J., 1960, Inshore estuarine sediments in the
    Haringvliet: Geol. en Mijn., v.39, p.701-710.

OPDYKE, N. D., 1972, Paleomagnetism of deep-sea cores: Rev. Geophys. and
    Space Phys., v.10, p.213-249.

PARK, J., 1905, On the marine Tertiaries of Otago and Canterbury with special
    reference to the relations existing between the Pareora and Oamaru
    Series: Trans. New Zealand Inst., v.37, p.489-551.

PARK, J., 1910, The geology of New Zealand: Whitcombe and Tombs, Wellington,
    488p.

PASSEGA, R., 1957, Texture as a characteristic of clastic deposition:
    Am. Assoc. Petr. Geol. Bull., v.41, p.1952-1984.

PASSEGA, R., 1964, Grain size representation of C-M patterns as a geological
    tool: Jour. Sed. Petr., v.34, p.830-847.

PASSEGA, R., 1972, Sediment sorting related to basin mobility and environment: Am. Assoc. Petr. Geol. Bull., v.56, p.2440-2450.

PELLETIER, B. R., 1958, Pocono paleocurrents in Pennsylvania and Maryland: Geol. Soc. Am. Bull., v.69, p.1033-1064.

PETTIJOHN, F. J., 1957, Sedimentary Rocks: Harper's Geoscience Series, 718p.

PIYASIN, S., 1966, Plio-Pleistocene geology of the Woodville area: Unpublished M.Sc. thesis, Victoria Univ., Wellington, New Zealand.

PLUMLEY, W. J., 1948, Black Hills terrace gravels: a study in sediment transport: J. Geol., v.56, p.526-577.

POTTER, P. E., AND PETTIJOHN, F. J., 1963, Paleocurrents and basin analysis: Academic Press, New York, 296p.

PRICE, P. B. AND WALKER, R. M., 1962, Chemical etching of charged particle tracks in solids: J. Applied Phys., v.33, p.3407-3412.

RAAF, J.F.M.de AND BOERSMA, J. R., 1971, Tidal deposits and their sedimentary structures: Geol. en Mijn., v.50, p.479-504.

REINECK, H. E., 1960, Uber die Entstehung von Linsen- und Flaserschichten: Abhandl. Deutsche Akad. Wiss. Berlin, v.3, p.369-374.

REINECK, H. E., 1963, Sedimentgefüge im Bereich der Sudlichen Nordsee: Abhandlungen der Senckenbergischen Naturforschenden Gesellschaft, v.505, 138p.

REINECK, H. E. AND WUNDERLICH, F., 1968, Classification and origin of flaser and lenticular bedding: Sedimentology, v.11, p.99-104.

RICH, C. C., 1959, Late Cenozoic geology of the lower Manawatu valley, New Zealand: Unpublished Ph.D. thesis, Harvard Univ. Cambridge, Mass., U.S.A., copy held at Victoria Univ. Wellington, New Zealand.

ROSS, C. S., MISER, H. D., AND STEPHSON, L. W., 1929, Waterlaid volcanic rocks of early Upper Cretaceous age in southwestern Arkansas, southeastern Oklahoma, and northeastern Texas: U.S. Geol. Surv. Prof. Paper 154-F, p.175-202.

SANDERS, J. E., 1963, Concepts of fluid mechanics provided by sedimentary structures: Jour. Sed. Petr., v.33, p. 173-179.

SANDERS, J. E., 1965, Primary sedimentary structures formed by turbidity currents and related resedimentation mechanisms: in MIDDLETON, G. V., ed., Primary sedimentary structures and their hydrodynamic interpretation, S.E.P.M.Spec. Pub., No.12, p. 192-219.

SELLEY, R. C., 1967, Palaeocurrents and Sediment Transport in Nearshore
        Sediments in the Sirte Basin, Libya: J. Geol., v.75, p.215-223.

SELLI, R., 1967, The Pliocene-Pleistocene boundary in Italian marine
        sections and its relationship to continental stratigraphies,
        In: SEARS, M., ed., Progress in oceanography, New York, Pergamon
        Press, v.4, p.67-86.

SHROCK, R. R., 1948, Sequences in layered rocks: McGraw Hill, New York,
        507p.

SHEPARD, F. P., 1963, Submarine geology: Harper's Geoscience Series, 557p.

SILK, E.C.H., AND BARNES, R. S., 1959, Examination of fission fragment
        tracks with an electron microscope: Phil. Mag., v.4, p.970-972.

SIMONS, D. B., AND RICHARDSON, E. V., 1961, Forms of bed roughness in
        alluvial channels: Am. Soc. Civil Engineers Proc., v.87, No.HY3,
        p.87-105.

STERNBERG, R. W., 1972, Measurement of incipient motion of sediment particles
        in the marine environment: Marine Geol., v.10, p.113-120.

SUNDBORG, A., 1956, The River Klaralven: a study of fluvial processes:
        Geograf.Ann., v.38, p.127-316.

SUPERIOR OIL CO., 1943, Geology of the Palmerston-Wanganui Basin, "West
        side", North Island, New Zealand, by Feldmeyer, A. E., Jones, B. C.,
        Firth, C. W., Knight, J. (Typescript and maps held with New
        Zealand Geol. Surv., Wellington.)

TANNER, W. F., 1955, Paleogeographic reconstructions from cross-bedding
        studies: Am. Assoc. Petr. Geol. Bull., v.39, p.2471-2483.

TANNER, W. F., 1959, Near-shore studies in sedimentology and morphology
        along the Florida Panhandle coast: Jour. Sed. Petr., v.29,
        p.564-574.

TANNER, W. F., 1967, Ripple mark indices and their uses: Sedimentology,
        v.9, p.89-104.

TAYLOR, G. A., 1958, The 1951 eruption of Mount Lamington, Papua: Dept of
        National Devt., Bureau of Mineral Resources, Geology and Geophysics,
        Bull. No. 38, 117p.

TEN HAAF, E., 1956, Significance of convolute lamination: Geol. en Mijn.,
        v.18, p.188-194.

TE PUNGA, M., 1953, The Geology of the Rangitikei Valley: N.Z. Geol.
        Surv. Mem. no.8, 46p.

TE PUNGA, M. T., 1957, Live anticlines in western Wellington: New Zealand
        Jour. Science and Technology, v.38, p.433-446.

THOMPSON, J. A., 1916, On stage names applicable to the divisions of the
        Tertiary in New Zealand: Trans. New Zealand Inst., v.48, p.28-40.

UREY, H. C., LOWENSTAM, H. A., EPSTEIN, S., AND McKINNEY, C. R., 1951,
        Measurement of paleotemperatures and temperatures of the Upper
        Cretaceous of England, Denmark and southeastern United States:
        Geol. Soc. Am. Bull., v.62, p.399-416.

VAN DER LINDEN, W.J.M., 1963, Sedimentary structures and facies interpretation
        of some Molasse deposits: Doctoral Thesis, Univ. of Utrecht.

VAN DER LINDEN, W.J.N., 1968, Textural, chemical and mineralogical analyses
        of marine sediments: New Zealand Oceanographic Institute
        Miscellaneous Publication, no. 39, 37p.

VAN DER LINGEN, G. J., 1968, Volcanic ash in the Makara Basin (upper Miocene),
        Hawke's Bay, New Zealand: New Zealand Jour. Geol. Geophys., v.11,
        p.693-705.

VAN STRAATEN, L.M.J.U., 1961, Sedimentation in tidal flat areas:
        Alberta Soc. Petr. Geol. Jour., v.9, p.203-226.

VELLA, P., 1963, Plio-Pleistocene cyclothems, Wairarapa, New Zealand:
        Trans. Royal Soc. New Zealand, v.2, p.15-50.

WALTERS, L. J., CLAYPOOL, G. E., AND CHOQUETTE, P. W., 1972, Reaction
        rates and $\delta^{18}O$ variation for the carbonate-phosphoric acid
        preparation method: Geochim. Cosmochim. Acta, v.36, p.129-140.

APPENDIX 1

Computer programme for the calculation of mean inclination and declination of NRM for cores taken from dipping strata. Programme modified after Lienert (1972).

This is followed by the results determined in the present study. K is the precision parameter, A95 is the cone of confidence at the 95% level, and R is the vector magnitude.

```
      REAL X2(2)
      DIMENSION GDEC(100),GINC(100),XL(100),XM(100),XN(100),
     1 DFC(100),DINC(100),TITLE(40)
    1 FORMAT(2A4,2(F6.1),3(F7.3))
    2 FORMAT(F4.1,E10.3,4(F5.1))
    3 FORMAT(/,1H ,2A4,2X,2(F8.3,2X),F10.3)
    4 FORMAT(1H0,'NO',13X,'DEC',7X,'INC',3X,'INTENSITY')
      READ(2,7)TITLE
    7 FORMAT(40A2)
      WRITE(3,51)TITLE
   51 FORMAT(1H0,40A2)
C     READ CONSTANT INPUT DATA
      READ(2,2)DELT,FACT,SLA,SLO,BD,BI
      WRITE(3,4)
      PI=3.14159265
C     READ DATA CARDS,N=NUMBER OF MEASUREMENTS PER LOCALITY
C     NO=SAMPLE NUMBER,OD=SAMPLE STRIKE,OI=SAMPLE INCLINATION
C     X,Y,Z ARE COMPONENTS MEASURED
   52 READ(2,11)N
   11 FORMAT(I3)
      IF(N)12,13,12
   12 DO 102 I=1,N
      READ(2,1)NO,OD,OI,X,Y,Z
C     CONVERT COMPASS BEARINGS TO DECLINATIONS OF Z AXIS FROM
C     TRUE NORTH
C     ADD 90 TO STRIKE TO GET SAMPLE DECLINATION
      ROD = (OD+DELT)*PI/180. +PI/2.
      RBD = (BD+DELT)*PI/180. +PI/2.
      ROI = OI*PI/180.
      RBI = BI*PI/180.
C     CALCULATE INTENSITY
      XD=SQRT(X*X+Y*Y+Z*Z)*FACT
      A=ROI
      B=ROD
      CA=COS(A)
      CB=COS(B)
      SA=SIN(A)
      SB=SIN(B)
```

```fortran
C    TRANSFORM COMPONENTS TO GEOGRAPHICAL AXIS
     YR=Y*CA-Z*SA
     XR=X*CI-Y*SA*SR-Z*SA*CA
     ZA=X*SR+Y*SA*C +Z*CA*CA
     A=XR
     B=SR.
     CA=COS(A)
     CR=COS(B)
     SA=SIN(A)
     SR=SIN(B)
C    TRANSFORM COMPONENTS TO BEDDING PLANE AXIS
     XG=Y*(1.+SR**2*(CA-1.0))+YR*SA*SR*CR*SA*(1.-CA)
     YG=YR*SA*Y*CA+ZR*SA*CR
     ZG=XR*CR*SR*(1.-CA)-YR*CR*SA+ZR*(1.+CR**2*(CA-1.))
C    CALCULATE DECLINATION AND INCLINATION RELATIVE TO
C    BEDDING PLANE
     GI=-ATAN(YG/SQRT(XG**2+ZG**2))
     GD=3.*PI/2.+ATAN(ZG/XG)
     IF(XG)2,1111,1111
   2 GD = GD - PI
1111 CONTINUE
     GDEC(I)=GD
     DINC(I)=GI
     GDEC(I)=GD*180./PI
     SINC(I)=GI*180./PI
102  WRITE(3,3)XG,GDEC(I),DINC(I),XP
C    CALCULATE FISHERS STATISTICS
     CONTINUE
     DO 111 I=1,N
     XL(I)=COS(DINC(I))*COS(DDEC(I))
     XM(I)=COS(DINC(I))*SIN(DDEC(I))
111  XN(I)=SIN(DINC(I))
     SL=0
     SM=0
     SN=0
     DO 22 I=1,N
     SL=SL+XL(I)
     SM=SM+XM(I)
22   SN=SN+XN(I)
```

```
C     CALCULATE MAGNITUDE OF VECTOR SUM
      R=SQRT(SL*SL+SN*SN+SN*SN)
C     CALCULATE PRECISION CONSTANT
      AXN=N
      XK=(AXN-1.)/(AXN-R)
C     CALCULATE MEAN DIRECTIONS
      DM=ATAN(SN/SL)+PI
      IF(SL)66,66,33
33    IF(SN)44,55,55
44    DM=DM+2.*PI
55    DM=DM+PI
C     CALCULATE HALF ANGLE OF CONE OF CONFIDENCE
66    XIM=ATAN((SN/R)/SQRT(1.-(SN/R)**2))*180./PI
      DM=DM*180./PI
      A=1.-((AXN-R)/R)*(EXP((1./(AXN-1.))*(ALOG(20.))-1.))
      A95=ATAN(SQRT(ABS(1.-A*A))/A))*180./PI
      WRITE(3,10)DM,XIM,XK,A95,R
10    FORMAT(18H MEAN DECLINATION=,F5.1,18H MEAN INCLINATION=,F5.1,
     118H K=,F5.1,3H A95=,F5.1,3H R=,F5.3)
      GO TO 52
13    STOP
      END
```

PRECLEANING

NO	DEC	INC	INTENSITY
R92B	32.313	-44.169	0.300E-06
R92D	59.948	-64.867	0.239E-06

MEAN DECLINATION= 42.5 MEAN INCLINATION=-55.2 K= 19.8 A95= 35.8 R=1.949

R91B	25.396	-71.175	0.239E-06
R91D	2.663	-56.622	0.634E-06

MEAN DECLINATION= 11.0 MEAN INCLINATION=-64.3 K= 43.3 A95= 23.9 R=1.976

R81B	166.323	-29.772	0.207E-07
R81D	126.457	-40.943	0.135E-07

MEAN DECLINATION=147.8 MEAN INCLINATION=-37.0 K= 11.4 A95= 48.4 R=1.912

R84B	14.653	2.973	0.570E-07

MEAN DECLINATION= 14.6 MEAN INCLINATION= 2.9 K= 0.0 A95= 0.1 R=0.999

R83A	330.358	-24.600	0.108E-07

R83B	168.707	47.909	0.499E-07
R83C	224.100	-4.603	0.637E-07

R82D	153.793	84.968	0.151E-07

MEAN DECLINATION=235.7 MEAN INCLINATION= 46.5 K= 1.3 A95=-70.3 R=1.710

R82B	77.532	-73.408	0.551E-07

R82C	24.167	-71.414	0.991E-07

MEAN DECLINATION= 49.2 MEAN INCLINATION=-74.1 K= 53.3 A95= 21.5 R=1.981

R9B	12.602	-20.540	0.865E-07

MEAN DECLINATION= 12.6 MEAN INCLINATION=-20.5 K= 0.0 A95= 0.1 R=0.999

R8A	257.661	74.139	0.366E-07

R8B	313.179	18.959	0.996E-07

MEAN DECLINATION=301.6 MEAN INCLINATION= 48.3 K= 3.4 A95=-75.0 R=1.706

```
R 74A    339.621    -69.253    0.166E-06
R 7B     247.674    -59.262    0.112E-05
R 72     305.305    -47.490    0.199E-06
MEAN DECLINATION=294.7 MEAN INCLINATION=-69.4 K= 11.7 A95= 25.7 R=2.929

R 73A     18.207    -58.911    0.226E-06
R 73C     54.272    -66.157    0.338E-05
R 73D     30.335    -57.821    0.230E-06
MEAN DECLINATION= 32.5 MEAN INCLINATION=-61.7 K= 73.6 A95= 13.0 R=2.972

R 71B    339.557    -72.629    0.796E-07
R 71C    295.561    -59.438    0.943E-07
MEAN DECLINATION=315.3 MEAN INCLINATION=-72.2 K= 67.9 A95= 19.0 R=1.965

R 6A     156.237    -71.495    0.232E-05

R 6B     249.205    -62.262    0.159E-06
MEAN DECLINATION=213.9 MEAN INCLINATION=-73.3 K= 11.6 A95= 47.9 R=1.913

R 4B     134.318     72.695    0.508E-07
R 4C     297.614    -33.935    0.495E-07
MEAN DECLINATION=268.6 MEAN INCLINATION= 35.7 K= 0.7 A95=-44.9 R=0.679
R 5A     146.790     75.770    0.113E-06

R 5C     106.897     20.789    0.601E-07
MEAN DECLINATION=119.8 MEAN INCLINATION= 53.0 K= 2.9 A95=-50.6 R=1.663

R 34B      3.479    -68.299    0.115E-06

R 34D    342.726    -54.128    0.119E-06
MEAN DECLINATION=350.7 MEAN INCLINATION=-61.5 K= 44.6 A95= 23.5 R=1.977
```

```
R33A     114.015    -13.926    0.303E-07
R33B     205.977    -54.039    0.389E-07
R33D      75.124     21.417    0.268E-07
MEAN DECLINATION=114.5 MEAN INCLINATION=-21.7 K= 1.6 A95=-85.0 R=1.807

R32       47.730    -36.326    0.606E-07
R3C      359.894    -64.536    0.495E-07
MEAN DECLINATION= 31.4 MEAN INCLINATION=-42.3 K= 8.3 A95= 37.8 R=1.880

R32A1      1.670    -82.491    0.293E-06
R3742    305.541    -72.247    0.245E-06
R322     290.463    -75.842    0.149E-06
MEAN DECLINATION=309.7 MEAN INCLINATION=-78.0 K= 89.8 A95=  8.9 R=2.977
R31A      64.945    -66.723    0.453E-07

R31B     295.759    -83.157    0.646E-07
MEAN DECLINATION= 78.9 MEAN INCLINATION=-80.7 K= 15.8 A95= 49.5 R=1.936

R12A     214.117     75.633    0.526E-07
R12B     175.267     76.519    0.764E-07
MEAN DECLINATION=191.7 MEAN INCLINATION= 73.9 K= 57.6 A95= 16.5 R=1.985

R11B     339.626     27.617    0.911E-07
R11C     354.F11     43.023    0.502E-07
MEAN DECLINATION=346.1 MEAN INCLINATION= 38.0 K= 23.7 A95= 52.6 R=1.957

R1A       82.544    -17.340    0.437E-07
R1B      189.927     11.426    0.389E-07
MEAN DECLINATION=137.3 MEAN INCLINATION= -5.4 K= 1.1 A95=-44.2 R=1.149
```

POST CLEANING AT 50 DEGREES C

NO	DEC	INC	INTENSITY
R83A	162.482	-58.491	0.131E-07
R83B	267.616	79.891	0.299E-07
R83C	191.027	-12.516	0.166E-07
R83D	124.173	37.894	0.486E-07

MEAN DECLINATION=172.3 MEAN INCLINATION= 13.9 <= 1.5 A95= 87.9 R=2.034

873A	13.602	-72.782	0.331E-06
873C	16.012	-66.624	0.365E-06
873D	11.358	-67.379	0.342E-06

MEAN DECLINATION= 13.6 MEAN INCLINATION=-68.9 K=545.3 A95= 3.6 R=2.996

// JFG GL56

POST CLEARING AT 100 DEGREES C

	DEC	INC	INTENSITY
R92A	34.081	-39.886	0.335E-06
R92C	359.085	-33.807	0.161E-06
R92D	23.104	-64.255	0.221E-06

MEAN DECLINATION= 17.4 MEAN INCLINATION=-47.0 K= 15.2 A95= 22.3 R=2.868

R93A	295.466	-36.394	0.170E-07
R93B	270.736	49.341	0.719E-07
R93C	205.323	-17.411	0.255E-07
R93D	134.046	34.640	0.453E-07

MEAN DECLINATION=227.8 MEAN INCLINATION= 15.0 K= 1.2 A95=-65.6 R=1.668

R7A	337.206	-72.418	0.138E-06
R7B	217.073	-35.226	0.125E-06
R7C	35.452	-65.137	0.136E-05
R7D	61.909	-69.291	0.131E-05

MEAN DECLINATION= 50.0 MEAN INCLINATION=-88.5 K= 3.1 A95= 33.9 R=3.415

R73A	356.338	-63.376	0.279E-06
R73C	26.691	-62.795	0.325E-06
R73D	30.648	-67.003	0.290E-06

MEAN DECLINATION= 17.5 MEAN INCLINATION=-65.1 K= 93.8 A95= 8.8 R=2.978

216.

R71A   300.453   -51.573   0.519E-07

R71B   281.015   -47.296   0.527E-07

R71C   3.601   -51.426   0.512E-07
R71D   6.064   -83.348   0.101E-06
MEAN DECLINATION=315.9 MEAN INCLINATION=-63.4 K= 9.4 A95= 23.9 R=3.683

R34C   297.026   -4.962   0.259E-07
MEAN DECLINATION=297.0 MEAN INCLINATION= -4.9 K= 0.0 A95= 0.1 R=0.999
R34A   335.373   -37.020   0.435E-07

R34B   330.368   -17.688   0.295E-07

R3C   26.517   -49.535   0.158E-07
MEAN DECLINATION=346.4 MEAN INCLINATION=-37.2 K= 8.2 A95= 31.2 R=2.756

R32A   117.274   -35.570   0.139E-06

R32B   176.364   -47.550   0.840E-07
MEAN DECLINATION=143.6 MEAN INCLINATION=-45.4 K= 6.7 A95= 65.8 R=1.851

R31B   226.663   -47.570   0.615E-07
MEAN DECLINATION=226.6 MEAN INCLINATION=-47.8 K= 0.0 A95= 0.1 R=0.999

POST CLEANING 150DEGREES C

NO. DATA	DEC	INC	INTENSITY
8998	207.723	18.998	0.240E-07
8999	157.930	55.367	0.492E-07
8990C	215.250	-29.561	0.269E-07
8990D	97.202	74.868	0.862E-07

MEAN DECLINATION=194.8 MEAN INCLINATION= 36.2 K= 2.3 A95= 57.2 R=2.739

8973A	1.386	-64.503	0.177E-06
8973C	24.028	-56.368	0.239E-06
8973D	351.851	-58.249	0.222E-06

MEAN DECLINATION= 9.6 MEAN INCLINATION=-63.9 K= 59.1 A95= 11.1 R=2.966

| 8971A | 306.746 | -53.124 | 0.395E-07 |
| 8971C | 59.535 | -65.718 | 0.517E-07 |

MEAN DECLINATION=344.9 MEAN INCLINATION=-69.9 K= 4.7 A95= 82.8 R=1.787

| 8346 | 194.141 | -31.387 | 0.746E-07 |
| 8341 | 111.364 | 3.180 | 0.622E-07 |

MEAN DECLINATION=148.8 MEAN INCLINATION=18.4 K= 1.8 A95=-38.6 R=1.468

218.

POST CLEANING 200 DEGREES C

NO	DEC	INC	INTENSITY
R83B	276.503	53.784	0.644E-07
R83C	143.455	-27.097	0.353E-07
R83D	102.733	57.968	0.640E-07

MEAN DECLINATION=157.1 MEAN INCLINATION= 58.0 $<=$ 1.3 A95=-44.5 R=1.469

R73A	13.402	-55.895	0.162E-06
R73C	28.243	-54.452	0.227E-06
R73D	180.179	-14.245	0.943E-07

MEAN DECLINATION= 77.6 MEAN INCLINATION=-77.7 $<=$ 1.8 A95= 84.7 R=1.932

R71A	90.770	-27.084	0.536E-07
R71C	299.197	-48.258	0.580E-07

MEAN DECLINATION= 32.4 MEAN INCLINATION=-65.2 K= 1.4 A95=-42.9 R=1.323

// XEQ GLS6

```
POST CLEANING 250DEGREES C

NO            DEC        INC      INTENSITY

R59A        231.439     17.039    0.240E-07

R58C        204.822     22.912    0.389E-07
R58D        202.290     48.316    0.395E-07
MEAN DECLINATION=214.1 MEAN INCLINATION= 30.0 K= 13.5 A95= 23.5 R=2.855

R7A          42.910    -61.934    0.364E-07
R7B          11.533    -21.582    0.433E-07
MEAN DECLINATION= 21.9 MEAN INCLINATION=-42.7 K=  8.3 A95= 68.1 R=1.942

R73A         88.474    -23.679    0.100E-06
R73C        305.742    -54.393    0.750E-07
R73D        193.133    -48.765    0.119E-06
MEAN DECLINATION=123.4 MEAN INCLINATION=-78.4 K=  2.0 A95= 79.2 R=2.007

R71A        138.969     62.438    0.200E-07

R71C        341.737    -71.135    0.512E-07
MEAN DECLINATION=101.6 MEAN INCLINATION=-16.0 K=  3.5 A95=-44.9 R=0.215

R34A          0.339     14.644    0.973E-08
R34B        143.480    -20.165    0.455E-07

R34D        348.487    -13.601    0.232E-07
MEAN DECLINATION= 17.6 MEAN INCLINATION=-14.9 K=  1.1 A95=-31.0 R=1.265
```

POST CLEANING AT 300 DEGREES C

NO	DEC	INC	INTENSITY
R7C	2.961	-74.135	0.593E-07
R7B	13.659	-53.679	0.643E-07

MEAN DECLINATION= 10.2 MEAN INCLINATION=-63.9 K= 30.1 A95= 25.8 R=1.966

R73A	30.013	-26.417	0.867E-07
R73C	89.482	-44.316	0.984E-07
R73B	125.438	-30.285	0.910E-07

MEAN DECLINATION= 81.4 MEAN INCLINATION=-41.1 K= 4.0 A95= 47.4 R=2.506

| R71C | 31.503 | 44.962 | 0.200E-07 |

MEAN DECLINATION= 31.5 MEAN INCLINATION= 44.9 K= 0.0 A95= 0.1 R=0.999

R34B	0.612	49.875	0.850E-07
R34C	15.966	-15.928	0.692E-07
R34D	5.833	9.567	0.510E-07

MEAN DECLINATION= 8.2 MEAN INCLINATION= 13.9 K= 5.8 A95= 37.9 R=2.657

| R3C | 217.532 | 43.661 | 0.271E-07 |
| R3B | 341.424 | -7.238 | 0.659E-07 |

MEAN DECLINATION=295.8 MEAN INCLINATION= 33.8 K= 1.0 A95=-44.6 R=1.012

| R31C | 107.103 | 13.036 | 0.105E-07 |
| R31C | 290.205 | 32.945 | 0.445E-07 |

MEAN DECLINATION= 88.6 MEAN INCLINATION= 79.4 K= 0.8 A95=-44.8 R=0.782
// XEQ GLS6

```
R3A          2.190      64.157   0.127E-07

R3B        217.726     -31.556   0.331E-07

R3C         44.059      -5.557   0.357E-07
MEAN DECLINATION= 21.4 MEAN INCLINATION= 28.6  K=  0.3  A95=-44.5  R=0.583

R31C       295.417      -1.597   0.445E-07

R31B       130.727      -6.351   0.562E-07
MEAN DECLINATION=214.3 MEAN INCLINATION=-27.5  K=  0.5  A95=-44.9  R=0.299
// XEQ GLS6
```

POST CLEANING AT 350 DEGREES C

NO	DEC	INC	INTENSITY
R92A	90.983	-6.883	0.143E-06
R92C	55.390	-20.659	0.792E-07
R92D	118.831	-41.743	0.835E-07

MEAN DECLINATION= 86.3 MEAN INCLINATION=-25.1 K= 6.1 A95= 36.8 R=2.675

R91B	34.108	-55.432	0.145E-06
R91C	16.289	-67.250	0.837E-06
R91D	69.553	-74.792	0.767E-06

MEAN DECLINATION= 35.7 MEAN INCLINATION=-67.0 K= 35.9 A95= 14.3 R=2.944

| R9?B | 7.924 | -40.228 | 0.902E-07 |
| R9?C | 195.715 | -36.535 | 0.150E-06 |

MEAN DECLINATION=261.7 MEAN INCLINATION=-84.7 K= 1.3 A95=-43.7 R=1.247

R84A	60.939	-39.915	0.667E-05
R84B	25.121	49.560	0.874E-07
R84C	238.775	78.296	0.295E-07

MEAN DECLINATION= 42.1 MEAN INCLINATION= 43.8 K= 1.4 A95=-62.8 R=1.591

| R81A | 204.994 | 35.266 | 0.432E-07 |
| R81B | 197.817 | 72.220 | 0.457E-07 |

MEAN DECLINATION=203.0 MEAN INCLINATION= 53.7 K= 9.6 A95= 53.4 R=1.895

```
R83A         155.186      46.266      0.232E-07
R83C         148.657      12.609      0.127E-07
R83D         138.267      10.282      0.127E-07
MEAN DECLINATION=149.1 MEAN INCLINATION= 23.2 K= 12.2 A95= 25.1 R=2.836
R8A          220.707      70.793      0.292E-07
R8B          301.846      41.694      0.559E-07
R8C          181.422      77.936      0.488E-07
MEAN DECLINATION=265.6 MEAN INCLINATION= 71.6 K= 7.2 A95= 33.4 R=2.725
R82A          89.963     -46.261      0.555E-07
R82B         212.795     -32.455      0.491E-07
R82C         123.463     -40.826      0.564E-07
R82D         126.807     -58.002      0.354E-07
MEAN DECLINATION=138.2 MEAN INCLINATION=-54.9 K= 4.7 A95= 35.5 R=3.372
R7A           16.645     -53.088      0.583E-07
R7B           13.646      16.524      0.327E-07
MEAN DECLINATION= 14.7 MEAN INCLINATION=-18.2 K= 2.7 A95=-52.7 R=1.641
R72A         311.776       2.702      0.906E-07
R73D          31.483     -57.686      0.608E-07
MEAN DECLINATION=337.4 MEAN INCLINATION=-23.3 K= 1.8 A95=-39.5 R=1.452
R71A         141.382      71.876      0.203E-07
R71C          91.994      52.589      0.302E-07
MEAN DECLINATION=108.2 MEAN INCLINATION= 64.1 K= 16.1 A95= 40.1 R=1.937
```

```
R6A        208.942    -71.751    0.186E-06
R6C         10.770     56.282    0.819E-07
R6D        192.428     67.291    0.623E-07
R6F        316.195      5.024    0.161E-06
MEAN DECLINATION=306.6 MEAN INCLINATION= 41.5 K=  1.1 A95==24.0 R=1.371

R4B        229.645     19.985    0.371E-07
R4C        285.455     39.304    0.635E-07
R4D        254.903     40.977    0.667E-07
MEAN DECLINATION=254.7 MEAN INCLINATION= 33.5 K=  9.8 A95= 28.3 K=2.796

R5A        171.582     58.591    0.167E-06
R5B        154.567     61.456    0.665E-07
R5C        165.899     53.478    0.458E-07
MEAN DECLINATION=164.3 MEAN INCLINATION= 58.0 K=182.1 A95=  6.3 R=2.989

R34Q       235.132     24.510    0.464E-07
R34L       ...         ...       ...
R34G        53.024      7.888    0.424E-07
MEAN DECLINATION=359.3 MEAN INCLINATION=-14.6 K=  1.0 A95==40.4 R=1.081

R33R       202.670     20.733    0.412E-07
R33G       182.343      1.107    0.771E-07
R33H       157.405     18.472    0.791E-07
R33J       165.192     37.657    0.209E-06
MEAN DECLINATION=177.2 MEAN INCLINATION= 20.3 K= 11.5 A95= 21.4 R=3.740
```

```
R30              117.971    -15.424    0.271E-07
R3C              150.173     17.828    0.200E-07   0.200E-07
MEAN DECLINATION=148.8 MEAN INCLINATION=  1.4  K=  2.7  A95=-32.4  R=1.641

R?D              125.160     12.576    0.453E-07
R?E              148.557     34.621    0.313E-07
R?C              140.492     23.429    0.435E-07
MEAN DECLINATION=148.2 MEAN INCLINATION= 25.2  K=  1.2  A95= 31.4  R=2.751

R21B              77.451     42.652    0.529E-07
R21C             111.135     32.806    0.346E-07
R?1D             139.224     69.013    0.114E-04
MEAN DECLINATION=103.4 MEAN INCLINATION= 50.3  K=  5.3  A95= 48.3  R=2.796

R12A              35.359     58.164    0.273E-07
R12B             213.090     51.931    0.123E-05
R12C               1.661     85.428    0.263E-07
MEAN DECLINATION= 23.9 MEAN INCLINATION= 87.3  K=  7.4  A95= 33.0  R=2.730

R11A             134.713    -43.679    0.456E-07
R11B              92.327     25.466    0.781E-07
R11C              29.042     50.447    0.355E-07
MEAN DECLINATION= 63.9 MEAN INCLINATION= 23.1  K=  1.6  A95=-81.5  R=1.767

R1A              199.130     36.319    0.268E-07
R1B              287.971      5.991    0.918E-07
R1C              290.196    -15.863    0.451E-07
MEAN DECLINATION=266.5 MEAN INCLINATION= 11.3  K=  2.3  A95= 69.8  R=2.145
```

APPENDIX 2

This appendix contains descriptions of stratigraphic sections, where the sequence is of considerable length (i.e. there are no single outcrop descriptions here).

Thicknesses were measured, except where stated, with a rod and level. Those under column A are unit thicknesses and those under B cumulative thicknesses.

COAST SECTION

Described 25/4/70. Base of section N137/374944, the base of the Butlers Shell Conglomerate.

BUTLERS SHELL CONGLOMERATE

Unit	- scoured base -	A(m)	B(m)

1   BUTLERS SHELL CONGLOMERATE

Conglomerate with sandy silt tongues increasing   3.0-7.0   3.0-7.0
in number both upwards and eastwards.
Conglomerate composed of rolled shells and
pebbles varying in abundance, in sandy glassy
matrix. Pebbles up to 0.2m diameter generally
well rounded, dominantly greywacke, but
others of weathered ignimbrite, rhyolite and
pumice. Other clasts are derived concretions,
with very irregular slightly platey form.
Shells, mollusca, often broken and rounded.
To the west the conglomerate is thin bedded,
conglomerate beds alternating with slightly
ashy silts, and cross bedded. Conglomerate
beds average 0.1m thick and silt beds 0.02m.
Cross bedding is large scale tangential, low
angle and often bipolar bimodal. Eastwards
the facies changes, with increasing silt beds,
up to several metres thick. Ripple, symmetric,
lingoid?, seen on broken fragments of silt on
the beach.

- sharp contact with relief up to 0.1m -

2   LOWER OKEHU SILTSTONE

Very thin bedded to laminated sandy silt and   20.0-22.0 23.0-29.0
silt. Dark blue, sometimes green-grey. A few
scattered molluscs. At the base, a conglom-
erate; pebbles up to 30 mm long; greywacke,
argillite, quartzite and very rarely rhyolite.
Also clasts of rolled concretions in a silty
fossiliferous sand.

- erosional contact with relief up to 0.5m -

Unit		A(m)	B(m)

3 OKEHU SHELL GRIT

Shelly sandy conglomerate. Thin bedded silty 0.0-8.3 37.3
sands alternating with thin to medium bedded
sandy conglomerates. Towards the top of the
unit, silts are thicker bedded and conglomerate
less common. Pebbles, greywacke and quartzite,
up to 30mm long, rounded. Shells generally
freshly broken, or complete, include molluscs
and echinoderms. Whole unit is cross-
stratified. Low angle, planar, large scale
bipolar-bimodal.

- contact gradational over 0.5m -

4 UPPER OKEHU SILTSTONE

Laminated to very thin bedded sandy silt. 5.2 42.5
Dominantly blue grey. The lower one metre is
conglomeratic, with pebbles of greywacke and
quartzite up to 35mm, well rounded, together with
a few rounded mollusc shells.

- sharp contact -

5 KAIMATIRA PUMICE SAND

Alternating sandy silt and medium sand. Brown, 6.6 49.1
thin bedded. Silts exhibit symmetrical ripples
sands frequently ripple-drift cross-laminated.

- sharp contact -

6 Gravelly coarse sand. Very friable, brown. 6.4 55.5
Pebbles of rhyolite, ignimbrite and pumice as
well as greywacke. Sand fraction tuffaceous.
Scattered molluscs. Large scale cross-
stratification common in the upper portion.

- sharp contact -

7 Alternating very coarse sand and sandy silt. Very 2.0 57.5
friable. Brown, very tuffaceous with
abundant hornblende crystals.

Molluscs especially abundant in the upper 0.5m.
Large scale cross-stratified, set thickness 2.0m.

SECTIONS IN THE WANGANUI VALLEY

Outcrop at the junction of Makirikiri Stream and
Wanganui Rivers, N138/640940. Section begins with the
Makirikiri Formation.

Unit		A(m)	B(m)
1	Basal conglomerate. Poorly sorted, lack of bedding. Clasts up to 0.15m long axis, of greywacke and quartzite, set in a coarse sandy matrix, iron stained.	0-1.0	1.0

- sharp contact -

2	Sand and silty sand. Brown yellow, medium, moderately well sorted, tuffaceous, thin bedded.	9.0-10.0	11.0

In basal 1m, intraformational breccia with
clasts of sandy siltstone up to 0.5m long,
angular, platey. Clasts tend to be imbricate.
Within this lower unit, also, convolute laminae
with very irregular geometry, height of the
convolutions up to 0.75m.
At 2m ripple-drift cross-lamination and large
scale cross-stratification. Higher in the
unit, again, large scale cross-stratification,
with some charred wood fragments up to 5mm
long.

- sharp contact -

3	Tephra, white, medium to fine.	1.0-1.3	12.3

- undulatory, sharp contact, with relief up to 0.5m -

4	Alternating sands and clayey silts, mottled blue, and yellow. Sand, medium, tuffaceous, very thin bedded, sometimes slightly wavey. Some asymmetric ripples in the silts. Towards the top, convolute laminations, up to 0.1m high.	1.1	13.4

- sharp contact -

Unit		A(m)	B(m)
5	Sand, grey yellow, medium, moderately well sorted, tuffaceous. Thin bedded, with some parallel laminations visible. Some large scale cross-stratification and ripple-drift cross-lamination.	4.5	17.9
	- sharp contact -		
6	Ash, white, gravelly very coarse sand.	0.5-1.0	18.9
	- sharp contact -		
7	Sand, grey brown, very coarse, moderately well sorted, pumiceous. Large scale cross-stratification.	1.5	20.4
	- sharp contact -		
8	Silt, light brown, no bedding visible.	0.7	21.1
	- sharp contact -		
9	Alternating sand and silty sand. Brown, thin bedded with plane parallel laminations.	2.0	23.1
	- top of outcrop -		
	Estimated break of 70m (Superior, 1943; Fleming, 1953), followed by a sequence of Kaimatira Pumice Sand at Kaimatira Bluff, N138/625908.	70.0	93.1
10	Silty very fine sand, thin bedded, with partings of medium-fine sand up to 5mm thick. Slightly tuffaceous.	1.5	94.6
	- sharp erosional contact -		
11	Pebbly shelly sand, with interbedded silt. Pebbles of greywacke, ignimbrite and pumice up to 30mm long. Sands, brown, very coarse, tuffaceous. Silts, pale brown, thin bedded tuffaceous. Shells, mollusca, often broken. Large scale planar cross-stratification; sets up to 1.5m high. Unimodal foreset dip.	3.0-5.0	99.6
	- sharp contact -		

Unit		A(m)	B(m)
12	Alternating sand and silty sand. Sand, brown,	19.0+	118.6+

12   Alternating sand and silty sand. Sand, brown,
often iron stained, medium to very coarse,
moderately well sorted, friable, tuffaceous,
with visible hornblende crystals. Silty sand,
pale brown, tuffaceous, thin to very thick
bedded, and thickening to west. Contact
between sands and silty sands, sharp, with many
examples of scouring of the silt by the sand.
Symmetrical ripple marks on base of silty sand
units. Some silty sand beds braded, with
ripple lamination in the lower portion and
plane parallel in the upper. Top of silty
sands often have load features (flames), with
maximum height of 20mm. Upper portion of some
silty sands, have burrows up to 25mm long.

Where silty sands thicker bedded, to west,
convolute laminations, with heights up to 1.0m
common.

Sands, all ripple-drift cross-laminated,
often with opposing foreset dip directions.

SECTION ALONG RAILWAY PARALLEL TO BRUNSWICK ROAD

Sequence is Kaimatira Pumice Sand, with first exposure at N138/580911.

Unit		A(m)	B(m)
1	Silt, pale brown, thin bedded	0.5	0.5
	- erosional contact -		
2	Alternating sand and silt. Sand, grey, pumiceous, with pumice pebbles up to 30mm long diameter, bipolar-bimodal large scale cross-stratification. Asymmetric ripples towards the top in the silt. Charcoal fragments common. Silts, grey, thin bedded, generally plane parallel laminated.	1.0-2.5	3.0
	- sharp contact -		
3	Alternating sand and silt. Sands, ripple-drift cross-laminated, grade up to silts which are plane parallel laminated.	4.2	7.2
	- sharp contact -		
4	Gravelly sand. Shelly-broken mollusca. Iron stained. Pebbles greywacke, well rounded. Whole unit is one set of large scale planar cross-stratification.	0.5	7.7
	- sharp contact -		
5	Sand, with silt flasers in the lower section. Bipolar-bimodal ripple-drift cross-lamination. Grades up to linsen bedding with small scale cross-laminated sandy silts and lenses of sand.	11.0	18.7
	- sharp contact -		
6	Alternating coarse sand and silt. Large scale cross-stratification, with set thickness generally greater than 1.0m.	2.1	20.8
	- sharp contact -		

Unit		A(m)	B(m)
7	Silts with some interbedded rippled medium sands.	0.5	21.3
	- erosional contact -		
8	Tephra, white. No apparent structures.	1.3	22.6
	- sharp contact -		
9	Sand. Medium. Varies laterally from ripple-drift cross-lamination to large scale sets with set thickness up to 200mm.	1.1	23.7
	- sharp contact -		
10	Sand. Medium. Ripple-drift cross laminated. - sharp contact -	1.8	25.5
11	Silt. Plane parallel laminated to thin bedded.	2.1	27.6
	- gradational contact -		
12	Sand. Brown grey, medium, well sorted, with bipolar-bimodal ripple-drift cross lamination, and silt flasers. Varies laterally to large slump folds to the north.	0.9	28.5
	- erosional contact -	1.5-3.0	31.5
13	Gravelly sand and silt. Thin bedded, large scale cross-stratification with sets greater than 1.0m high. Very pumiceous. Intraformational conglomerate - silt clasts - at base.		
	- sharp contact -		
14	Alternating sand and silt. Latter rippled.	1.2	32.7
	- sharp contact -		
15	Tephra. Sand, coarse, white.	1.5	34.2
	- top of exposure marked by fault -		
	GAP OF UNKNOWN THICKNESS		
16	Sand, pale brown, medium, friable, tuffaceous. Ripple-drift cross-lamination. A few silt flasers.	3.0	3.0
	- gradational contact -		

Unit		A(m)	B(m)
17	Alternating medium sand and sandy silt. Grey, friable, very thin bedded. Sands are small scale cross bedded.	1.1	4.1

- erosional contact -

| 18 | Sand. Medium, brown, pebbly shelly with lenses of silty very fine sand up to 1.0m long and 0.2m thick. Large scale tangential cross-stratification. | 0.25 | 4.35 |

- erosional contact -

| 19 | Alternating sand and silty fine sand. Pale brown, very thin bedded. Each bed graded. Contact between individual beds sharp. Base of each unit has ripple-drift cross-stratification which grades up to plane parallel lamination in the finer material. | 0.6-2.0 | 6.35 |

- gradational contact -

| 20 | Sand. Brown, medium, pebbly, shelly, tuffaceous. Pebbles all greywacke, up to 0.2m long diameter. Shells broken. Large scale tangential cross-stratification. | 0.8 | 7.15 |

- sharp contact -

| 21 | Alternating coarse and very fine sand. Thin bedded, passes laterally to shelly sands as unit 5. | 2.1 | 9.25 |

- erosional contact -

| 22 | Sands. Brown, coarse, tuffaceous. Numerous Amphidesma, broken but not rounded, lying parallel to bedding. | 1.0 | 10.25 |

- top of exposure -

KAUKATEA ROAD   Loc. 148

Position at base N139/710892. Base at road level. Measured
10/4/71.

Unit		A(m)	B(m)
1	Sand. Yellow grey, fine to medium, very tuffaceous. Thin bedded.	2.1	2.1

                  - erosional contact over 0.5m -

| 2 | Sand. Medium to coarse with pebbles. Lateral change very strong, pebbles increase in size to the west until the unit becomes conglomeratic with boulders up to 1.5m long. Clasts of greywacke, andesite and siltstone haphazardly deposited in a coarse lithic sand. Base of conglomerate is erosional contact with the underlying unit. Sands are large scale cross-stratified, with some ripple drift, which has bipolar-bimodal foreset dips. This whole unit is very disordered. | 1.0-2.5 | 4.6 |

                       - sharp contact -

| 3 | Alternating sand and silt. Yellow grey. Sand fine, thin bedded. Some irregular convolute laminations. At 2.1m lens of very coarse pumiceous hornblende rich gravelly sand, large scale cross bedded, with thin beds of fine sand. Amphidesma shells, some broken but not abraded, very abundant in this lens. | 3.5 | 8.1 |

                       - sharp contact -

| 4 | Alternating medium and very fine sand. Yellow grey, well sorted, tuffaceous. Thin bedded. Very fine sands rippled. | 13.0 | 21.1 |

                       - sharp contact -

| 5 | Sandy silt. Grey brown, plane parallel lamination just distinguishable. Whole mollusc shells - Chlamys gemmulata. | 3.0 | 24.1 |

                 - sharp, slightly wavy contact -

Unit		A(m)	B(m)
6	Tephra, white, fine sand to silt size. Whole unit is a mass of large convolutions which are emphasised on the weathered surface.	4.1	28.1

- top of exposure -

RANGITIKEI SECTION

The section is exposed along the road from Pakihikura Bridge to the
top of Rewa Hill. Base of outcrop along the road just south of the
junction of Pakihikura Stream and the Rangitikei River, at N139/137839.
Section description begins with the Makirikiri Tuff formation.

Unit		A(m)	B(m)
1	Sand. Grey, medium, friable, tuffaceous. Medium to thick bedded. Some large scale cross-stratification.	13.1	13.1
	- sharp contact -		
2	Sand. Grey brown, coarse, tuffaceous, inter-bedded pale yellow brown, fine. Thin bedded.	2.3	15.4
	- sharp contact -		
3	Sand. Very coarse interbedded with medium to fine. All tuffaceous. Plane parallel lamination and some ripple-drift cross-lamination.	1.5	16.9
	- sharp contact -		
4	Sand. Brown, coarse; plane parallel lamination grades up to large scale cross-stratification.	1.0	17.9
	- sharp contact -		
5	Tephra. White grades up to grey. Massive.	0.5	18.4
	- gradational contact -		
6	Silt. Grey, thin to medium bedded. Very tuffaceous.	0.7	19.1
	- erosion surface with 200mm relief -		
7	Sand. Grey brown, coarse. Some small scale cross-stratification.	0.9	20.0
	- sharp contact -		
8	Silt. Grey, thin to very thin bedded.	1.2	21.2
	- sharp contact -		
9	Clayey silt. Weathers white, fresh surface blue grey. Massive.	2.0	23.2
	- sharp contact -		

Unit		A(m)	B(m)
10	Sand. Grey, medium, tuffaceous, with some silt lenses, which increase in number upwards.	7.0	30.2
	- sharp contact -		
11	Sand and silt. Pale green grey passes up to dark grey to a lignite bed near the top, 100mm thick. Crystals of gypsum on the lignite.	1.6	31.8
	- sharp contact -		
12	Sand. Grey, medium, poorly sorted, with laminae of blue brown silt. Mollusc shells common. Lignite bed 60mm thick at the base.	0.9	32.7
	- sharp contact -		
13	Sand. Brown grey, pebbly, coarse, friable.	8.5	41.2
	- grass covered contact -		
14	Interbedded sand and silt. Grey, tuffaceous, thin bedded. Some beds graded. One tephra at 4.0m, 90mm thick. This unit is the Ridge Ash.	4.5	45.7
	- sharp contact -		
15	Sand. Brown grey, very coarse to coarse, friable. Large scale, low angle cross-stratification, up to 1m high. Convolute lamination near the top, with very sharp peaks.	4.4	50.1
	- gradational contact -		
16	Alternating sandy silt and medium to coarse sand. White to yellow grey, very tuffaceous. Thin bedded. (Lower sequence of Mangapipi Ash Member).	2.6	52.7
	- grass covered contact -		
17	Sandy silt with some beds of medium sand. Blue grey to yellow grey, some tuffaceous beds. Lignite lenses.	9.8	62.5
	- sharp contact -		
18	Sand and silt. Blue grey and yellow grey with a white tephra at 5.0 metres (Mangapipi Ash, upper tephra). Large scale cross-stratification.	5.6	68.1
	- sharp contact -		

Unit		A(m)	B(m)
19	Sand. Grey brown, medium, very tuffaceous. At base convolute laminations, and in the bed above, intraformational breccia, with blocks of siltstone up to 0.3m long. Anticlines of convolutions are sharply truncated by the brecciated bed above. The latter passes up into medium to fine sands, with decreasing ash content to brown sands at the top, and a few dark grey clay beds.	14.4	82.5

<div align="center">- gradational contact -</div>

20	Sand and sandy silt. Grey, thin bedded, only slightly tuffaceous. Several silt units have a very blue weathered surface. Some beds large scale cross bedded. Blocks that have fallen down from the cliff have symmetrical ripples on the bedding plane.	28.0	110.5

<div align="center">- sharp contact -</div>

21	Sand. Blue grey, medium, tuffaceous. Some pumice lenses up to 0.1m long, 10mm thick. Mollusc shells.	7.1	117.6

<div align="center">- sharp contact -</div>

22	Clayey silt. Blue grey, plane parallel laminations. Abundant mollusc shells.	6.4	124.0

<div align="center">- sharp contact -</div>

23	Silt. Blue grey, very thin bedded. No fauna. At 8.5m there is a gradational coarsening of the sediment to medium sand, grey brown. Near the top there is another sandy unit. (Okehu Siltstone).	approx 105m (Te Punga, 1953)	229.0

<div align="center">- sharp contact -</div>

24	Sand. Brown, medium, micaceous. At approximately 40m large scale trough cross-stratification in coarse brown sand. Lower unit of each trough defined by sandy silt up to 0.1m thick with rippled surface. Just beneath the large scale cross-beds the sand is ripple-drift cross-laminated.	58.0	287.0

<div align="center">- sharp contact -</div>

Unit		A(m)	B(m)
25	Sand. Grey, very coarse, medium, tuffaceous with silt lenses up to 30mm thick. Bedding very irregular with convoluted small scale cross-stratification. Broken mollusc shells common. (Beginning of Kaimatira Pumice Sand Formation).	4.8	291.8

- sharp contact -

26	Sand. Brown yellow, medium to coarse, tuffaceous. Small scale cross-stratification.	0.9	292.7

- sharp contact -

27	Sand. Grey, medium to coarse, tuffaceous, thin bedded.	3.2	295.9

- erosion surface with 0.2m relief -

28	Sand. Brown, medium at base to fine at top, tuffaceous and friable. Lower 3m has large scale cross-stratification up to 1m high, emphasised by laminae of ferromagnesian minerals. Within this lower unit are a few scattered pebbles and broken mollusc shells. Also some small 'armoured' silt clasts. Large fine sandy silt flasers up to 4m long and 120mm thick common. Upper surface of the flasers display flame structures. Base of some are rippled. Lower contact of the flasers always unconformable on the underlying sands.	6.8	302.7

The upper section of this unit has a higher percentage of ferromagnesian minerals and grades vertically and laterally into thin bedded plane parallel laminated grey, tuffaceous, medium sands. Towards the top these plane beds give way to ripple-drift cross-laminated fine sands.

- sharp contact -

29	Sand. Grey, medium to fine, tuffaceous. Thin bedded with plane parallel lamination.	1.5	304.2

- sharp contact -

Unit		A(m)	B(m)
30	Sand. Grey, very fine to fine, with some greywacke and andesite clasts up to 20mm diameter. At 1.5m a thin bed of mollusc shells. In the upper half of the unit are large convolute laminations in very fine sand, height up to 0.7m, with very peaked anticlines. Some exhibit rupturing of the anticlines. Some anticlines have concentrations of pumice in the nodes.	9.1	313.3
	- sharp contact -		
31	Sand and sandy silt. Grey, tuffaceous, thin bedded. Large scale trough cross-stratification in the lower section. At 4m lenses of intra-formational breccia with clasts up to 0.4m diameter, quite rounded. At the top of the unit the sand is coarser and large scale trough cross-stratification up to 0.3m high is well developed.	6.8	320.1
	- contact erosional with 0.2m relief -		
32	Conglomerate. Tephra. All clasts pumice with a tuffaceous matrix. Rewa Pumice.	1.5	321.6
	- sharp contact -		
33	Sand. Weathers white, very tuffaceous, fine, parallel laminated, thin bedded.	0.7	322.3
	- sharp contact -		
34	Sand. Pale grey, coarse with andesite and greywacke pebbles up to 20mm diameter. A few scattered molluscs.	1.0	323.3
	- sharp irregular contact -		
35	Sand. Brown, iron stained, medium, tuffaceous.	2.7	326.0
	- grass covered contact -		
36	Sand and silty sand. Brown, medium to fine, thin to medium bedded.	3.1	329.1
	- sharp contact -		

Unit		A(m)	B(m)
37	Sand. Brown, medium to coarse. Convolutions up to 1m high. Small normal faults within the convolutions.	2.0	331.1

- sharp contact -

| 38 | Sand. Grey, medium to fine, tuffaceous, well sorted, thin bedded. Ripple-drift cross-lamination at the base of each bed grades up to plane parallel lamination in very fine sand at the top. Some silt beds up to 50mm thick. Some of the silts have been eroded by the overlying sands. A few burrows. | 4.4 | 335.5 |

- gradational contact over 0.2m -

| 39 | Sand. Grey, medium to fine, tuffaceous, well sorted. Symmetrical ripples on sandy silt lenses. | 0.9 | 336.4 |

- gradational contact -

| 40 | Sand as unit 39, but gradual increase in silt and fine sand content until at the top, the dominant texture is silty fine sand and sandy silt. Bedding increases from thin to medium. In the lower half, channel cuts with fills of sandy silt common. Width of channels up to 10m, height up to 0.5m. | 7.7 | 344.1 |

- gradational contact -

| 41 | Dominantly fine silty sand. Grey, thin bedded. Also very thin beds of fine sand, pumiceous with some carbonaceous material. One shelly sand bed 0.1m thick. | 2.3 | 346.4 |

- sharp contact -

| 42 | Sandy silt. Grey brown, thin bedded. Some ripple-drift cross-lamination and some symmetrical ripples on the siltier lenses. Small burrows, up to 10mm long passing down from the top of the beds are distinctly clayey. | 14.5 | 360.9 |

- sharp contact -

Unit		A(m)	B(m)
43	Conglomerate. Red brown, poorly sorted. Clasts up to 30mm long of greywacke and andesite in a coarse sand matrix. Graded upwards. Large scale cross-stratification.	1.2	362.1
	- sharp contact -		
44	Sand. Weathers grey brown, medium to fine. Ripple-drift cross-lamination.	3.0	365.1
	- grass covered contact -	8.6	373.7
45	Sand. Brown, medium with flaser of very fine sand and silt. Sand generally plane parallel laminated. Near the base, a thin shelly lens 0.3m maximum thickness, with large scale planar cross-stratification.	1.0	374.7
	- gradational contact -		
46	As above unit but with increasing number and thickness of silt units upwards.	12.4	387.1
	- grass covered contact -	5.2	392.3
47	Alternating silty fine sand and sand. Thin to very thin bedded. Slightly tuffaceous. At 9m very irregularly shaped lenses of conglomerate up to 0.5m thick, with pumice clasts up to 0.3m long. Most clasts, however, greywacke.	13.0	405.3
	- sharp contact -		
48	Sand and silty fine sand. Thin bedded. Brown grey, very friable, tending to slump easily, tuffaceous.	4.8	410.1
	- sharp contact -		
49	Sand. Grey, medium, with alternating silt beds. Tuffaceous. Thin bedded.	11.1	421.2
	- gradational contact -		
50	As above unit with increase in ash content.	3.2	424.4
	- sharp contact -		

Unit		A(m)	B(m)
51	Sand. Brown, medium to fine. Plane parallel laminated. Some silt and very fine sand flasers.	1.6	426.0
	- sharp contact -		
52	Sand. Pale brown to grey, fine, well sorted. Some plane parallel lamination, and some large scale cross-stratification.	10.0	436.0
	- sharp contact -		
53	Tephra (Potaka Pumice). White, fine sand size. Convolute lamination and large scale cross-stratification.	1.3	437.3
	- sharp contact -		
54	Tephra. White, fine sand size, plane parallel laminated.	1.5	438.8
	- sharp contact -		
55	Tephra. White, sand size with some pumice pebbles.	3.2	442.0
	- sharp contact -		
56	Tephra. White, very coarse sand size to conglomerate. Large scale trough cross bedded. Inverse grading in many beds, with clast of pumice up to 0.1m at the top of some beds.	1.3	443.3
	- sharp contact -		
57	Tephra. White, coarse sand and silt size. Channel cut with a depth of 1m and width 3m. Large scale trough cross-stratification common. Silt dominantly plane parallel laminated.	3.7	447.0
	- sharp contact -		
58	Tephra. White, medium to fine sand size. Bedding.	1.0	448.0

Unit		A(m)	B(m)
60	Tephra. White to grey, coarse sand size. Large scale cross-stratification. Hornblende crystals visible.	0.5	449.3
	– sharp contact –		
61	Silt. Brown, bedding indistinct.	0.4	449.7
	– sharp contact –		
62	Medium sand and silt. Brown, generally thin bedded, with plane parallel lamination common in the sand.	16.4	466.1

top of section

OROUA SECTION

Base of section at London Ford Bridge on the Oroua River. Section down river very obscured by bush, therefore this description is based on both river and road sections. Base of Makirikiri Tuff Formation not seen.

Unit		A(m)	B(m)
1	Sand. Grey, fine, tuffaceous grading up to white tephra. Thin to medium bedded.	4.0	4.0
	- sharp contact -		
2	Tephra with interbedded lignite tongues. Tephra, grey, fine sand size. Lignite varies from 0 to 200mm thickness over 22m.	1.5	5.5
	- sharp contact -		
3	Sand and silt. Grey, very tuffaceous. Thin bedded.	2.5	8.0
	- sharp contact -		
4	Sand and silt. Grey brown, very tuffaceous. At 2.3m a white tephra bed 1m thick.	11.0	19.0
	- grass cover -	22.5	41.5
5	Sandy silt. Varies from brown to blue grey. Thin to very thin laminated, otherwise generally structureless. (This is an estimated thickness, based on road and river sequences.)	35.0	76.5
	- sharp contact -		
6	Sand. Brown, iron stained, medium, very tuffaceous, generally thin bedded. Higher up the section are lenses of poorly sorted very coarse pebbly sands with large scale cross bedding. Fault running through this outcrop, in a north-south direction.	20.0	96.5
	- grass cover -	27.0	123.5

Unit		A(m)	B(m)
7	Alternating medium fine sand and silty sand. Grey brown, very friable, pumiceous, quite well sorted. Sequence displays a series of fining upwards beds with a maximum thickness of 200mm. At the base of these beds is plane parallel lamination, passing up to ripple-drift cross-lamination, finally to asymmetric ripples and sometimes to plane parallel again.	6.0	129.5

– interbedded contact –

| 8 | Shelly conglomerate. Poorly sorted, red brown, iron stained. Clasts up to 30mm long mostly greywacke but a few volcanic. Shells broken but include _Amphidesma_. | 1.5 | 131.0 |

– irregular contact –

9	Sand. Brown, medium to fine. Thin bedded to laminated.	2.0	133.0
	– grass cover –	25.0	158.0
10	Sand. Brown, coarse, very pumiceous. Lenses of light brown silty sands. Whole unit large scale trough cross bedded, height of sets generally greater than 0.5.	2.3	160.3
	– scree contact over 1m –	1.0	161.3
11	As unit 10 with slightly smaller cross-stratification and some convolute lamination. Passes up to plane parallel laminated medium to fine sands.	3.2	164.5

– slightly interbedded gradational contact –

| 12 | Sand. Brown, coarse, pumiceous. Tangential large scale cross-stratification, with height of sets 200-300mm. | 1.3 | 165.8 |

COAL CREEK

Position at base N144/326644. Measured 12/1/72. Kaimatira Pumice Sand.

Unit		A(m)	B(m)
	- Grass cover -		
1	Sand. Brown, very coarse to coarse, pumiceous. Large scale cross-stratification.	9.0	9.0
	- gradational contact -		
2	Sand. Coarse and medium, thin bedded, pumiceous. Large scale cross-stratification. Convolute lamination near the top.	4.1	13.1
	- sharp, wavy (100mm relief) contact -		
3	Tephra. Sand, pink white, medium to very fine. Fairly well cemented. Massive.	0.9	14.0
	- sharp contact -		
4	Sand. Brown grey, medium, very tuffaceous. Thin bedded with plane parallel laminations.	7.4	21.4
	- gradational contact -		
5	Sand. Grey, weathers blue grey, medium to fine, tuffaceous. Some alternating silt layers. Thin to very thin bedded. Some small scale cross-stratification, some ripple flasers.	2.5	23.9
	- gradational contact -		
6	Sand. Brown, medium, very tuffaceous, friable. Plane parallel laminated.	14.2	38.1
	- sharp contact -		
7	Tephra. Sand, white, fine. Bluff former.	0.7	38.8
	- sharp contact -		
8	Sand. Grey, medium to fine, very tuffaceous. Plane parallel laminated.	13.5	52.3
	- sharp contact -		
9	Sand. Grey to brown, fine to medium, very tuffaceous.	20.0+	72.3+

top of outcrop

OROUA VALLEY, NORTH OF TABLE FLAT ROAD.   Loc. 105

Position at base N139/442855. (Base is the contact with blue grey
Nukumaruan strata.)

Unit		A(m)	B(m)
1	Sandy silt. Grey, very tuffaceous. Generally moderately well sorted. Thin carbonized lignite lenses in lower 0.5m.	0.95	0.95
	- sharp contact -		
2	Sandy silt. Grey, very tuffaceous. Thick bedded. Beds all show upward grading.	1.9	2.85
	- sharp contact -		
3	Silty fine sand. Grey, very tuffaceous. Medium to thick bedded. Wood fragments scattered in thin laminae.	1.00-1.3	4.15
	- sharp contact -		
4	Sand. Grey, medium. Low angle small scale planar crossbedding. At top of unit is a lignite tongue 0-90mm thick.	1.4	5.55
	- sharp contact -		
5	Conglomerate tongue. Graded upwards. All pebbles subangular, greywacke. Maximum clast size 50mm at base, 20mm at top. Coarse lithic sand matrix.	0-1.0	6.55
	- gradational contact over 0.5m -		
6	Sand. Grading up from coarse to medium; lithic, angular fragments, friable. Bedding indistinct.	2.0	8.55
	- sharp contact -		
7	Tephra and lignite beds. Tephra grey yellow, silt size, moderately well sorted. Lignite, one unit at western side, bifurcates to two in east with ash in between. Lignite beds from 30-200mm thick, varying across the unit.	0-1.3	9.85
	- irregular contact -		

Unit		A(m)	B(m)
8	Tephra. Sands, very coarse to coarse, grey, laminated. Whole unit comprised of ash and pumice. Large scale tangential cross bedding, in places.	6.0	15.85
	- sharp contact -		
9	Silt. Grey, very tuffaceous, with lignite lenses up to 300mm thick.	3.0	18.85
	- sharp contact -		
10	Sand, grey, fine, very tuffaceous. Large scale planar crossbedding.	1.0	19.95
	- gradational contact -		
11	Sand. Fine, grey, tuffaceous with silt lenses up to 1m long, 50mm thick.	5.0	24.95
	- sharp contact -		
12	Alternating sand and silt. Grey-yellow, tuffaceous thin bedded.	6.0	30.95
	- sharp contact -		
13	Silt-fine sand, grey yellow, tuffaceous, with 2 lignite beds up to 100mm thick.	1.0	31.95
	- sharp contact -		
14	Sandy silt, yellow grey, tuffaceous. Bedding indistinct.	2.0	33.95
	- sharp contact -		
15	Sand, grey, yellow, very fine to fine, tuffaceous.	1.5	35.45
	- sharp contact -		
16	Alternating silt and fine sand. Grey brown, tuffaceous. Conglomerate lens at 5.5m, 0-3.5m thick. Maximum boulder size 0.2m; all boulders greywacke, subangular in brown coarse sand matrix. No bedding in conglomerate, poorly sorted, dumped appearance.	7.0	42.45
	- sharp contact -		
17	Sand. Brown, medium to fine, Bedding indistinct.	1.5	43.95

Unit		A(m)	B(m)
18	Sand and silty fine sand. Grey yellow, tuffaceous, thin bedded.	12.0	55.95
	- sharp undulatory contact -		
19	Conglomerate. Poorly sorted, disordered. Greywacke clasts up to 100mm long, in coarse brown sand matrix. Iron stained.	3.0-4.0	59.95
	- sharp contact -		
20	Silt. Grey yellow, tuffaceous. Plane parallel lamination.	4.0	63.95
	- sharp contact -		
21	Conglomerate as unit 19.	3.0-4.0	67.95
	- sharp contact -		
22	Sand and silt. Tuffaceous, thin bedded. Some lignite beds up to 50mm thick.	3.1	71.05
	- sharp contact -		
23	Conglomerate as unit 19.	1.5	72.55
	- sharp contact -		
24	Silt. Grey yellow, tuffaceous.	1.3	73.85
	- sharp contact -		
25	Conglomerate as unit 19.	2.0	75.85
	- sharp contact -		
26	Silt. Grey yellow, tuffaceous.	2.0	77.85
	- sharp contact -		
27	Conglomerate as unit 19.	2.0	79.85

Unit 20-27 are high in the cliff and thicknesses are
therefore estimates.

POHANGINA RIVER VALLEY   Loc. 183

Position at base N144/395715. Base of section is conformable
contact with the Nukumaru Group.

Unit		A(m)	B(m)
1	Silt. White, ashy, thickens to the north.	0.0-1.5	1.5
	- contact erosional over 0.4m -		
2	Silt. Green grey, weathers with rectangular fractures. Channel cut and fill structures with channel width up to 2.2m.	0.4-1.0	2.5
	- sharp contact -		
3	Silt. Blue grey. Lignite bed 0.2m thick near the base.	1.5	4.0
	- sharp contact -		
4	Conglomerate. Red brown. Silty sand, iron stained matrix, pumiceous. Clasts in conglomerate, greywacke, up to 60mm long diameter. Large scale, slightly tangential, cross bedding.	9.0	13.0
	- sharp contact -		
5	Sand. Brown grey, very coarse, tuffaceous. Plane parallel lamination near the base followed upwards by large scale cross-stratification. Convolute lamination near the top of the unit.	16.5	29.5
	- sharp contact -		
6	Silt. Blue grey. Lignite bed 100mm thick near the top.	2.0	31.5
	- contact erosional over 0.8m -		
7	Conglomerate with fine sand matrix. All clasts greywacke, largest 100mm long diameter. Conglomerate interfingers with grey green fine siltstone tongue near the base, where the conglomerate also channels into the underlying unit.	5.5	37.0
	- gradational contact over 1.0m -		
8	Sandy silt. Tuffaceous. Lignite bed, 80mm thick at the top.	6.0	43.0
	- grass covered contact -	15.0	58.0

Unit		A(m)	B(m)
9	Sand. Brown, medium, well sorted, massive.	1.2	59.2
	- contact grass covered -	6.3	65.5
10	Sand. Green brown, medium, well sorted, massive.	5.3	70.8
	- sharp contact -		
11	Silty sand. Dark blue grey. Plane parallel laminated with some low angle planar large scale cross beds.	5.4	76.2
	- sharp contact -		
12	Silt. Blue grey. Two lignite beds, each about 50mm thick, one at 2m, the other at 4.3m.	4.5	80.7
	- sharp contact -		
13	Silt. Blue grey. Indistinct plane parallel lamination.	3.0	83.7
	- sharp contact -		
14	Conglomerate. Red brown, iron stained. Sand matrix. Clasts all greywacke up to 40mm long diameter, but for a few clasts of lignite.	1.4	85.1
	- gradational contact -		
15	Sandy conglomerate. Similar to unit 14 but with a higher percentage of sand and no lignite.	0-0.7	85.7
	- sharp contact -		
16	Sand. Brown, medium, very friable. Grades up to silt. Plane parallel lamination.	13.5	99.3
	- sharp contact -		
17	Sand. Light brown, medium brown, ashy. Plane parallel lamination. At 7.5m lignite bed 20mm thick.	19.5	118.8
	- sharp contact -		
18	Lignite with obvious charred fragments.	0.2	119.0
	- sharp contact -		
19	Sand. Grey, fine very tuffaceous.	1.5	120.5
	- sharp contact -		

Unit		A(m)	B(m)
20	Lignite as unit 18.	0.3	120.8
	- sharp contact -		
21	Sand. Grey, fine, tuffaceous	2.5	123.3
	- sharp contact -		
22	As unit 18.	0.7	130.0
	- sharp contact -		
23	Sand. Grey, medium to fine, tuffaceous	2.5	126.5
	- sharp contact -		
24	Tephra. White, fine sand size	1.5	128.0
	top of outcrop		

Outcrop in old meander of the Manawatu River, 600m north
of the Tua Paka. Position at base N149/215380. Measured
18/6/71.

Unit		A(m)	B(m)
1	Conglomerate. Poorly sorted with medium sand matrix. Clasts all greywacke up to 150mm long diameter. Gradual upward decrease in size with an average of 60mm at the base to 20mm at the top. Some bedding visible. Some silt-fine sand lenses up to 50mm thick.	2.0	2.0

- contact erosional over 0.9m -

2	Sand. Grey brown, fine to medium, ashy. Massive with some indistinct plane parallel lamination. Channel cut at the base. Charred wood near the base and a few greywacke clasts up to 40mm across. Upwards silt flasers.	4.4-6.0	8.0

- sharp contact -

3	Conglomerate. Grey brown with sandy matrix. Poorly sorted. Clasts all greywacke, from 20-300mm diameter. Clasts at the base tend to be more rounded. No obvious stratification.	2.0	10.0

- grass covered contact -

4	Sand. Grey brown, medium, micaceous. Pumice beds of very coarse sand and pebble size material up to 20mm thick at intervals of about every 300mm. Small scale cross lamination in places. Rare siltstone clasts up to 40mm long.	5.0	15.0

- contact erosional over 1.5m -

5	Conglomerate. Sandy matrix. Clasts all greywacke, average size at base 40mm, at top 100mm. Incipient horizontal stratification visible.	17.0	32.0

- gradational contact -

6	Conglomerate. Sandy matrix. Clasts all greywacke from 10 to 60mm long diameter. Whole unit is one set of large scale cross-stratification.	3.0	35.0

- sharp contact -

Unit		A(m)	B(m)
7	Conglomerate. As unit 6 but with horizontal bedding.	1.0	36.0
	- sharp contact -		
8	Tephra. White, medium, well sorted.	1-2.0	38.0
	- sharp contact -		
9	Conglomerate. As unit 5 but clasts now average 10mm long diameter.	1.5	39.5
	- contact erosional over 2m -		
10	Sand. Grey yellow, fine, pumiceous. Plane parallel lamination.	3.0+	42.5+

Position at base sharp conformable contact with the
Nukumaru Group, N144/285506.

Unit		A(m)	B(m)
1	Sand. Grey brown, medium, tuffaceous. Small convolute laminae throughout the unit.	30.0	30.0
	- sharp contact -		
2	Alternating tephra and lignite. Eight lignite beds up to 100mm thick with a charred appearance. Sands, white, or purple stained at contact with lignite, fine to very fine.	2.3	32.3
	- sharp contact -		
3	Sand. Grey brown, fine to medium, tuffaceous. Plane parallel lamination.	5.2	37.5
	- grass covered contact -		
4	Sand. Grey brown, medium to fine, tuffaceous. Medium bedded with horizontal lamination within the beds. Some small convolute laminations. At 34.5m a lignite 70mm thick is followed by 0.7m thick blue grey very fine sand.	45.0	82.5
	- grass covered contact -		
5	Sand. Orange brown, medium, well sorted, tuffaceous. Medium bedded with horizontal lamination within the beds. Thin beds of coarse sand size pumice.	32.0	114.5
	- gradational contact over 2m -		
6	Tephra. White, medium sand size.	4.0	118.5
	- erosional contact with 0.7m relief -		
7	Sandy conglomerate. Red brown, iron stained, poorly sorted. Clasts in conglomerate all greywacke. Matrix coarse pumiceous sand. Large scale trough cross bedding. Some lenses of fine sand up to 100mm thick.	10.0-11.0	129.5
	- sharp contact -		

Unit		A(m)	B(m)
8	Sand. Brown, medium, well sorted, very tuffaceous. Medium bedded with horizontal lamination within the beds.	56.5	186.0
	- sharp contact -		
9	Conglomerate. Red brown, poorly sorted. Clasts all greywacke up to 20mm diameter. Matrix pumiceous sand.	3.0	189.0
	- sharp contact -		
10	Sand. As unit 8 with some herring bone cross-stratification.	10.0+	199.0+

top of outcrop

MAKOHINE STREAM   Loc. 157

Base is sharp conformable contact with the Nukumaru
Group, at N144/288513.

Unit		A(m)	B(m)
1	Sand. Brown, fine to medium, well sorted. Medium bedded with plane parallel laminations. Some large scale cross-stratification with sets averaging 100mm high in the lower section, and 0.5m high in the upper.	7.5	7.5

                        - sharp contact -

| 2 | Sand, alternating with lignite beds. Sand, grey, fine, tuffaceous. Some coarse pumice laminae. Plane parallel lamination. Lignite beds from 10-50mm thick. | 0.8 | 8.3 |

                        - sharp contact -

| 3 | Sand. Blue, alternating coarse and fine laminae. Tuffaceous. Plane parallel lamination. | 0.85 | 9.15 |

                        - sharp contact -

| 4 | Tephra. White, silt size detritus. | 0.35 | 9.5 |

                        - sharp contact -

| 5 | Sand. Blue grey, medium to fine. Ripple-drift cross-lamination. | 2.7 | 12.2 |

                        - sharp contact -

| 6 | Sand. Blue grey mottled brown, medium, pumiceous. Plane parallel lamination. | 2.3 | 14.5 |

                        - sharp contact -

| 7 | Tephra. White, alternating laminae fine to very coarse sand size. | 3.0 | 17.5 |

                    - slump and soil cover -   6.0   23.5

| 8 | Sand and silt. Grey brown, alternating plane parallel laminae. | 1.0 | 24.5 |

                        - sharp contact -

Unit		A(m)	B(m)
9	Tephra. Grey, fine to coarse sand size. 100mm lignite bed near the base.	1.5	26.0
	- slump cover -	20.0	46.0
10	Sand. Brown, medium, well sorted, with a few lenses of coarse pumiceous sands. Some ripple-drift.	6.3	52.3
	- sharp contact -		
11	Silt at base, 40-100mm thick, purple grey, root structures penetrating down. Silt grades up to darker purple to a black organic rich layer 500mm thick. Palaeosol.	0.2	52.5
	- sharp contact -		
12	Sand. Grey, medium, tuffaceous. Bipolar bimodal ripple-drift cross-lamination.	1.4	53.9
	- sharp contact -		
13	Alternating sand and silt. Silt 10-100mm thick, sand 40-110mm thick. Silt, blue; sand yellow brown. Channel cut infilled with silt, 90mm deep, 0.2m wide. Ripples on siltstone beds vary in direction by 45°.	1.9	55.8
	- sharp contact -		
14	Sand. Blue grey, very fine. Plane parallel lamination.	1.5	57.3
	- sharp contact -		
15	Sand grading to silt and then again to sand. Blue grey with brown mottle. Very tuffaceous. Ripple-drift cross-lamination.	6.4	63.7
	- sharp contact -		
16	Alternating silt and fine sand. Thinly bedded. Three lignite beds 50-100mm thick.	7.9	71.6
	- contact covered -	3.0	74.6

Unit		A(m)	B(m)
17	Sand. Brown, medium, well sorted, tuffaceous. Large scale cross bedding.	1.9	76.5
	- sharp contact -		
18	Sand. Brown orange, medium, well sorted, tuffaceous. Thick bedded.	6.3	82.8
	- sharp contact -		
19	Sand. Grey brown, very fine, thinly bedded, alternating with grey brown, fine, laminated. Some large scale cross beds.	0.6	83.4
	- sharp contact -		
20	Silt. Very thin bedded to laminated. A few laminae of fine ash. One lignite bed, 20mm thick near the top.	9.0	92.4
	- sharp contact -		
21	Sand. Medium, well sorted. Thinly bedded with parallel lamination within the beds.	20.5	112.9
	- erosion surface with 200mm relief -		
22	Conglomerate. Red brown, iron stained. Clasts all greywacke. Matrix, tuffaceous medium sand. Large scale tangential cross beds.	1.3	114.2
	- sharp contact -		
23	Sand as unit 21.	11.7	125.9
	- sharp contact -		
24	Conglomerate. Red brown, iron stained, poorly sorted. Some horizontal bedding visible. Clasts all greywacke, up to 200mm long diameter, subangular to subrounded. Matrix, ashy medium sand. A few lenses of brown, medium sand form 0.1 to 1.5m thick. Some large scale cross bedding in the conglomerate.	8.5	134.4
	- sharp contact -		

Unit		A(m)	B(m)
25	Sand. Light brown, very coarse, pumiceous. A few 'floating' greywacke pebbles, up to 20mm diameter.	1.5	135.9

- gradational contact -

26	Sand. Brown, fine to medium, tuffaceous. At 10m this grades into a 2-3m very tuffaceous coarse sand unit with low angle large scale planar cross-stratification. This grades back to the brown sands. At 20m rippledrift cross-lamination, and some mollusc shells.	24.0	159.9

top of exposure

APPENDIX 3

Locality and/or sample numbers referred to in text and in appendices.

Prefix B represents Butlers Shell Conglomerate

Prefix M represents Makirikiri Tuff

Prefix LO represents Lower Okehu Siltstone

Prefix OO represents Okehu Shell Grit

Prefix UO represents Upper Okehu Siltstone

Prefix O represents Undifferentiated Okehu Siltstone

Prefix K represents Kaimatira Pumice Sand.

The number following the above letters is the writer's field locality number. If several samples were taken from one locality, this number is then followed by a letter, and the position of the sample at the locality or the lithological horizon is noted under "comments".

Locality No. (Sample No.)	VUW No. (if any)	Grid ref.	Comments
B01A		N137/374944	Base of B.S.C.
B01B		"	0.7m above base
B01CA		N137/376943	Base of B.S.C.
B01CB		"	0.7m above base
B01CC		"	0.9m above base
B01CD		"	1.1m above base
B01CE		"	3m above base
B01CF		"	5m above base
L002A		N137/418930	0.5m above base
U002A		"	3.0m above base
K02A		"	0.5m above base
K02B		"	Top cross bedded unit
M03A	11530	N137/484959	Both tephra with ripples
M03B		"	B is 2m above M03A
O04A		N137/420941	Shelly gravel
L004A		"	
B05A		N137/457947	Basal silt bed
B05B		"	Sandy bed above 5A
B05D		"	Shell conglomerate
O07A		N137/489958	Shelly gravelly sand
K08TB		N138/625908	Lower and upper members
K08TT		"	of cycles
K08CS		N138/625908	Sands with ripple-
K08VC		"	drift cross-
K08MS		"	lamination
M09A		N138/656948	Basal conglomerate
M09C	11531	"	Tephra
M09D		"	Sandy beds above tephra
M10A		N138/656949	Conglomerate
M10B		"	Tephra
M11A		N138/780940	Tuffaceous sand
M11B		"	Shelly sand
M12A		N138/725935	Shelly bed
M12B		"	Tuffaceous bed near base
M13A		N138/640940	Bipolar-bimodal ripple drift
M13B		"	2m above 13A
L014A		N138/680920	1m beneath O014A
U014A		"	1m above O014A

Locality No. (Sample No.)	VUW No. (if any)	Grif Ref.	Comments
0014A		N138/680920	Shelly gravel
M15		N138/684926	
M16	11553	N138/638938	
K20A		N138/569928	Silt
K20B	11532	"	Sand near base
K21A		N138/567928	Tephra sampled at
K21B	11533	"	0.45m vertical
K21C		"	intervals
M22A		N138/798898	Conglomerate
M22B		"	Sand 0.15m above conglomerate
M23	11560	N138/796903	
0025A		N138/849869	
0026A		N138/844853	
M27A		N139/022833	Sand, climbing ripples
M27B		"	Silt above sand
M29	11534	N139/137839	Pakihikura Pumice
K30D	11535	N144/125797	Rewa Pumice
M32A	11536	N144/310752	Basal sand, large cross bed
M33		N139/355809	Parallel laminated sand
M34		N139/355808	
M35		N139/353806	
M36		N139/352805	
M37		N139/302837	Bipolar-bimodal ripple-drift
M38	11554	N139/314285	Tephra
M39	11537	N139/323283	Tephra with ripple cross-lamination.
M40		N139/219837	
M41		N139/219832	
M42		N139/237826	
M43		N139/239827	
M44		N139/242829	
K45		N137/442927	Shelly gravelly sand
M46	11555	N139/315846	Tephra - large cross bed
M47		N139/315843	Tephra - large cross bed
M48	11556	N144/381714	Tephra - climbing ripples
M49		N144/376712	
K50	11538	N144/372694	
K51A	11539	N144/131798	Tephra - lowest bed, climbing ripples

Locality No. (Sample No.)	VUW No. (if any)	Grid Ref.	Comments
K51B		N144/131798	Tephra - immediately above 51A. Large crossbed
K52		N137/446926	
M53A	11557	N137/438940	Large cross bed
M53B		"	Shelly gravelly sand
M54		N137/438941	Shelly gravelly sand
M55		N137/439940	
M56		N137/440939	
M57		N137/441942	Climbing ripples
M58		N137/441942	Shelly gravelly sand
M59A		N137/456951	Parallel laminated sand
M59B		N137/456951	Shelly gravelly sand
M60		N137/490957	
M061A		N137/495951	
K62		N138/580910	
K63		N138/580911	
K64A		N138/581912	Ripple-drift cross-laminated sand.
K64B		"	Pebbly shelly sands
K65		N138/570924	
K66		N138/581912	
K67	11558	N138/583910	Tephra, plane parallel laminated
M69		N139/130824	Parallel laminated sand
K71A		N144/124796	Bipolar-bimodal ripple-drift
K71B		N144/125796	
K71C		N144/126798	
K71F	11540	N144/130797	Tephra
K72	11541	N144/216794	Tephra
K73		N138/843843	
K74		N138/842841	
K75		N138/843852	
K76	11542	N138/844853	
K77		N138/846862	
K78		N138/846863	
M79		N138/847864	Parallel laminated sand
M80		N138/848870	
M81A		N138/852875	
M81B		"	
M82	11543	N138/853883	Large cross bed

Locality No. (Sample No.)	VUW No. (if any)	Grid Ref.	Comments
M83		N138/854884	
M84		N139/264845	Parallel laminated sand
M85		N139/298838	
M86		N139/299838	
M87		N139/304832	
M88		N139/303830	
M89		N139/302827	
K90	11544	N139/302820	
K91		N139/296810	
K92	11545	N144/289787	
K93		N144/291779	
K94		N144/289777	
K95		N144/278765	
K97		N144/237766	
K98		N144/246749	
M99		N144/350780	Parallel lamination
M100		N144/348780	
M101		N144/348768	Large cross bed
M102		N144/348767	
M103		N144/349765	
M104		N144/351750	
M105A	11546	N139/442855	Lowermost tephra bed
M105B		"	Lowermost conglomerate
M111		N144/316716	
M115		N144/306723	
M118		N144/270730	
M121		N144/293734	Large cross bed
M122		N144/296732	
M124		N144/298726	
K131		N144/318700	
K132		N144/315694	
K133		N144/305688	
K134		N144/310672	
K135	11547	N144/293652	Tephra, large cross bed
K136		N144/309671	
K137	11548	N144/300662	
K138		N144/294657	
-140A	11549	N139/255585	} Finnis Rd tephras
-140D	11550	N139/255585	} 'D' is lower

Locality No. (Sample No.)	VUW No. (if any)	Grid Ref.	Comments
K141	11551	N144/016776	
K142		N139/125810	
K145		N138/808874	
K146		N138/804874	
K147		N138/772856	
K148A	11559	N138/710892	Basal hornblende sands
K148D	11552	"	Kaukatea Ash
K149		N138/718892	
K150		N138/725893	
K152		N149/220370	
M153		N149/215380	
M154		N149/325346	
K156		N144/285506	
M157		N144/288513	
M169		N138/882896	
M183		N144/374696	
M184		N139/237817	
M185		M139/235814	
M186		N139/233809	
M187		N139/227806	
M188		N139/226804	
K189		N139/225801	
K190		N138/907833	
K191		N138/908833	
K192		N138/968829	
K193		N139/015825	
K194		N139/014823	
M195		N149/255436	Tephra
M196		N149/253438	
M197		N139/153847	
M198		N139/168853	
K200		N144/326644	
M202		N144/342645	

Locality No. (Sample No.)	VUW No. (if any)	Grid Ref.	Comments

APPENDIX 4

The following tables list the size analysis data used in Part II, Chapter 3. Geographical localities of samples are recorded in Appendix 3.

Sample No.	Percentiles (∅)							Folk graphical statistics (∅)			
	5	16	25	50	75	84	95	Mean	Standard deviation	Skewness	Kurtosis
B01A	-3.57	-2.18	-1.56	0.06	1.44	1.96	3.09	-0.05	2.05	-0.09	0.91
B01B	-2.83	-2.08	-1.57	0.46	2.15	2.41	2.91	0.27	1.99	-0.14	0.63
B01GA	-5.57	-4.45	-4.02	-1.49	1.84	2.45	3.27	-1.17	3.06	0.11	0.62
B01GB	-2.34	-0.62	1.23	2.21	2.58	2.72	2.93	1.44	1.63	-0.71	1.60
B01GC	-2.82	-2.01	-1.59	0.99	1.95	2.16	2.46	0.38	1.84	2.08	-0.44
B01CD	-2.53	-1.41	0.65	2.43	3.92	5.32	8.56	2.11	3.36	-0.02	1.39
B01CE	4.55	4.98	5.37	6.08	7.42	8.15	10.13	6.40	1.64	0.38	1.12
L002A	3.34	3.57	3.85	5.28	7.45	8.35	10.31	5.73	2.25	0.36	0.79
U002A	3.78	3.98	4.33	5.07	6.76	7.70	10.76	5.58	1.99	0.52	1.18
K02	-2.20	-1.40	-0.94	0.02	0.60	0.85	2.12	-0.18	1.22	-0.15	1.15
M03A	4.43	4.74	4.86	5.25	6.29	6.98	9.30	5.66	1.30	0.60	1.39
M05B	2.61	3.42	3.93	5.10	6.29	6.83	8.20	5.12	1.70	0.06	0.97
0004A	-1.72	-1.12	-0.64	1.22	3.82	7.13	7.96	2.41	3.53	0.41	0.89
L004A	3.83	4.58	4.89	5.86	7.27	8.04	9.63	6.16	1.75	0.28	1.00
B05A	3.46	4.05	4.17	4.53	4.81	5.11	5.87	4.56	0.63	0.10	1.53
B05B	-1.09	0.15	0.48	0.83	1.17	1.32	1.76	0.77	0.72	-0.26	1.71
B05D	-3.05	-1.40	-0.49	0.71	1.37	2.12	3.16	0.47	1.82	-0.20	1.37
0007A	-2.72	-2.14	-1.79	-0.90	1.03	2.13	2.96	-0.30	1.93	0.39	0.83
K08TB	3.25	3.65	3.88	4.53	5.31	5.72	6.84	4.63	1.06	0.22	1.03
K08TT	3.57	3.77	3.98	4.65	5.53	6.12	8.94	4.84	1.43	0.40	1.48
K08CS	-2.52	-1.54	-0.63	0.67	2.05	2.49	3.15	0.54	1.86	-0.11	0.87
K08VG	-0.75	0.19	0.43	0.88	2.36	2.79	3.38	1.29	1.28	0.34	0.88
K08MS	2.99	3.36	3.51	3.97	4.44	4.69	5.33	4.01	0.69	0.12	1.03

Sample No.	Percentiles (ø)							Folk graphical statistics (ø)			
	5	16	25	50	75	84	95	Mean	Standard deviation	Skewness	Kurtosis
M09A	-5.66	-4.59	-4.18	-3.52	0.23	1.21	2.11	-2.30	2.63	0.54	0.72
M10B	4.55	5.19	6.01	6.76	7.53	7.91	9.08	6.62	1.37	-0.07	1.22
M11A	-2.51	-1.56	-0.57	0.24	0.80	1.17	2.75	-0.05	1.48	-0.18	1.57
M11B	3.35	3.96	4.46	5.34	6.13	6.95	8.70	5.41	1.56	0.17	1.32
M12A	-3.59	-2.40	-1.96	-0.31	1.01	1.29	2.45	-0.47	1.84	-0.11	0.83
M12B	3.61	4.22	4.49	4.93	5.81	6.58	9.57	5.25	1.46	0.47	1.79
M13A	1.60	1.99	2.17	2.47	2.76	2.90	3.31	2.45	0.49	-0.04	1.20
M13B	-4.10	-3.28	-2.95	-1.78	0.90	1.94	2.73	-1.04	2.34	0.37	0.73
OO14A	-3.06	-1.87	-1.41	-0.52	0.33	0.79	4.61	-0.53	1.83	0.16	1.81
LO14A	3.69	4.40	4.69	5.54	7.24	8.26	10.28	6.06	1.96	0.43	1.06
UO14A	3.95	4.77	5.23	6.47	7.96	9.22	10.90	6.82	2.17	0.26	1.05
M15A	2.59	2.74	2.80	2.89	3.15	3.29	3.51	2.97	0.28	0.39	1.09
K20A	4.29	5.01	5.51	6.48	7.88	8.76	10.60	6.75	1.89	0.26	1.09
K20A	2.11	3.68	4.72	6.11	7.55	8.46	10.42	6.08	2.45	0.01	1.20
K20B	-0.70	-0.35	-0.19	0.47	0.75	0.88	1.71	0.33	0.67	-0.15	1.05
K21A	3.89	4.96	5.29	5.86	7.19	7.88	10.88	6.23	1.79	0.41	1.51
K21A	5.49	5.76	5.86	6.15	7.47	9.08	11.05	7.00	1.67	0.76	1.41
K21C	4.71	5.35	5.65	6.28	7.27	7.94	9.95	6.52	1.44	0.34	1.32
M22A	-6.81	-5.83	-5.46	-4.67	-1.72	0.86	1.93	-3.21	3.00	0.58	0.96
M22B	-1.29	-0.23	0.30	2.42	2.83	3.03	3.47	1.74	1.54	-0.59	0.77
OO25A	4.59	5.06	5.56	6.78	8.40	9.41	11.71	7.08	2.16	0.30	1.03
OO26A	3.45	3.87	4.07	4.76	5.79	6.68	9.09	5.10	1.56	0.45	1.35
M27A	0.88	1.86	2.39	3.04	3.47	3.95	5.92	2.95	1.29	0.01	1.92

Sample No.	Percentiles (∅)							Folk graphical statistics (∅)			
	5	16	25	50	75	84	95	Mean	Standard deviation	Skewness	Kurtosis
M27B	4.08	4.62	4.83	5.48	6.83	7.68	10.36	5.93	1.72	0.50	1.29
M32A	1.90	2.19	2.31	2.49	2.80	2.97	3.41	2.55	0.42	0.21	1.25
M33	1.54	1.93	2.06	2.32	2.65	2.86	4.48	2.37	0.68	0.31	2.04
M35	1.96	2.41	2.61	2.96	3.30	3.48	3.96	2.95	0.57	-0.02	1.17
M37	2.51	2.74	2.83	2.96	3.23	3.37	3.83	3.02	0.36	0.31	1.32
M38	4.57	5.31	5.61	6.13	6.79	7.28	8.55	6.24	1.10	0.19	1.37
M39	2.88	3.45	3.75	5.71	6.40	6.63	6.98	5.26	1.42	-0.40	0.63
K45	-3.73	-3.19	-2.15	0.32	0.87	1.14	2.21	-0.57	1.98	-0.49	0.81
M46	-0.57	0.55	1.61	3.17	5.12	5.68	7.31	3.13	2.48	0.02	0.92
M47	-2.53	-1.44	-0.80	0.20	0.81	1.11	1.86	-0.05	1.30	-0.26	1.12
M48	3.62	4.09	4.62	5.41	6.16	6.79	8.33	5.43	1.39	0.13	1.26
M49	2.81	3.60	3.92	4.54	5.32	5.91	7.72	4.68	1.32	0.24	1.43
K50	2.18	2.46	2.60	2.90	4.13	6.93	11.62	4.10	2.55	0.82	2.53
K51A	2.87	3.71	3.99	5.42	6.42	7.15	9.57	5.43	1.87	0.12	1.13
K51B	1.32	2.14	2.51	3.09	3.59	3.85	4.53	3.03	0.91	-0.11	1.21
M53A	0.22	1.07	1.41	2.12	2.38	2.78	3.27	1.99	0.89	-0.24	1.07
M53B	2.34	2.97	3.20	3.59	4.44	5.19	6.63	3.92	1.20	0.43	1.42
M54	-3.22	-3.01	-2.09	0.22	1.36	2.06	2.78	-0.24	2.18	-0.21	0.71
M55	1.12	1.69	2.01	2.41	2.75	2.91	3.35	2.34	0.64	-0.17	1.24
M58	-3.06	-2.29	-1.87	0.26	1.36	2.21	4.22	0.06	2.23	-0.02	0.93
M59A	0.63	1.52	1.87	2.55	3.18	3.42	3.99	2.50	0.98	-0.11	1.05
M59B	-2.95	-1.34	-0.56	1.48	3.61	4.12	5.49	1.42	2.64	-0.04	0.83
U061A	3.49	3.90	4.30	5.68	7.31	8.18	10.05	5.92	2.06	0.25	0.89

Sample No.	Percentiles (ϕ)							Folk graphical statistics (ϕ)			
	5	16	25	50	75	84	95	Mean	Standard deviation	Skewness	Kurtosis
K64A	2.55	2.88	3.00	3.22	3.39	3.58	4.05	3.23	0.40	0.06	1.57
K64B	-1.36	-0.31	0.08	0.70	1.39	1.72	2.40	0.70	1.08	-0.05	1.18
K67	3.90	4.74	5.15	5.91	6.85	7.54	9.56	6.07	1.56	0.23	1.37
M69	2.19	2.55	2.68	2.92	3.23	3.39	3.93	2.95	0.47	0.14	1.29
K71A	2.35	2.52	2.59	2.80	3.04	3.23	3.62	2.85	0.37	0.24	1.18
K71C	-3.97	-2.93	-2.17	-0.94	0.10	0.54	2.04	-1.11	1.78	-0.08	1.08
M79	1.19	1.36	1.42	1.59	1.92	2.23	2.98	1.73	0.49	0.50	1.48
K81A	3.60	3.92	4.10	4.74	5.51	5.91	10.02	4.85	1.47	0.41	1.88
K81B	3.93	5.04	5.12	5.44	5.55	5.71	5.96	5.40	0.47	-0.35	1.94
M82	1.75	2.23	2.41	2.81	3.29	3.62	5.96	2.88	0.98	0.33	1.96
M84	2.30	2.55	2.64	2.84	3.11	3.26	3.48	2.88	0.36	0.12	1.03
M85	0.91	2.24	2.73	3.31	3.83	4.47	6.31	3.34	1.38	0.08	2.01
M99,1	1.08	1.41	1.55	1.89	2.22	2.38	2.81	1.89	0.50	0.04	1.07
M99,2	1.19	1.42	1.52	1.88	2.25	2.42	2.87	1.91	0.50	0.13	0.95
M101	1.84	2.13	2.24	2.44	2.70	2.83	3.10	2.47	0.37	0.07	1.13
M111	2.36	2.67	2.82	3.11	3.42	3.63	3.95	3.14	0.48	0.07	1.09
M105A	-0.13	1.12	1.73	2.93	3.76	4.41	6.50	2.82	1.83	-0.01	1.34
M105B	-4.01	-3.57	-3.23	-1.87	-0.22	0.67	2.24	-1.59	2.01	0.26	0.85
M121	-0.26	0.20	0.35	0.68	1.17	1.46	2.67	0.78	0.76	0.29	1.46
K135	1.16	1.69	1.98	2.65	3.65	4.12	6.06	2.82	1.35	0.30	1.24
M140	2.36	2.64	2.77	2.97	3.24	3.38	3.80	3.00	0.40	0.14	1.24
M144	1.32	1.70	2.01	2.65	3.27	3.64	5.11	2.67	1.06	0.16	1.24

APPENDIX 5

Etching and staining of grains (modified after Bailey and Stevens, 1960).

1. Grains mounted in Lakeside cement on a thin section glass.

2. Grains etched for 1min. 30secs. in the fumes of 40% HF at 90°C.

3. Slide washed in running water.

4. Slide dipped in a saturated solution of sodium cobaltinitrite.

5. Slide dipped in 5% barium chloride solution for 30-45 secs.

6. Slide washed under running water for at least one minute.

7. Slide dipped in sodium rhodizonate solution (0.05 gms in 20 mls water).

8. Slide washed again.

This staining technique gives the following results:

K feldspar is yellow

Ca feldspar is red

Quartz has a thin white coating

APPENDIX 6

Petrographic descriptions of some typical clasts from the conglomerate horizons. Nomenclature of sedimentary clasts is that of Folk et al (1970) wherever possible.

1. Butlers Shell Conglomerate and Makirikiri Tuff Formation

Locality 1, N137/374944

Clast 1: Ignimbrite

Phenocrysts of plagioclase, quartz and hypersthene in glass groundmass with a eutaxitic texture.

Clast 2: Poorly sorted medium sandstone:feldsparenite

Poorly sorted subangular to angular grains in a sericitic matrix. Quartz, the dominant mineral present, is subangular with a mean diameter up to 0 phi. The quartz grains are generally monocrystalline, clear, with slight undulose extinction. Feldspar grains vary from almost euhedral to rounded and from a state of unaltered to highly altered by sericitization. The composition of the feldspars is dominantly within the oligoclase range. Rock fragments, rounded to subrounded, are dominantly volcanic, displaying a trachytic texture. A few chert grains appear to be the product of alteration of grains of volcanic detritus. A few volcanic grains show spherulitic development. Accessory minerals include serpentine, muscovite and epidote. Both the former are often bent around larger grains.

Rarely small laths of prehnite are recognised.

This specimen and others similar to it show properties similar to those described by Reed (1957) for the Lower Mesozoic rocks of the Wellington district, New Zealand. It may be assumed then that these clasts were derived from the basement "greywackes".

Clast 3: Quartz micrite

Very fine sand sized, subangular to subrounded grains of monocrystalline
quartz and subordinate plagioclase in a calcite mud.

Locality 5, N137/457947

Clast 1: Pumice

Extremely rare phenocrysts of quartz and plagioclase in a vesicular glass
matrix.

Clast 2: Pumice

As above but with a few rare hypersthene phenocrysts.

Clast 3: Moderately sorted medium sandstone: Sublitharenite

Subangular, monocrystalline quartz grains with undulose extinction form more
than 80% of the rock. Most of these grains have dust trails and a very few
show evidence of overgrowths. Grain to grain contact show "saw-tooth"
development suggestive of pressure solution. Other sand sized components
are altered rock fragments, and in lesser amounts altered feldspar and
muscovite. Zircon is a very rare accessory mineral. The matrix, less than
5%, is entirely of sericite.

Clast 4: Quartzite (metamorphic)

Quartz crystals with coarsely interdigitating contact. Undulose extinction
dominant. Dust trails common.

Clast 5: Poorly sorted coarse sandstone: Lithic feldsarenite.

Poorly sorted angular to subangular grains in an iron stained sericitic
matrix. Quartz grains forming 25-30% of the rock are angular, generally
monocrystalline and with slight undulose extinction. Untwinned potassium
feldspar and microcline are subordinate to plagioclase. All feldspars show
varying degrees of alteration but the orthoclase is the most extreme in all
cases. All plagioclase feldspars fall in the range of albite-oligoclase.

Rock fragments tend to be rounded to subrounded and are mostly fine grained volcanic with a very few argillite. Accessory minerals include bent laths of biotite and chlorite.

Clast 6: Intraclast bearing micrite

Microcrystalline calcite, sometimes with a fibrous radiating texture, with small rounded areas of dense dark cryptocrystalline calcite and rare intraclasts of a quartz micrite.

This pebble is probably a reworked calcite concretion.

Clast 7: Quartzite (metamorphic)

Interdigitating quartz, with inclusions of biotite, and altered grains of alkali feldspar. Muscovite and chlorite occur rarely as very small grains.

Locality 9, N138/656949

Clast 1: Poorly sorted medium sandstone: litharenite

Quartz grains, generally angular, monocrystalline, with slightly undulose extinction form up to 25% of the rock. Feldspars forming less than 10% of the rock are very altered. Rock fragments are the major sand sized component and are up to -1 phi (2mm). Their dominant lithology is volcanic; most show trachytic texture but the more coarsely crystalline may be altered spillites. Very rarely chert and argillite grains are evident. Accessory minerals include biotite (frequently altering to chlorite), epidote, hypersthene. The matrix is of fine grained sericitic, iron stained material.

Clast 2: Poorly sorted sandy conglomerate: polymictic rudite.

Rounded clasts up to 8mm long. Dominant lithology is micaceous chloritic mudstone - very low grade metamorphic as evidence by parallel alignment of micas, and presence of chlorite. Others include altered volcanics. The sand size particles are dominantly altered feldspars, quartz and altered volcanic rock fragments including andesite. Chlorite and biotite occur rarely.

Clast 3:   Poorly sorted medium sandstone: litharenite

Similar to clast 1.

Clast 4:   Poorly sorted fine sandstone: feldspathic litharenite

Similar to clast 1 but with a higher percentage of feldspar.

Clast 5:   Altered andesite

Phenocrysts of zoned plagioclase, hypersthene, augite and altered hornblende

and xenoliths of andesine feldspar in a cryptocrystalline groundmass.

Clast 6:   Poorly sorted coarse sandstone: litharenite

Similar to clast 1, but with volcanic grains larger and more frequent.

Clast 7:   Poorly sorted medium sandstone: feldspathic litharenite

Similar to clast 1 but with a higher percentage of feldspar and polycrystalline

quartz grains.

Clast 8:   Ignimbrite

Phenocrysts of plagioclase in a banded glass and microlite feldspar

groundmass.

Clast 9:   Poorly sorted medium sandstone: feldspathic litharenite

Similar to clast 1 but with a higher percentage of feldspar and chlorite.

Clast 10:   Poorly sorted very fine sandstone: litharenite

Similar to clast 1 but with micas bent around larger grains.

Clast 11:   Poorly sorted very fine sandstone: litharenite

Similar to clast 1 but with a higher percentage of prehnite.

Clast 12:   Poorly sorted medium sandstone: feldspathic litharenite

Similar to clast 1 but with a higher percentage of feldspar and chlorite.

Clast 13:   Poorly sorted fine sandstone: litharenite

Similar to clast 1 but with a higher percentage of prehnite.

Locality 12, N138/725935

Clast 1: Moderately sorted fine sandstone: feldspathic litharenite

Angular to subangular grains in a fine grained chloritic matrix. Both grains and groundmass except quartz are very altered. Quartz, grains, forming less than 20% of the rock are generally angular to subangular, monocrystalline with very slightly undulose extinction. The feldspars are are altered, most of them almost completely such that it is difficult to estimate proportions of potassic to plagioclase. Rock fragments form the main component of the rock. The main type appears to be made of quartz and feldspar microliths but identification is not clear as the fragments show chloritisation. Rare laths of prehnite are evident, as well as rare rounded grains of epidote.

Clast 2: Pumice

Rare lithic fragments in a vesicular glass.

Locality 36, N139/352805

Clast 1: Poorly sorted medium sandstone: lithic felds-arenite

Angular to sub angular grains in an iron stained micaceous matrix. Quartz forms up to 30% of the rock. It is generally monocrystalline with straight or very slightly undulose extinction. Graphic intergrowths of quartz and feldspar occur rarely. Feldspar is the dominant grain present. Potassium feldspar is more dominant than plagioclase, and is generally more weathered. Microcline was noted rarely. Plagioclase varies in composition from albite to oligoclase, and varies from very fresh to highly altered. Rock fragments are generally volcanic, some recognisably andesitic and others with a trachytic texture. Most are altered and some show development of spherulitic texture. Chert and argillite are minor forms. The only accessory mineral is muscovite which is often bent around other grains. Chlorite and prehnite are present as alteration products.

Locality 111, N144/316716

Clast 1: Poorly sorted fine sandstone: litharenite

Angular to subangular grains in a sericitic matrix. Quartz grains are generally monocrystalline with sharp to very slightly wavy extinction. Plagioclase feldspar albite to oligoclase is dominant over potassium. All feldspars show some sericitic alteration. Muscovite, bent around grains, is the dominant accessory mineral. Rock fragments, which tend to be larger than the other detrital grains, are mostly volcanic, with subordinate metamorphic.

Locality 10, N138/656949

Clast 1: Poorly sorted very fine sandstone: litharenite
Similar to above.

Clast 2: Poorly sorted medium sandstone: litharenite
Similar to above but with epidote as an additional accessory.

Clast 3: Poorly sorted coarse sandstone: litharenite
Subangular quartz grains, often polycrystalline form 5% of the rock. They are all smaller than the modal size. Feldspar is often so highly altered that it is difficult to distinguish from the groundmass. Rock fragments are subrounded to rounded; the dominant lithology is volcanic, although these too are generally highly altered. Accessory grains are rare but include hypersthene, augite, and serpentine. Chloritic alteration is common.

Clast 4: Ignimbrite
Phenocrysts of plagioclase in a groundmass of banded devitrified glass. (Development of spherulites in glass very obvious). Rare euhedral opaques and one grain of subrounded zircon.

Clast 5: Ignimbrite
Phenocrysts of plagioclase in a (devitrified) glass groundmass.

Clast 6: Ignimbrite

Phenocrysts of plagioclase in a (devitrified) glass groundmass.

Clast 7: Ignimbrite

Phenocrysts of plagioclase in a glass groundmass which has a
eutaxitic texture.

2. Okehu Shell Grit Formation

Locality 7, N137/489958

Clast 1: Lutite

This rock has been highly altered by the introduction of quartz along
veins such that the general appearance is of cloudy chert.

Clast 2: Altered arenite

Quartz veining has altered the rock such that it now has a cherty
appearance with aggregates of mica. Biotite with alteration to chlorite
occurs rarely.

3. Kaimatira Pumice Sand Formation

Locality 148, N139/710892

Clast 1: Augite hypersthene andesite

Phenocrysts of plagioclase, hypersthene and augite in a groundmass with
a hyalopilitic texture (glass in minute interspaces between microlites
of feldspar in haphazard orientation).

Clast 2: Augite hypersthene andesite

Phenocrysts of plagioclase, hypersthene and augite in a groundmass with
a pilotaxitic texture.

Clast 3: Augite hypersthene andesite

Phenocrysts of plagioclase (some zoned), hypersthene, and augite in a
groundmass with a hyalopilitic texture.

Clast 4: Lamprobolite andesite

Phenocrysts and xenoliths of plagioclase (some zoned) and lamprobolite
in a groundmass with a hyalopilitic texture.

Clast 5: Hypersthene andesite

Phenocrysts of plagioclase (some zoned) and hypersthene in a groundmass
of altered feldspar and glass.

Clast 7: Augite hypersthene and andesite

Phenocrysts of plagioclase (some zoned), hypersthene and augite in a
groundmass with a pilotaxitic texture with an iron oxide stain.

Clast 8: Augite hypersthene andesite

Phenocrysts of plagioclase (some zoned), hypersthene and augite in a
groundmass with a trachytic texture, with bands of iron oxide staining.

Clast 9: Augite hypersthene andesite

Similar to clast 3.

Clast 10: Augite hypersthene andesite

Similar to clast 3.

Clast 12: Augite hypersthene andesite

Similar to clast 3.

Clast 13: Augite hypersthene andesite

Similar to clast 8.

Clast 14: Augite hypersthene andesite

Phenocrysts and xenoliths of plagioclase (some zoned), hypersthene and
augite in a groundmass with a pilotaxitic texture and with an iron oxide
stain.

Clast 11: Vesicular andesite

Occasional phenocrysts of plagioclase in a pilotaxitic very vesicular
groundmass.

Clast 29:   Ignimbrite

Phenocrysts of plagioclase, hypersthene, magnetite and more rarely
quartz and biotite and lithic fragments in a glass groundmass with a
eutaxitic texture.

Other clasts from this horizon were lithic arenites similar to those
already described in the other formations.

APPENDIX 7

Computer programme used in the palaeocurrent analysis.

This is followed by the computed output for all cosets measured. The output reads - Formation, grid reference, sedimentary structure measured, unit if measured within a long section (see Appendix 2), site no., vector mean, confidence interval at the 95% level, number of readings taken within each coset, vector magnitude computed as a percent, and the true azimuth for the readings.

```
// FOR
*IOCS(CARD,1132PRINTER)
*ONE WORD INTEGERS
*LIST SOURCE PROGRAM
      REAL MAG
      REAL LOCET(19)
      REAL LOCMO(2)
      DIMENSION A(500), M(200), T(40)
C  THIS PROGRAM CALCULATES VMEAN, STANDARD DEVIATION ETC FOR ANY NUMBER
C  OF SETS OF DATA. NUMBER OF DATA ITEMS IN A SET MUST NOT EXCEED 200.
C  RESULTS APPEAR ON THE LINEPRINTER.
C  ALL VALUES ROUNDED OFF. PROGRAM ELIMINATES BLANKS FROM INPUT. PUNCH O
C  AS 360 DEGREES.
C  A M ARRAYS STORE AZIMUTHS REAL AND INTEGER. T IS STUDENTS T TABLE
      READ(2,40)(T(I),I=1,35)
   40 FORMAT(20F4.2/20F4.2)
      WRITE(3,5)
    5 FORMAT (1H1////' VECTOR MEAN, STANDARD DEVIATION, CONFIDENCE INTER
     1VAL (95 PCT) '/19X, 'FOR VECTORIAL DATA')
      GO TO 96
    1 WRITE (3,2)
    2 FORMAT(1H1////)
   96 P=0
      P=1
C  M=NO OF READINGS, MAG = MAGNETIC DECLINATION, LOCET IS FOR
C  STRATIGRAPHIC AND LOCALITY DATA TO BE PRINTED WITH OUTPUT.
   90 READ(2,20)N,MAG,LOCET
   20 FORMAT(I3,F4.0,1X,18A4)
      WRITE(3,21)LOCET
   21 FORMAT(1H0,20A4)
      IF(N)90,91,92
   92 CONTINUE
      P=P+1
      READ(2,22)LOCMO,(A(I),I=1,N)
   22 FORMAT (2A4,18F4.0/(8X,18F4.0))
C  ELIMINATES BLANKS IN DATA
      L=N
      I=1
      N=1
```

```
      DO 2 J=1,L
      IF(A(I)) 90,90,91
90    N=N-1
      GOTO 82
91    A(N)=A(I)
92    I=I+1
93    N=N+1
 2    N=N-1
C     CONVERT READINGS TO TRUE NORTH
      DO 50 I=1,N
      AZ = A(I) + MAG
      IF(AZ - 360.) 51,52,52
51    A(I) = AZ
      GOTO 50
52    A(I) = AZ - 360.
50    CONTINUE
      A(1) = A(1)
      IF (N-1) 90,93,94
93    GOTO 95
94    CONTINUE
C     CALCULATE R AND VECTOR MEAN
C     CALCULATE SUMS OF SINS AND COSINES
      SS=0.0
      SC=0.0
      DO 3 I=1,N
      SS=SS+SIN(A(I)*0.01745)
      SC=SC+COS(A(I)*0.01745)
3     R=SQRT(SS*SS+SC*SC)
      VMEAN=(ATAN(SS/SC)*180./3.14159)
      IF(SS)61,62,62
62    IF(SC)63,64,64
64    VMEAN=VMFAN
      GOTO 66
63    VMEAN=VMEAN+180.
      GOTO 65
61    IF(SC)63,65,65
65    VMEAN=VMEAN+360.
66    CONTINUE
      EL=R*100.0/N
      SUMY=0.0
```

```
      DO 30 I=1,N
      DIFF=(VMEAN-A(I))
      IF(DIFF-180.0)31,33,33
33    DIFF=A(I)+360.0-VMEAN
      GOTO 35
31    IF(DIFF+180.0)34,34,35
34    DIFF= VMEAN+360.0-A(I)
35    CONTINUE
      W(I)=A(I)
30    SUMV=SUMV+DIFF**2.
      STDEV=SQRT(SUMV/(N-1))
      IF(N-35)41,42,42
41    TE=T(N-1)
      GOTO 49
42    TE=2.03
49    Z=N
      CON=TE*STDEV/SQRT(Z)
      VMEAN = VMEAN + 0.5
      STDEV=STDEV+0.5
      CON=CON+0.5
      WRITE(3,4)VMEAN,STDEV,CON,N,EL
4     FORMAT('  VEC MEAN=',F4.0,1X,    ' ST DEV=',F4.0,
     1 ' CON INTVL=',F4.0,' READINGS=',I3,  ' VEC MAG(PCT)=',F6.2)
53    FORMAT(' TRUE AZIMUTH ',11I5)
95    WRITE (3,53) (W(I),I=1,N)
      IF (P-12)90,1,1
91    CALL EXIT
      END
```

288.

VECTOR MEAN, STANDARD DEVIATION, CONFIDENCE INTERVAL (95 PCT)
       FOR VECTORIAL DATA

MAKIRIKIRI   N137/374944   RIPPLE STRIKE UNIT 2   001
VEC MEAN=197.   ST DEV= 18. CON INTVL=159. READINGS= 2 VEC MAG(PCT)= 97.63
TRUE AZIMUTH 210 185

MAKIRIKIRI   N137/374944   LARGE XBED   UNIT 2   001
VEC MEAN=113.   ST DEV= 19. CON INTVL= 47. READINGS= 3 VEC MAG(PCT)= 96.39
TRUE AZIMUTH 100 105 135

MAKIRIKIRI   N137/374944   LARGE XBED   UNIT 1   001
VEC MEAN=285.   ST DEV= 19. CON INTVL= 30. READINGS= 4 VEC MAG(PCT)= 96.05
TRUE AZIMUTH 260 305 290 285

OKEHU   N137/418930   LARGE XBED   002
VEC MEAN=308.   ST DEV= 19. CON INTVL= 16. READINGS= 8 VEC MAG(PCT)= 95.02
TRUE AZIMUTH 320 280 305 280 325 325 300 325

OKEHU   N137/418930   LARGE XBED   002
VEC MEAN=141.   ST DEV= 19. CON INTVL= 16. READINGS= 8 VEC MAG(PCT)= 95.34
TRUE AZIMUTH 175 125 130 130 160 145 145 120

KAIMATIRA   N137/418930   LARGE XBED   002
VEC MEAN=125.   ST DEV= 11. CON INTVL= 18. READINGS= 4 VEC MAG(PCT)= 98.57
TRUE AZIMUTH 115 126 118 140

KAIMATIRA   N137/418930   RIPPLE STRIKE   002
VEC MEAN=190.   ST DEV= 5. CON INTVL= 12. READINGS= 3 VEC MAG(PCT)= 99.74
TRUE AZIMUTH 190 195 185

KAIMATIRA   N137/418930   RIPPLE FLOW   002
VEC MEAN=100.   ST DEV= 5. CON INTVL= 12. READINGS= 3 VEC MAG(PCT)= 99.74
TRUE AZIMUTH 100 105 95

MAKIRIKIRI
N137/484959   RIPPLE DRIFT   003
VEC MEAN=285.   ST DEV=13. CON INTVL= 33. READINGS=   3 VEC MAG(PCT)= 98.23
TRUE AZIMUTH 275 300 280

MAKIRIKIRI
N137/484959   RIPPLE DRIFT   003
VEC MEAN=106.   ST DEV=20. CON INTVL= 25. READINGS=   5 VEC MAG(PCT)= 95.28
TRUE AZIMUTH 130 80 105 95 120

MAKIRIKIRI
N137/484959   RIPPLE STRIKE   003
VEC MEAN=195.   ST DEV=20. CON INTVL= 25. READINGS=   5 VEC MAG(PCT)= 95.28
TRUE AZIMUTH 185 210 220 170 195

MAKIRIKIRI
N137/457947   LARGE XBED   005
VEC MEAN= 62.   ST DEV=10. CON INTVL= 26. READINGS=   3 VEC MAG(PCT)= 98.90
TRUE AZIMUTH 65 50 70

OKEHU
N137/489958   LARGE XBED   007
VEC MEAN=143.   ST DEV=20. CON INTVL= 32. READINGS=   4 VEC MAG(PCT)= 95.49
TRUE AZIMUTH 123 135 146 170

OKEHU
N137/489958   RIPPLE DRIFT   007
VEC MEAN=259.   ST DEV= 9. CON INTVL= 14. READINGS=   4 VEC MAG(PCT)= 99.07
TRUE AZIMUTH 270 250 254 263

OKEHU
N137/489958   RIPPLE STRIKE   007
VEC MEAN=169.   ST DEV= 9. CON INTVL= 14. READINGS=   4 VEC MAG(PCT)= 99.07
TRUE AZIMUTH 180 160 164 173

KAIMATIRA
N138/625908   LARGE XBED   UNIT 1   008
VEC MEAN=124.   ST DEV= 8. CON INTVL= 9. READINGS=   6 VEC MAG(PCT)= 99.12
TRUE AZIMUTH 120 124 132 116 115 135

KAIMATIRA
N138/625908   RIPPLE STRIKE   UNIT 2   008
VEC MEAN=205.   ST DEV=10. CON INTVL= 7. READINGS= 11 VEC MAG(PCT)= 98.70
TRUE AZIMUTH 195 204 189 213 197 198 215 208 205 215 219

MAKIRIKIRI   N138/656949   LARGE XBED   009
TRUE AZIMUTH   140

MAKIRIKIRI   N138/656949   LARGE XBED   009
TRUE AZIMUTH   270

MAKIRIKIRI   N138/780940   RIPPLE STRIKE   011
VEC MEAN=358.   ST DEV= 8. CON INTVL= 9. READINGS= 6 VEC MAG(PCT) = 99.10
TRUE AZIMUTH   355 359 348 355 13 1

MAKIRIKIRI   N138/780940   RIPPLE FLOW   011
VEC MEAN=273.   ST DEV= 9. CON INTVL= 23. READINGS= 3 VEC MAG(PCT) = 99.14
TRUE AZIMUTH   265 283 271

MAKIRIKIRI   N138/725935   LARGE XBED   012
VEC MEAN=131.   ST DEV= 4. CON INTVL= 9. READINGS= 3 VEC MAG(PCT) = 99.86
TRUE AZIMUTH   135 130 128

MAKIRIKIRI   N138/640940   RIPPLE DRIFT UNIT 2   013
VEC MEAN=205.   ST DEV= 15. CON INTVL= 18. READINGS= 5 VEC MAG(PCT) = 97.42
TRUE AZIMUTH   215 185 195 220 210

MAKIRIKIRI   N138/640940   LARGE XBED UNIT 2   013
VEC MEAN=135.   ST DEV= 5. CON INTVL= 12. READINGS= 3 VEC MAG(PCT) = 99.74
TRUE AZIMUTH   130 135 140

MAKIRIKIRI   N138/640940   LARGE XBED UNIT 2   013
VEC MEAN=232.   ST DEV= 8. CON INTVL= 19. READINGS= 3 VEC MAG(PCT) = 99.40
TRUE AZIMUTH   240 225 230

MAKIRIKIRI   N138/640940   RIPPLE DRIFT UNIT 4   016
VEC MEAN=288.   ST DEV= 8. CON INTVL= 19. READINGS= 3 VEC MAG(PCT) = 99.40
TRUE AZIMUTH   290 295 280

```
MAKIRIKIRI     N138/640940      LARGE XBED    UNIT 5              016
VEC MEAN=135.  ST DEV= 5.  CON INTVL= 12.  READINGS=  3  VEC  MAG(PCT)= 99.74
TRUE AZIMUTH   140  135  130

MAKIRIKIRI     N138/640940      LARGE XBED    UNIT 7              016
VEC MEAN=209.  ST DEV= 5.  CON INTVL= 44.  READINGS=  2  VEC  MAG(PCT)= 99.81
TRUE AZIMUTH   206  213

KAIMATIRA      N138/569928      LARGE XBED                       020
VEC MEAN=109.  ST DEV= 9.  CON INTVL= 9.  READINGS=  6  VEC  MAG(PCT)= 99.07
TRUE AZIMUTH   95  105  117  115  107  116

KAIMATIRA      N138/567928      LARGE XBED                       021
TRUE AZIMUTH   290

KAIMATIRA      N138/567928      LARGE XBED                       021
VEC MEAN=125.  ST DEV= 19.  CON INTVL= 20.  READINGS=  6  VEC  MAG(PCT)= 95.35
TRUE AZIMUTH   115  116  107  150  150  115

MAKIRIKIRI     N138/798898      LARGE XBED    UNIT 3              022
VEC MEAN=260.  ST DEV= 5.  CON INTVL= 12.  READINGS=  3  VEC  MAG(PCT)= 99.74
TRUE AZIMUTH   250  265  255

MAKIRIKIRI     N138/798898      LARGE XBED    UNIT 4              022
VEC MEAN=235.  ST DEV= 23.  CON INTVL= 37.  READINGS=  4  VEC  MAG(PCT)= 93.83
TRUE AZIMUTH   240  210  225  265

MAKIRIKIRI     N138/798898      LARGE XBED    UNIT 5              022
VEC MEAN=275.  ST DEV= 17.  CON INTVL= 21.  READINGS=  5  VEC  MAG(PCT)= 96.54
TRUE AZIMUTH   270  275  285  250  295

MAKIRIKIRI     N138/796903      RIPPLE DRIFT  UNIT 2              023
VEC MEAN= 33.  ST DEV= 3.  CON INTVL= 8.  READINGS=  3  VEC  MAG(PCT)= 99.90
TRUE AZIMUTH   32  36  30
```

```
MAKIRIKIRI     N138/796903     RIPPLE DRIFT   UNIT 2         023
VEC MEAN=207.  ST DEV= 3. CON  INTVL= 8. READINGS=    3 VEC MAG(PCT)= 95.90
TRUE AZIMUTH   210 208 204

MAKIRIKIRI     N138/796903     LARGE XBED     UNIT 2         023
VEC MEAN=207.  ST DEV= 6. CON  INTVL= 10. READINGS=   4 VEC MAG(PCT)= 99.52
TRUE AZIMUTH   210 205 200 215

MAKIRIKIRI     N139/137839     RIPPLE STRIKE  UNIT 7         029
VEC MEAN=142.  ST DEV= 9. CON  INTVL= 8. READINGS=    8 VEC MAG(PCT)= 98.91
TRUE AZIMUTH   145 149 139 160 132   139 137 135

MAKIRIKIRI     N139/137839     RIPPLE DRIFT   UNIT 7         029
VEC MEAN= 46.  ST DEV= 3. CON  INTVL= 5. READINGS=    4 VEC MAG(PCT)= 99.89
TRUE AZIMUTH   42 49 47 45

MAKIRIKIRI     N139/137839     RIPPLE DRIFT   UNIT 7         029
VEC MEAN=238.  ST DEV= 9. CON  INTVL= 14. READINGS=   4 VEC MAG(PCT)= 99.10
TRUE AZIMUTH   235 239 229 250

MAKIRIKIRI     N139/137839     LARGE XBED     UNIT 7         029
VEC MEAN= 95.  ST DEV= 21. CON INTVL=191. READINGS=   2 VEC MAG(PCT)= 96.59
TRUE AZIMUTH   70 100

MAKIRIKIRI     N139/137839     LARGE XBED     UNIT 4         029
VEC MEAN=216.  ST DEV= 18. CON INTVL= 44. READINGS=   3 VEC MAG(PCT)= 96.84
TRUE AZIMUTH   235 200 213

KAIMATIRA      N144/125797     RIPPLE FLOW    UNIT 28        030
VEC MEAN=192.  ST DEV= 10. CON INTVL= 26. READINGS=   3 VEC MAG(PCT)= 98.90
TRUE AZIMUTH   195 200 180

KAIMATIRA      N144/125797     RIPPLE STRIKE  UNIT 28        030
VEC MEAN=106.  ST DEV= 10. CON INTVL= 7. READINGS=   11 VEC MAG(PCT)= 98.58
TRUE AZIMUTH   105 120 100 90 107 115 119 110   110 105 90
```

```
KAIMATIRA     N144/125797     LARGE XBED     UNIT 28          030
VEC MEAN=298.  ST DEV= 6. CON INTVL= 7. READINGS= 5  VEC MAG(PCT)= 99.63
TRUE AZIMUTH  300  290  300  305  297

MAKIRIKIRI    N144/310752     LARGE XBED                      032
VEC MEAN=145.  ST DEV= 5. CON INTVL= 11. READINGS= 3  VEC MAG(PCT)= 99.79
TRUE AZIMUTH  145  149  140

MAKIRIKIRI    N139/353806     LARGE XBED                      035
TRUE AZIMUTH  240

MAKIRIKIRI    N139/352805     IMBRICATE PEBBLES               036
TRUE AZIMUTH  100

MAKIRIKIRI    N139/352805     LARGE XBED                      036
VEC MEAN=106.  ST DEV= 8. CON INTVL= 76. READINGS= 2  VEC MAG(PCT)= 99.45
TRUE AZIMUTH  100  112

MAKIRIKIRI    N139/302837     LARGE XBED     UNIT             037
VEC MEAN=300.  ST DEV= 46. CON INTVL= 39. READINGS= 8  VEC MAG(PCT)= 73.34
TRUE AZIMUTH  240  250  248  320  310  0.  330  335

MAKIRIKIRI    N139/302837     LARGE XBED     UNIT             037
VEC MEAN=130.  ST DEV= 5. CON INTVL= 12. READINGS= 3  VEC MAG(PCT)= 99.74
TRUE AZIMUTH  130  135  125

MAKIRIKIRI    N139/302837     LARGE XBED     UNIT             037
VEC MEAN=135.  ST DEV= 8. CON INTVL= 13. READINGS= 4  VEC MAG(PCT)= 99.24
TRUE AZIMUTH  145  135  125  135

MAKIRIKIRI    N139/302837     RIPPLE DRIFT   UNIT             037
VEC MEAN=269.  ST DEV= 40. CON INTVL= 42. READINGS= 6  VEC MAG(PCT)= 80.86
TRUE AZIMUTH  265  257  260  205  310  315
```

MAKIRIKIRI   N139/302837   BEACH MARKS   037
TRUE AZIMUTH   299

MAKIRIKIRI   N139/302837   RIPPLE FLOW   037
VEC MEAN=100.   ST DEV= 3. CON INTVL= 5. READINGS= 4 VEC MAG(PCT)= 99.87
TRUE AZIMUTH   100   97   105   100

MAKIRIKIRI   N139/302837   RIPPLE STRIKE   037
VEC MEAN=190.   ST DEV= 29. CON INTVL= 22. READINGS= 9 VEC MAG(PCT)= 89.69
TRUE AZIMUTH   190   187   195   175   167   170   115   220
190

MAKIRIKIRI   N139/166854   LARGE XBED   039
VEC MEAN= 36.   ST DEV= 25. CON INTVL= 26. READINGS= 6 VEC MAG(PCT)= 92.35
TRUE AZIMUTH   50   30   10   5   55   65

MAKIRIKIRI   N139/166854   RIPPLE DRIFT   039
VEC MEAN=199.   ST DEV= 16. CON INTVL=140. READINGS= 2 VEC MAG(PCT)= 98.16
TRUE AZIMUTH   210   188

MAKIRIKIRI   N139/166854   RIPPLE DRIFT   039
VEC MEAN= 17.   ST DEV= 19. CON INTVL= 24. READINGS= 5 VEC MAG(PCT)= 95.50
TRUE AZIMUTH   5   26   28   36   349

MAKIRIKIRI   N139/166854   RIPPLE STRIKE   039
VEC MEAN=109.   ST DEV= 17. CON INTVL= 16. READINGS= 7 VEC MAG(PCT)= 96.26
TRUE AZIMUTH   120   98   116   126   95   79   118

MAKIRIKIRI   N139/219837   CONVOLUTE LAM   040
VEC MEAN=290.   ST DEV= 2. CON INTVL= 4. READINGS= 3 VEC MAG(PCT)= 99.97
TRUE AZIMUTH   292   290   289

MAKIRIKIRI   N139/219837   LARGE XBED   040
VEC MEAN=281.   ST DEV= 4. CON INTVL= 38. READINGS= 2 VEC MAG(PCT)= 99.86
TRUE AZIMUTH   284   278

```
MAKIRIKIRI    N139/2219832    LARGE XBED                    041
VEC MEAN=193.  ST DEV=19. CON INTVL= 23. READINGS=  5 VEC MAG(PCT)= 95.77
TRUE AZIMUTH  205 176 186 180 220

MAKIRIKIRI    N139/2219832    LARGE XBED                    041
TRUE AZIMUTH  354

MAKIRIKIRI    N139/2423829    LARGE XBED                    044
VEC MEAN=232.  ST DEV=26. CON INTVL= 27. READINGS=  6 VEC MAG(PCT)= 91.91
TRUE AZIMUTH  195 215 220 244 260 255

KAIMATIRA     N137/4442927    LARGE XBED                    045
VEC MEAN=145.  ST DEV=5. CON INTVL= 12. READINGS=  3 VEC MAG(PCT)= 99.74
TRUE AZIMUTH  145 150 149

KAIMATIRA     N137/4442927    RIPPLE STRIKE                 045
VEC MEAN= 73.  ST DEV=7. CON INTVL= 16. READINGS=  3 VEC MAG(PCT)= 99.57
TRUE AZIMUTH  73 80 67

MAKIRIKIRI    N139/315843     LARGE XBED       UNIT 8       047
VEC MEAN=226.  ST DEV=17. CON INTVL= 28. READINGS=  4 VEC MAG(PCT)= 96.53
TRUE AZIMUTH  205 245 235 220

MAKIRIKIRI    N139/315843     LARGE XBED       UNIT 8       047
VEC MEAN=235.  ST DEV=29. CON INTVL= 72. READINGS=  3 VEC MAG(PCT)= 91.69
TRUE AZIMUTH  240 260 203

MAKIRIKIRI    N139/315843     LARGE XBED       UNIT 8       047
VEC MEAN= 34.  ST DEV=12. CON INTVL= 13. READINGS=  6 VEC MAG(PCT)= 98.13
TRUE AZIMUTH  35 55 28 38 21 28

MAKIRIKIRI    N139/315843     LARGE XBED       UNIT 10      047
VEC MEAN=267.  ST DEV=30. CON INTVL= 31. READINGS=  6 VEC MAG(PCT)= 89.19
TRUE AZIMUTH  295 271 305 231 255 238
```

```
                                              047
KAKIRIKIRI     N139/315843       LARGE XBED   UNIT 10
VEC MEAN=134.  ST DEV= 36. CON INTVL= 90. READINGS= 3  VEC MAG(PCT) = 87.08
TRUE AZIMUTH   107 122 176

                                              047
KAKIRIKIRI     N139/315843       LARGE XPED   UNIT 11
VEC MEAN=281.  ST DEV= 21. CON INTVL= 34. READINGS= 4  VEC MAG(PCT) = 94.93
TRUE AZIMUTH   283 295 250 295

                                              049
KAKIRIKIRI     N144/376712       LARGE XBED
VEC MEAN=130.  ST DEV= 7. CON INTVL= 11. READINGS= 4  VEC MAG(PCT) = 99.43
TRUE AZIMUTH   125 125 130 140

                                              051
KAIMATIRA      N144/313279       LARGE XPED
VEC MEAN=297.  ST DEV= 32. CON INTVL= 80. READINGS= 3  VEC MAG(PCT) = 89.78
TRUE AZIMUTH   320 310 260

                                              051
KAIMATIRA      N144/313279       RIPPLE FLOW
VEC MEAN=304.  ST DEV= 15. CON INTVL= 38. READINGS= 3  VEC MAG(PCT) = 97.67
TRUE AZIMUTH   320 290 301

                                              052
KAIMATIRA      N137/446926       RIPPLE STRIKE
VEC MEAN= 91.  ST DEV= 34. CON INTVL= 54. READINGS= 4  VEC MAG(PCT) = 86.97
TRUE AZIMUTH   65 60 110 130

                                              052
KAIMATIRA      N137/446926       RIPPLE DRIFT
VEC MEAN=325.  ST DEV= 7. CON INTVL= 64. READINGS= 2  VEC MAG(PCT) = 99.61
TRUE AZIMUTH   330 320

                                              052
KAIMATIRA      N137/446926       LARGE XBED
VEC MEAN=340.  ST DEV= 35. CON INTVL= 44. READINGS= 5  VEC MAG(PCT) = 85.86
TRUE AZIMUTH   350 300 35 330 330

                                              052
KAIMATIRA      N137/446926       LARGE XBED
VEC MEAN=244.  ST DEV= 28. CON INTVL= 35. READINGS= 5  VEC MAG(PCT) = 90.56
TRUE AZIMUTH   275 250 265 210 220
```

KAIWATIRA   N137/446926   LARGE XBED   052
VEC MEAN=162.   ST DEV= 8. CON   INTVL= 19. READINGS=   3 VEC MAG(PCT)= 99.40
TRUE AZIMUTH   170 155 160

MAKIRIKIRI   N137/438940   LARGE XBED   053
VEC MEAN=105.   ST DEV= 55. CON   INTVL=137. READINGS=   3 VEC MAG(PCT)= 71.55
TRUE AZIMUTH   50 105 160

MAKIRIKIRI   N137/438941   LARGE XBED   054
VEC MEAN=115.   ST DEV= 2. CON   INTVL= 5. READINGS=   3 VEC MAG(PCT)= 99.95
TRUE AZIMUTH   115 113 117

MAKIRIKIRI   N137/439940   LARGE XBED   055
TRUE AZIMUTH   330

MAKIRIKIRI   N137/439940   LARGE XBED   055
TRUE AZIMUTH   145

MAKIRIKIRI   N137/440939   SMALL XBED   056
VEC MEAN= 62.   ST DEV= 8. CON   INTVL= 19. READINGS=   3 VEC MAG(PCT)= 99.42
TRUE AZIMUTH   70 55 62

MAKIRIKIRI   N137/441942   RIPPLE STRIKE   057
VEC MEAN=177.   ST DEV= 7. CON   INTVL= 7. READINGS=   7 VEC MAG(PCT)= 99.27
TRUE AZIMUTH   180 170 176 190 180 170

MAKIRIKIRI   N137/441942   LARGE XBED   058
VEC MEAN=103.   ST DEV= 3. CON   INTVL= 7. READINGS=   3 VEC MAG(PCT)= 99.92
TRUE AZIMUTH   105 104 100

MAKIRIKIRI   N137/456951   LARGE XBED   059
TRUE AZIMUTH   320

```
MAKIRIKIRI      N127/490957      LARGE XBED                    060
VEC MEAN= 86.   ST DEV= 10. CON INTVL= 25. READINGS=  3 VEC MAG(PCT) = 98.98
TRUE AZIMUTH     82  97  78

KAIMATIRA       N138/580911      LARGE XBED                    063
VEC MEAN=235.   ST DEV= 5. CON INTVL= 12. READINGS=  3 VEC MAG(PCT) = 99.74
TRUE AZIMUTH    230  240  236

KAIMATIRA       N138/581912      LARGE XBED      UNIT 3        064
VEC MEAN=163.   ST DEV= 8. CON INTVL= 19. READINGS=  3 VEC MAG(PCT) = 99.40
TRUE AZIMUTH    155  170  165

KAIMATIRA       N138/581912      RIPPLE DRIFT    UNIT 4        064
VEC MEAN=345.   ST DEV= 7. CON INTVL= 64. READINGS=  2 VEC MAG(PCT) = 99.61
TRUE AZIMUTH    350  340

KAIMATIRA       N138/581912      RIPPLE DRIFT    UNIT 4        064
VEC MEAN=165.   ST DEV= 11. CON INTVL= 17. READINGS=  4 VEC MAG(PCT) = 98.67
TRUE AZIMUTH    155  160  180  165

KAIMATIRA       N138/581912      RIPPLE STRIKE   UNIT 4        064
VEC MEAN= 82.   ST DEV= 8. CON INTVL= 19. READINGS=  3 VEC MAG(PCT) = 99.40
TRUE AZIMUTH     80  90  75

KAIMATIRA       N138/581912      LARGE XBED      UNIT 5        064
VEC MEAN=162.   ST DEV= 6. CON INTVL= 14. READINGS=  3 VEC MAG(PCT) = 99.66
TRUE AZIMUTH    155  165  165

KAIMATIRA       N138/556928      RIPPLE STRIKE                 065
VEC MEAN=207.   ST DEV= 14. CON INTVL= 13. READINGS=  7 VEC MAG(PCT) = 97.57
TRUE AZIMUTH    220  215  221  190  215  200  190

KAIMATIRA       N138/556928      LARGE XBED                    065
VEC MEAN=121.   ST DEV= 19. CON INTVL= 16. READINGS=  8 VEC MAG(PCT) = 95.45
TRUE AZIMUTH    125  100  140  130  110  90  140  130
```

```
KAIMATIRA      N138/556928      RIPPLE DRIFT              065
VEC MEAN=263.  ST DEV= 12. CON INTVL= 29. READINGS=  3 VEC MAG(PCT) = 98.65
TRUE AZIMUTH   250 270 270

KAIMATIRA      N138/570924      RIPPLE DRIFT              065
VEC MEAN= 95.  ST DEV=  7. CON INTVL= 64. READINGS=  2 VEC MAG(PCT) = 99.61
TRUE AZIMUTH   100  90

KAIMATIRA      N138/570924      LARGE XBED                065
VEC MEAN=246.  ST DEV= 40. CON INTVL= 99. READINGS=  3 VEC MAG(PCT) = 84.65
TRUE AZIMUTH   260 200 275

KAIMATIRA      N138/581912      LARGE XBED                066
VEC MEAN= 62.  ST DEV= 60. CON INTVL= 96. READINGS=  4 VEC MAG(PCT) = 66.80
TRUE AZIMUTH   160  49  35  43

KAIMATIRA      N138/583910      LARGE XBED                067
VEC MEAN=250.  ST DEV= 42. CON INTVL=104. READINGS=  3 VEC MAG(PCT) = 82.96
TRUE AZIMUTH   270 200 275

KAIMATIRA      N138/583910      LARGE XBED                067
VEC MEAN=100.  ST DEV= 10. CON INTVL= 25. READINGS=  3 VEC MAG(PCT) = 98.98
TRUE AZIMUTH    90 100 110

KAIMATIRA      N138/583910      RIPPLE STRIKE             067
VEC MEAN=170.  ST DEV= 22. CON INTVL= 54. READINGS=  3 VEC MAG(PCT) = 95.23
TRUE AZIMUTH   145 180 185

KAIMATIRA      N144/132795      RIPPLE STRIKE  UNIT 38    071
VEC MEAN=201.  ST DEV= 34. CON INTVL= 29. READINGS=  8 VEC MAG(PCT) = 85.13
TRUE AZIMUTH   220 210 190 175 165 160 240 250

KAIMATIRA      N144/132795      RIPPLE DRIFT   UNIT 38    071
VEC MEAN=291.  ST DEV= 40. CON INTVL= 33. READINGS=  8 VEC MAG(PCT) = 80.18
TRUE AZIMUTH   310 300 300 265 250 225 330 340
```

```
KAIMATIRA       N144/127797    RIPPLE DRIFT    UNIT 38         071
VEC MEAN=111.   ST DEV= 34. CON INTVL= 29. READINGS= 8 VEC MAG(PCT)= 85.13
TRUE AZIMUTH    130 120 100  85  75  70 150 150 160

KAIMATIRA       N144/133793    RIPPLE DRIFT    UNIT 42         071
VEC MEAN=117.   ST DEV= 15. CON INTVL= 38. READINGS= 3 VEC MAG(PCT)= 97.64
TRUE AZIMUTH    129 100 130

KAIMATIRA       N144/133793    RIPPLE DRIFT    UNIT 42         071
VEC MEAN=297.   ST DEV= 15. CON INTVL= 38. READINGS= 3 VEC MAG(PCT)= 97.64
TRUE AZIMUTH    300 280 310

KAIMATIRA       N144/133794    LARGE XBED      UNIT 42         071
VEC MEAN=335.   ST DEV= 7. CON INTVL= 64. READINGS= 2 VEC MAG(PCT)= 99.61
TRUE AZIMUTH    330 340

KAIMATIRA       N144/132795    LARGE XBED      UNIT 43         071
VEC MEAN=135.   ST DEV= 7. CON INTVL= 64. READINGS= 2 VEC MAG(PCT)= 99.61
TRUE AZIMUTH    130 140

KAIMATIRA       N144/132795    LARGE XBED      UNIT 45         071
VEC MEAN=244.   ST DEV= 15. CON INTVL= 37. READINGS= 3 VEC MAG(PCT)= 97.69
TRUE AZIMUTH    242 260 230

KAIMATIRA       N144/133794    LARGE XBED      UNIT 42         071
VEC MEAN=155.   ST DEV= 5. CON INTVL= 12. READINGS= 3 VEC MAG(PCT)= 99.74
TRUE AZIMUTH    150 160 155

KAIMATIRA       N144/133794    LARGE XBED      UNIT 60         071
VEC MEAN=247.   ST DEV= 11. CON INTVL= 95. READINGS= 2 VEC MAG(PCT)= 99.14
TRUE AZIMUTH    240 255

KAIMATIRA       N144/133794    LARGE XBED      UNIT 56         071
VEC MEAN=268.   ST DEV= 8. CON INTVL= 19. READINGS= 3 VEC MAG(PCT)= 99.40
TRUE AZIMUTH    275 260 270
```

```
KAIMATIRA        N138/842841       LARGE XBED                          074
VEC MEAN= 88.    ST DEV= 8. CON    INTVL= 19. READINGS=   3 VEC MAG(PCT) = 99.42
TRUE AZIMUTH     88  80  95

KAIMATIRA        N138/842841       LARGE XBED                          074
VEC MEAN=302.    ST DEV= 3. CON    INTVL= 7. READINGS=    3 VEC MAG(PCT) = 99.91
TRUE AZIMUTH     305 300 300

KAIMATIRA        N138/843852       RIPPLE DRIFT                        075
VEC MEAN=268.    ST DEV= 3. CON    INTVL= 6. READINGS=    3 VEC MAG(PCT) = 99.93
TRUE AZIMUTH     270 265 268

KAIMATIRA        N138/843852       RIPPLE DRIFT                        075
VEC MEAN= 83.    ST DEV= 8. CON    INTVL= 19. READINGS=   3 VEC MAG(PCT) = 99.40
TRUE AZIMUTH     85  75  90

KAIMATIRA        N138/843852       RIPPLE STRIKE                       075
VEC MEAN=195.    ST DEV= 6. CON    INTVL= 6. READINGS=    6 VEC MAG(PCT) = 99.60
TRUE AZIMUTH     200 195 198 195 185 200

KAIMATIRA        N138/846862       LARGE XBED                          077
VEC MEAN=162.    ST DEV= 24. CON   INTVL= 59. READINGS=   3 VEC MAG(PCT) = 94.41
TRUE AZIMUTH     135 170 180

MAKIRIKIRI       N138/847864       RIPPLE STRIKE                       079
VEC MEAN= 96.    ST DEV= 38. CON   INTVL= 94. READINGS=   3 VEC MAG(PCT) = 85.98
TRUE AZIMUTH     140 80  70

MAKIRIKIRI       N138/847864       LARGE XBED                          079
VEC MEAN=149.    ST DEV= 6. CON    INTVL= 10. READINGS=   4 VEC MAG(PCT) = 99.52
TRUE AZIMUTH     151 158 145 144

MAKIRIKIRI       N138/852875       RIPPLE DRIFT                        081
VEC MEAN= 3.     ST DEV= 12. CON   INTVL= 30. READINGS=   3 VEC MAG(PCT) = 98.50
TRUE AZIMUTH     5   14  350
```

```
MAKIRIKIRI                   081
N138/852875      RIPPLE STRIKE
VEC MEAN=273. ST DEV= 12. CON INTVL= 30. READINGS= 3 VEC MAG(PCT)= 98.51
TRUE AZIMUTH  275  284  760

MAKIRIKIRI                   083
N139/854884      LARGE XBED
VEC MEAN=296. ST DEV= 44. CON INTVL= 55. READINGS= 5 VEC MAG(PCT)= 78.15
TRUE AZIMUTH  340  280  305  225  320

MAKIRIKIRI                   085
N139/298838      LARGE XBED
VEC MEAN=266. ST DEV= 41. CON INTVL= 66. READINGS= 4 VEC MAG(PCT)= 82.00
TRUE AZIMUTH  240  330  255  250

MAKIRIKIRI                   087
N139/304832      LARGE XBED
VEC MEAN=145. ST DEV= 9. CON INTVL= 15. READINGS= 4 VEC MAG(PCT)= 99.05
TRUE AZIMUTH  155  150  140  135

MAKIRIKIRI                   088
N139/303830      LARGE XBED
VEC MEAN=296. ST DEV= 18. CON INTVL= 28. READINGS= 4 VEC MAG(PCT)= 96.53
TRUE AZIMUTH  315  305  275  290

MAKIRIKIRI                   088
N139/303830      LARGE XBED
VEC MEAN=125. ST DEV= 9. CON INTVL= 10. READINGS= 6 VEC MAG(PCT)= 98.90
TRUE AZIMUTH  130  115  140  125  123  116

MAKIRIKIRI                   089
N139/302827      LARGE XBED
TRUE AZIMUTH  265

KAIMATIRA                    C90
N139/302820      LARGE XBED
VEC MEAN=277. ST DEV= 10. CON INTVL= 26. READINGS= 3 VEC MAG(PCT)= 98.90
TRUE AZIMUTH  280  265  285

KAIMATIRA                    092
N144/289787      LARGE XBED
VEC MEAN=143. ST DEV= 13. CON INTVL= 31. READINGS= 3 VEC MAG(PCT)= 98.39
TRUE AZIMUTH  130  145  155
```

```
KAIMATIRA     N144/291779      LARGE XBED         093
VEC MEAN=141. ST DEV= 2. CON INTVL= 5. READINGS= 3 VEC MAG(PCT)= 99.95
TRUE AZIMUTH  140 139 143

KAIMATIRA     N144/291779      RIPPLES ASYM       093
VEC MEAN=147. ST DEV= 3. CON INTVL= 7. READINGS= 3 VEC MAG(PCT)= 99.92
TRUE AZIMUTH  145 150 146

KAIMATIRA     N144/237766      RIPPLES ASYM       097
VEC MEAN=162. ST DEV= 19. CON INTVL= 47. READINGS= 3 VEC MAG(PCT)= 96.39
TRUE AZIMUTH  140 175 170

MAKIRIKIRI    N144/350780      LARGE XBED         099
VEC MEAN=220. ST DEV= 18. CON INTVL= 23. READINGS= 5 VEC MAG(PCT)= 95.96
TRUE AZIMUTH  220 215 200 250 215

MAKIRIKIRI    N144/348786      LARGE XBED    UNIT 1   101
VEC MEAN=207. ST DEV= 20. CON INTVL= 21. READINGS= 6 VEC MAG(PCT)= 95.17
TRUE AZIMUTH  205 240 185 210 190 215

MAKIRIKIRI    N144/348768      LARGE XBED    UNIT 2   101
VEC MEAN=190. ST DEV= 5. CON INTVL= 12. READINGS= 3 VEC MAG(PCT)= 99.74
TRUE AZIMUTH  185 195 199

MAKIRIKIRI    N144/351750      LARGE XBED         104
TRUE AZIMUTH  270

MAKIRIKIRI    N139/442855      SMALL XBED         105
VEC MEAN=238. ST DEV= 10. CON INTVL= 26. READINGS= 3 VEC MAG(PCT)= 98.90
TRUE AZIMUTH  230 250 235

MAKIRIKIRI    N139/442855      SMALL XBED         105
VEC MEAN=135. ST DEV= 5. CON INTVL= 11. READINGS= 3 VEC MAG(PCT)= 99.79
TRUE AZIMUTH  135 139 130
```

```
MAKIRIKIRI    N139/442855      IMBRIC-N                              105
VEC MEAN= 35.  ST DEV= 14.  CON INTVL=127.  READINGS=  2  VEC MAG(PCT) = 98.48
TRUE AZIMUTH   45   25

MAKIRIKIRI    N144/306725      LARGE XBED                           115
VEC MEAN=286.  ST DEV= 34.  CON INTVL= 54.  READINGS=  4  VEC MAG(PCT) = 87.13
TRUE AZIMUTH  250  310  320  265

MAKIRIKIRI    N144/270730      LARGE XBED                           118
VEC MEAN=219.  ST DEV= 33.  CON INTVL= 52.  READINGS=  4  VEC MAG(PCT) = 85.07
TRUE AZIMUTH  175  220  225  255

MAKIRIKIRI    N144/293734      LARGE XBED                           121
VEC MEAN=332.  ST DEV=  4.  CON INTVL=  6.  READINGS=  4  VEC MAG(PCT) = 99.85
TRUE AZIMUTH  335  330  329  336

MAKIRIKIRI    N144/293734      LARGE XBED                           121
VEC MEAN=167.  ST DEV= 11.  CON INTVL= 95.  READINGS=  2  VEC MAG(PCT) = 99.14
TRUE AZIMUTH  175  160

MAKIRIKIRI    N144/296732      LARGE XBED      UNIT  6              122
VEC MEAN=180.  ST DEV= 13.  CON INTVL= 33.  READINGS=  3  VEC MAG(PCT) = 98.23
TRUE AZIMUTH  185  190  165

MAKIRIKIRI    N144/296732      RIPPLE DRIFT   UNIT  7              122
VEC MEAN=130.  ST DEV=  7.  CON INTVL= 54.  READINGS=  2  VEC MAG(PCT) = 99.61
TRUE AZIMUTH  125  135

MAKIRIKIRI    N144/296732      RIPPLE DRIFT   UNIT  7              122
VEC MEAN=309.  ST DEV=  8.  CON INTVL= 10.  READINGS=  5  VEC MAG(PCT) = 99.17
TRUE AZIMUTH  305  315  305  320  300

MAKIRIKIRI    N144/297727      LARGE XBED      UNIT 10             122
VEC MEAN= 87.  ST DEV= 11.  CON INTVL= 14.  READINGS=  5  VEC MAG(PCT) = 98.54
TRUE AZIMUTH   90  100   85   90   70
```

```
MAKIRIKIRI        N144/297727      LARGE XBED      UNIT 10                          122
VEC MEAN=322.     ST DEV= 16. CON INTVL= 20. READINGS= 5   VEC MAG(PCT)= 96.88
TRUE AZIMUTH      310 335 330 335 300

MAKIRIKIRI        N144/297728      LARGE XBED      UNIT 12                          122
VEC MEAN=297.     ST DEV= 6. CON INTVL= 14. READINGS= 3    VEC MAG(PCT)= 99.66
TRUE AZIMUTH      300 290 300

MAKIRIKIRI        N144/297728      LARGE XBED      UNIT 12                          122
VEC MEAN=107.     ST DEV= 4. CON INTVL= 32. READINGS= 2    VEC MAG(PCT)= 99.90
TRUE AZIMUTH      110 105

MAKIRIKIRI        N144/298726      LARGE XBED                                       124
VEC MEAN=273.     ST DEV= 8. CON INTVL= 19. READINGS= 3    VEC MAG(PCT)= 99.40
TRUE AZIMUTH      265 275 280

KAIMATIRA         N144/318700      LARGE XBED                                       131
VEC MEAN=275.     ST DEV= 5. CON INTVL= 12. READINGS= 3    VEC MAG(PCT)= 99.74
TRUE AZIMUTH      280 270 274

KAIMATIRA         N144/305683      LARGE XBED                                       133
VEC MEAN=164.     ST DEV= 9. CON INTVL= 14. READINGS= 4    VEC MAG(PCT)= 99.16
TRUE AZIMUTH      165 155 160 175

KAIMATIRA         N144/293652      LARGE XBED                                       135
VEC MEAN=258.     ST DEV= 16. CON INTVL= 40. READINGS= 3   VEC MAG(PCT)= 97.39
TRUE AZIMUTH      265 270 240

KAIMATIRA         N144/309671      LARGE XBED                                       136
VEC MEAN=167.     ST DEV= 4. CON INTVL= 32. READINGS= 2    VEC MAG(PCT)= 99.90
TRUE AZIMUTH      165 170

KAIMATIRA         N144/309671      LARGE XBED                                       136
TRUE AZIMUTH      100
```

```
KAIMATIRA      N144/309571          LARGE XBED                                           136
TRUE AZIMUTH   325

KAIMATIRA      N144/309662          LARGE XBED                                           137
VEC MEAN= 0.   ST DEV= 0.  CON INTVL= 0.  READINGS= 2  VEC MAG(PCT)= 99.99
TRUE AZIMUTH   0   0

KAIMATIRA      N144/309662          LARGE XBED                                           137
VEC MEAN= 97.  ST DEV= 25.  CON INTVL=222.  READINGS= 2  VEC MAG(PCT)= 95.37
TRUE AZIMUTH   70  105

KAIMATIRA      N144/309662          LARGE XBED                                           137
VEC MEAN=205.  ST DEV= 17.  CON INTVL= 27.  READINGS= 4  VEC MAG(PCT)= 96.79
TRUE AZIMUTH   225  185  200  210

KAIMATIRA      N144/294557          LARGE XBED                                           139
VEC MEAN=307.  ST DEV= 12.  CON INTVL= 29.  READINGS= 3  VEC MAG(PCT)= 98.65
TRUE AZIMUTH   320  300  300

KAIMATIRA      N144/016776          LARGE XBED                                           141
VEC MEAN=274.  ST DEV= 60.  CON INTVL=148.  READINGS= 3  VEC MAG(PCT)= 67.73
TRUE AZIMUTH   325  200  300

KAIMATIRA      N139/125810          RIPPLE FLOW                                          142
VEC MEAN=252.  ST DEV= 38.  CON INTVL= 95.  READINGS= 3  VEC MAG(PCT)= 85.74
TRUE AZIMUTH   210  260  285

KAIMATIRA      N139/125810          RIPPLE STRIKE                                        142
VEC MEAN=156.  ST DEV= 34.  CON INTVL= 85.  READINGS= 3  VEC MAG(PCT)= 88.58
TRUE AZIMUTH   120  170  185

KAIMATIRA      N139/125810          LARGE XBED                                           142
TRUE AZIMUTH   240
```

```
                            142                LARGE XBED

KAIMATIRA         N139/125810
TRUE AZIMUTH     75

KAIMATIRA              147
VEC MEAN=211.    N138/772856   LARGE XBED
TRUE AZIMUTH     ST DEV= 39. CON INTVL= 40. READINGS=   6  VEC MAG(PCT)= 82.15
                 215  190  170  165  245  275

KAIMATIRA              147
VEC MEAN=142.    N138/772856   LARGE XBED
TRUE AZIMUTH     ST DEV= 8. CON INTVL= 19. READINGS=   3  VEC MAG(PCT)= 99.40
                 135  150  140

KAIMATIRA              148
VEC MEAN=106.    N138/710892   LARGE XBED     UNIT 2
TRUE AZIMUTH     ST DEV= 17. CON INTVL= 16. READINGS=   7  VEC MAG(PCT)= 96.20
                 110  85  90  110  95  115  135

KAIMATIRA              148
VEC MEAN= 95.    N138/710892   RIPPLE DRIFT   UNIT 2
TRUE AZIMUTH     ST DEV= 3. CON INTVL= 6. READINGS=   3  VEC MAG(PCT)= 99.93
                 95  93  98

KAIMATIRA              148
VEC MEAN=262.    N138/710892   RIPPLE DRIFT   UNIT 2
TRUE AZIMUTH     ST DEV= 13. CON INTVL= 21. RFADINGS=   2  VEC MAG(PCT)= 98.39
                 250  275  260

KAIMATIRA              148
VEC MEAN=176.    N138/710892   RIPPLE STRIKE   UNIT 4
TRUE AZIMUTH     ST DEV= 11. CON INTVL= 9. READINGS= 10  VEC MAG(PCT)= 98.27
                 185  183  188  160  185  170  165  161  188  175

KAIMATIRA              149
VEC MEAN=282.    N138/718892   LARGE XBED
TRUE AZIMUTH     ST DEV= 4. CON INTVL= 32. READINGS=   2  VEC MAG(PCT)= 99.90
                 285  280

KAIMATIRA              149
VEC MEAN=157.    N138/718892   RIPPLE STRIKE
TRUE AZIMUTH     ST DEV= 12. CON INTVL= 29. READINGS=   3  VEC MAG(PCT)= 98.65
                 150  170  150
```

149
KAIMATIRA   N138/718992   LARGE XBED
VEC MEAN= 99. ST DEV= 15. CON INTVL= 25. READINGS= 4 VEC MAG(PCT) = 97.28
TRUE AZIMUTH   90 95 100 120

150
KAIMATIRA   N138/725893   LARGE XBED
VEC MEAN=280. ST DEV= 0. CON INTVL= 1. READINGS= 2 VEC MAG(PCT) = 99.99
TRUE AZIMUTH   280 280

150
KAIMATIRA   N138/725892   LARGE XBED
VEC MEAN= 85. ST DEV= 7. CON INTVL= 64. READINGS= 2 VEC MAG(PCT) = 99.61
TRUE AZIMUTH   90 80

152
KAIMATIRA   N149/220370   LARGE XBED   UNIT 3
VEC MEAN=312. ST DEV= 16. CON INTVL= 38. READINGS= 3 VEC MAG(PCT) = 97.57
TRUE AZIMUTH   330 306 301

153
MAKIRIKIRI   N149/215380   RIPPLE DRIFT UNIT 4
VEC MEAN=277. ST DEV= 4. CON INTVL= 32. READINGS= 2 VEC MAG(PCT) = 99.90
TRUE AZIMUTH   275 280

153
MAKIRIKIRI   N149/215390   LARGE XBED   UNIT 6
VEC MEAN=266. ST DEV= 21. CON INTVL= 33. READINGS= 4 VEC MAG(PCT) = 95.24
TRUE AZIMUTH   265 270 240 290

154
MAKIRIKIRI   N149/325346   LARGE XBED
VEC MEAN=296. ST DEV= 24. CON INTVL= 25. READINGS= 6 VEC MAG(PCT) = 93.13
TRUE AZIMUTH   300 315 280 295 260 325

154
MAKIRIKIRI   N149/325346   LARGE XBED
VEC MEAN=112. ST DEV= 8. CON INTVL= 19. READINGS= 3 VEC MAG(PCT) = 99.40
TRUE AZIMUTH   105 110 120

156
KAIMATIRA   N144/285506   RIPPLE DRIFT UNIT 1
VEC MEAN=258. ST DEV= 8. CON INTVL= 19. READINGS= 3 VEC MAG(PCT) = 99.40
TRUE AZIMUTH   260 250 265

```
KAIMATIRA       N144/285506         RIPPLE DRIFT   UNIT  1                        156
VEC MEAN= 80.   ST DEV= 7. CON INTVL= 17. READINGS=  3 VEC MAG(PCT)= 99.50
TRUE AZIMUTH     80  87  73

KAIMATIRA       N144/285506         LARGE XBED     UNIT  4                        156
VEC MEAN=336.   ST DEV= 9. CON INTVL= 14. READINGS=  4 VEC MAG(PCT)= 99.15
TRUE AZIMUTH    334 345 340 325

KAIMATIRA       N144/285506         LARGE XBED     UNIT  6                        156
VEC MEAN=360.   ST DEV= 15. CON INTVL= 23. READINGS=  4 VEC MAG(PCT)= 97.60
TRUE AZIMUTH      0  15   3 340

KAIMATIRA       N144/285506         RIPPLE STRIKE  UNIT  1                        156
VEC MEAN=170.   ST DEV= 7. CON INTVL=  8. READINGS=  6 VEC MAG(PCT)= 99.30
TRUE AZIMUTH    160 170 180 170 175 163

MAKIRIKIRI      N144/288513         LARGE XBED     UNIT  1                        157
VEC MEAN=265.   ST DEV= 2. CON INTVL=  5. READINGS=  3 VEC MAG(PCT)= 99.95
TRUE AZIMUTH    263 266 267

MAKIRIKIRI      N144/288513         RIPPLE STRIKE  UNIT 12                        157
VEC MEAN= 12.   ST DEV= 12. CON INTVL= 30. READINGS=  3 VEC MAG(PCT)= 98.45
TRUE AZIMUTH     24  16   0

MAKIRIKIRI      N144/288513         RIPPLE STRIKE  UNIT 13                        157
VEC MEAN=285.   ST DEV= 13. CON INTVL=121. READINGS=  2 VEC MAG(PCT)= 98.62
TRUE AZIMUTH    295 275

MAKIRIKIRI      N144/288513         RIPPLE STRIKE  UNIT 13                        157
VEC MEAN=347.   ST DEV= 4. CON INTVL= 32. READINGS=  2 VEC MAG(PCT)= 99.90
TRUE AZIMUTH    350 345

KAIMATIRA       N144/288513         LARGE XBED     UNIT 19                        157
VEC MEAN=232.   ST DEV= 9. CON INTVL= 21. READINGS=  3 VEC MAG(PCT)= 99.26
TRUE AZIMUTH    240 232 223
```

```
KAIMATIRA      N144/288513      LARGE XBED    UNIT 22     157
VEC MEAN=295.  ST DEV=  2.  CON INTVL=  5.  READINGS= 3  VEC MAG(PCT)= 99.95
TRUE AZIMUTH   295 293 297

KAIMATIRA      N144/288513      LARGE XBED    UNIT 24     157
VEC MEAN=240.  ST DEV=  5.  CON INTVL= 11.  READINGS= 3  VEC MAG(PCT)= 99.79
TRUE AZIMUTH   240 245 236

KAIMATIRA      N144/288513      LARGE XBED    UNIT 26     157
VEC MEAN=272.  ST DEV= 14.  CON INTVL= 35.  READINGS= 3  VEC MAG(PCT)= 98.02
TRUE AZIMUTH   278 256 282

KAIMATIRA      N144/288513      RIPPLE DRIFT  UNIT 26     157
VEC MEAN=353.  ST DEV=  8.  CON INTVL= 19.  READINGS= 3  VEC MAG(PCT)= 99.40
TRUE AZIMUTH     0 345 355

MAKIRIKIRI     N138/882396      LARGE XBED                169
VEC MEAN=238.  ST DEV= 18.  CON INTVL= 23.  READINGS= 5  VEC MAG(PCT)= 96.00
TRUE AZIMUTH   210 250 245 230 255

MAKIRIKIRI     N144/374696      LARGE XBED    UNIT  5     183
VEC MEAN=138.  ST DEV= 23.  CON INTVL= 28.  READINGS= 5  VEC MAG(PCT)= 93.93
TRUE AZIMUTH   170 135 120 115 150

KAIMATIRA      N144/367673      LARGE XBED    UNIT 11     183
VEC MEAN=192.  ST DEV= 13.  CON INTVL= 16.  READINGS= 5  VEC MAG(PCT)= 97.96
TRUE AZIMUTH   205 200 175 182 199

MAKIRIKIRI     N139/237817      LARGE XBED                184
VEC MEAN= 91.  ST DEV=  5.  CON INTVL= 12.  READINGS= 3  VEC MAG(PCT)= 99.77
TRUE AZIMUTH    95  86  93

MAKIRIKIRI     N139/237817      CHANNELS                  184
VEC MEAN=150.  ST DEV= 14.  CON INTVL=127.  READINGS= 2  VEC MAG(PCT)= 98.48
TRUE AZIMUTH   160 140
```

MAKIRIKIRI
N139/235814   LARGE XBED   185
VEC MEAN=137. ST DEV= 37. CON INTVL= 59. READINGS= 4 VEC MAG(PCT)= 95.0x
TRUE AZIMUTH 185 148 104 113

MAKIRIKIRI
N139/233869   RIPPLE STRIKE   186
VEC MEAN= 10. ST DEV= 17. CON INTVL= 43. READINGS= 3 VEC MAG(PCT)= 96.96
TRUE AZIMUTH 350 20 29

MAKIRIKIRI
N139/227806   RIPPLE STRIKE   187
VEC MEAN=139. ST DEV= 10. CON INTVL= 25. READINGS= 3 VEC MAG(PCT)= 98.96
TRUE AZIMUTH 150 131 135

MAKIRIKIRI
N139/226804   LARGE XBED   188
VEC MEAN=150. ST DEV= 2. CON INTVL= 19. READINGS= 2 VEC MAG(PCT)= 99.96
TRUE AZIMUTH 149 152

KAIMATIRA
N139/225801   LARGE XBED   189
VEC MEAN= 73. ST DEV= 23. CON INTVL= 56. READINGS= 3 VEC MAG(PCT)= 94.90
TRUE AZIMUTH 95 75 50

KAIMATIRA
N139/225801   LARGE XBED   189
VEC MEAN=269. ST DEV= 35. CON INTVL= 88. READINGS= 3 VEC MAG(PCT)= 87.63
TRUE AZIMUTH 300 275 230

KAIMATIRA
N138/907833   LARGE XBED   190
VEC MEAN=126. ST DEV= 6. CON INTVL= 10. READINGS= 4 VEC MAG(PCT)= 99.54
TRUE AZIMUTH 125 135 125 120

KAIMATIRA
N138/908833   RIPPLE DRIFT   191
VEC MEAN=127. ST DEV= 9. CON INTVL= 10. READINGS= 6 VEC MAG(PCT)= 98.90
TRUE AZIMUTH 120 125 140 135 115

KAIMATIRA
N138/908833   RIPPLE DRIFT   191
VEC MEAN=302. ST DEV= 4. CON INTVL= 32. READINGS= 2 VEC MAG(PCT)= 99.90
TRUE AZIMUTH 300 305

KAIMATIRA   N138/969829   LARGE XBED   192
VEC MEAN=257.   ST DEV= 8. CON INTVL= 19. READINGS=   3   VEC MAG(PCT) = 99.40
TRUE AZIMUTH   205 215 200

KAIMATIRA   N138/969829   RIPPLE STRIKE   192
VEC MEAN=143.   ST DEV= 10. CON INTVL= 24. READINGS=   3   VEC MAG(PCT) = 98.90
TRUE AZIMUTH   155 135 140

KAIMATIRA   N139/015825   LARGE XBED   193
VEC MEAN=159.   ST DEV= 3. CON INTVL= 7. READINGS=   3   VEC MAG(PCT) = 99.91
TRUE AZIMUTH   160 155 160

KAIMATIRA   N139/015825   LARGE XBED   193
VEC MEAN= 15.   ST DEV= 42. CON INTVL=381. READINGS=   2   VEC MAG(PCT) = 86.57
TRUE AZIMUTH   345   45

KAIMATIRA   N139/015825   RIPPLE STRIKE   193
VEC MEAN= 76.   ST DEV= 12. CON INTVL= 11. READINGS=   7   VEC MAG(PCT) = 98.09
TRUE AZIMUTH   100   85   70   65   70   75   70

KAIMATIRA   N139/015825   RIPPLE DRIFT   193
TRUE AZIMUTH   340

KAIMATIRA   N139/015825   RIPPLE DRIFT   193
VEC MEAN=160.   ST DEV= 4. CON INTVL= 6. READINGS=   4   VEC MAG(PCT) = 99.80
TRUE AZIMUTH   160 155 160 165

KAIMATIRA   N139/015842   LARGE XBED   193
VEC MEAN=122.   ST DEV= 5. CON INTVL= 6. READINGS=   6   VEC MAG(PCT) = 99.65
TRUE AZIMUTH   125 125 130 120 115 120

KAIMATIRA   N139/015823   LARGE XBED   193
VEC MEAN=130.   ST DEV= 7. CON INTVL= 64. READINGS=   2   VEC MAG(PCT) = 99.61
TRUE AZIMUTH   125 135

MAKIRIKIRI   N139/255436   LARGE XRED   195
VEC MEAN=263.   ST DEV= 17. CON INTVL= 21. READINGS=   3 VEC MAG(PCT)= 96.55
TRUE AZIMUTH   260 245 285 275 250

MAKIRIKIRI   N139/153847   LARGE XRED   197
VEC MEAN=230.   ST DEV= 26. CON INTVL= 27. READINGS=   4 VEC MAG(PCT)= 91.90
TRUE AZIMUTH   250 245 247 195 240

MAKIRIKIRI   N139/153847   LARGE XRED   197
VEC MEAN= 27.   ST DEV= 10. CON INTVL= 26. READINGS=   3 VEC MAG(PCT)= 98.90
TRUE AZIMUTH   15 30 35

MAKIRIKIRI   N139/168853   LARGE XRED   198
VEC MEAN=170.   ST DEV= 4. CON INTVL= 10. READINGS=   3 VEC MAG(PCT)= 99.83
TRUE AZIMUTH   175 179 163

MAKIRIKIRI   N139/172955   LARGE XRED   199
VEC MEAN=177.   ST DEV= 4. CON INTVL= 32. READINGS=   2 VEC MAG(PCT)= 99.90
TRUE AZIMUTH   175 180

KAIMATIRA   N144/326644   LARGE XRED   UNIT 2   200
VEC MEAN=162.   ST DEV= 4. CON INTVL= 32. READINGS=   2 VEC MAG(PCT)= 99.90
TRUE AZIMUTH   160 165

KAIMATIRA   N144/326644   SMALL XRED   UNIT 5   200
VEC MEAN=242.   ST DEV= 4. CON INTVL= 32. READINGS=   2 VEC MAG(PCT)= 99.90
TRUE AZIMUTH   245 240

KAIMATIRA   N144/326644   LARGE XRED   UNIT 9   200
VEC MEAN=126.   ST DEV= 16. CON INTVL= 19. READINGS=   5 VEC MAG(PCT)= 97.04
TRUE AZIMUTH   145 140 115 120 110

KAIMATIRA   N144/326644   LARGE XRED   UNIT 9   200
VEC MEAN=255.   ST DEV= 21. CON INTVL=191. READINGS=   2 VEC MAG(PCT)= 96.59
TRUE AZIMUTH   240 270

314.

KAIMATIPA   N144/326644   RIPPLE STRIKE UNIT ?   200
VEC MEAN=155. ST DEV= 7. CON INTVL= 64. READINGS= 2 VEC MAG(PCT)= 99.61
TRUE AZIMUTH 150 160

MAKIRIKIRI   N144/342645   RIPPLE DRIFT   202
VEC MEAN=161. ST DEV= 11. CON INTVL= 18. READINGS= 4 VEC MAG(PCT)= 98.60
TRUE AZIMUTH 175 150 165 155

MAKIRIKIRI   N144/342645   LARGE XBED   202
VEC MEAN=177. ST DEV= 6. CON INTVL= 19. READINGS= 3 VEC MAG(PCT)= 99.40
TRUE AZIMUTH 175 170 185